ROLE OF HIPPOCAMPAL ΔFOSB IN BEHAVIORAL RESPONSES TO CHRONIC STRESS

By

Claire Elena Manning

A DISSERTATION

Submitted to
Michigan State University
in partial fulfillment of the requirements
for the degree of

Neuroscience — Doctor of Philosophy

2019

ABSTRACT

ROLE OF HIPPOCAMPAL ΔFOSB IN BEHAVIORAL RESPONSES TO CHRONIC STRESS

By

Claire Elena Manning

Depression is a highly prevalent mood disorder which affects up to 20% of the population. While women are twice as likely as men to be diagnosed with a mood disorder, the neurophysiological basis of this disparity is unclear. The hippocampus (HPC) is a limbic brain region implicated in clinical depression and preclinical rodent models that is uniquely susceptible to stress-induced changes in gene expression and cell function. The transcription factor ΔFosB regulates spatial learning and cell proliferation in HPC and is induced in dorsal HPC by stress. In this thesis, I elucidate the contributions of ΔFosB in dorsal dentate gyrus (DG) influence to neural proliferation and spatial learning, and in ventral HPC projections to stress-induced depression-like behavior in both sexes. Specifically, I show that DG subgranular zone *FosB* gene products are necessary for normal neurogenesis and learning. As the vHPC is implicated in affective learning and memory through its connectivity to other limbic regions, I examined the role of vHPC ΔFosB in stress-induced behaviors. I describe divergent patterns of behavior in males, wherein ΔFosB in vHPC-NAc is necessary and sufficient for resilience to stress but ΔFosB in vHPC-BLA is necessary for the expression of fear and anxiety. These results demonstrate that individual genes can have disparate roles within a single brain region, based not only on heterogenous cell types but on the specific projections of the neurons in which they are expressed. I also show a basal sex difference in stress susceptibility that is mediated by the vHPC-NAc circuit and adult testosterone. These data show vHPC-

NAc activity is causally linked to the sex difference in susceptibility to stress-induced anhedonia. This relationship is dependent upon long-term adaptation of vHPC-NAc projections that I show can be manipulated with hormones or chemogenetics. Thus, this work uncovers a potential biological underpinning of female vulnerability to mood disorders related to stress and sets the stage to develop novel, sex-specific treatments for depression.

For my community, family, and especially Federico. This document is a testament to their invaluable support.

ACKNOWLEDGEMENTS

This research was supported through a variety of funding sources including the following:

- Dr. A.J. Robison's start-up funds, a Whitehall Foundation grant, and a NIMH R01MH111604
- Dr. Andrew Eagle was awarded a NARSAD young investigator, and Dr. Elizabeth Williams was awarded Spectrum Health Scholarships.
- Claire Manning was funded through Dissertation Continuation and Completion Fellowships from the College of Natural Science at Michigan State University and a T32 to Michigan State University.

This work was also completed with significant contributions from A.L. Eagle and E.S. Williams in chapters 4 and 5, respectively. These contributions include the ex vivo slice electrophysiology and surgical assistance, as well as A.L.E. performing Temporally Displaced Passive Avoidance assays.

I am extremely lucky to have worked alongside astute, frank, and generous scientists at Michigan State University. Foremost in my mind, I would like to thank my advisor Dr. A.J. Robison. From the beginning, his encouragement and endless patience set the tone for my graduate school experience. His mentorship shaped my philosophy and approach to science. I will be forever grateful for our discussions of science, art, and academia. I also owe a great debt to my committee, Drs. Cheryl Sisk. Hongbing Wang, and Gina Leinninger. Their availability, unfettered support, helpful critiques,

and collaborations enhanced my dissertation. I would also be remiss not to thank the work of the neuroscience and physiology program's administrative staff in facilitating my graduate school experiences.

Throughout my time in the Robison lab I have been blessed to work closely alongside a truly phenomenal group of people in the Robison/Mazei-Robison group. This spans from our superlative lab manager Ken Moon, through our post-doctoral fellows (especially Dr. Andrew Eagle), to graduate students past and present. I would particularly like to thank Amber Garrison, Marie Doyle, and Christine Kwiatkowski for their scientific discussions, editing prowess, and friendship. Nearest to my heart are Drs. Sarah Simmons, Paula Kurdziel, and Elizabeth Higginson. Their enthusiasm for science, active collaborations, and close personal friendships formed a bastion for my academic growth. Together the positive working environment illustrated that it takes a village to raise a scientist.

I would like to thank other collaborators who contributed to this work. Dr. Rachel Neve and her viral core at Massachusetts General Hospital generated several new viruses for work done in Chapters 4 and 6. The Maze Lab and genomics core at Mt. Siani School of Medicine generously processed TRAP tissue and parsed RNA-seq reads for chapters 4 and 5. The Jordan Lab taught me how to make hormone pellets and provided the pellets and testosterone used in chapter 5. Finally, Dr. Sandra O'Reilly ran mice through metabolic cages quantified in chapter 6. In addition, the floxFosB line, floxedAR line, and Rosa26L10-GFP were all generous donations gifted to AJ Robison from Drs. Eric Nestler, Aritro Sen, and Gina Leinninger, respectively. All of these faculty contributed to experiments described herein.

TABLE OF CONTENTS

LIST OF TABLES

LIST OF FIGURES

CHAPTER 1: INTRODUCTION

Note: Some content was concerning the stress response and immediate early genes was previously published in Kwiatkowski et al., 2019, and Manning et al., 2017

Author contributions for Kwiatkowski et al.

Wrote the paper: Kwiatkowski, Manning, Eagle, Robison

Author contributions for Manning et al.

Wrote the paper: Manning, Williams, Robison

Depression Overview

Depression is a highly prevalent disease state, affecting 6-20% of the US population [1-3]. This disease manifests in many mood disorders classified by the DSM-V, the most prominent being Major Depression Disorder (MDD). Although initially this disease state was described as melancholy [4, 5], referring to a persistent low mood, this description has been refined over time and subdivided into a number of distinct syndromes. There are no specific biomarkers for a depressed state or MDD, although several SNPs or genetic mutations are associated with an increased probability for major depression disorder [6, 7]. Thus, mood disorders are primarily diagnosed by psychiatrists interacting with individuals and their own report of their psychological symptoms. Major depressive disorder (MDD) is classified by exhibiting two episodes of depressed mood and/or loss of pleasure in life activities for two weeks at a time, coupled with an additional five out of a potential nine symptoms. These include experiences such as: depressed mood throughout the day, diminished interest in life activities, changes in weight, sleep, or motor behaviors, loss of energy, feelings of guilt, diminished ability to concentrate or make

decisions, or suicidality [8]. These diagnostic criteria are oftentimes comorbid with other serious medical problems including other psychiatric conditions like substance use disorder, PTSD and anxiety disorders [8, 9].

The first line of treatment for patients suffering from MDD is Selective Serotonin Reuptake Inhibitors (SSRIs) which block serotonin transporters to increase serotonin levels in the synapse [10-14]. Other pharmacotherapies include other selective catecholamine reuptake inhibitors, monoamine oxidase inhibitors (MAOis) to reduce the enzymatic breakdown of monoamines like dopamine and serotonin, and more recently, atypical rapidly acting antidepressants derived from ketamine which presumably act on specific glutamate receptors [14, 15]. Although SSRIs act acutely for this physiological effect, several weeks of treatment are needed to observe their antidepressant effects, and they are only effective in up to 40% of patients [16]. The time course of these treatments suggests that relief from MDD symptoms comes from changes in persistent signaling mechanisms between neurons, rather than from acute changes in catecholamine signaling that occur within minutes of the first SSRI dose [14].

MDD diagnoses are frequently precipitated by chronic or traumatic stress, including environmental and interpersonal stressors, further implicating long-term changes in neuroplasticity underlying this disease [17]. However, an estimated 85 percent of people will be exposed to a traumatic event throughout their lives and only a subset of individuals who undergo similar stressors succumb to depression [18, 19]. Thus, some individuals are more susceptible to stress, and these individual differences in responses to stress may be due to differences in basal neurobiology or neuroadaptations to stress.

One critical difference of note is that *women in the United States are twice as likely to be diagnosed with MDD compared to men [1]*. This gender disparity in diagnostic rates may be due to cultural contributions, including gender biases against seeking help or acceptance of negative feelings [20, 21]. However, depression in women more frequently diagnosed than in men across the world [2, 3], and both human and animal model basic science has revealed sex differences in brain regions and molecular pathways central to mood disorders [22-24], indicating that biology may underlie, in part, the disparity in diagnostic rates. To this end, the contributions of the organizational effects of sex chromosomes and sex determining genes are unclear, although circulating hormones may play a role. Women's diagnoses with mood disorders are often concordant with changes in their reproductive status including puberty, postpartum, menopause, and menstruation [25-29]. In addition, in a meta-analysis, men who suffered from MDD experienced significant reduction in their symptoms with treatment by testosterone [30]. Taken together, these data suggest that gonadal hormones in both men and women can regulate depression symptoms.

Despite these correlations, the causal biological underpinnings of depression are not well understood. Access to human brain tissue is limited to imaging studies and postmortem samples. Therefore, to uncover the neurobiological substrates of depression researchers have developed several preclinical models using rodents. Although unable to communicate feelings and impressions, rodents in preclinical models of mood disorders have stress-induced behaviors which mimic many facets of MDD, including changes in weight, anhedonia, social withdrawal and related anxiety behaviors. These allow

scientists to assay neurobiological changes associated with stress-induced behaviors and therefore depression-like symptoms.

Preclinical Models of Depression

There are many rodent manipulations which model various aspects of mood disorders resulting in differing levels of pharmacological, face, and etiological validity [31]. These models include breeding lines predisposed to behavior deficits, application of acute stressors, and exposure to chronic stressors [32]. Paradigms inducing a stress-based depression-like phenotype include experiences like: injections of glucocorticoids, restraint, social isolation, tail suspension, foot shock, forced swim, application of ether, predator odors, early life stresses, and variations of social subjugaton [33-45]. Chronic social defeat stress (CSDS) emerged as a robust model as it displays face, etiological, and pharmacological validity for MDD in across many rodent species [35, 46-50]. Social subjugation displays etiological (i.e. construct) validity as it is a form of social stress which occurs naturally in territorial rodents and is considered analogous to social stressors experienced by humans that can precipitate MDD in some individuals [51, 52]. Some rodents that undergo CSDS show reduced sucrose preference and increased social withdrawal compared to nonstressed animals, clear reductions in previously pleasurable behaviors that mimic anhedonia in MDD patients. As in humans, some mice are resilient to CSDS, displaying no anhedonic behaviors, indicating face validity for the varied nature of stress outcomes [46, 49, 53]. In addition, chronic (but not acute) application of antidepressants like imipramine and fluoxetine is sufficient to reverse the behavioral phenotype elicited by CSDS [53, 54], again mimicking the human condition, wherein the

same compounds require weeks of administration to have antidepressant effects. Because CSDS displays multiple forms of validity as a model of MDD, there is enhanced confidence in the translational potential of CSDS based findings. However, there are two major caveats of this method. The first is that behavioral phenotypes arising from social subjugation paradigms cannot be divorced from the physicality of subjugation [38, 55]. It is possible that the physical encounter itself, which often results in wounding, could drive subsequent behaviors. The second major caveat is that social subjugation relies upon territorial aggression which is not normally displayed by or toward females in polygynous breeding species [56], including common lab mouse strains of *mus musculus* like C57 and CD1. This means that in rats and mice, the canonical CSDS model cannot be applied to females and precludes the generalization of findings of CSDS-induced behaviors to females. This echoes a larger issue in biomedical research, in which male studies outnumber female studies 5.5:1 [57]. This is highly problematic as women, typically aligned with female sex, are more likely to experience depression compared to men (see above) and are not represented in this otherwise robust preclinical model.

Chronic Stress Models for Both Sexes:

Several research groups have adapted the CSDS paradigm to elicit female mouse and rat subjugation. These models include the use of maternal aggression in lactating dams [42], manipulation of sensory cues [58], directly manipulating aggression circuitry to elicit aggression [37, 59], vicarious experiences of CSDS [39], or threat against a mated pair [60]. These paradigms allow the dissection of facets of CSDS experience: whether it is intrasexual aggression, aggression by a male, and/or effects of the etiologically relevant aggression. Although these modified CSDS paradigms undoubtedly contribute new

knowledge about female subjects of aggression, the confounding differences in experimental design prevent direct comparisons to previous male CSDS research. In addition, these manipulations are novel, resource intensive, and provide mixed behavioral outcomes. Most female subjection paradigms were published in the last five years, have not yet been reproduced, and social withdrawal is not elicited in all models, which complicates interpretation of the findings of these studies.

Other groups have utilized chronic unpredictable stresses (CUS), which is a general term for an array of experimenter administered interventions which can elicit behaviors related to mood disorders in adult animals of both sexes [61]. The variable (i.e. unpredictable) nature of the stresses prevents the habituation to a single chronic stressor and allows for the assessment of the neurobiological consequences after an amalgamation of stressful experiences. These paradigms are variable in length and content and include some combination of the following stressors: restraint on laboratory shakers, noise exposure, foot shocks, tail suspension, social isolation, and social subjugation [44, 45, 62]. Unlike CSDS, CUS paradigms allow the inclusion of both sexes in studies, thereby acutely addressing the disparity of females in preclinical research [57]. Among the variations of CUS is subchronic variable stress (SCVS), an abbreviated paradigm originally published in 2015 [63]. SCVS includes six days of stress and results in decreases in animals' preference for sucrose, increases in latency to feed in the novelty suppressed feeding task, increased circulating corticosterone, and reduced time spent auto-grooming following stress. These results are interpreted as indications of anhedonia, anxiety, HPA axis activation, and reduced self-soothing behaviors. Critically, this suite of stress-induced behaviors was *only observed in females*, while males were resilient to such stress-

induced behaviors. The SCVS paradigm has been replicated in several labs since its inception [64, 65]. SCVS represents a high-throughput method to recapitulate the gender difference seen in human MDD symptoms. Thus, SCVS is an attractive paradigm to study potential sex differences in the neurobiology of stress-induced behaviors.

Stress response

Many different preclinical models of depression rely upon stress to elicit their effects. Stress as a concept was articulated by Hans Selye as the nonspecific response of the body to adapt to perturbations in its environment [66]. This core idea, that environmental stimuli elicit adaptive responses, has evolved into an understanding of the acute effects of arousing stimuli and how the body utilizes homeostatic feedback to return the body to baseline. The process is present in rodents and humans and is termed the stress response.

The stress response is a two-step, interconnected system involving the Autonomic Nervous System (ANS) and the hypothalamic pituitary (HPA) axis. The ANS is a subsystem of the peripheral nervous system composed of the sympathetic and parasympathetic components which act in physiological antagonism to escalate and deescalate the immediate stress response [67]. The sympathetic nervous system, in particular, prepares the body to respond to acute stressors by mobilizing peripheral systems to engage in the classic "fight or flight" response by increasing oxygen and blood flow throughout the body and concurrently suppressing functions less essential to immediate survival (e.g., digestion) [68]. When the acute stress response is over, the parasympathetic nervous system aids in the return to baseline function [67], activating

the systems important for long-term survival. In tandem, the HPA axis also mobilizes to modulate the central nervous system (CNS) and PNS response using circulating hormones to communicate across the entire body. The HPA axis ultimately stimulates the production of glucocorticoids (e.g. cortisol in humans) in the periphery, which can coordinate a number of brain and peripheral systems to continue the stress response, including increasing metabolism to provide energy through glucose production. Notably, the HPA axis responds over a slower time course than the ANS, with the duration of its acute effects progressing during the hour following the onset of an acute stressor [69, 70]. Thus, the stress response involves a dramatic shift in physiological function that extends well beyond the experience of the initial stressor.

Acute stress modulation involves a rapid evaluation of stimulus and context before influencing the interconnected systems of the ANS and HPA axis. This is not to say the ANS and HPA axis are static under normal conditions; even common events in the environment elicit responses. However, frequent and extreme disruptions in the normal function of stress coping mechanisms can cause prolonged dysregulation of these systems. It follows that dysregulation manifests in a reduced ability to correctly identify and contextualize potential aversive and rewarding stimuli. Of particular risk is the HPA axis due to the prolonged nature of its signaling cascades, as the HPA axis mobilizes to modulate protracted stress responses using stable and widely circulating hormones to communicate across the brain and body over a prolonged period of time [69-73]. Thus, the HPA system provides both a shift in physiological function that extends beyond the stressor and a nexus by which to alter stress modulation circuitry.

In view of the relationship between the ANS and HPA axis, mobilization of the HPA axis is centrally mediated by many of the same regions responsible for activating the autonomic stress response [74]. Specifically, the hypothalamus, a ventral brain structure, initiates a neuroendocrine signaling pathway that begins with the release of corticotropin-releasing hormone (CRH, also known as corticotropin-releasing factor CRF) release. CRH diffuses through the adjacent portal system of the anterior pituitary to stimulate adrenocorticotropic hormone (ACTH, also known as corticotropin) release into the peripheral bloodstream [75]. As ACTH circulates throughout the body, plasma ACTH stimulates the adrenal glands to secrete glucocorticoids into the bloodstream. Glucocorticoids then circulate to targets all over the body to serve as a primary regulator of the stress response and prepare the body to better respond to future stress [76, 77]. The role of glucocorticoids is not fully understood, but is generally dependent upon where the target organ is and glucocorticoid concentration [77]. Glucocorticoids potentiate the ANS response in some cases and inhibit the overall stress system in others [70]. For example, glucocorticoids increase cardiac output in response to general stressors, but inhibit the stress response during hemorrhage in order to prevent vasoconstrictive stress hormones from overcompensating and stopping the heart [77]. Glucocorticoids are also critical for providing negative feedback to the hypothalamus and anterior pituitary to suppress the secretion of stress hormones. As such, interruptions of glucocorticoid signaling can dramatically affect the entire process of the HPA axis.

Corticosteroid receptors:

Glucocorticoids primarily exert their actions through two receptors: the mineralocorticoid receptors (MR) and glucocorticoid receptors (GR). MRs will bind to several corticosteroid

hormones with regularity and are considered activated under baseline conditions; though they are protected from excessive glucocorticoid stimulation through enzyme activity. In contrast, the GR is more selective for glucocorticoids and can be stimulated through elevated glucocorticoid concentrations [78]. Both of these receptors canonically exert their effects through genomic mechanisms: binding to their ligands and translocating to the cell nucleus to alter gene transcription [76, 79]. As such, prolonged exposure to glucocorticoids can dramatically impact systematic health and contribute to the pathophysiology of stress vulnerability.

Indeed, measurements of peripheral cortisol levels and GRs under baseline or stress conditions collectively indicate that individuals suffering psychiatric disorders associated with stress have altered HPA activity. Individuals suffering from unmedicated depression have elevated baseline cortisol and reduced numbers of peripheral GRs [80-82], indicating that there is reduced efficacy of glucocorticoids on their receptors, which is thought to be causal in at least some forms of depression. In contrast, individuals suffering from PTSD have normal or lower baseline cortisol [83], and normal pituitary and adrenal function [84], but peripheral GRs are more reactive to cortisol [85], indicating heightened reactivity under normal conditions. In anxiety disorders, which are often concomitant with both depression and PTSD, the relationship to HPA axis activity is less clear. Anxious persons may have slightly elevated cortisol at baseline and increased cortisol during exposure therapy sessions may facilitate a reduction in anxiety, such as in phobia extinction, but these results are not significant in meta-analyses [86, 87]. Taken together, this suggests that common maladaptive HPA activity in humans may be ascribed in part

to differences in GR reactivity to traumatic or prolonged stresses evidenced by changes in GRs in the periphery.

However, the principle mechanism by which cortisol exposure induces maladaptive responses to stress is by changing the brain. When GRs expressed within the HPA axis are bound, they result in a negative feedback cycle which attempts to return the body to normal function. However, other brain regions whose connectivity underlie reward-related processing and behaviors are also enriched for GR expression in mammals [88, 89], and thus are also sites of cortisol action. Although acute stress exposure can render the body capable of more quickly responding to threat, chronic stress can have deleterious consequences at the cellular level in these regions. Research in animals indicates that chronic stress results in cognitive impairments and less regulatory control over the stress response, likely via changes in neural function (I.e. neuroadaptations) driven by chronic activation of GRs in these areas [77, 90, 91], and such changes are considered the initial mediators of stress susceptibility.

Limbic Circuitry and Stress Behaviors:

Stress-induced behaviors (some of which are associated with a depression-like phenotype) are inextricably tied to the limbic system of the brain. The limbic circuitry is a number of brain regions whose connectivity underlie suites of natural and maladaptive reward-related processes and behaviors [92, 93]. These regions were initial identified by James Papez, and refined by Paul MacLean, and include the hippocampus (HPC), prefrontal cortex (PFC), basolateral amygdala (BLA), nucleus accumbens (NAc), and ventral tegmental area (VTA) (Fig 1) [94, 95]. Since depression is commonly characterized by decreased mood, social withdrawal, and anhedonia, this points to

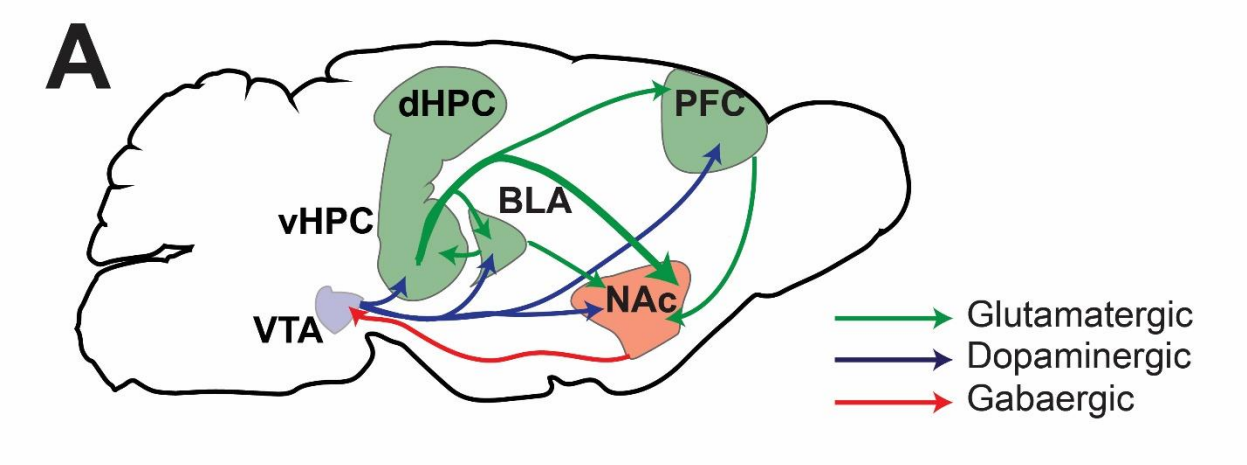

Figure 1 | Limbic Circuitry Connectivity (A) A schematic of the limbic circuitry. VTA sends dopaminergic (blue) projections to the vHPC, BLA, NAc and PFC. The NAc integrates both dopaminergic (blue) and glutamatergic (green) inputs from BLA, PFC, and vHPC, all implicated in affective states.

deficits in reward processing, perhaps through neuroadaptations which prevent normal limbic function. In addition, several of the limbic regions also express enhanced GRs, thereby positioning the limbic circuitry at the nexus of maladaptive stress responses and depression symptoms. Examining stress-induced alterations in limbic circuitry in conjunction with stress-induced behaviors in rodents provides a neurobiological model for the divergent behavioral responses to stress in humans: susceptible and resilient phenotypes. Understanding these behavioral responses in rodents will increase understand of the biological underpinnings of depression symptoms.

Mesolimbic Dopamine and the NAc

One of the core facets underlying both natural and maladaptive reward behavior is the mesolimbic dopamine system. The Ventral Tegmental Area (VTA) is one of two canonical sites of dopamine synthesis in the brain. The VTA is made of primarily dopamine producing neurons, with minority populations of inhibitory and excitatory neurons. The

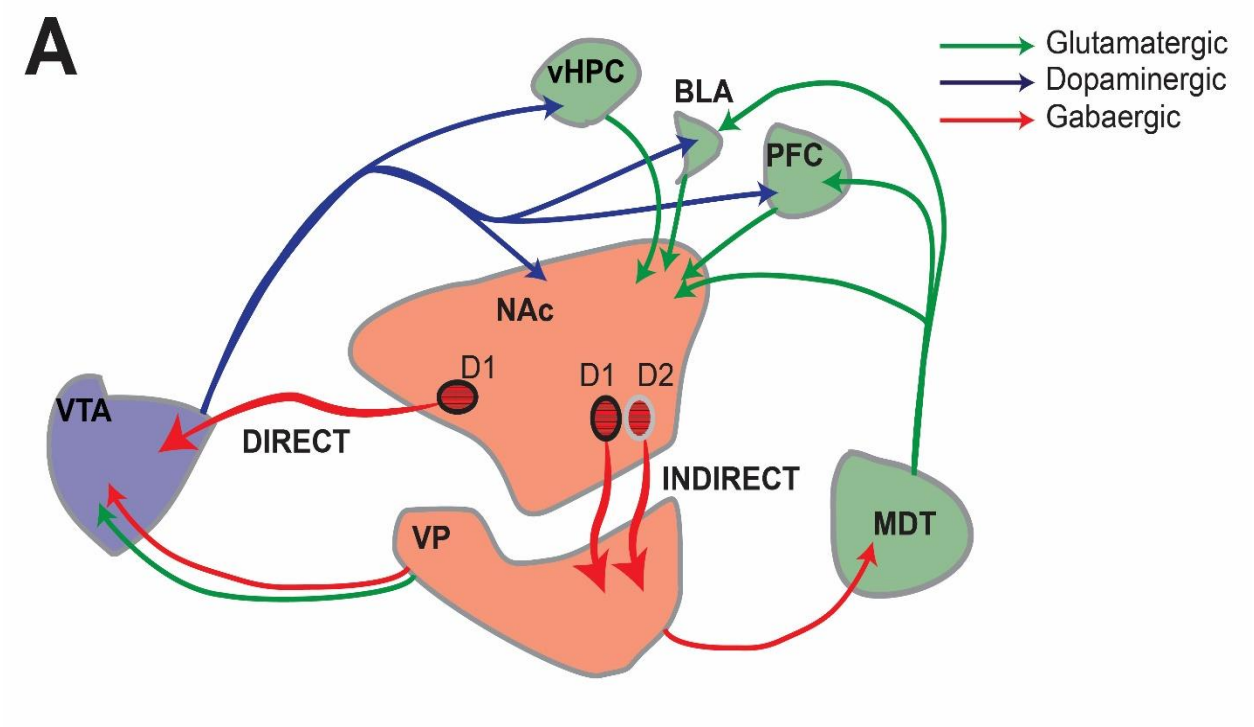

Figure 2 | NAc connectivity underlying motivated behavior. (A) A schematic of NAc's innervation and projections which drive to motivated behaviors. Both dopaminergic (blue) and glutamatergic (green) inputs converge on γ-aminobutyric acid (GABA) expressing medium spiny neurons (MSNs) (red) in the NAc. NAc MSNs project to the VTA either directly (mediated by D1 expressing MSNs) or indirectly (mediated by both D1 and D2 expressing MSNs) through intermediary Ventral Pallidal (VP) neurons. VP activity also reduces glutamatergic tone on NAc through intermediate projections to the Mediodorsal Thalamus (MDT).

VTA sends dopaminergic projections across the brain, primarily to the frontal cortex (mesocortical projection) and the NAc (mesolimbic projection)[92].

Dopamine release in NAc acts upon multiple populations of NAc neurons. The majority of NAc neurons are termed dopamine receptor D1 (D1) or dopamine receptor D2 (D2) medium spiny neurons (MSNs) for the near mutually exclusive nature of D1 vs D2 receptor expression [96]. MSNs are the largest cell population of the NAc, accounting for 95% of neurons and rendering the structure a prominent site of dopaminergic action [97]. Dopamine receptors are heterotrimeric G-protein coupled receptors, and their underlying

differences in function are a direct result of the specific coupled Gα subunit. D1 receptors are Gαs are coupled, and therefore the binding of D1 receptors causes activation of adenyl cyclases, leading to the production of cAMP, phosphorylation of PKA, and ultimately increased excitatory responses to glutamate [98-100]. Conversely D2 receptors are Gαi coupled resulting in the inhibition of adenyl cyclases, reduction of PKA phosphorylation, and subsequent reduced excitability of D2 MSNs in response to glutamate [100-102]. Thus, MSN responses to dopamine are reflected by the form of dopamine receptor they produce.D1 and D2 MSNs in the dorsal striatum constitute separate populations and distinct projection targets, with D1 MSN connectivity leading to the disinhibition of thalamus and subsequent behavior, (i.e, the “direct” pathway) and D2 MSNs forming the “indirect” pathway through ultimately decreasing thalamocortical drive. However, this rigid functional segregation of MSNs does not hold true for NAc [103, 104]. NAc MSNs project to the VTA either directly (mediated by D1 expressing MSNs) or indirectly (mediated by both D1 and D2 expressing MSNs) through intermediary Ventral Pallidal (VP) neurons (Fig 2) [104]. The direct projections from NAc to VTA synapse on cells dependent on anatomical location [105], which cause changes in dopaminergic signaling sufficient to drive changes in motivated behaviors[106, 107] [108]. The dorsal striatal indirect pathway canonically has a directly opposing role, but again, this is less clear in the NAc. For example, both D1 and D2 MSNs of the indirect pathway can disinhibit thalamic neurons to drive behavior through the activity of downstream inhibitory VP neurons (Fig 2) [104, 109, 110]. In addition, both D1 and D2 MSNs engage excitatory and inhibitory VP neurons which in turn project to VTA. Most VP projections to VTA are inhibitory and can either directly impede dopamine release or facilitate the process

through disinhibition, while glutamatergic VP to VTA activity is uniquely implicated in aversive states [111]. D2 neuronal activity is associated with sensitivity to aversive states [112-115] and almost half D1 MSNs project to VP where they instead implicated in rewarding states [104, 113]. Taken together, this suggests that while the indirect pathway in reward is complex, its activation reinforces affective state behavior based on the identity of the intermediate VP neuron [111]. To that end, dopamine release in the NAc stimulates the direct pathway and a subpopulation of the indirect pathway, leading to disinhibition of VTA dopamine neurons (direct pathway) and prevention of inhibition (indirect path). Thus, VTA dopamine contributes to reward behaviors through the downstream connectivity of its NAc projections.

Dopamine release in the NAc is critical for reward processing, both for natural and synthetic rewards [116]. It follows that deficits in reward behavior (i.e. anhedonia and social withdrawal) can be attributed to changes in this pathway. Indeed, CSDS can alter this circuit [46, 117, 118] to change both neuronal activity after stress and patterns of gene expression. These neuroadaptations result in reduced reward behaviors like social interaction and sucrose preference (proxies for withdrawal and anhedonia) while increasing despair behaviors such as latencies to immobility in the forced swim or tail suspension test (in some ways modelling despair or suicidality). Thus, there is direct evidence for contributions of the mesolimbic dopamine pathway to stress behaviors through its release onto the NAc.

The NAc is a complex site of motivational processing and this is evident in both its structure and neuronal inputs. The NAc is subdivided into core and the shell regions and is cellularly heterogenous in that D1 and D2 MSNs are intermixed throughout the

structure. The core surrounds the anterior commissure and is more mediodorsal, while the shell encompasses the core and extends laterally. These anatomical distinctions correlate with differential contributions to reward related behavior. For example, approaches to rewarding stimuli are mediated through the core [119-121], while implementing learned behavioral flexibility utilizes the shell [122, 123]. The contributions of anatomical location and MSN subtype to specific behaviors such as anhedonia and social withdrawal are still unclear. However, D1 shell neurophysiology and gene expression changes in response to CSDS, while D2 neurons in the shell do not respond in the same manner [45, 114, 124-126]. This implies that stress effects on the direct and indirect pathways differentially contribute to suites of stress-induced behavior.

Chronic stress experiments, including those of physiological manipulations and post-stress tissue collection described above, elucidate some of the neuronal mechanisms of behavioral responses to stress. However, as there is individual variability in stress behaviors [53, 127], assessment post-stress precludes information of the neuronal mechanisms which *establish* susceptible or resilient phenotypes. Thus, although the phenotypic variation undoubtedly depends upon intrinsic differences between individuals, the technical difficulties associated with within-subjects experimental designs for brain function impede studies on the prevention of stress susceptibility. In other words, it is not currently possible to biopsy brain regions for molecular analysis both before and after stress in the same animal without directly affecting the animal's behavioral response. Current work hypothesizes that mechanisms of susceptibility may be uncovered by observing NAc neuronal activity under baseline and stressed conditions through *in vivo* fiber photometry. This work suggests resiliency to social withdrawal is associated with

basal increases in D1-MSN activity in response to rewarding stimuli, although these methods rely upon the identification of MSNs for their conclusions [128]. This paves the way for future studies to examine preventative interventions, perhaps priming resilient stress responses in otherwise vulnerable populations. However, the NAc is a complex site of reward processing and the various contributions to baseline MSN activity are not yet fully characterized.

This lack of understanding is magnified because the NAc receives more than dopaminergic input from the VTA. The NAc receives numerous glutamatergic inputs from a diverse set of brain regions which include, but are not limited to, the Prefrontal Cortex (PFC), Basolateral Amygdala (BLA), and Hippocampus (HPC) [129, 130]. These inputs can synapse throughout the core and shell on D1 and/or D2 MSNs [130]. While the BLA and PFC afferents bias for the core, the HPC biases for projections to the NAc shell and contributes the majority of glutamatergic inputs to the NAc [130]. This complex integration of glutamate and dopamine signaling undoubtedly contributes the susceptible or resilient phenotypes following stress, but the nature of each circuit and their interactions are only now being probed. The glutamatergic inputs from each of these limbic regions may provide differential information about the experience of stress to drive different behavioral aspects of susceptible and resilient phenotypes.

BLA

The BLA is a highly heterogenous brain region which is important for assigning and integrating valence to stimuli [131, 132]. The BLA has been classically associated with fear and aggression, and the view that BLA contributes to processing of both negative and positive valenced experiences is relatively recent. BLA is also a site of HPA axis

integration and particularly well known for its role in fear memory and anxiety behaviors [133, 134]. However, BLA projections to NAc increase reward behaviors, and this requires HPC activity [135-137]. This suggests the HPC in gating BLA-NAc connectivity, potentially through monosynaptic HPC connections to BLA [138]. In addition, vHPC and BLA are both implicated in aspects of contextual fear learning which supports the role of vHPC-BLA regulating both rewarding and aversive stimuli [139]. However, BLA also has reciprocal projections with the HPC itself [140, 141], and these projections have functional relevance in the context of chronic stress. Decreasing the activity of BLA inputs to the HPC drives basal pro-social behaviors [142] and anxiolytic behaviors [143]. Unlike other neurons in the BLA, BLA-HPC neurons do not encode valence [144]. This indicates that increased activity of these projections prevents exploratory behaviors. After stress, these BLA-HPC neurons become enlarged and correlate to anxiety behavior [145]. This suggests that BLA-HPC neurons don't encode valence, but rather drive stress-induced neophobia. Conversely, glutamatergic vHPC-BLA projections are critical for the long-term generalization of fear learning, but not short-term generalization nor behavioral responses to immediate noxious stimuli [146, 147]. Together this suggests vHPC-BLA circuits may contribute to affective memory reconsolidation.

PFC

The PFC is located in the anterior cerebrum and contributes to the explicit monitoring of behaviors to achieve goals (i.e. executive function). The medial PFC (mPFC), known for its role in behavioral inhibition and regulation of reward behavior, is subdivided into the infralimbic (IL) and prelimbic (PrL) cortices, and these are anterior to the orbitofrontal cortex (OFC) [148]. Afferents from these subdivisions of the mPFC are biased toward

different subregions of the NAc: the IL preferentially synapses in the shell while PrL tends to synapse in the core [149]. mPFC afferents to NAc contribute to goal-directed behaviors, particularly behavioral initiation, and their neuronal activity are thought to be gated in part through HPC and BLA inputs onto the PFC [150-152]. Thus, both the BLA and PFC can contribute to reward behavior through their projections to NAc, but these are modulated by the HPC.

Hippocampus

The hippocampus is a bilateral "c"-shaped brain region located in the medial temporal lobe. The hippocampus has been well known for its role in rodent learning and memory since the 1960s, and its translational relevance to human memory has been directly confirmed by human lesion case studies [153-155]. The human HPC and rodent HPC are differentially oriented, although they occupy similar locations in the brain (Fig 3). The human HPC is rotated about 100 degrees compared to the rodent hippocampus and the anterior human HPC correlates the caudal/ventral aspect of the rodent HPC. HPC in rodents is critical for the integration of encoding and consolidation of memories (i.e. integrating external stimuli and proprioceptive information of an experience for future recollection), especially spatial memories [156, 157]. The HPC has a well-known role in declarative and episodic memories in humans [158], and a current hypothesis is that the hippocampus integrates stimuli and context, while other medial temporal cortices specifically identify item information and context information [159-161]. To that end, the molecular underpinnings of hippocampal memory formation have been extensively studied in rodents. Memory processes engage the neuroanatomy of HPC on a molecular level to facilitate memory formation and reconsolidation.

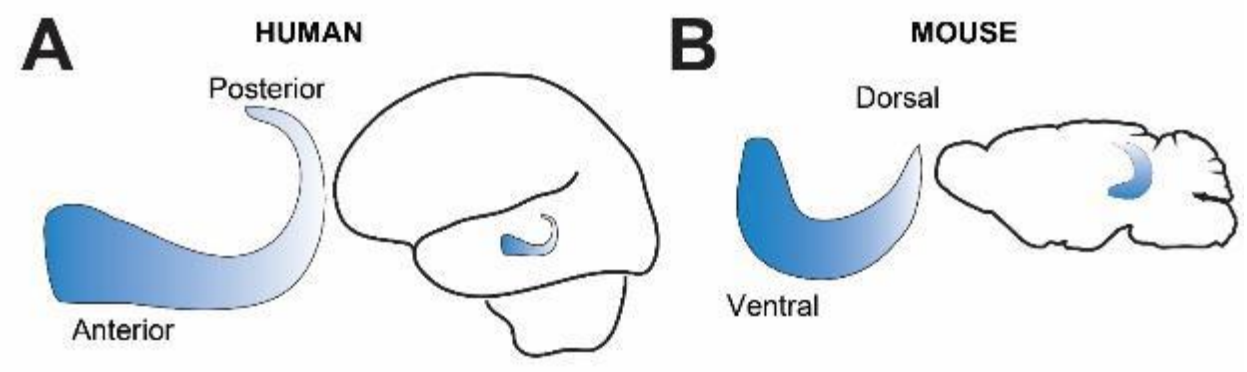

Figure 3 | Homologous hippocampal morphology between species. (A) A schematic of the human hippocampus morphology and its placement within the brain, compared to the mouse hippocampus shown in **(B).**

Neurophysiology of Memory

The HPC has three robust cell layers, the anatomical basis of the trisynaptic circuit of information flow. Glutamatergic inputs (termed the perforant pathway) enter the HPC from the entorhinal cortex of the medial temporal lobe and synapse in the dentate gyrus (DG). Axons from DG neurons form dense projections termed mossy fibers to the cornu ammonis 3 (CA 3). CA3 axons form Schaffer collaterals which then project onto the neurons of CA 1, which then commonly synapse onto subiculum, the primary output structure of the hippocampus projecting back to the entorhinal cortex. The neurons in this pathway are almost all glutamatergic, and therefore are activated in a feedforward loop following an experience or stimulation [162, 163]. As a result of stimulation, these synapses can undergo activity-dependent changes in postsynaptic strength [164, 165]. Individual experiences will engage unique patterns of neurons within these cell layers (i.e. a memory trace or engram), and with repeated engagement this will result in long-term changes in these specific neurons to causes the consolidation of a memory [166].

The strength of concordant neuronal activity in the memory trace is a physiological correlate of the strength of the memory. Changes in the synchronicity or relative frequency of activation of the memory trace elicit changes in the synapses among these neurons through morphological changes at the synapse or adaptations of their expressed receptors [167-169]. Thus, plasticity of the synapse plays a critical role in memory trace maintenance and is a mechanism for memory consolidation. Synaptic plasticity comes about through a two-phase process. The early phase involves acute changes in receptor activity and availability. The late phase stabilizes and maintains the acute change in synaptic plasticity via alterations in gene expression and protein synthesis [170, 171]. Synaptic plasticity can be bidirectional, either enhancing the memory trace through the potentiation of a synapse (LTP) or weakening the memory trace through long term depression (LTD) [172].

Long term potentiation (LTP) is the process by which two neurons strengthen their connectivity at the level of the synapse after prolonged or enhanced stimulation. These changes can be long lasting, existing on the order of hours and even days. LTP requires changes in postsynaptic neuron signaling cascades. These changes are dependent on expression of specific postsynaptic receptors. In glutamatergic synapses, glutamate release from the presynaptic neuron will bind to its ionotropic receptors, a-amino-3-hydroxy-5-methyl-4-isoxazolepropionic acid receptors (AMPARs) and the LTP-critical *N*-methyl-d-aspartate receptors (NMDARs) [173, 174]. Only AMPARs pores will open in response to initial glutamate release and ligand binding, because the NMDARs have a Mg^{2+} ion preventing any ion flux. Open AMPARs allow sodium influx and subsequent depolarization of the membrane. The depolarization of the postsynaptic membrane then

relieves the Mg^{2+} block. This, in combination to ligand binding, enables the flow of calcium ions through NMDARs. Ca^{2+} is a complex intracellular signaling molecule, acting through many Ca^{2+}-dependent proteins including kinases and adenyl cyclases. A bolus of NMDAR-mediated Ca^{2+} influx increases both the number and function of AMPARs on the postsynaptic surface through insertion and phosphorylation, which occur independent of gene expression (early phase of plasticity) [99, 175, 176]. Ca^{2+}influx through NMDARs also leads to changes in transcription factor activity and subsequent gene expression which are required for the maintenance of long term memories (late phase of plasticity) [177-183]. Thus, glutamate signaling in hippocampal neurons can enhance future responses to glutamate through short and long term mechanisms and provides a mechanism for increased coordination between neurons.

Hippocampal LTD can also act through postsynaptic glutamatergic signaling cascades at Schaffer collateral synapses onto CA1 neurons. In contrast to the bolus nature of Ca^{2+} influx in LTP, CA1 LTD occurs through smaller influxes of Ca^{2+}. This typically occurs as a result of low-frequency glutamate release activating a smaller number of NMDARs and/or metabotropic glutamate receptors and recruiting Ca^{2+}-dependent phosphatases, all of which leads to the endocytosis of AMPARs. This results in the postsynaptic neuron's reduced ability to respond to future glutamate stimulation (early phase) [172]. Long term changes in gene expression are also necessary for prolonged maintenance of LTD (late phase) [184, 185]. The late phase of both LTD and LTP requires changes in gene expression [164, 186], and preventing either neuronal activity or late phase gene expression also prevents learning and memory[187]. A number of genes are activity-dependent (also known as immediate early genes: IEGs) and are stimulated by neuronal

activity. These IEGs mark activated neurons and are positioned to underlie the formation of late phase plasticity through changes in transcription, and some IEGs will be discussed in detail below. Changes in transcription provide a prolonged molecular mechanism for integrating the external stimuli and proprioceptive information of an experience required for the neurophysiological changes associated with memory consolidation.

Functional segregation of HPC:

Historically, the hippocampus was thought to be uniform in its function across the entire structure. The more rostral/dorsal (dHPC) aspects of the rodent hippocampus were robustly studied leaving the caudal/ventral (vHPC) aspects understudied (Fig 3B). Initial analysis hinting that the dHPC and vHPC may have differential functions arose in 1998, after 30 years of hippocampal study [188]. However, the hypothesis languished for a decade before its resurgence [189]. The functional difference hypothesis posits that differences in HPC function in non-affective and affective memories can be attributed the dHPC and vHPC, respectively. The dHPC, but not vHPC, is necessary for spatial and context learning tasks [190-192]. Conversely the vHPC has been implicated in behavior related to valenced memories and its associated context and cues [189, 193-197]. Thus, vHPC can integrate emotional valence with memory, like the negative associations of stressful events associated with an affective memory. This is supported by anatomical differences between the connectivity of dHPC and vHPC. The dHPC CA1 neurons project specifically to the dorsal subiculum (dSub) and subsequently the entorhinal cortex described in the trisynaptic loop [198]. In contrast, the vHPC CA1 (vCA1) and ventral subiculum (vSub) sends afferents to many other limbic structures. These afferents including reciprocal connections to BLA [199, 200], projections to PFC [151], and

particularly dense projections to the NAc [129, 130, 201], and projections that can indirectly influence the VTA through the lateral septum [202]. Because the vHPC afferents to limbic circuitry can convey some aspects of affective memories, they are poised to elicit subsequent behavioral responses to valenced stimuli. The vHPC CA1 glutamatergic cells projecting to NAc have emerged as a population of interest in driving reward behavior. VHPC-NAc neurons have baseline individual variability in excitability [127] and can also undergo activity-dependent synaptic plasticity [45] (described above) [45, 125, 126, 194]. Furthermore, changes in vHPC-NAc plasticity drive reward behavior [45]. This implicates long term changes in gene expression of vHPC afferents, required for late phase LTP, in driving stress-induced behaviors in response to chronic or traumatic stress, including those reward-related behaviors that define resilience and susceptibility to depression-like phenotypes.

Adult Neurogenesis:

A key contributor to hippocampal volume is adult neurogenesis, or the generation of new neurons. The DG contains one of the two canonical sites for adult neurogenesis in rodents: the subgranular zone (SGZ) [203, 204]; the other is the subventricular zone (SVZ) of the rostral migratory stream and olfactory bulb [205], although adult neurogenesis may occur at low levels in other brain regions [206]. Whether humans have adult neurogenesis is still a hotly debated topic. SGZ cellular proliferation does occur in humans, but the contention is whether this process continues into adulthood and results in integrated neurons [196, 207-210]. Within the SGZ of the DG are self-renewing neural stem cells. These stem cells can also proliferate through mitotic division and are not committed to neuronal cell fates and can generate either glia or neurons [203]. Some of

these cells will commit to a cell fate (i.e. fate specification) followed by migration out of the SGZ and into the granule cell layer. As the newborn neurons settle in new locations, they extend neurites and synaptically integrate with surrounding tissue. Throughout this process, they undergo proscribed patterns of gene expression as they move through each step until neuronal maturation, which typically takes several weeks [203, 211, 212]. Tracking the progress of RGC to mature cells is complicated by the self-renewing properties of RGCs and NPCs. However, mitotic cells can be marked *in vivo*, via the thymine analog 5-bromo-2'-deoxyuridine (BrdU), and examined for specific proteins to ascertain their stage of maturation, such as NeuN (Neuronal Nuclei, a protein expressed in mature neurons) or GFAP (Glial fibrillary acidic protein, a glial protein which marks astrocytes). This process of mitotic renewal and differentiation of new cells in HPC is necessary to maintain hippocampal volume in rodents [213]. Thus, appropriate adult neurogenesis perhaps plays a protective role stress associated volume loss in rodents and humans.

However, the role of adult neurogenesis in normal behaviors is still incompletely understood. Many, but not all, research groups see that increases in adult neurogenesis are concordant with improved cognition and performance on hippocampal-dependent memory tasks [214]. This is predicted to occur through synaptic plasticity of the memory trace. This suggests that adult neurogenesis facilitates learning and memory by providing new potential connections during an encoding of a changed aspect of the world. These new connections may be recruited by altered or novel stimuli and through synaptic plasticity form a discrete memory trace [215-217]. The existence of an increasing number of discrete memory traces may prevent the overgeneralization of behavior by facilitating

discrimination between stimuli. However, this may result in an unsustainable increase in metabolic load. A separate hypothesis suggests that increasing neurogenesis strengthens new memories at the expense of older memories and is essential in forgetting information [218, 219]. Nevertheless, increases in neurogenesis increase performance on pattern separation tasks, promote behavioral inhibition, and improve cognitive flexibility [220, 221]. Thus, proliferation of new neurons results in enhanced behavioral discrimination to contextual stimuli in non-stress contexts.

The role of neurogenesis in stress behavior has primarily been investigated independently of its contributions to cognition, especially since the contributions of neurogenesis to normal memory processes are still unclear. As rodents and humans who have been exposed to stress have reduced hippocampal volume and cognitive deficits, methods for increasing hippocampal volume have arisen as potential mechanism of stress intervention. The first evidence for this was correlational. For example, wheel running increases SGZ proliferation in rodents [222] and also ameliorates stress behaviors in rodents and is reputed to have mood lifting properties in humans [223-226]. In addition, antidepressants also increase neurogenesis [227, 228]. The most compelling evidence for the role of adult neurogenesis in stress resilience and depression is that two different classes of antidepressants require adult neurogenesis for their behavioral effects, and that adult neurogenesis is sufficient for antidepressant effects in rodent chronic stress models [229-231]. Furthermore, running and antidepressants have been reported to increase hippocampal volume in the humans, acting in part through cell proliferation [232-234]. This highlights a common mechanism of stress resilience in both rodents and humans. How increasing neurogenesis may specifically confer its antidepressant effects

is not fully understood, but it acts in part through inhibition of mature granule cells specifically in the ventral aspect of the HPC [235]. This indicates the function of neurogenesis in stress behavior is not consistent across the dorsoventral axis. Taken together, most data indicate that neurogenesis is protective against the deleterious effects of chronic stress both in terms of neuronal volume and stress-induced behavior, and this depends upon the discrete functions of the HPC dorsoventral axis.

Chronic stress and Hippocampal Neurophysiology:

The HPC has long been associated with emotional state and valanced behavior and intersects with the HPA axis [94, 95, 236, 237]. The HPC is enriched with both mineralcorticoid receptors (MRs) and glucocorticoids (GRs) [77], and is especially vulnerable to the adverse effects of stress [91, 236, 238]. In a healthy brain, stress-based activation of GRs leads to short-term reductions in neuronal excitability that are hypothesized to return the hippocampus to its baseline firing rate and protect information encoded during acute stress [239, 240]. This mechanism is critical for long-term memories in rodents and humans [241-243]. However, prolonged exposure to glucocorticoids results in impairments in hippocampal-dependent spatial memory performance [91], thereby weakening recall of contextual knowledge during stimulus processing. Underlying this spatial memory impairment are glucocorticoid-related functional and morphological changes in hippocampal neurons. For example, reductions in hippocampal activity associated with chronic, but not acute, stress result in changes in glutamatergic tone and impairments in LTP [91, 244-249]. During chronic stress, hippocampal cells also become more vulnerable to damage due to unsustainable demands on their cellular resources [239], and ultimately memories can also be

weakened [250]. Consistent with these findings, elevated glucocorticoid levels stemming from chronic stress are associated with atrophy of hippocampal neurons, such as retraction of dendritic processes and a general reduction in hippocampal volume in rodents, as well as reduced GR expression [90, 91, 251]. Importantly, structural differences in the hippocampus are observed in humans exposed to stress. For example, hippocampal volume is reduced in association with MDD or witnessing traumatic stress [252-255]. This suggests that stress can create risk for memory impairments and context generalization by affecting either synaptic plasticity and/or hippocampal cell number and health.

Transcriptional Responses to Stress and Antidepressants

Any experience results in some neuronal activation, the potential for memory formation, and behavioral responses. However chronic stressors are sufficient to elicit prolonged changes in function and/or plasticity in the suites of neurons involved in the memory of the stress, stress responses, and maladaptive reward processes, processes driven by long term changes in gene expression [228, 256-260]. Chronic stress produces changes in gene expression that can arise through a number of mechanisms, including through epigenetic modifications, noncoding RNAs, or activation of transcription factors [93, 261]. Humans that were depressed and died by suicide displayed robust changes in RNA profiles compared to non-depressed controls, and these changes were sexually dimorphic [262, 263]. This indicates that gene expression profiles linked to depression have natural variation between the sexes. Therefore, the molecular profiles associated with susceptible and resilient stress-behaviors could also be sexually dimorphic and this

may drive sex-specific pathophysiology of depression. These changes in gene expression in response to stress differ by brain region, as described below.

Hippocampus:

The hippocampus is particularly responsive to chronic stress paradigms and antidepressants. In rodents, chronic stress affects transcription to alter a number of systems including corticosteroid receptor production, monoaminergic signaling, and mediators of plasticity like cAMP (cyclic adenosine monophosphate, a intracellular second messenger) and ERK1/2 (extracellular signal–regulated kinases involved intracellular signaling to the nucleus) [41, 264-266]. Complementing these studies in rodents, depressed humans also had deficits in the plasticity mediators ERK1/2 and MAPK2 (mitogen-activated protein kinase kinase, an enzyme which phosphorylates ERK1/2) [267], kinases mediating pathways that converge on a decreased activation of the transcription factor CREB. Indeed, decreases in the expression of CREB are found following stress in rodent paradigms, which has been replicated in postmortem human brain [268, 269]. This indicates that CREB can modify suites of gene expression in the HPC after stressful experiences. Furthermore, antidepressant treatment increases this transcription factor, pointing to its bidirectional effects under stress/depression and antidepressant conditions [47, 270-272]. These gene expression changes in the HPC following stress contribute to changes in synaptic plasticity, neurogenesis, dendritic outgrowth, and spine formation, perhaps indicating the integration of gene expression and morphology changes [266]. As blocking transcription inhibits memory formation, this suggests that these changes in transcription underlie the memory trace of stress [164, 259]. These experiments were done primarily in males, but studies of both sexes suggest

sex differences in HPC stress neuroadaptations. For example, females have higher rates of basal vDG neurogenesis than males [273]. In addition, males, but not females, show increased dopamine metabolism following acute stress [274] and decreased corticosteroid receptors expression following chronic stress [275]. Taken together this points to differential, and possibly divergent, stress-induced molecular adaptations in the hippocampus between males and females.

VTA and NAc:

Much of the work underlying changes in gene expression following chronic stress has focused on the male rodent VTA and NAc. The VTA and NAc are robust mediators of reward behavior, and so deficits in these reward regions were explored in response to CSDS. These initially included assessment of whole tissue expression of specific genes associated with stress and maladaptive reward behaviors, like the CREB-dependent expression of BDNF(brain derived neurotrophic factor) and ERK, followed by microarrays of candidate genes including voltage gated potassium channels, glutamate receptors, and Ca^{2+} signaling molecules [46, 53]. The evidence indicated increased firing of VTA neurons elicited susceptible behaviors (i.e. decreased time spent with novel animals, decreased sucrose preference). Susceptible behaviors were reversed by the expression of voltage-gated potassium channels driving activity back down to baseline levels (an active mechanism of resilience). These changes in excitability were accompanied by epigenetic changes in many genes in whole samples of NAc [53, 118, 276, 277]. This implicates patterns of VTA and NAc neuronal excitability, driven by transcription, as mechanisms underlying various stress responses.

Other studies focused on the NAc specifically, looking at the patterns of activity-dependent gene expression after stress. This included the induction of IEGs. Although IEGs are markers of neuronal activity, IEGs can themselves be tightly regulated activity-dependent transcription factors [278, 279]. For example, the Fos family of transcription factors which include cellular oncogene fos(c-fos) and splice varients of the FBJ murine osteosarcoma viral oncogene homolog B (FosB) gene: FosB and ΔFosB can bind to DNA and alter gene expression (mechanism described in detail below) [280-287]. ΔFosB, but not FosB or c-fos, was differentially induced in the NAc following chronic stress and antidepressant treatment, and specifically changes in its expression within the NAc shell corresponded with stress resilience [284, 285, 288-290]. Furthermore, ΔFosB in the NAc intersects with Ca^{2+} signaling cascades through its phosphorylation by Calmodulin-dependent protein Kinase IIα (CaMKIIα). ΔFosB can also induce CaMKIIα gene expression, suggesting a feed-forward loop [291, 292]. As CaMKIIα is upstream of CREB activation, ΔFosB can affect downstream CREB activity, and CREB is necessary for FosB gene expression[293], suggesting another potential loop. CREB activation is critical in NAc shell for appropriate behavioral responses to affective stimuli [294, 295].

In addition to changes seen in transcription factors, CSDS also results in NAc epigenetic histone modifications (Hdac2 [53, 276], Cdk5 [296], SIRT1 [297]), DNA methylation (Dnmt3a [44, 63], Tet1 [298]), and microRNAs [299]. Although CSDS studies initially took a candidate-based approach, evidence for extensive changes in gene expression facilitated the use of unbiased transcriptional profiling following chronic stress. There are pronounced differences in the transcriptional signatures concordant with [300], and causative of [194], male susceptibility and resilience to stress in the NAc. Furthermore, in

SCVS paradigms which include female test subjects, there are sex differences the NAc transcriptomes [63] and mircoRNA networks [299] following stress which rely in part on gonadal hormone signaling [64]. This is consistent with the sex differences reported in female MDD transcriptomes and further supports sexually dimorphic pathophysiology of stress phenotypes.

These differences in transcriptome analysis, while informative, do not allow the functional segregation of D1 and D2 MSNs. The NAc's heterogenous nature prevents the attribution of molecular changes to either D1 or D2 neurons, perhaps even masking cell-type specific effects. Because D1 and D2 neurons are differentially implicated in stress phenotypes (see Reward Circuits above), some labs are using candidate-based approaches in male mouse models allowing individual manipulation and examination of D1 and D2 populations. This strategy revealed that increases in D2-MSN expression of the ion transporter Slc6a15 is pro-resilient following CSDS [301]. Conversely, CSDS stress-susceptibility is tied to dendritic atrophy of D1-MSNs through increased expression of the IEG Egr-3 and the GTPase RhoA and/or decreased expression of cell adhesion proteins like neuroligin-2 [124, 302, 303]. This suggests that patterns of gene expression directly contribute to the cell-type specific changes in NAc neuroadaptations which drive behavioral responses to stress. The IEG ΔFosB can be induced in both D1 vs D2 MSNs following stress but only ΔFosB expression in D1 MSNs is associated with stress resilience [304, 305]. This association was tested for causality through viral CRISPR-Cas9epigenetic regulation of the *FosB* gene in NAc MSNs. It was found that D1 enhancement of the *FosB* gene is pro-resilient, while enhancement in D2-MSNs is pro-susceptible, further indicating the importance of cell-type functional transcriptome

regulation in stress-induced behavior [287].Thus, the HPC and NAc undergo robust changes in gene expression following chronic stress, and there are sex differences in gene expression in both human and rodent brains following MDD or its preclinical models. As the human disease state shows robust gender differences in diagnostic rates, it is possible that sexually dimorphic patterns of gene expression after chronic stress may be the biological underpinning of this health disparity. Given the HPC's role in memory formation, increasing HPC volume, and the stress response, further study of the sexually dimorphic long-term transcriptional underpinnings of neurogenesis, learning and memory, and stress behaviors is warranted. In particular, the vHPC is a site of integration of the HPA axis, affective memories, and reward behavior and sends the strongest glutamatergic projections to the NAc. vHPC-NAc neurons show individual basal differences in excitability which could contribute to individual differences in stress susceptibility or behavioral resilience through their connectivity in the NAc [127, 128]. Although several studies have examined vHPC-NAc activity and plasticity in the context of chronic stress [45, 127], changes in gene expression of this neuronal population have not been studied. Thus, in my thesis I sought to characterize how long-term changes in transcription may underlie stress vulnerability in male and female mice. To this end I utilized the chronic activity dependent IEG ΔFosB to examine how long-term changes in gene expression affect stress susceptibility.

ΔFosB:

ΔFosB is an IEG previously implicated in both dHPC learning and memory processes and in the NAc for behavioral responses to stress [287, 305, 306]. ΔFosB is a member of the Fos family of proteins, and it results from splice variation in the *FosB* gene resulting in a

premature stop codon and truncation of a large portion of the c-terminal transactivation domain ([280] and Fig 4A). This truncation removes a ubiquitination site in the c-terminus, reducing ΔFosB targeting for degradation [307]. Thus, while other Fos proteins have half-lives of hours, ΔFosB has a prolonged half-life, up to a week *in vivo [308]*. This splice variant is also non-preferred and thus is induced at low levels basally [309]. This combination of prolonged half-life and low induction rate provides a mechanism to reflect chronic stimulation and allow ΔFosB to accumulate in cells with prolonged activation, making it a marker of chronic activity.

In order to bind DNA and alter transcription, ΔFosB forms a variant of the activator protein 1 (AP-1) complex in conjunction with its canonical binding partner JunD ([280, 310] and Fig 4B). These proteins dimerize along leucine-rich zipper regions leaving positively charged residues outside of the zipper. This forms a basic loop helix loop configuration transcription factor wherein the basic residues interact with DNA [310]. The interactions between ΔFosB and DNA promote transcriptional activation at some genes, while other genes are repressed by ΔFosB [281, 307, 311]. The downstream targets of ΔFosB are still under study, but candidate gene and microarray protocols some have yielded targets from various brain areas. These include a number of epigenetic modifiers and transcription factors like sirtuins, Calb1, *NFκB,* CDK5, c-fos, and the histone methyltransferase G9A, all contributing to suites of gene expression governing neuronal maturation, immune and energy regulation, and cell survival [312-317]. Another class of ΔFosB targets include glutamate receptor subunits and downstream effectors (GRIA2, CAMK2A, NMDAR1) with direct implications on the formation of both early and late phase LTP [291, 292, 318-320]. Furthermore, ΔFosB can even accumulate in microglia, and

stimulate the activation genes C5aR1 and C5aR, which are implicated in synaptic loss [321-323]. In addition to ΔFosB's prolonged stability *in vivo*, the nature of ΔFosB's targets across the brain suggest that ΔFosB can directly and indirectly drive swaths of persistent changes in gene expression in response to chronic activity.

Specific studies investigating the role of hippocampal ΔFosB in persistent gene expression, neuronal physiology, and animal behavior are sparse, especially regarding stress. However, several of ΔFosB's targets regulate cell survival and maturation and germline *FosB* gene knockout reduces hippocampal neurogenesis and increases behavioral despair in forced swim conditions [324, 325]. This shows that hippocampal *FosB* gene products contribute to neurogenesis and are associated with increased stress-induced behavior. Furthermore, hippocampal ΔFosB accumulates in the dHPC following several chronic stress paradigms and antidepressants, while vHPC has not been studied [284, 286, 326-328].

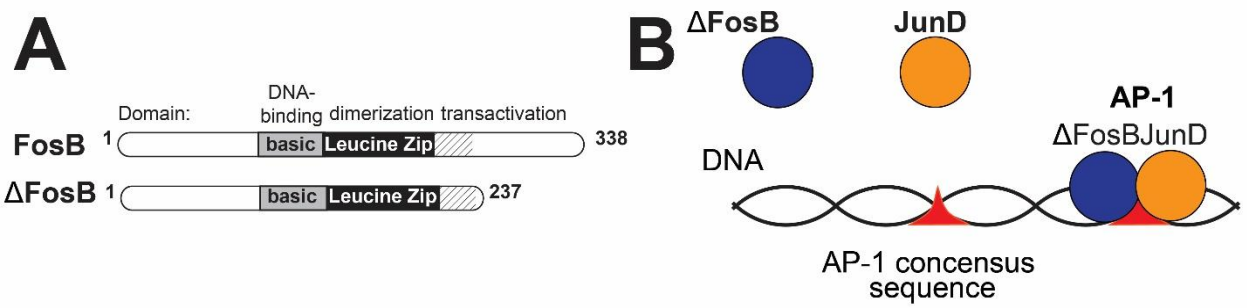

Figure 4 | ΔFosB structure and function **(A)** A schematic of splice variants of the *FosB* gene: full length FosB (above) and ΔFosB (below). ΔFosB and FosB both contain the same DNA-binding and dimerization domains, but ΔFosB lacks a degron domain compared to the full-length isoform. **(B)** Schematic of ΔFosB's actions as a transcription factor. ΔFosB binds with JunD to form an AP-1 complex and bind to DNA.

ΔFosB can alter hippocampal neuron function and learning and memory. Specifically, work from our group in the dHPC which used viral-mediated transcriptional antagonism of ΔFosB decreased the number of spines on dorsal CA1 neurons and increased CA1

excitability. Conversely, general dHPC ΔFosB overexpression increased CA1 spines and decreased CA1 excitability [306, 329]. These findings suggest that ΔFosB regulates hippocampal dendritic morphology and homeostatic excitability which are associated with synaptic plasticity and learning and memory. Hippocampal ΔFosB mediated changes in gene expression may therefore underlie changes in plasticity in response to chronic stress. This would be concordant with the concept of ΔFosB playing a role in activity-dependent memory trace plasticity and memory processes.

Moreover, both general viral-mediated inhibition and overexpression of ΔFosB's transcriptional actions in dHPC lead to impairments in hippocampal-dependent memory tasks [306]. These seemingly discordant behavioral results are hypothesized to result from the non-selective transfection across the subregions of dHPC thereby indiscriminately changing HPC neuronal excitability and preventing the formation of a discrete hippocampal memory trace. This supports the idea that cell-specific dHPC ΔFosB expression is critical in spatial and contextual memory formation. Because HPC ΔFosB has been implicated in spatial memory formation, direct manipulation of hippocampal ΔFosB may also regulate neurogenesis, affective memories, and/or stress behaviors. However, no study has been published about hippocampal ΔFosB's role in dHPC neurogenesis, any role in the vHPC, or examined its function in female hippocampus. These are all critical knowledge gaps I sought to address in my thesis. Therefore, in my thesis I sought to elucidate ΔFosB's contributions in hippocampal subregions along specific behavioral domains: DG influences on neurogenesis and spatial learning and vHPC in stress-behavior in both sexes.

Hypothesis and Specific Aims

Central hypothesis: Cell-specific hippocampal ΔFosB drives behavioral responses to chronic stress

Aim 1: Examine ΔFosB in antidepressant regulation of hippocampal neurogenesis and cognition

- Aim 1A | Genetic SGZ ΔFosB knockout in regulated neurogenesis
- Aim 1B | Genetic SGZ ΔFosB knockout in hippocampal dependent learning

Aim 2: Quantify hippocampal induction of ΔFosB by chronic stress

- Aim 2A | ΔFosB induction in dHPC and vHPC after stress in both sexes
- Aim 2B | ΔFosB induction in projection-specific vHPC cells after stress

Aim 3: Test the necessity and sufficiency of Projection-specific vHPC ΔFosB function in behavioral responses to chronic stress

- Aim 3A | Projection-specific vHPC *FosB* gene editing in male and female stress resilience
- Aim 3B | Projection-specific vHPC ΔFosB overexpression in male and female stress resilience

CHAPTER 2: MATERIALS AND METHODS

Animals and Genotyping

Adult male and female mice (>8 weeks) were used in these studies. Adult mice were group housed 4-5 per cage in a 12 h light/dark cycle and provided *ad libitum* food and water. In some cases, a wheel was provided for *ad libitum* wheel running (see results below). All experiments were approved by the Institutional Animal Care and Use Committee at Michigan State University and performed in accordance with AAALAC and NIH guidelines.

In chapter 3 Neurotensin receptor-2 IRES-Cre ($NtsR2^{cre/+}$) mice lacking the frt-flanked blocking cassette were crossed with Cre-inducible $Rosa26^{eGFP\text{-}L10a}$ mice (referred to as $L10^{loxSTOPlox\text{-}GFP}$), so that any cells expressing NtsR2/Cre are permanently marked with GFP [330]. $NtsR2^{cre/+}$ mice were crossed with floxed *FosB* ($FosB^{lox/lox}$) mice [331]to generate progeny with intact *FosB* ($NtsR2^{+/+};FosB^{lox/lox}$) and those lacking *FosB* in NtsR2 cells ($NtsR2^{Cre/+};FosB^{lox/lox}$). In chapter 4, the floxed *FosB* ($FosB^{lox/lox}$) mouse line was crossed to the Cre-inducible $Rosa26^{eGFP\text{-}L10a}$ line to produce progeny with Cre-inducible *FosB* knockout marked with GFP ($L10^{loxSTOPlox\text{-}GFP};FosB^{lox/lox}$) and wildtype littermates ($L10^{loxSTOPlox\text{-}GFP};FosB^{+/+}$). In chapters 5 and 6 the Cre-inducible GFP line, $L10^{loxSTOPlox\text{-}GFP}$ mice were used. All other experiments were performed on group housed C57BL6/J mice (>8 weeks) from Jackson. Mice were genotyped using standard PCR with the following primers:

- Cre:

  IRES-Cre forward: 5' – GGACGTGGTTTTCCTTTGAA – 3'

  IRES-Cre reverse: 5' – AGGCAAATTTTGGTGTACGG – 3'

- Rosa26EGFP-L10a:

  mutant forward: 5' – TCTACAAATGTGGTAGATCCAGGC – 3'

  wild type forward: 5' – GAGGGGAGTGTTGCAATACC – 3'

  common reverse: 5' – CAGATGACTACCTATCCTCCC – 3'

- Floxed *FosB*:

  FB loxPu sequence: 5' – GCT GAA GGA GAT GGG TAA CAG – 3'

  LIPz sequence: 5' – AAG CCT GGT GTG ATG GTG A – 3'

  LNEo1 sequence: 5' – AGA GCG AGG GAA GCG TCT ACC TA – 3'.

Surgeries

Gonadectomies:

In chapter 5, mice were anesthetized with a mixture of ketamine and xylazine 0.9/0.1 mg/kg and their testes or ovaries removed at 8 weeks old [332]. In capsule replacement studies, either empty 1.5 cm silastic pellets or pellets filled with .6 cm of testosterone (Sigma 1001774366) were placed subcutaneously between the scapulae and sutured at time of gonadectomy [333]. Mice then either recovered for 10 or 28 days in accordance with experimental protocol.

Intracranial Injections:

In chapters 4-6, stereotaxic surgeries were performed as previously described [306]. Male and female mice were anesthetized with a mixture of ketamine and xylazine 0.9/0.1 mg/kg, placed in a stereotax and injected with 0.5uL/hemisphere of virus or 0.3/dorsoventral injection with Hamilton glass syringes (see Table 1 for Bregma coordinates). Frequently in studies, Cre-dependent viral vectors were injected at one

region while another viral vector containing Cre was injected at another site, leading to projection specific expression of the particular construct (i.e.: Cas9, ΔFosB, hm3D and hM4D). Viruses were obtained from Addgene (DREADDs) or UNC (AAVs) or Dr. Rachael Neve from MGHVC (HSVs), shown in Table 2.

Table 1 | Surgical Coordinates

Region	Angle	AP	ML	DV
NAc	10	+1.6	+1.5	-4.4
BLA	0	-1.3	+3.4	-4.5
vHPC	3	-3.4	+3.2	-4.8
dHPC	10	-2.2	+2.0	-2.1/-1.9
vHPC	5	-3.6	+3.2	-4.8/-3.0

Table 2 | Viral vectors used in chapters 4 through 6

Viral Vector	Full Virus Description	Product Number
Retrograde mCherry	HSV-hEf1α-mCherry	(RN403)
Retrograde Cre	HSV-heF1α-Cre	(RN425)
Persistent Local GFP	AAV2-CMV-GFP	(AV7713)
Persistent Local ΔJunD	AAV2-CMV-ΔJunD-GFP	(AV4954E)
Local Cas9 and gRNA	HSV-syn-Cas9-gRNA-IRES-GFP	(RN made to order)
Local GFP	HSV-CMV-GFP	(RN1)
Retrograde Cre-dependent Cas9	HSV-heF1α-LS1L-myc-Cas9	(RN603)
Local scr-gRNA	HSV-IE4/5-TB-eYFP-CMV-IRES-Cre	(RN made to order)
Local FosB-gRNA	HSV-IE4/5-TB-FosB gRNA-CMV-eYFP-IRES-Cre	(RN made to order)
Retrograde Cre-dependent Cas9 and Cre-dependent ΔFosB	HSV-hEF1α-LSIL-ΔFosB-myc-Cas9	(RN made to order)
Retrograde Cre-dependent ΔFosB	HSV-hEF1α-LSIL-ΔFosB-IRES-GFP	(RN made to order)
Persistent Local Cre	AAV2-CMV-Cre-GFP	(AV4954E)
Retrograde Cre-dependent G_q DREADD	rAAV2-hSyn-DIO-hM3D-mCherry	(44361-AAV2)
Retrograde Cre-dependent G_i DREADD	rAAV2-hSyn-DIO-hM4D-mCherry	(44362-AAV2)

Immunocytochemistry (IHC)

Mice were transcardially perfused with cold PBS followed by 10% formalin. Brains were post-fixed for 24 hours in 10% formalin, cryopreserved in 30% sucrose, and sliced into 35µm sections. Following an optional 0.05% sodium borohydride (sigma 452882-25g lot:SHBK0324) in PBS antigen retrieval protocol the following primary antibodies were used: Anti-FosB (FosB 5G4, 1:1000, rb, #2251S, Cell Signaling Technologies), Anti-NeuN (1:1000, ms, MAB377 Millipore), Anti-GFP (1:1000, gt, ab5450, Abcam or ms, A11120, Invitrogen), Anti-BrdU (1:1000, rat, MCA2060, Bio-Rad), Anti-Doublecortin (1:1000, gt, sc-8066, Santa Cruz), and Anti-Androgen Receptor (1:1000, rb, ab52615, Abcam). The following corresponding secondary antibodies were then used: Donkey anti-rabbit Cy3 (1:200, 711-165-152, Jackson Immunoresearch), Donkey anti-goat Ig bitotin (1:200, 705-065-147 Jackson Immunoresearch), Donkey anti-goat Alexa Fluor 488 (1:200, 705-545-147 Jackson Immunoresearch), Donkey anti-goat Alexa Fluor 568 (1:200, A11057 Invitrogen), Donkey anti-mouse Cy3 (1:200, 715-165-150 Jackson Immunoresearch), Donkey anti-mouse Alexa Fluor 488 (1:200, 715-545-150 Jackson Immunoresearch), Donkey anti-rat Cy3 (1:200, 712-165-150 Jackson Immunoresearch), and biotin-conjugated secondary antibody (Jackson Immunoresearch) then visualized by 3,3′-diaminobenzidine staining (Vector Laboratories). Images of IHC were taken with an Olympus FluoView 1000 filter-based laser scanning confocal microscope, and by a blinded experimenter using Fiji software. Pseduo-3D image was generated by compiling a z-stack of 40 0.5 micrometer slices using the Olympus FluoView 1000 software.

Western Blots

After cervical dislocation, 12G bilateral punches of hippocampus were isolated from 1mm coronal slices of dHPC and vHPC and flash frozen. Samples were then thawed in 80uL RIPA buffer (ph 7.4) with phosphatase and protease inhibitors cocktails (Sigma P8340-1ML 1:100, Sigma P0044 1:100, Sigma P57261:100), and subjected to DC protein assay (Biorad 5000112EDU). Following the addition of 5x lamelli buffer, 20ug of protein were loaded in each lane of a 4-15% precast Biorad gel. Protein was then transferred from gels to PVDF membranes at 80mV for 20 minutes at room temperature. Membranes were blocked in 5% nonfat dry milk in 1x PBS-Tween20 for 1 hour, prior to primary incubation overnight at 4C with Anti-FosB (FosB 5G4, 1:1000, rb, #2251S, Cell Signaling Technologies) in 5% Bovine Serum Albumin in 1xPBST. The following day, membranes were rinsed and incubated with Donkey anti-rb HRP (PI-1000; 1:40,000; Vector) followed by development with Western Substrate Dura and imaged with a film developer. Films were then quantified using Fiji Software and normalized to a total protein stain.

CRISPR Guide RNA design and testing

gRNAs targeting exon 2 of the *FosB* gene were designed using e-CRISP software (www.e-CRISP.org). The top four sequences were:

gRNA1: TACACCGGGAGCCGGAGTCG

gRNA2: TTACGATCTAAAACTTACCT (this gRNA was most effective and was selected for all *in vivo* work described in the current manuscript; also referred to as AJR4 as it was the fourth gRNA produced for our lab)

gRNA3: TCAACATCCGCTAAGGAAGA

gRNA4: CCGTCTTCCTTAGCGGATGT

Each gRNA was tested by transfection in a mammalian expression plasmid also containing Cas9. Briefly, Neuro2a cells (N2a, American Type Culture Collection) were cultured in EMEM (ATCC) supplemented with 10% heat-inactivated fetal bovine serum (ATCC) in a 5% CO_2 humidified atmosphere at 37° C. Cells were plated into 12-well plates, and 24 h later (when cells were ~30% confluent) cells were transiently transfected using Effectene (Qiagen) with a total of 200 ng DNA per well. Cells were transfected with empty vector, Cas9 alone, or Cas9 with a gRNA to be tested. Cells were then serum starved for 24 h, then refed for 4 h to induce *FosB* gene expression. Cells were pelleted, samples were run on gradient polyacrylamide gels and transferred to PVDF membranes, and Western blot was performed using rabbit anti-FosB antibody (2251; 1:500; Cell Signalling) and HRP conjugated anti-rabbit secondary at (PI-1000; 1:40,000; Vector). Signal was detected on film and quantified using ImageJ software.

qPCR

RNA was isolated using TriZol (Invitrogen) homogenization and chloroform layer separation. The clear RNA layer was then processed (RNAeasy MicroKit, Qiagen #74004) and analyzed with NanoDrop. A volume of 10uL of RNA was reverse transcribed to cDNA (High Capactiy cDNA Reverse Transcription Kits Applied BioSystens # 4368814). Prior to qPCR, cDNA was diluted to 200 uL. The reaction mixture consisted of 10 uL PowerSYBR Green PCR Master Mix (Applied Biosystems; #436759), 2uL each of forward and reverse primers and water, and 4 uL cDNA template. Samples were then heated to 95 °C for 10 min (Step 1) followed by 40 cycles of 95 °C for 15 s, 60 °C for 15 s,

and 72 °C for 15 s (Step 2), and 95 °C for 15 s, 60 °C for 15 s, 65°C for 5s and 95 °C for 5s(Step 3). Analysis was carried out using the ΔΔC(t) method[334] Samples were normalized to *Gapdh*.

- ADCY1
    - Forward: AAACACAGTCAATGTGGCCAGTCG
    - Reverse: ACTTTGCCTCTGCACACAAACTGG
- ADRA2A
    - Forward: CAAGATCAACGACCAGAAGT
    - Reverse: GTCAAGGCTGATGGCGCACAG
- ARHGAP36
    - Forward: ACTTAGAGCAGTCCTTGCGG
    - Reverse: GGTAGAGCTCTGTCCGGCT
- ELAVL2
    - Forward: GGTACCGCCGCCAGGAAACACAACTGTCTAATGGG
    - Reverse: GCGGCCGCACTGAGGACAAGAGCTCATTAGGCTTTGT
- FOSB
    - Forward: GTGAGAGATTTGCCAGGGTC
    - Reverse: AGAGAGAAGCCGTCAGGTTG
- ΔFOSB
    - Forward: AGGCAGAGCTGGAGTCGGAGAT
    - Reverse: GCCGAGGACTTGAACTTCACTCC
- GAA
    - Forward: CCCAAAGGATGTGCTGACCT

    - Reverse: TTGTGTTCAGCAACACTCGG
- GAPDH
    - Forward: AGGTCGGTGTGAACGGATTTG
    - Reverse: TGTAGACAATGTAGTTGAGGTCA
- IGFBP6
    - Forward: GGTCTACAGCCCTAAGTGCG
    - Reverse: AGGGGCCCATCTCACTATCT
- KCTD9
    - Forward: CGGGTCACGCTGTTCTTGA
    - Reverse: ACAGCACATCATCATCCCTGA
- NEFM
    - Forward: CAGCTACCAGGACACCATCCAG
    - Reverse: GTGTACAGAGGCCCGGTGAT
- PEG10A
    - Forward: CCGATACACGCGTTTCCAAC
    - Reverse: TAAAACCCGCCTGTTCCACA
- PEG10B
    - Forward: AATCCTCGTGTGGAACAGGC
    - Reverse: TCATCATCTTCGGCGTCAGG
- PRKCB
    - Forward: CAGAGATTGCCATCGGTCTGT
    - Reverse: CCCCTCAGAATCCAGCATCA
- SCG5

    - Forward: ATCAAGGCTACCCAGACCCT
    - Reverse: GGATTGACACTCCTCCGCTT
- SVIL
    - Forward: TACACGAGTGTGATGAAGGCTCCGAGC
    - Reverse: CCAGAGGAGCTGCTGAGGATGAACAG

Stress Paradigms

Subchronic Variable Stress:

SCVS was performed according to previously published protocols [63, 335] Briefly, group-housed mice were exposed to a stressor every day for six days under white light conditions. These stresses were given in the following order: group foot shock of 10 conspecific animals with 100 random foot shocks over an hour at .45mA, one hour tail suspension, and one hour restraint stress. Restraint tubes were manufactured from 50mL falcon tubes.

Chronic social defeat stress (CSDS):

CSDS was performed as previously described [326, 328]. In brief, mice were placed into the home cage of an aggressive retired breeder CD1 mouse containing a perforated plexiglass divider placed between the walls of the cage. The experimental mice were allowed to physically interact with the CD1 for 10 min. Following the aggressive encounter, the mice were placed into the other side of the divider from the CD1 aggressor mouse allowing sensory, but not physical, contact for 24 hours. This protocol was repeated daily for 10 days with a new aggressor every day. Behavioral testing began the day following the final day of stress.

Subchronic defeat stress:

Also called a microdefeat, subchronic defeat is an abbreviated social defeat stress protocol [53, 336]. Mice were placed in the home cage of an aggressive retired breeder CD-1 mouse and allowed to interact for 3-5 min, then removed and allowed to rest in their homecage for 15 min. This was repeated for a total of 3 consecutive encounters in a single day. Behavioral testing began the following day.

Behavioral Tasks

All behavioral tests were performed under red light conditions after an hour habituation, except sucrose preference which was tested in the home cage.

Elevated Plus Maze:

EPM was performed as previously described [337]. In brief, Animals were placed with their heads in the center of the maze parallel to the open arms and allowed to roam for 5 minutes. The amount of time spent in the open arms was assessed as a measure of anxiety, and distance travelled was quantified as a measure of locomotor behavior. Animals who fell or jumped from the arena were excluded from analysis.

Open Field:

Open field was performed essentially as previously described [337]. Animals were placed into a 38x38 arena and allowed to roam freely. Activity was recorded with a digital CCD camera connected to a computer running automated video tracking software package (Clever Sys). Time spent within the center of the box (the center starts approximately 9.5cm from the edge of the wall) and distance moved were measured as anxiety-like and locomotor behaviors.

Novel Object Recognition (NOR):

NOR was assessed using a 3-day paradigm as described previously [337]. Briefly, mice were placed into the open-field (OF) apparatus for one hour (Day 1). 24 hours later mice were exposed to two identical objects placed in opposite corners of the open-field (OF) box and allowed to explore the apparatus for 30 min (Day 2). Twenty-four hours later, mice were tested for NOR. One object was removed and replaced with a dissimilar object, and mice were allowed to freely explore the apparatus for 5 min (Day 3).

Temporally dissociative passive avoidance (TDPA) (performed by ALE):

TDPA testing was conducted as previously described[337, 338]. Briefly, mice were placed into the lit side of light dark box. After 2 min of exploration, a door allowing entry into the dark side was raised. Upon entry (full body, excluding tail) into the dark side, the door was lowered and, after 5 min, mice received a mild footshock (0.7 mA, 2 s). Mice were returned to their homecage after 30 s. Testing (all of the same conditions including footshock) was repeated daily for 5 d. The latency (s) to “cross over” from the light side to dark side was manually recorded daily.

Splash Test:

Splash test was performed according to previously published protocols [63, 335]. Mice were sprayed twice on their backs with a 10% sucrose solution and placed solitary in an empty cage and then videotaped for 5 minutes. The time spent autogrooming was hand scored by blind observers. After splash tests animals were singly housed for the remainder of behavioral tests.

Novelty Suppressed Feeding:

After an overnight fast prior to testing, mice were placed into a corner of a bare novel arena, measuring 38x38cm, with a single pellet of chow at the center of the arena, and videotaped up to 10 minutes. The videos were then scored for the latency to feed. Feeding was defined as using forepaws during mastication.

Sucrose Preference:

Mice were given a two-bottle choice test from which they could drink freely. During the first day, the two bottles contained water and allowed habituation to the bottles. On the following day, one bottle was replaced with a 1% sucrose solution. The mice were then allowed to drink freely from the bottles over two days, and their intake was weighed and recorded daily. The bottles were switched every day to prevent side bias.

Social Interaction:

SI was performed as previously described [326]. Briefly, experimental animals were placed into the corner of an 38x38 arena with a mesh cage at one end. After 3 minutes of habituation to the arena, a novel stimulus animal was placed into the mesh cage, and the experimental animal was again allowed to move around the arena for 3 minutes. Time spent within a 5 cm radius of the stimulus animal was recorded for both sessions. SI ratio is a ratio of the time spent in the interaction radius while the novel animal is present to the time spent in the same location without a social stimulus.

Intraperitoneal injections

Fluoxetine (20 mg/kg; dissolved in 0.9%saline) or a 0.9% saline solution was injected into the i.p cavity once daily. BrdU (50mg/kg) was diluted in saline and injected i.p. every 3

days. Clozapine N-oxide (CNO) (Fischer Scientific NC1044836) was diluted into 5%DMSO and 95% 0.9% saline vehicle solution. Either CNO or just vehicle was administered i.p. at 0.3mg/kg daily an hour prior to the stressor or behavior.

Translational ribosomal affinity purification (TRAP) and cDNA library preparation (performed with assistance from Maze Lab)

Three weeks following injection of retrograde HSV-Cre into NAc, Cre-dependent L10-GFP-expressing mice (*Rosa26*$^{eGFP/L10a}$) were sacrificed and brains were immediately dissected into 1 mm coronal sections. Transduced tissue from ventral hippocampi (vHPC) of both wildtype and *FosB*$^{fl/fl}$ mice (chapter 4) or male vs females (chapter 5) were collected using 14 gauge biopsy punches guided by a fluorescent dissecting microscope (Leica) and stored at -80° C until processing (*n* = 3/group, 3-4 mice pooled per *n*). Polyribosome-associated RNA was affinity purified as previously described [339, 340]. Briefly, tissue was homogenized in ice-cold tissue-lysis buffer (20 mM HEPES [pH 7.4], 150 mM KCl, 10 mM MgCl2, 0.5 mM dithiothreitol, 100 µg/ml cycloheximide, protease inhibitors, and recombinant RNase inhibitors) using a motor-driven Teflon glass homogenizer. Homogenates were centrifuged for 10 min at 2000 *g* (4° C), supernatant was supplemented with 1% NP-40 (AG Scientific, #P1505) and 30 mM DHPC (Avanti Polar Lipids, #850306P), and centrifuged again for 10 min at 20000 *g* (4°C). Supernatant was collected and incubated with Streptavidin MyOne T1 Dynabeads (Invitrogen, #65601) that were coated with anti-GFP antibodies (Memorial Sloan-Kettering Monoclonal Antibody Facility; clone names: Htz-GFP-19F7 and Htz-GFP-19C8, 50 ug per antibody per sample) using recombinant biotinylated Protein L (Thermo Fisher Scientific,[SEP]#

29997) for 16-18 h on a rotator (4° C) in low salt buffer (20 mM HEPES [pH 7.4], 350 mM KCl, 1% NP-40, 0.5 mM dithiothreitol, 100 µg/ml cycloheximide). Beads were isolated and washed with high salt buffer (20 mM HEPES [pH 7.4], 350 mM KCl, 1% NP-40, 0.5 mM dithiothreitol, 100 µg/ml cycloheximide) and RNA was purified using the RNeasy Micro Kit (Qiagen, #74004). In order to increase yield, each RNA sample was initially passed through the Qiagen MinElute™ column 3 times. Following purification, RNA was quantified using a Qubit fluorometer (Invitrogen) and RNA quality was analyzed using a 4200 Agilent Tapestation (Agilent Technologies). cDNA libraries from 5 ng total RNA were prepared using the SMARTer® Stranded Total RNA-Seq Kit (Takara Bio USA, #635005), according to manufacturer's instructions. cDNA libraries were pooled following Qubit measurement and TapeStation analysis, with a final concentration ~7 nM. Sequencing was performed at the Icahn School of Medicine at Mount Sinai Genomics Core Facility (https://icahn.mssm.edu/research/genomics/core-facility).

Metabolic Cages and Bruker

Bruker:

For analysis of body composition, alert, non-anesthetized mice were individually placed in a time-domain nuclear magnetic resonance (TD-NMR) instrument (Minispec mq7.5, Bruker Optics). This acquires and analyzes all photons of mice, resulting in body composition analysis of fat, free body fluid, and lean tissue of each mouse.

Metabolic Cages:

In experiments involving energy balance, mice were singly housed in metabolic cages (PhenoMaster, TSE Systems, Chesterfield, MO) for 72 hours to measure metabolic

performance, activity, plus feeding and drinking behavior [341]. The first 48 hours were considered acclimation period, and only data from the last 24 hour cycle were used for analysis.

Electrophysiology (performed by ALE and ESW)

Ex vivo acute brain slices were prepared from 9-13 week old male or female L10-GFP transgenic mice. Animals were anesthetized with isofluorane and transcardially perfused with ice-cold sucrose artificial cerebrospinal fluid (sucrose aCSF, in mM: 234 sucrose, 11 D-glucose, 26 NaHCO3, 2.5 KCl, 1.25 NaH2PO4, 10 MgSO4, 0.5 CaCl2). Animals were decapitated and brains rapidly removed and placed in oxygenated (95% O2, 5% CO2) slurried sucrose aCSF for 15 seconds. Brains were blocked and transferred to a vibratome slicing chamber (Leica; Germany) containing aCSF (in mM: 126 mM NaCl, 2.5 KCl, 1.25 NaH2PO4, 2 MgCl, 2 CaCl2, 26 NaHCO3, 10 glucose). Coronal slices (250 □m) were obtained and transferred to an incubation chamber containing oxygenated aCSF. Slices were incubated at 34C for 30 minutes and then at room temperature for a minimum of 30 min before recording. Whole-cell patch clamp recordings were made with slices held in a submersion chamber perfused at 2 mL/min with oxygenated aCSF held at 30(± 2) C using a single inline heater (Warner Instruments; Hamden, CT). Borosilicate glass electrodes with a tip resistance of 3-6 M□ were filled with internal solution (in mM: 115 potassium gluconate, 20 KCl, 1.5 MgCl, 10 phosphocreatine-Tris, 2 Mg-ATP, 0.5 Na3-GTP; pH 7.2-7.4; 280-290 mOsm). L10-GFP+ cells representing vHPC-NAc or vHPC-BLA projections were visualized in the ventral CA1 region of the hippocampus with an upright epifluorescent microscope (BX51WI Olympus; Japan). Pyramidal cells were distinguished from other cell types by their morphology and location in the cell body layer

of the CA1 region. Recordings were made from projection cells using a Multiclamp 700B amplifier and Digidata 1440A digitizer (Molecular Devices; San Jose, CA). Membrane properties and cell excitability data were sampled (10 kHz), filtered (10 kHz), and stored on a PC for analysis. Membrane capacitance, membrane resistance, and access resistance were automatically calculated by pClamp 10 software (Molecular Devices; San Jose, CA). Any cell with a resting membrane potential more positive than -60mV or access resistance >25 M□ were omitted from analyses. Resting membrane potential was measured automatically by the Multiclamp 700B Commander while injecting no current (I=0); this value was recorded immediately after breaking into a cell. Rheobase measurements were taken by administering 250ms, +5pA steps starting from 0pA with 250ms between current injections. The first current level issued to elicit a spike was recorded as rheobase for each cell. Action potential (AP, or spike) numbers were measured using a +25pA increasing current step protocol. The number of spikes at each step from 0 to 300 pA was manually counted. Input resistance was determined as the slope of the line best fit to the I-V plot generated by the input-output current clamp protocol, with the minimum current step being that which generated a voltage of approximately -120 mV. Sag ratio was determined using peak and steady-state potentials obtained at the first current step that reached lower than -120 mV and was calculated as steady-state/peak. Spontaneous event frequency and amplitude were determined using Minianalysis software (Synaptosoft, Inc.) by manual selection of events from the first 60-120 seconds of gap free voltage clamp recording from each cell.

For DREADD validation, projection cells were identified as described above and recordings were obtained in regular aCSF. After initial baseline recordings were collected,

aCSF + Clozapine-N-Oxide (CNO, 1 □M) was washed onto the slice. Approximately 8 minutes were allowed for the solution to reach the bath from the reservoir and for the DREADDs to bind CNO before excitability was measured again. For flutamide studies, vehicle vHPC-NAc recordings were collected with the slice washed in aCSF + vehicle (DMSO, 0.001%). The slices were incubated as described above, now with the addition of 0.001% DMSO in the aCSF. Treatment recordings were collected from slices incubated and bathed in aCSF plus flutamide (100 nM) and picrotoxin (100 □M) in DMSO. Picrotoxin was included due to the ability of flutamide to affect GABAergic transmission.

Statistics

Analyses of one independent variable were performed using PRISM 8.0 (GraphPad Software) using fixed-effect models and treating all samples as independent, except for within-subject experiments. Normality and equal variance were tested using D'Agostino & Pearson test, and F-tests, respectively. If comparisons met these criteria they were tested using unpaired student's t-tests, and were otherwise tested with the nonparametric Mann-Whitney test. Analyses of two independent variables, including sex differences analyses data were analyzed with Laverene's and Shapiro-Wilks tests for normal distributions and equal variances, respectively, in in SPSS 25.0, followed by 2x2 factorial ANOVA or Repeated Measures 2x2 ANOVA if appropriate, otherwise an extension of the nonparametric Kruskal-Wallis test was applied. In cases of interaction between variables, multiple comparisons were tested using Sidak's post-hoc tests. A cutoff of alpha=0.05 was used in all analyses. Refer to Tables 4-6 for all omnibus statistical results.

CHAPTER 3: HIPPOCAMPAL SUBGRANULAR ZONE *FOSB* EXPRESSION IS CRITICAL FOR NEUROGENESIS AND LEARNING

Note: Figures and the text were previously published in (Manning et al., 2019).

Author contributions:

Conceived and designed the experiments: Manning, Leinninger, Robison

Performed the experiments: Manning, Eagle, Achargui, Potter, Woodworth, Robison

Analyzed the data: Manning, Kwiatkowski, Robison

Contributed reagents/materials/analysis tools: Ohnishi, Leinninger

Wrote the paper: Manning, Leinninger, Robison

Introduction

As described in the previous chapter, learning and memory are thought to develop through repeated activation of discrete networks of neurons and activity-dependent immediate early genes (IEGs) are critical mediators of learning and memory processes. Indeed, many studies have linked various IEGs to the creation and expression of memories[342-345], including IEG transcription factors that orchestrate the sweeping changes in gene expression underlying the formation of stable engrams central to learning. As the process of learning and memory consolidation can take place over timescales of up to days or weeks, mechanisms controlling gene expression over these timescales, including epigenetics[259, 346, 347], have become a key area of study in the learning field. The IEG ΔFosB, a transcription factor produced by the *FosB* gene, is unique in its stability, with a half-life *in vivo* of around eight days[307, 308, 348], allowing it to accumulate in neurons and regulate gene expression after repeated stimulation[349].

Moreover, hippocampal ΔFosB is critical for learning[306], though its mechanism(s) of action in hippocampal function are not fully understood.

ΔFosB function has been implicated in learned rewarding and social behaviors. For example, transcriptional silencing of ΔFosB in the nucleus accumbens (NAc) impairs experience-induced facilitation of sexual behavior[350] and NAc ΔFosB is necessary for learning association of spatial context with positive reinforcers, like cocaine[351]. ΔFosB is induced by the antidepressant fluoxetine in the NAc[305, 326] and its function there is critical for antidepressant effects on social interaction[305]. Fluoxetine also induces ΔFosB in the dentate gyrus (DG) of the dHPC[326], and its antidepressant efficacy is dependent on neurogenesis in the DG[227, 229], so probing the link between ΔFosB and neurogenesis may provide new insights into learning and antidepressant function.

Mice lacking expression of the *FosB* gene in all tissues from conception (*FosB* knockout mice) have a variety of hippocampal malformations, including thinning of the DG granular cell layer, and display reduced hippocampal neurogenesis[324]. However, such global, germline *FosB* knockout cannot indicate the specific contribution of hippocampal neurogenesis to behavior. Our group has shown that ΔFosB regulation of transcription in dorsal hippocampus (dHPC) is necessary for spatial memory[306]. However, these studies used a viral method that inhibited ΔFosB activity in fully differentiated CA1 and DG neurons of dHPC, and thus did not address a role for ΔFosB-driven neurogenesis in learning. Moreover, it is critical to consider how specific hippocampal subregions may be involved in learning and memory. Of particular note is the subgranular zone (SGZ) of the DG, an important site of neurogenesis in the brain. SGZ neurogenesis has been tied to learning and memory in the context of spatial learning tasks[219], stress-induced

behaviors[231, 352], and fear[353]**.** I therefore used *NtsR2-Cre* mice, in which hippocampal Cre expression is confined to the SGZ, to test the hypothesis that knockout of *FosB* gene products specifically in the SGZ of mice inhibits neurogenesis and impairs performance in learning and memory-related tasks.

Results

NtsR2-Cre;GFP mice identify cells in the dentate gyrus subgranular zone:

Previous reports indicate that NtsR2 is sparsely expressed in adult mouse brain, and this expression is predominantly in glia[330, 354-356]. Additionally, adult NtsR2$^{Cre/+,GFP}$ mice exhibit robust GFP-expression in cells of the SGZ of the DG and in the pyramidal layer of CA3 in the adult dHPC (Fig 5). However, the NtsR$^{Cre/+,GFP}$ transgenic line permanently expresses GFP independent of current NtsR2 expression and NtsR2 expression is thought to be phasic in new cells, peaking in P5-P15[357]. As the SGZ is a region enriched in neuroprogenitor cells, I sought to determine the developmental status of the GFP-positive cells. I performed immunohistochemistry for NeuN and Doublecortin (DCX), markers of mature and immature neurons, respectively in two animals (Fig 5A, B). In the CA3 pyramidal neurons, there was extensive colabeling with NeuN but not DCX, indicating that many of these GFP-positive cells were mature neurons. However, in the SGZ, there was significant overlap between DCX- and GFP-positive cells (Fig 5B), indicating that NtsR2$^{Cre/+,GFP}$ expresses in neuroprogenitor cells in this region.To determine whether these NtsR2-GFP labeled cells of the SGZ are indeed neuroprogenitor cells undergoing division, we used BrdU labeling to mark newly divided cells. We injected adult male NtsR2$^{Cre/+,GFP}$ mice with 50mg/kg BrdU daily for five days, during which they

had *ad libitum* access to a running wheel, as wheel running promotes hippocampal neurogenesis in rodents [358]. Subsequent immunohistochemistry revealed distinct BrdU-staining in nuclei of some NtsR2-GFP cells of the SGZ (Fig 6A), indicating that some of the NtsR2$^{Cre/+,GFP}$ cells had undergone mitosis in the previous five days. Additional immunostaining revealed that ΔFosB was present in some NtsR2$^{Cre/+,GFP}$ cells.

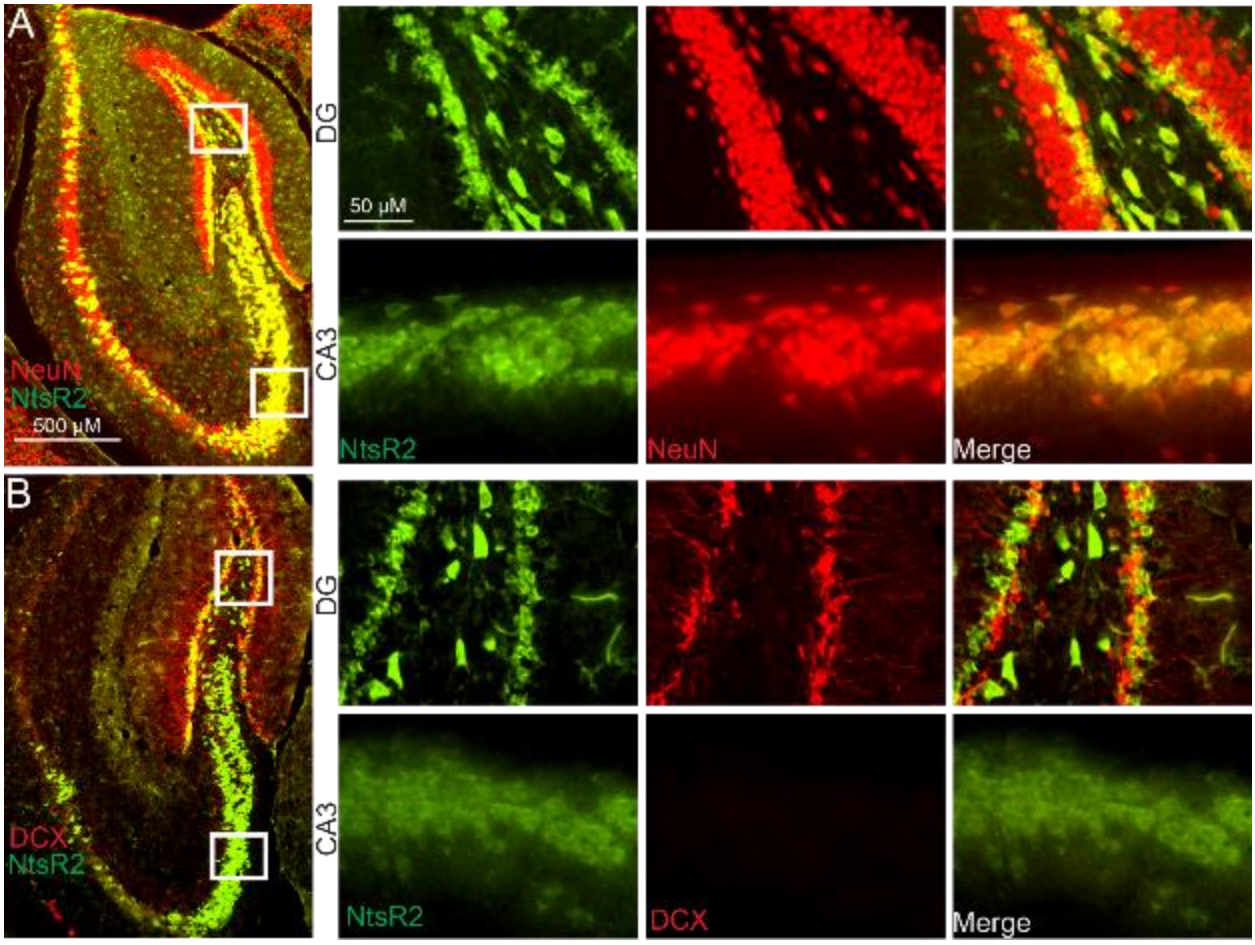

Figure 5 | NtsR2-Cre expresses in the DG and CA3 of the dHPC. (A) 4x and 40x images showing that NtsR2-positive cells colocalize with NeuN in DG and CA3. **(B)** 4x and 40x images showing that NtsR2-positive cells colocalize with doublecortin (DCX) in the DG, but this staining is absent in the CA3.

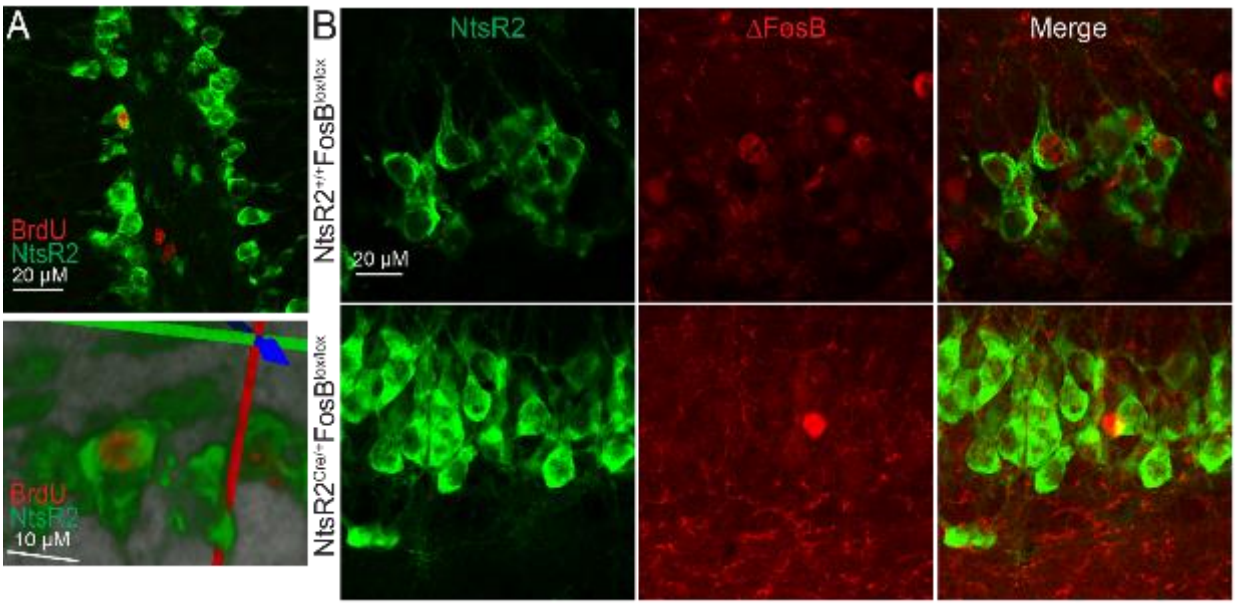

Figure 6 | NtsR2-Cre expresses in newly-dividing SGZ progenitor cells, some of which express *FosB.* (A) Some NtsR2-Cre cells are stained with BrdU in the SGZ of the DG (100x, top), and this is confirmed by 3D reconstruction from confocal imaging (bottom). **(B)** NtsR2-Cre cells also express with ΔFosB in the SGZ.

However, $NtsR2^{Cre/+,GFP}$;$FosB^{lox/lox}$ mice did not exhibit ΔFosB immunoreactivity in GFP-positive SGZ cells (Fig 6B). Taken collectively, these data indicate that $NtsR2^{Cre/+,GFP}$ marks multiple cell types in the dHPC, including newly dividing cells in the SGZ, and that some of these cells express *FosB* gene products that can be knocked out using this Cre/lox approach.

***FosB* in the SGZ is critical for induced neurogenesis:**

It has been previously suggested that the *FosB* gene is critical for adult hippocampal neurogenesis, as germline *FosB* knockout mice show reduced BrdU staining in response to kainic acid[324]. Moreover, multiple antidepressants induce hippocampal neurogenesis, and *FosB* gene products are critical for the behavioral effects of

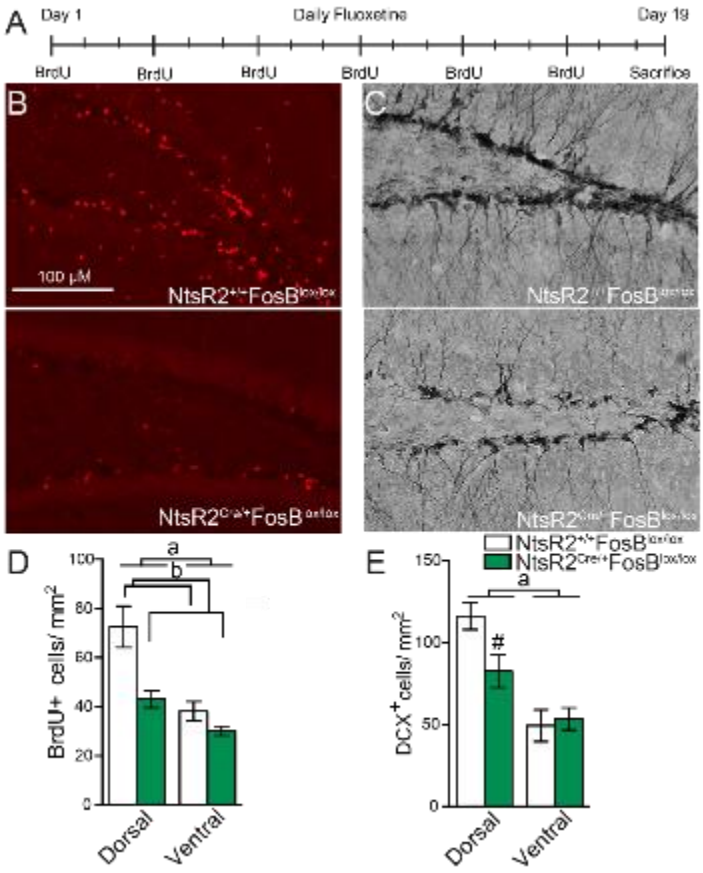

Figure 7 | Genetic Knockout of FosB in SGZ reduces neurogenesis. (A) Timeline of experiment. Representative images of BrdU **(B)** and doublecortin **(C)** staining in the dorsal HPC of WT or Cre-positive animals after 18 days of daily fluoxetine. **(D** and **E)** Cre-positive animals have significantly fewer BrdU ((a):p=0.039 for effect of Cre; (b):p=0.007 for dHPC vs vHPC) with no effect on DCX positive cells ((#):p=0.0507 for interaction between genotype and dorsoventral axis; (a):p=0.0001 for dHPC vs vHPC).

antidepressants like fluoxetine[292, 305]. To examine if *FosB* gene expression in the hippocampal SGZ is necessary for fluoxetine-induced hippocampal neurogenesis, I studied NtsR2$^{Cre/+,GFP}$ mice crossed onto the FosB$^{lox/lox}$ line, providing developmental *FosB* knockout in a subset of hippocampal cells including the SGZ. 4 NtsR2$^{Cre/+,GFP}$;FosB$^{lox/lox}$ mice (referred to as Cre-positive) and 5 littermates lacking Cre (referred to as WT) were injected i.p with fluoxetine (2mg/kg) daily and BrdU (50mg/kg) every 3rd day for 18 days to both induce neurogenesis and mark dividing cells,

respectively (Fig 7A). Mice were sacrificed 24 hours after the last injection (Fig 7A) and brains were then immunolabeled for BrdU and DCX, (Fig 7B, C). Cre-positive animals showed reduced BrdU staining compared to WT animals (Fig 7D), with main effect of genotype on BrdU labeled cells and dorsoventral axis of the brain (dorsal vs ventral HPC) ($H_{(1)}$=4.218; p=0.039 and $H_{(1)}$=7.25; p=0.007, respectively), without interaction between the two variables ($H_{(1)}$=0.206; p=0.649). DCX staining was significantly reduced in the vHPC compared to dHPC (Fig 7E). I found a main effect of the dorsoventral axis, but not genotype ($F_{(1,13)}$=29.64, p=0.0001 and $F_{(1,13)}$=2.832, p=0.1162, respectively), with a trend for an interaction between the genotype and dorsoventral axis ($F_{(1,13)}$=4.634, p=0.0507). These indicate that mitotic division, but not differentiation into a neuronal lineage, are reduced with *FosB* SGZ knockout, and that these effects are exaggerated in the dHPC.

FosB KO in the SGZ does not alter basal anxiety behaviors:

Enhanced neurogenesis is thought to be one of the mechanisms behind antidepressant drug effects, and neurogenesis has been linked to abnormalities in anxiety behaviors[231, 326, 359]. Therefore, 30 adult NtsR2$^{Cre/+,GFP}$;FosB$^{lox/lox}$ mice and 35 NtsR2$^{+/+,GFP}$;FosB$^{lox/lox}$ littermates were tested in both the open-field and the elevated plus maze (EPM). Despite the developmental knockout, there were no differences between these two genotypes in the percent of total time spent in the center of the open field arena, nor the percent of center entries (Fig 8A, B; group medians of 13.05 and 12.13 Mann Whitney U=503.5, p=0.93 and $t_{(62)}$=1.186, p=0.24). In EPM, there was no difference in percentage of open arm time or percentage of open arm entries between genotypes (Fig 8C, D; $t_{(52)}$=0.719, p=0.475 and $t_{(52)}$=0.344, p=.732). Taken together, these data suggest that *FosB* SGZ knockout causes no changes in anxiety-like behavior.

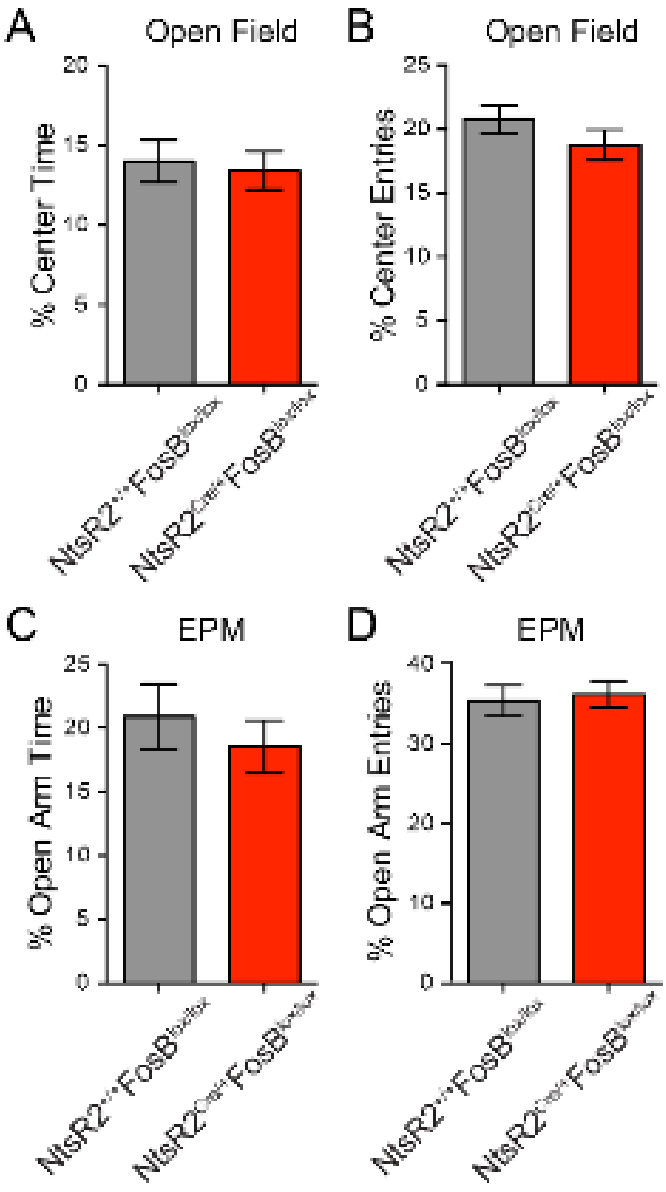

Figure 8 | Genetic knockout of FosB in SGZ does not alter basal anxiety behaviors FosB SGZ knockout caused differences in the percentage of total time spent **(A)**, nor in the percentage of entries **(B)** into the center of the open field (p=0.93 and p=0.24, respectively). There were also no differences in the percentage of total time spent **(C)** or percentage of entries **(D)** into the open arms of the elevated plus maze (p=0.475 and p=0.732, respectively).

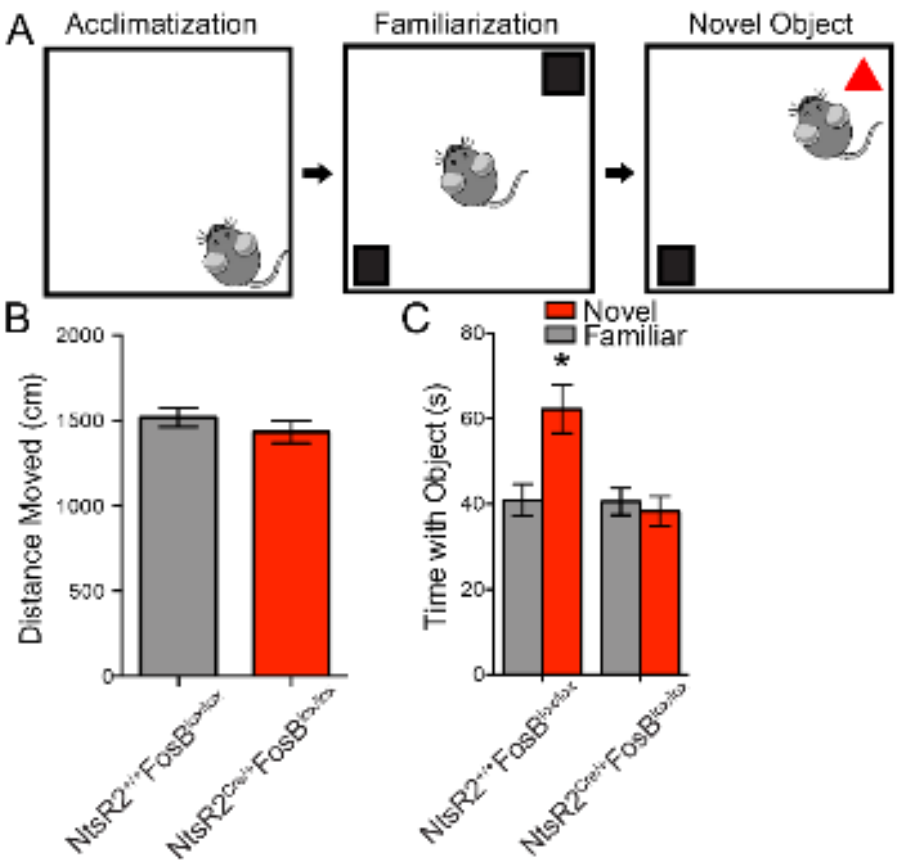

Figure 9 | Genetic knockout of FosB in SGZ reduces hippocampus-dependent memory. (A) Schematic of the NOR task. **(B)** Cre-positive and WT littermates show no differences in locomotor behaviors in the acclimatization phase. **(C)** Cre-positive mice display reduced time spent with a novel object compared to WT littermates (*:p=0.0038).

FosB SGZ Knockout impairs learning:

Reductions in neurogenesis have been linked to abnormalities in hippocampus-dependent learning[203, 214, 218, 360, 361]. Therefore, 29 adult NtsR2$^{Cre/+,GFP}$;FosB$^{lox/lox}$ mice and 35 wild-type littermates also underwent novel object recognition (NOR; Fig 9A) to test for deficits in a hippocampal-dependent task. During the acclimatization phase, Cre-positive mice and wild-type littermates showed no difference in locomotor behavior (Fig 9B; $t_{(62)}$=0.96, p=0.342). As long term memory is dependent upon protein synthesis [362], and *FosB* gene products are transcription factors, a 24 hour timepoint was chosen

to test long-term memory as opposed to a more immediate timepoint which results from non-genomic actions [168]. 24 hours after familiarization with two identical objects, wildtype mice spent significantly longer interacting with a novel object (Fig 9C; $F_{(1,60)}$=9.086, p=0.0038, followed by Sidak *post hoc* test) compared to Cre-positive mice, with main effects of Cre decreasing total exploration time ($F_{(1,60)}$=8.363, p=0.0053) and time around novel objects ($F_{(1,60)}$=5.908, p=0.0181). Thus, *FosB* SGZ knockout induces a deficit in hippocampus-dependent learning.

Discussion

In this chapter I used NtsR2$^{Cre/+,GFP}$ mice crossed onto the FosB$^{lox/lox}$ background to investigate the role of *FosB* in hippocampal SGZ cells. NtsR2 labeling has previously indicated glia and has not been explicitly characterized on neurons throughout the adult brain[330, 357]. Nevertheless, NtsR2 has reported in the dentate gyrus of both rodents [357] and primates[363]. As the scope of this study was to explore subregion specific effects on learning and memory, the NtsR$^{Cre/+,GFP}$ line allowed me to limit Cre-mediated deletion of FosB to a discrete cell population in the hippocampus to investigate how the *FosB* gene affected both neurogenesis and learning.

Previous studies of hippocampal ΔFosB could not address neither subregion nor cell type specificity, as they employed either germline whole body knockouts, local viral effects, or correlations[324, 364, 365]. Here I show that specifically knocking out *FosB* in a subset of DG and CA3 cells overlapping strongly with the SGZ caused both reduced cellular proliferation in the SGZ and learning deficits, without altering basal anxiety or locomotor behavior. Changes in neurogenesis have been causally linked to stress-induced

behaviors and antidepressant efficacy[72, 229, 235], while fluoxetine increases memory retrieval and cognitive flexibility processes in hippocampal dependent tasks such as the T-maze, NOR, and the Barnes maze, but not memory acquisition[366-368]. Importantly fluoxetine induces neurogenesis concurrently with increased long-term memory performance[368, 369]. These studies suggest that *FosB* gene products may be a molecular mechanism that underlies these two effects. This is intriguing as standard treatment with SSRIs requires several weeks for efficacy, pointing to long-term changes in the brain mediating antidepressant responses as opposed to acute actions at serotonin receptors. Although the timeline for antidepressant response is consistent with the timeline for neuronal maturation[203, 234], the specific molecular mechanisms which underlie neuronal division, survival, and maturation are incompletely understood.

Previous work has highlighted that ΔFosB's long half-life contributes to prolonged effects of gene expression[307, 308], and indeed its accumulation in the NAc is critical for resilience to stress and the antidepressant effects of fluoxetine[292, 305]. In addition, ΔFosB is also induced in the dHPC after stress and several antidepressant treatment regimens including fluoxetine, ketamine, and exercise, and it is necessary in the ventral CA3 for the prophylactic effects of the non-traditional antidepressant ketamine[284, 326, 348, 370]. The finding that knocking out *FosB* in a subset of SGZ cells reduced cell proliferation is concordant with the idea that hippocampal *FosB* gene products, including ΔFosB, support fluoxetine-induced neurogenesis and perhaps adaptive responses to stress.

Hippocampal ΔFosB is also linked to preclinical models of comorbid diseases which have cognitive associated deficits, like Alzheimer's disease and epilepsy. Germline *FosB* KO

mice have depressive phenotypes and spontaneous seizures[324]. In addition, ΔFosB accumulates in the dHPC in response to natural seizures, kainic acid, and pilocarpine models of epilepsy, as well as in Alzheimer's disease mouse models and patients [324, 371, 372]. This accumulation could be neuroprotective, but general ΔFosB viral overexpression in the dHPC results in impaired cognition, while viral inhibition of ΔFosB impairs cognition in wild type mice but prevents cognitive decline in an Alzheimer's model[306, 314]. Coupled with data from this chapter that shows SGZ *FosB* is necessary for normal cognition, this suggests that cell-specific hippocampal ΔFosB is necessary for normal cognition, but aberrant or non-specific ΔFosB may result in cognitive deficits.

The importance of appropriate expression of ΔFosB in normal behavior is reinforced by its unique molecular characteristics. ΔFosB accumulation in the dHPC results in a number of downstream changes in gene expression, including epigenetic alterations at target genes. Of note is histone deacetylation at the *Calb1* gene, a calcium binding protein and marker of mature neurons[314, 315, 371, 373], whose regulation by ΔFosB may be critical for the altered neurogenesis I report in *FosB* SGZ knockout. Alternatively, ΔFosB may directly regulate microglia through C5aR1 and C5aR2[321], and this in turn may elicit the altered neurogenesis I report in *FosB SGZ* knockout[374]. Thus, future studies from our group will focus on identifying downstream transcriptional targets of ΔFosB in both glia and neurons to provide insight into mechanisms of hippocampal function and potential insight into diseases in which neurogenesis may play a role, such as Alzheimer's disease and depression.

The experiments I performed in this chapter suggest that *FosB* gene products in DG neurons are critical for hippocampal neurogenesis and learning. However, these studies

suggest that dHPC, but not vHPC are preferentially impacted by this manipulation under baseline conditions. As dHPC and vHPC are thought to have differential contributions to non-valenced and affective memories, in the next chapter I sought to test the contributions of ΔFosB in the vHPC during stress contexts.

CHAPTER 4: CIRCUIT-SPECIFIC HIPPOCAMPAL ΔFOSB UNDERLIES RESILIENCE TO STRESS

Author contributions:

Conceived and designed the experiments: Manning, Eagle, and Robison

Performed the experiments: Manning, Eagle, Williams, Bastle, Gawjewski, Wirtz, Akgun,

Analyzed the data: Williams, Manning, Robison

Contributed reagents/materials/analysis tools: , Ohnishi, Mazei-Robison, Maze, Neve

**Eagle and Manning contributed equally to this work, Eagle on electrophysiology and avoidance experiments and Manning on stress experiments*

Introduction

The ventral hippocampus (vHPC) is uniquely positioned to regulate emotional responses to stress that may underlie neuropsychiatric diseases such as depression, discussed in chapter 1[189, 375]. Glutamatergic vHPC neurons project to regions important in stress susceptibility and mood, including NAc and BLA, and activity of NAc-projecting vHPC neurons mediates reward behavior[376] and susceptibility to stress-induced social withdrawal[377]. However, we don't have a clear understanding of the dual role of the vHPC and its modulation of these target regions in depressive and anxiety disorders. Stress alters gene expression in vHPC neurons[378-380], but the molecular mechanisms underlying circuit-specific vHPC gene expression and activity in response to stress are poorly understood.

As discussed in chapter 1 and chapter 3, ΔFosB is a remarkably stable transcription factor[381, 382] found throughout the brain and induced by chronic neuronal activity[383].

ΔFosB has a well-established role in NAc in mediating stress susceptibility[305, 384, 385] and regulates synaptic and intrinsic properties of NAc medium spiny neurons[386]. It is also necessary in dorsal hippocampus (dHPC) for learning[337], and regulates the excitability of dHPC CA1 neurons[387]. ΔFosB is induced in dHPC by stress and antidepressant treatment[326, 328, 384, 388], and vHPC CA3 ΔFosB is critical for the prophylactic effects of ketamine on stress responses[388]. This indicates that ΔFosB is a critical modulator of vHPC function and may orchestrate long-term alterations in gene-expression underlying depressive and anxiety disorders.

There are many viral and transgenic methods for manipulating and investigating a gene in a specific cell type or region within the brain. However, because we hypothesize that the *FosB* gene product ΔFosB plays a specific role in vHPC neurons projecting to NAc in resilience to anhedonia and social withdrawal following stress, we needed to develop a novel method to manipulate the expression of the *fosB* gene specifically in these neurons, and not in other projections in the same brain region. Thus, we developed a dual-virus circuit-specific CRISPR gene editing system allowing the first circuit-specific mutation of genomic DNA in a living organism. Here, we use this technology to reveal a previously unknown role for ΔFosB in vHPC neurons projecting to NAc in resilience to

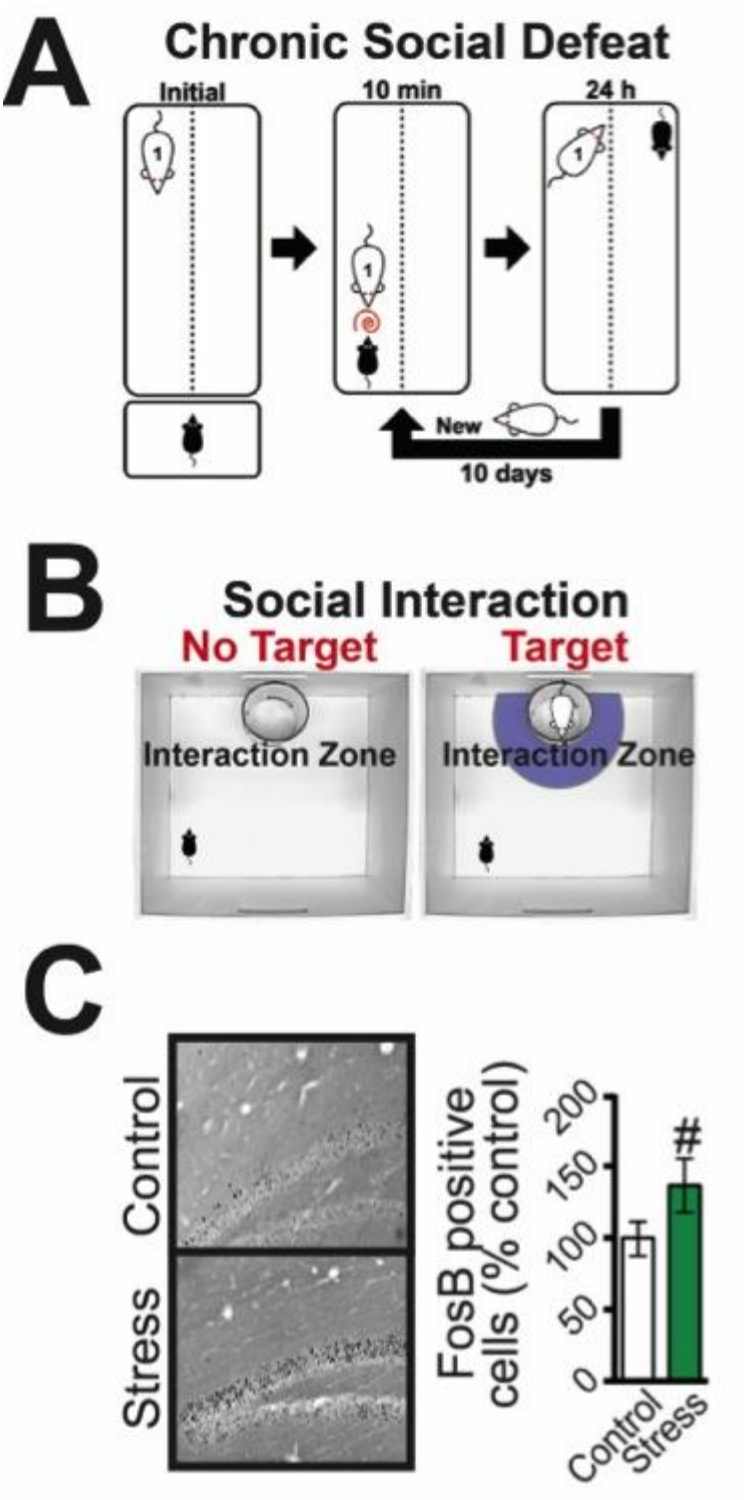

Figure 10 | Social defeat stress induces ΔFosB in ventral hippocampus. (A) Schematic of CSDS and **(B)** social interaction test. **(C, left)** Representative photomicrographs of coronal sections (4X) stained for ΔFosB in vHPC from control handled and stressed mice, quantified in **(C, right)** $^{\#}P<0.10$ (n=12 control, n=8 stress; independent samples t-test compared to control)**.**

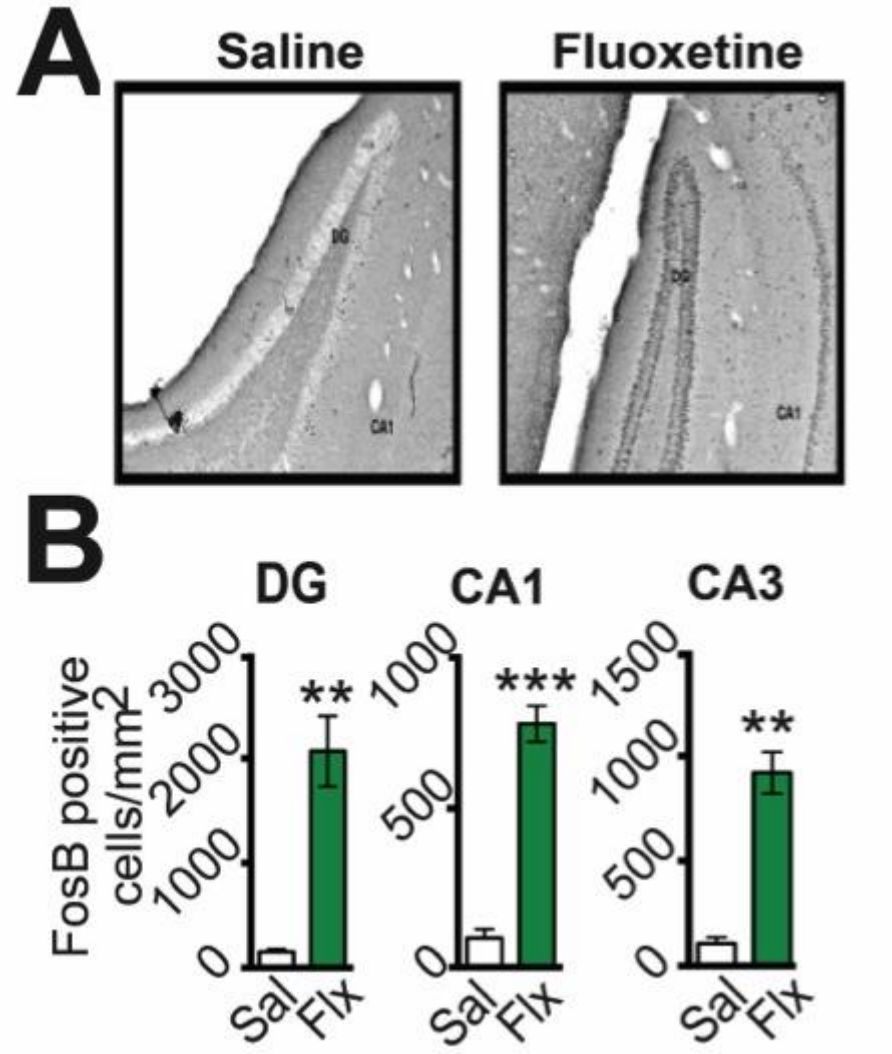

Figure 11 | Fluoxetine induces ΔFosB in ventral hippocampus. (A) Representative photomicrographs stained for ΔFosB in vHPC subregions (CA1, CA3, DG) from mice treated with chronic saline (Sal) or fluoxetine (Flx), quantified in **(B)** ***P*<0.01, ****P*<0.001 (n=4 saline, n=4 fluoxetine; independent samples t-tests compared to saline). (n=12 control, n=8 stress; independent samples t-test compared to control)**.**

social defeat stress-induced social avoidance. Furthermore, we show that ΔFosB regulates the excitability of this circuit and we identify potential downstream gene targets in this circuit that may underlie stress resilience.

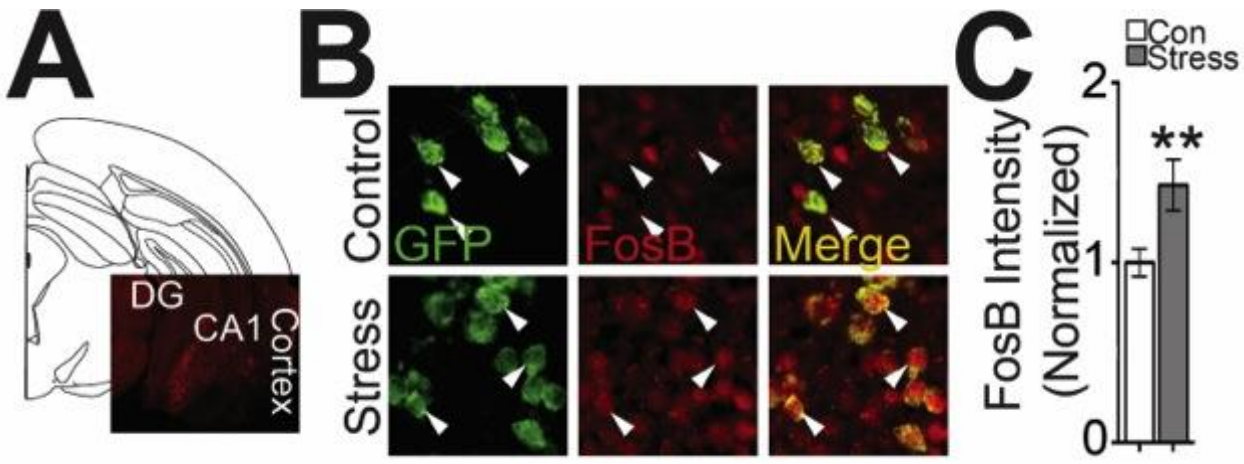

Figure 12 | ΔFosB accumulates in vHPC neurons projecting to NAc after CSDS. **(A)** Schematic and coronal section (4X) showing mCherry expression in vHPC of mice infused with retrograde mCherry in NAc 3 weeks prior to sacrifice **(B)** Representative images of vHPC CA1 coronal sections (40X) showing immunofluorescent labeling of NAc-projecting neurons expressing GFP (left), ΔFosB (red, middle) and merge (right). Stressed mice (bottom panels; n=109 cells) show increased ΔFosB signal in GFP-positive cells compared to controls (top panels; n=147 cells), as indicated by white arrows and quantified in **(C)** $^{**}P<0.01$ (independent samples t-test compared to Control).

Results

ΔFosB is induced in vHPC by Stress and Antidepressants:

To investigate the induction of ΔFosB in vHPC by stress, we exposed male C57Bl6/J mice to chronic social defeat stress (CSDS, Fig 10A), which produces a depressive-like anhedonia and social avoidant phenotype in stress-susceptible mice (measure through SI, Fig 10B)[46, 389, 390]. Stress increased the number of ΔFosB+ dentate gyrus neurons in vHPC (Fig 10C). Expanding upon our previous findings in the dHPC[326, 328], we found that ΔFosB was also induced in all subregions of the vHPC following repeated treatment with the antidepressant fluoxetine (Fig 11A,B), a selective serotoninreuptake inhibitor. Thus, ΔFosB is induced in vHPC by both stress and antidepressants, which

strongly suggests that stress-induction of ΔFosB in vHPC is a compensatory response to counteract the effects of stress, i.e. mediating stress resilience as it does in NAc[305]. Because the excitability of afferent projections from vHPC CA1 extending to NAc mediate CSDS susceptibility[377] and ΔFosB regulates excitability of dHPC CA1 neurons[387], we set out to investigate the role of vHPC projection neuron ΔFosB in CSDS susceptibility. To label vHPC-NAc neurons, we utilized a mouse line expressing Cre-dependent GFP (*Rosa26*$^{eGFP\text{-}L10a}$), and injected into NAc a persistent, retrograde viral vector expressing Cre (HSV-hEf1α-Cre). 3 weeks after surgery into the NAc, expression of retrograde viral vectors can be observed in ventral CA1 of vHPC (vCA1) and in ventral subiculum (vSub) (Fig 12A). Mice were then exposed to CSDS and immunostained for ΔFosB and GFP, and we found that CSDS induced ΔFosB in vHPC-

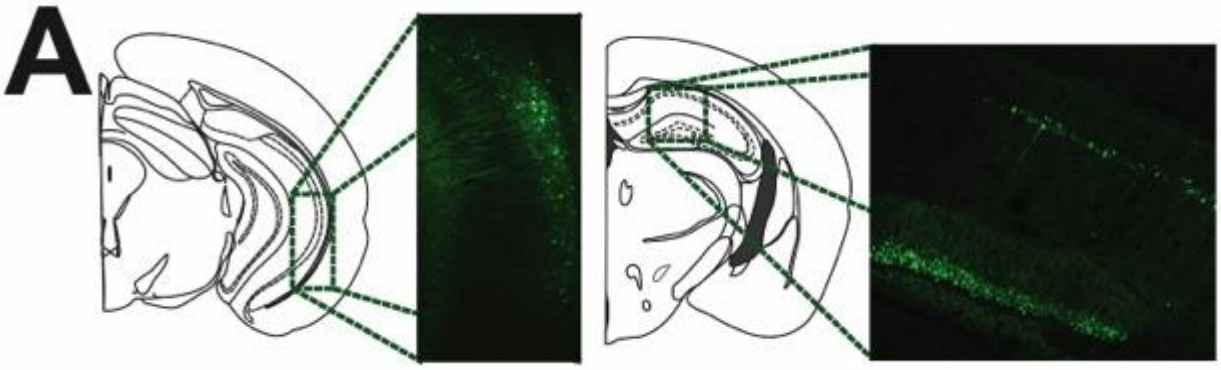

Figure 13 | Targeting of dorsal and ventral hippocampus. (A) Representative figures and coronal sections showing viral-mediated GFP expression in ventral and dorsal HPC.

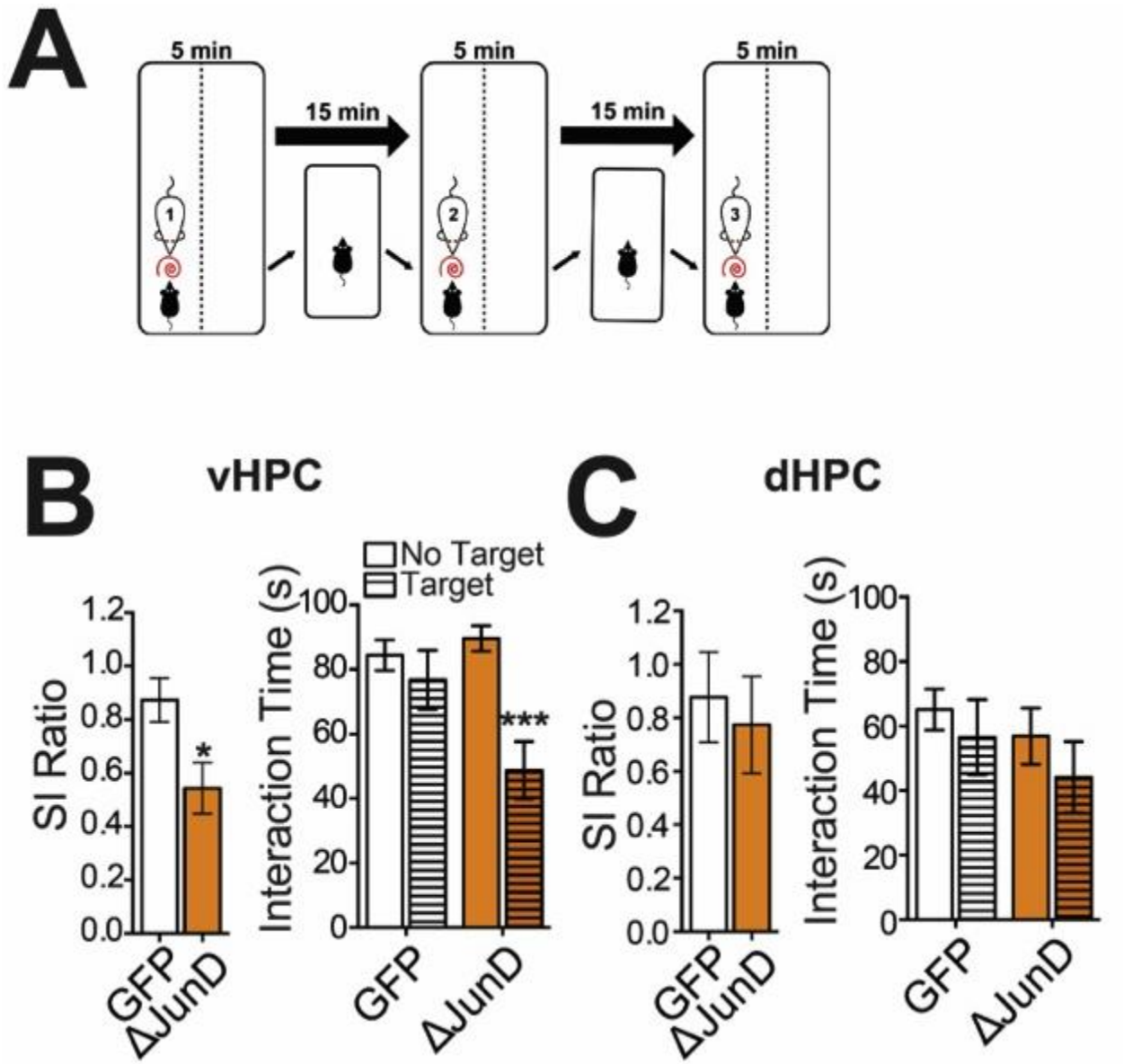

Figure 14 | ΔFosB expression in the ventral hippocampus is necessary for CSDS resilience. (A) Experimental design for subthreshold defeat. **(B)** ΔJunD inhibition of ΔFosB in vHPC reduced SI ratio (left) and decreased investigation time of the social target (right). **P*<0.05, ****P*<0.001 (n=19 GFP, n=18 ΔJunD; SI ratio: independent samples t-test compared to GFP; Investigation time: two-way mixed ANOVA with Holm-Sidak post-test GFP No Target vs Target). **(C)** ΔJunD expression in dHPC did not affect stress-induced social avoidance (n=9/group).

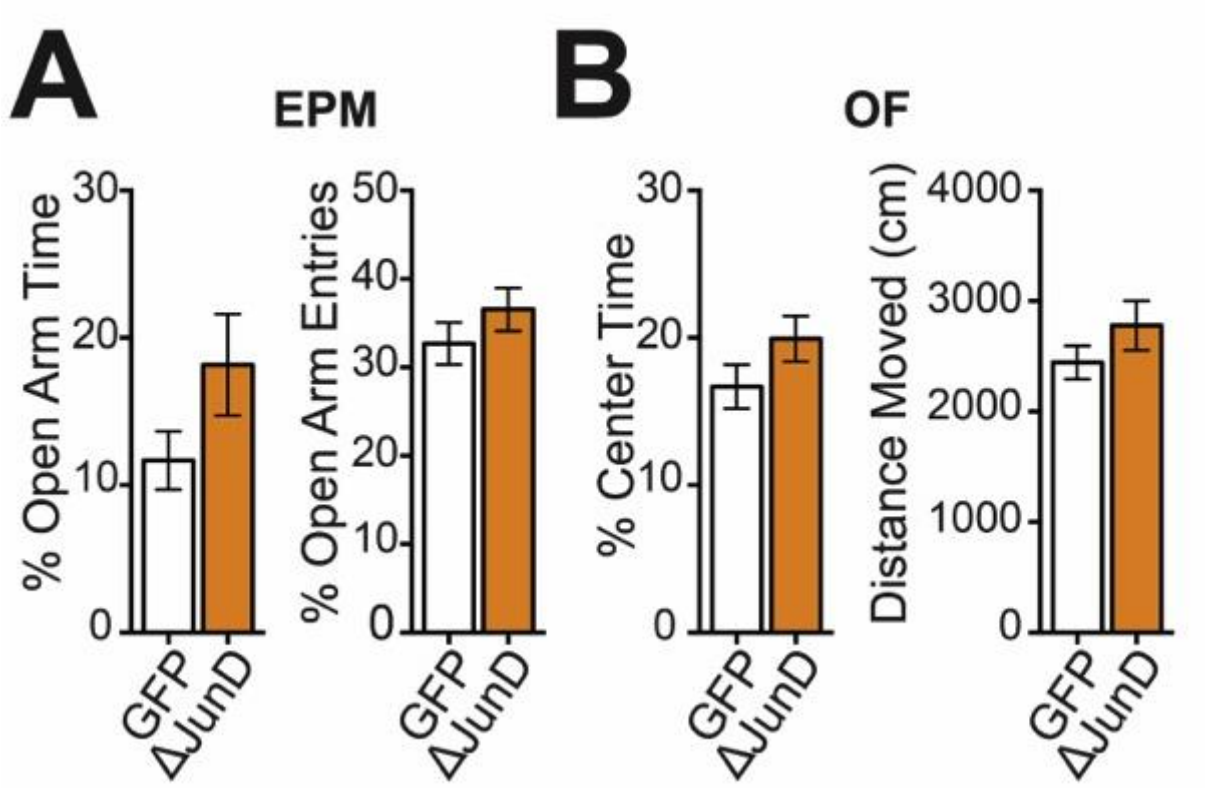

Figure 15 | ΔFosB inhibition in ventral hippocampus does not alter locomotor activity or anxiety-like behavior. (A) ΔJunD expression in vHPC caused no differences in time spent in the open arms or entries into the open arms of elevated plus maze (n=11 GFP, n=14 ΔJunD). **(B)** ΔJunD expression in vHPC did not alter time spent in the center of an open field or total distance moved.

NAc projections (Fig 12B,C), demonstrating that chronic stress increases ΔFosB expression in vHPC neurons projecting to NAc.

ΔFosB in vHPC is necessary for stress resilience:

To probe whether ΔFosB-mediated transcriptional regulation in vHPC is critical in stress resilience, we virally overexpressed ΔJunD, a mutant of ΔFosB binding partner and transcriptional inhibitor of ΔFosB[305], in either the vHPC or dHPC (Fig 13A) and exposed mice to a subthreshold microdefeat stress (Fig 14A) which produces a social avoidant phenotype only in mice sensitized to stress[389, 390]. Transcriptional inhibition of ΔFosB in vHPC reduced social interaction and ΔJunD mice spent less time interacting with a

social target (Fig 14B). Conversely, inhibition of ΔFosB in dHPC did not produce a stress susceptible phenotype (Fig 14C). Furthermore, vHPC ΔFosB inhibition but did not affect baseline (unstressed) anxiety or locomotor activit1y (Fig 5A,B). Thus, ΔFosB is induced in vHPC following stress, and its function in vHPC is necessary for resilience to stress, but its circuit-specific role remained unknown.

Development of *FosB* targeted CRISPR/Cas9 System:

Because tools to test the circuit-specific role of an individual gene have not previously been described, we developed an innovative CRISPR-Cas9 viral toolset to manipulate ΔFosB expression in a circuit-specific manner (Figs 16, 17, and 18; chapter 2). Using CRISPR, we developed and screened guide RNAs (gRNA) specific to the *FosB* gene, which encodes ΔFosB, and tested these in cultured mouse neuroblastoma (Neuro2A) cells. Transfection of cells with Cas9 and gRNA specific to exon I of the *FosB* gene reduced ΔFosB expression (gRNA2; Fig 16A,B). To confirm this *in vivo*, an HSV expressing GFP and both Cas9 and the gRNA was infused into dHPC of adult mice. Transduced dHPC neurons had significantly reduced ΔFosB expression compared to GFP only controls (Fig 17A,B), indicating that the CRISPR-Cas9 vector successfully mutated the *FosB* gene and silenced expression of ΔFosB protein (*FosB* KO) in mouse brain.

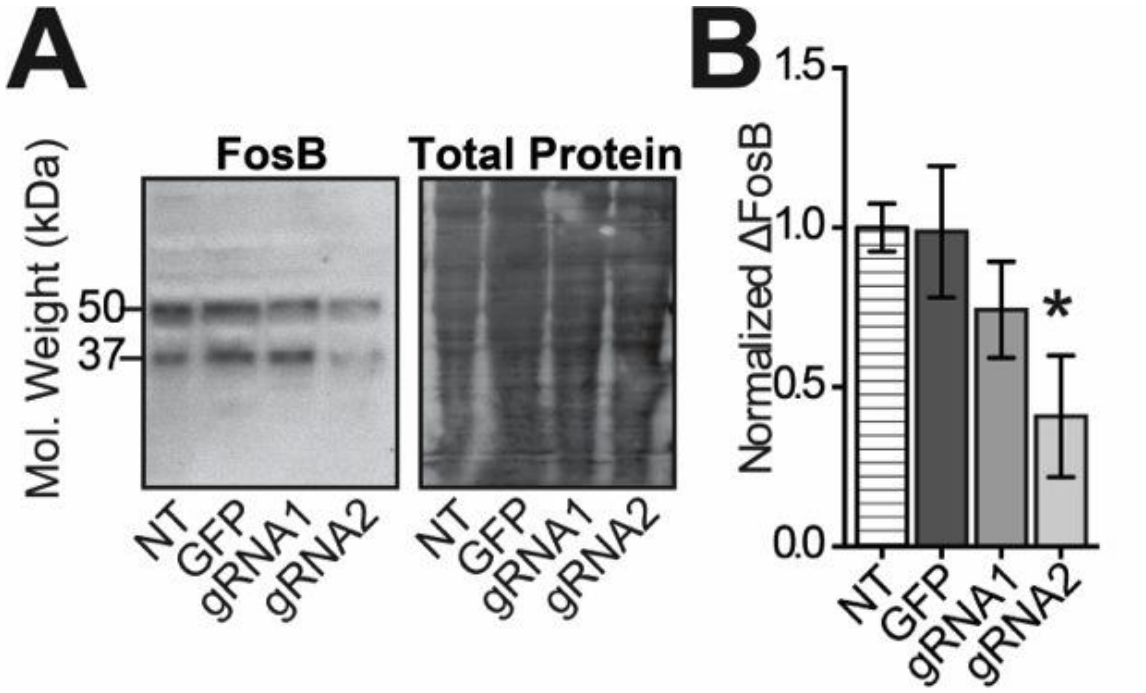

Figure 16 | Development of CRISPR/Cas9 guideRNA to knockout *FosB*. (A) Representative Western blot showing FosB (55 kDa) and ΔFosB (37 kDa) and total protein stain from Neuro2A cells that were not transfected (NT) or transfected with GFP, or Cas9 plus guide RNAs specific to the FosB gene; quantified in **(B)** **P*<0.05 (n=4/group; independent samples t-test).

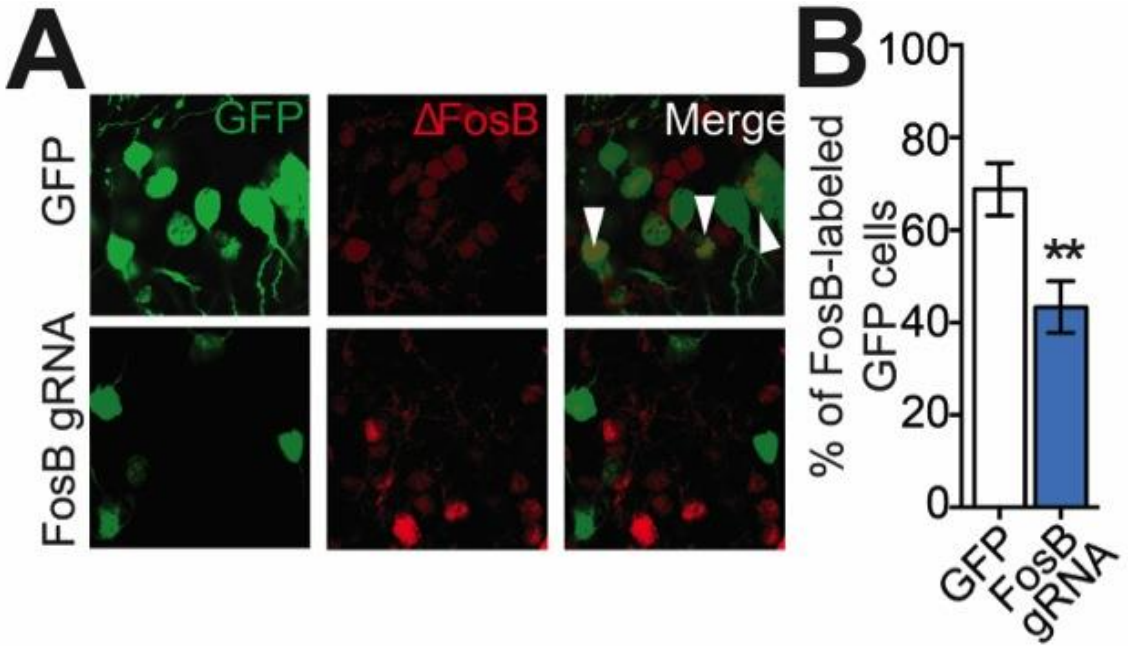

Figure 17 | *In vivo* validation of CRISPR/Cas9 constructs to knockout *FosB*. (A) Representative images (100x) from dHPC of mice infused with HSV expressing GFP or GFP plus Cas9 and FosB gRNA2 stained for GFP and ΔFosB. Percentage of FosB-positive cells quantified in **(B)** ***P*<0.01 (n=8 GFP, n=17 FosB gRNA; independent samples t-test compared to GFP alone).

To produce a circuit-specific tool to efficiently target *FosB* gene expression only in specific vHPC afferent neurons, we split the CRISPR constructs (Cas9 and gRNA) into two separate viral vectors to allow a circuit-specific intersection approach (Fig 18A). Thus, we injected a retrograde viral vector into a projection target region and a locally expressing vector into the somatic region. Retrograde virus encoded a Cre-dependent Cas9 (HSV-hEf1α-LS1L-Cas9) and was injected into NAc; mice were allowed to recover for three weeks for maximal retrograde expression. We then injected into the vCA1/vSub an HSV that locally-expresses Cre and *FosB* gRNA (HSV-IE4/5-TB-gRNA-eYFP-CMV-IRES-Cre), or control HSV (HSV-IE4/5-TB-eYFP-CMV-IRES-Cre). Similar to our finding with the single-vector CRISPR strategy, the dual vector approach specifically reduces the expression of ΔFosB in co-labeled GFP and Cas9 vHPC cells, i.e. in NAc-projecting vHPC neurons (Fig 18B-D). Thus, this system mutates the *FosB* gene and decreases ΔFosB expression in a circuit-specific manner, allowing investigation of *FosB* gene products' contributions to affective behavior in vHPC afferents.

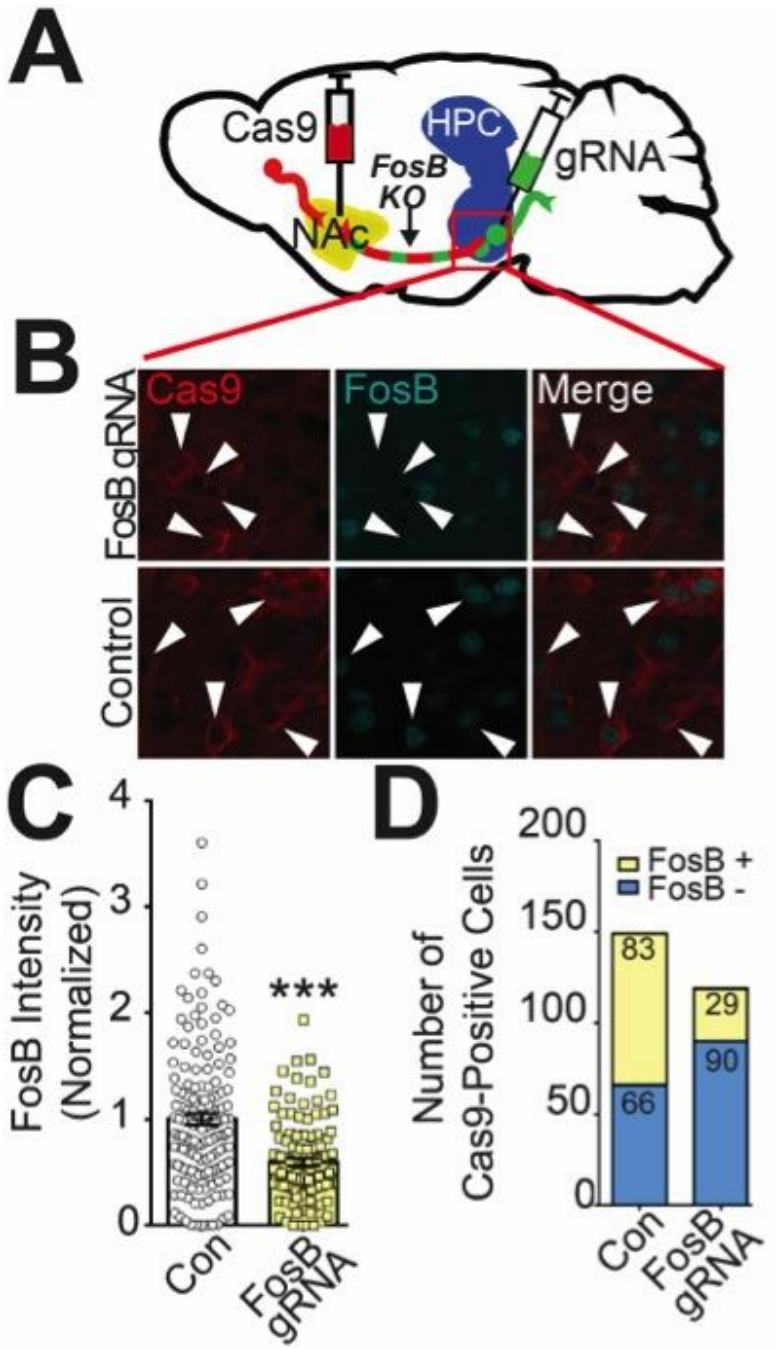

Figure 18 | Validation of circuit-specific *FosB* knockout. (A) Illustration of dual vector experiment design to knockout *FosB* in vHPC neurons projecting to NAc. Retrograde virus expressing Cre-dependent Cas9 is injected into NAc while local vector expressing FosB gRNA and Cre is infused into vHPC. *FosB* knockout (FosB KO, red & green) occurs in co-transduced NAc-projecting vHPC neurons. **(B)** Representative images of Cas9 (red, left), FosB (cyan, middle), and merged image from vHPC of mice that receive control (no gRNA) or *FosB* KO vectors (FosB gRNA). Intensity of FosB staining quantified in **(C)** ***P<0.001 (n=149 control cells; n=119 FosB gRNA cells; independent samples t-test compared to control). **(D)** Qualitative analysis of number of Cas9+ cells co-expressing FosB in the nucleus.

Circuit-specific silencing of the *FosB* gene reveals dissociable roles of vHPC-NAc and vHPC-BLA in stress phenotypes:

Previously, vHPC-NAc excitability has been shown to underlie resilience to social stress, while ΔFosB reduces the excitability of HPC neurons [127, 337]. As our tool produced a circuit-specific reduction in ΔFosB protein expression in vHPC cells projecting to NAc, we then examined if *FosB* gene products in this circuit were necessary for resilience to CSDS. Adult mice that received *FosB* KO in the vHPC-NAc circuit (Fig 19A) were subjected to CSDS and assayed for social avoidance. *FosB* KO in vHPC-NAc enhanced stress-induced social avoidance (Fig 19B) and caused a small decrease in locomotor activity (Fig 19C). These findings suggest that ΔFosB likely regulates locomotor activity and stress susceptibility through the vHPC-NAc circuit. This is consistent with previous reports showing that vHPC afferents to NAc regulate locomotor activity [391, 392]. It is critical to note that this manipulation of *FosB* in vHPC-NAc neurons did not affect passive avoidance learning (Fig 20A) or baseline anxiety (Fig 20B), behaviors not associated with vHPC-NAc projections. Therefore, ΔFosB expression in vHPC-NAc afferents appears to be critical for a normal response to stress, and in its absence, mice are sensitized specifically to the social aspects of this stress response. Taken together, these data reveal that vHPC *FosB* gene products regulate phenotypes in a circuit-specific manner and provide rationale for previously dissonant findings about vHPC's role in stress behaviors.

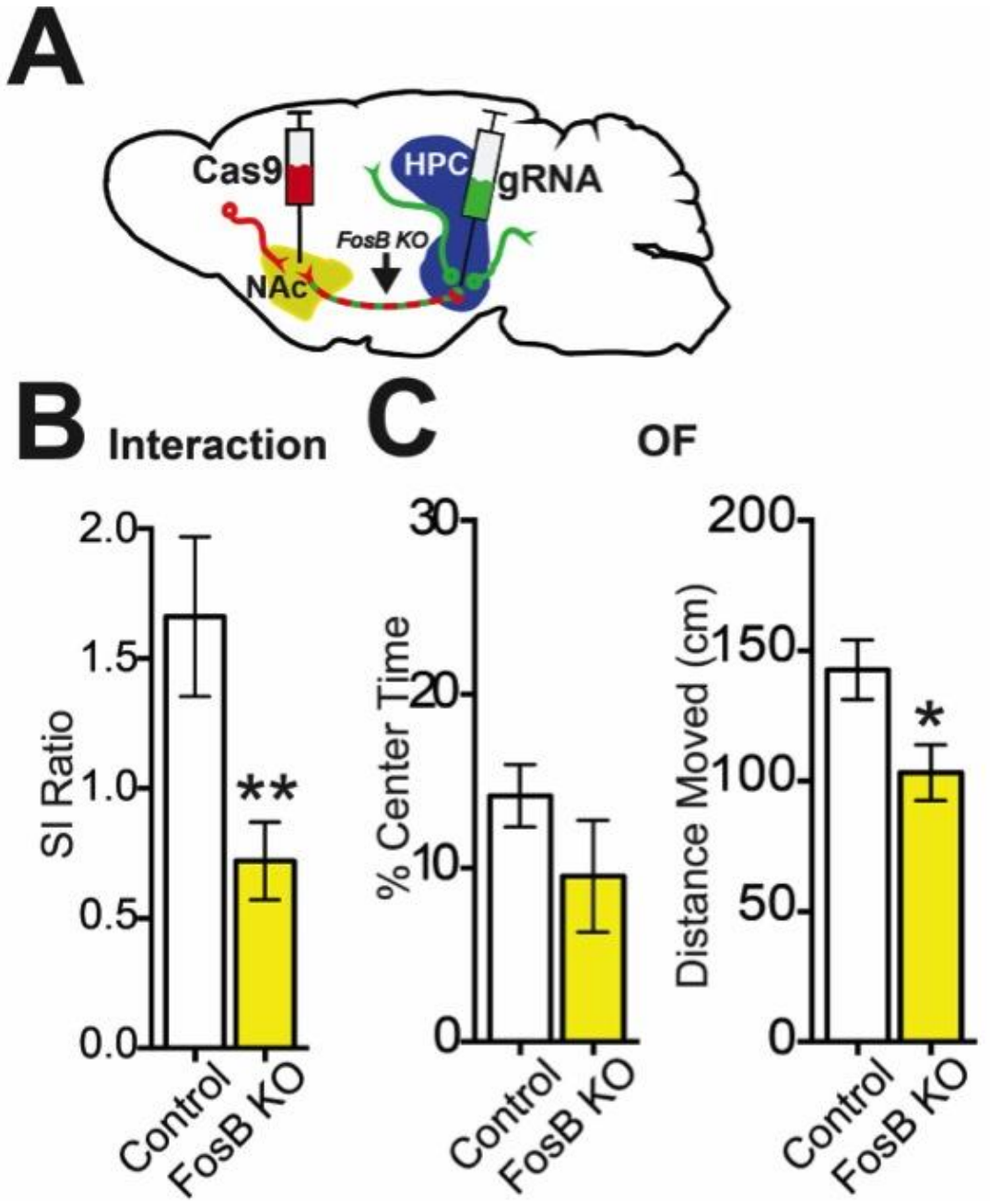

Figure 19 | Circuit-specific silencing of *FosB* gene in ventral hippocampal afferents to nucleus accumbens. (A) Schematic of dual-vector CRISPR tool to silence *FosB* in vHPC-NAc afferent neurons. Retrograde vector expressing Cre-dependent Cas9 (Cas9; red) is injected into NAc while local vector expressing Cre and *FosB* guide RNA (gRNA; green) is injected into vHPC. *FosB* silencing (*FosB* KO) occurs only in co-transduced vHPC-NAc neurons. **(B)** *FosB* silencing in vHPC-NAc neurons heightens stress-induced social avoidance. ***P*<0.01 (n=6 control, n=9 FosB KO; independent samples t-test compared to control). **(C, left)** *FosB* knockout in vHPC-NAc neurons reduces total activity in the open field, **(C,right)** but not time spent in the center. **P*<0.05 (n=7 control, n=8 FosB KO; independent samples t-test compared to Control).

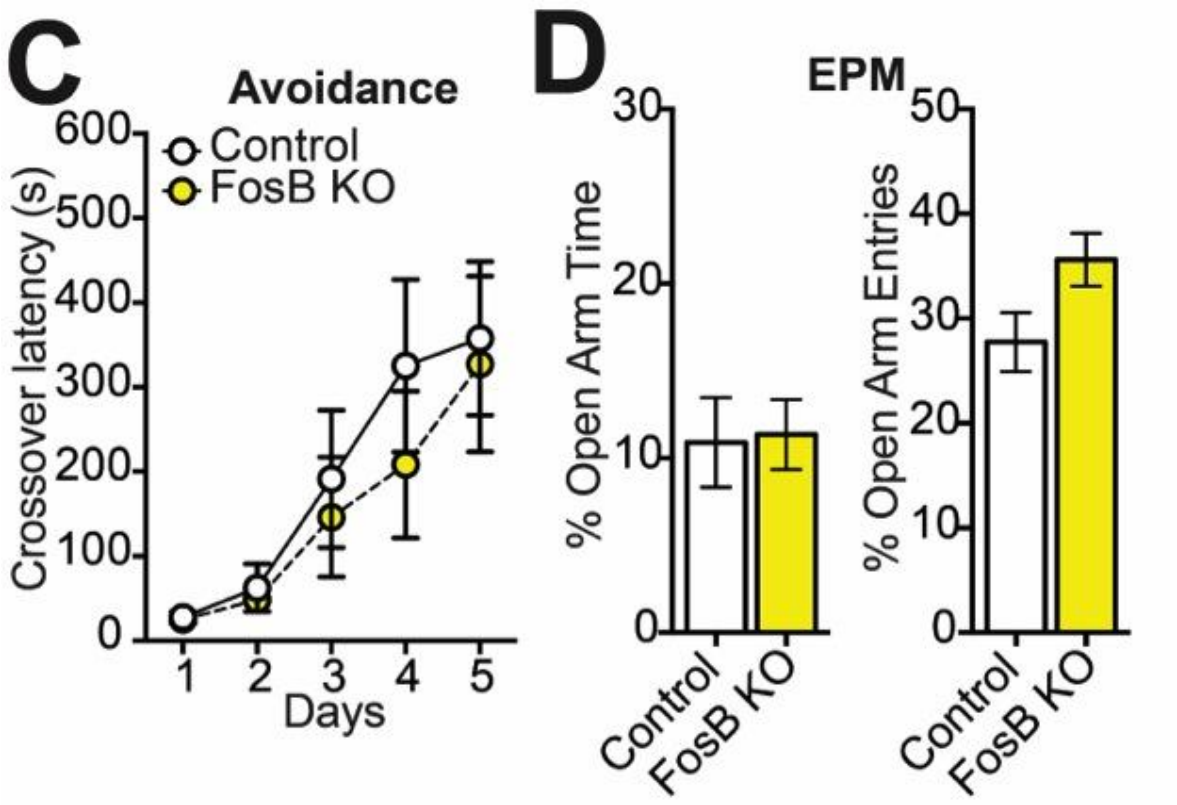

Figure 20 | *FosB* knockout in vHPC-NAc on anxiety-like behavior. (A) Dual-vector CRISPR *FosB* silencing in vHPC-NAc does not affect crossover latency in the passive avoidance learning paradigm (n=7 control, n=8 FosB KO), or **(D)** anxiety-like behavior in the elevated plus maze (EPM). t-test compared to control).

vHPC sends projections to other brain regions implicated in stress responses, including the basolateral amygdala (BLA), an area important in fear learning and anxiety[393-395]. In order to determine the circuit-specificity of our ΔFosB manipulations, we also assessed stress-induced social avoidance after *FosB* KO in the vHPC-BLA circuit (Fig 21A). *FosB* KO in vHPC-BLA did not impair stress-induced social avoidance or locomotor activity (Fig 21B,C). Interestingly, however, it significantly impaired passive avoidance learning (Fig 22A) and reduced anxiety-like behavior (Fig 22B). Similar observations, e.g. decreased anxiety, fear expression, and fear extinction, have been shown after vHPC lesions[375, 395, 396], which suggests that ΔFosB in vHPC-BLA projections is necessary for the expression of fear and anxiety and that knockout of ΔFosB in this circuit is anxiolytic.

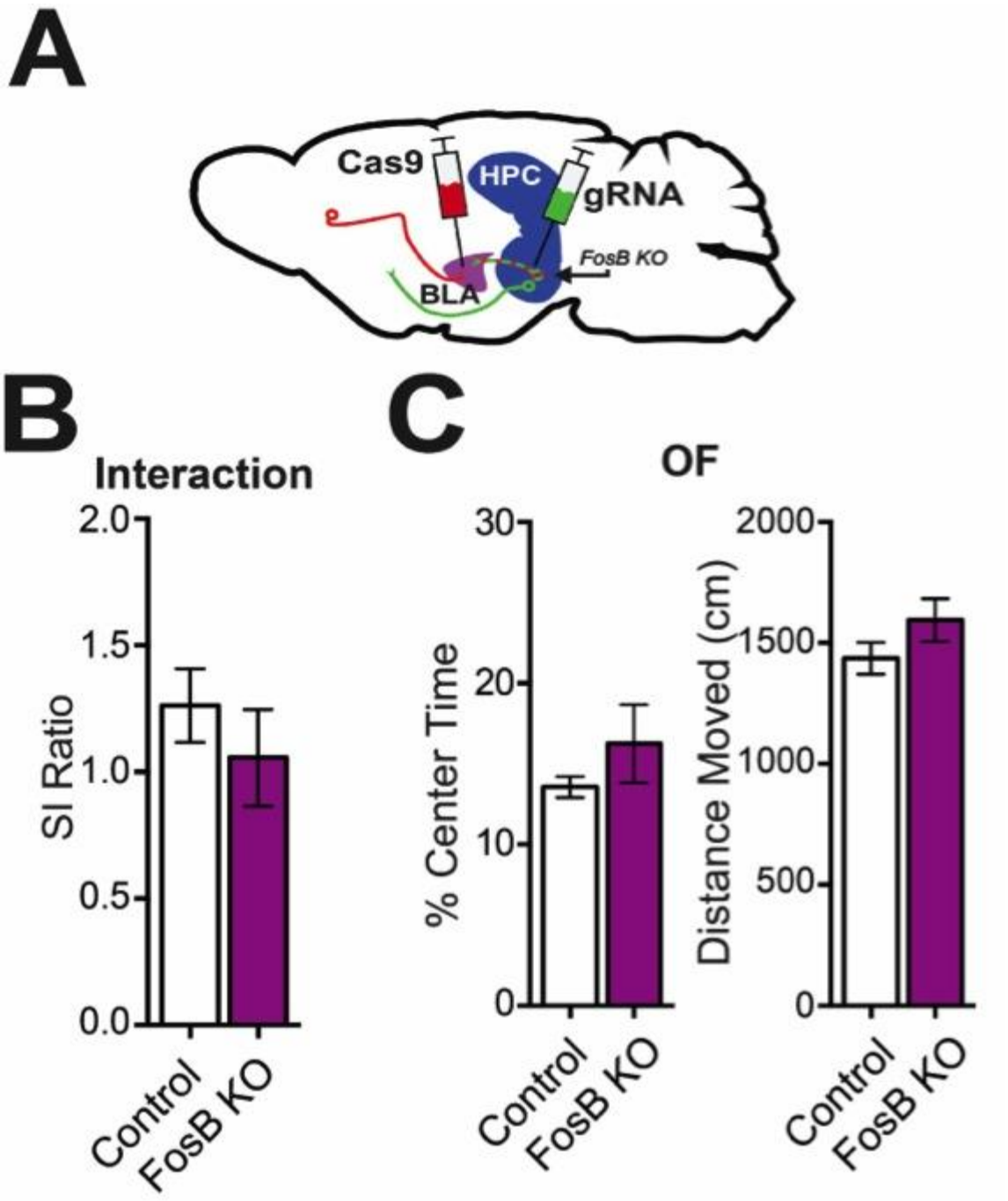

Figure 21 | Circuit-specific silencing of *FosB* gene in ventral hippocampal projection neurons to amygdala. (A) Schematic of dual-vector CRISPR silencing *FosB* in vHPC-BLA neurons. **(B)** *FosB* silencing in vHPC-BLA does not affect stress-induced social avoidance (n=11 control, n=10 FosB KO). **(C)** Locomotor activity was unaffected by CRISPR *FosB* knockout in vHPC-BLA neurons (n=6 control, n=8 FosB KO).

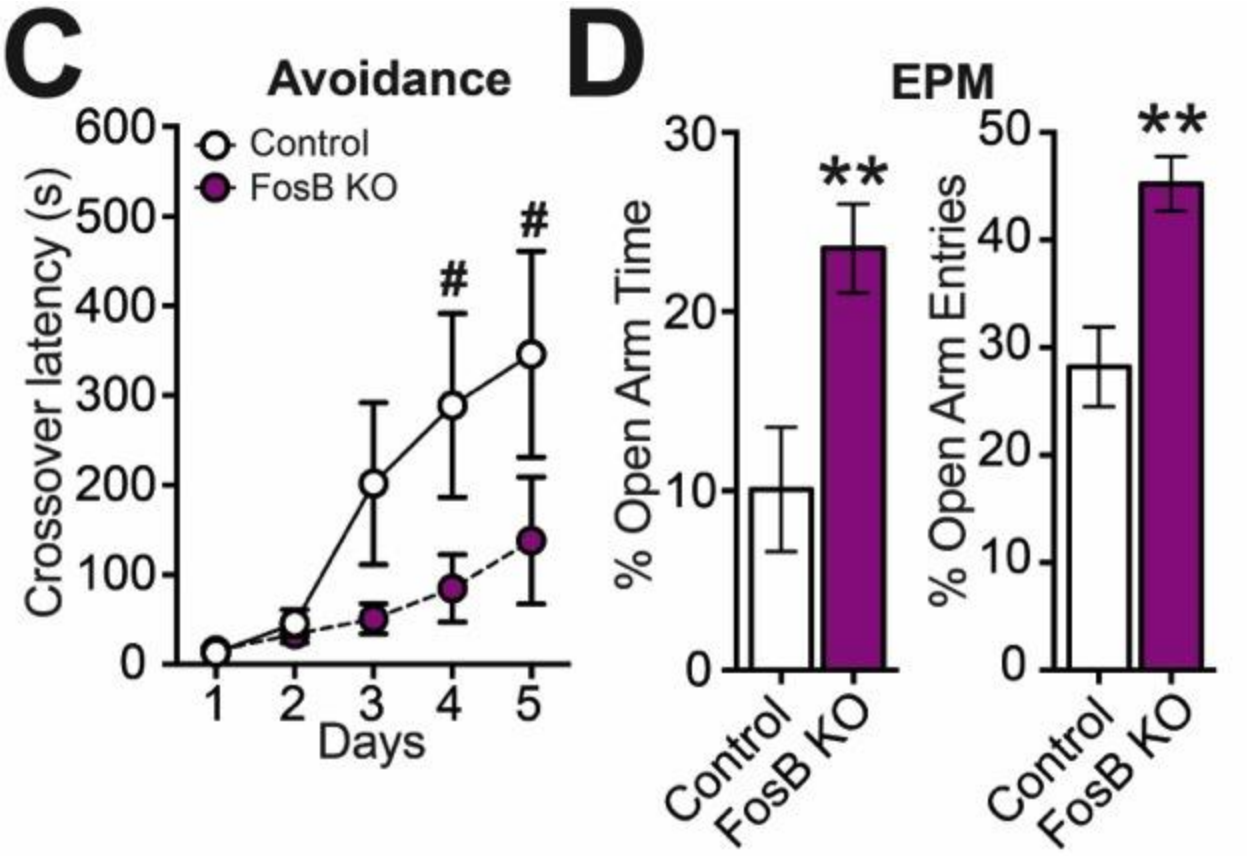

Figure 22 | *FosB* knockout in vHPC-BLA decreases anxiety-like behavior. (A) *FosB* silencing in vHPC-BLA impairs avoidance learning. $^{\#}P<0.10$ (n=6 control, n=8 FosB KO; two-way mixed ANOVA with Holm-Sidak post-tests compared to control). **(D)** *FosB* silencing in vHPC-BLA decreases anxiety-like behavior in the EPM, increasing time spent and entries into the open arms. $^{**}P<0.01$ (independent samples t-test compared to control).

Circuit-specific rescue of ΔFosB ameliorates effects of *FosB* silencing and is sufficient for stress resilience:

The *FosB* gene encodes multiple isoforms, including full-length FosB and ΔFosB, and neuronal activity induces both of these isoforms[282, 383, 397, 398]. It is therefore possible that any or all of these isoforms are important for the functional effects of *FosB* silencing in vHPC-NAc projections on stress-induced social avoidance. To investigate the specific role of ΔFosB in vHPC projections to NAc in stress-induced behaviors, we developed an additional intersecting viral strategy that would allow us to overexpress

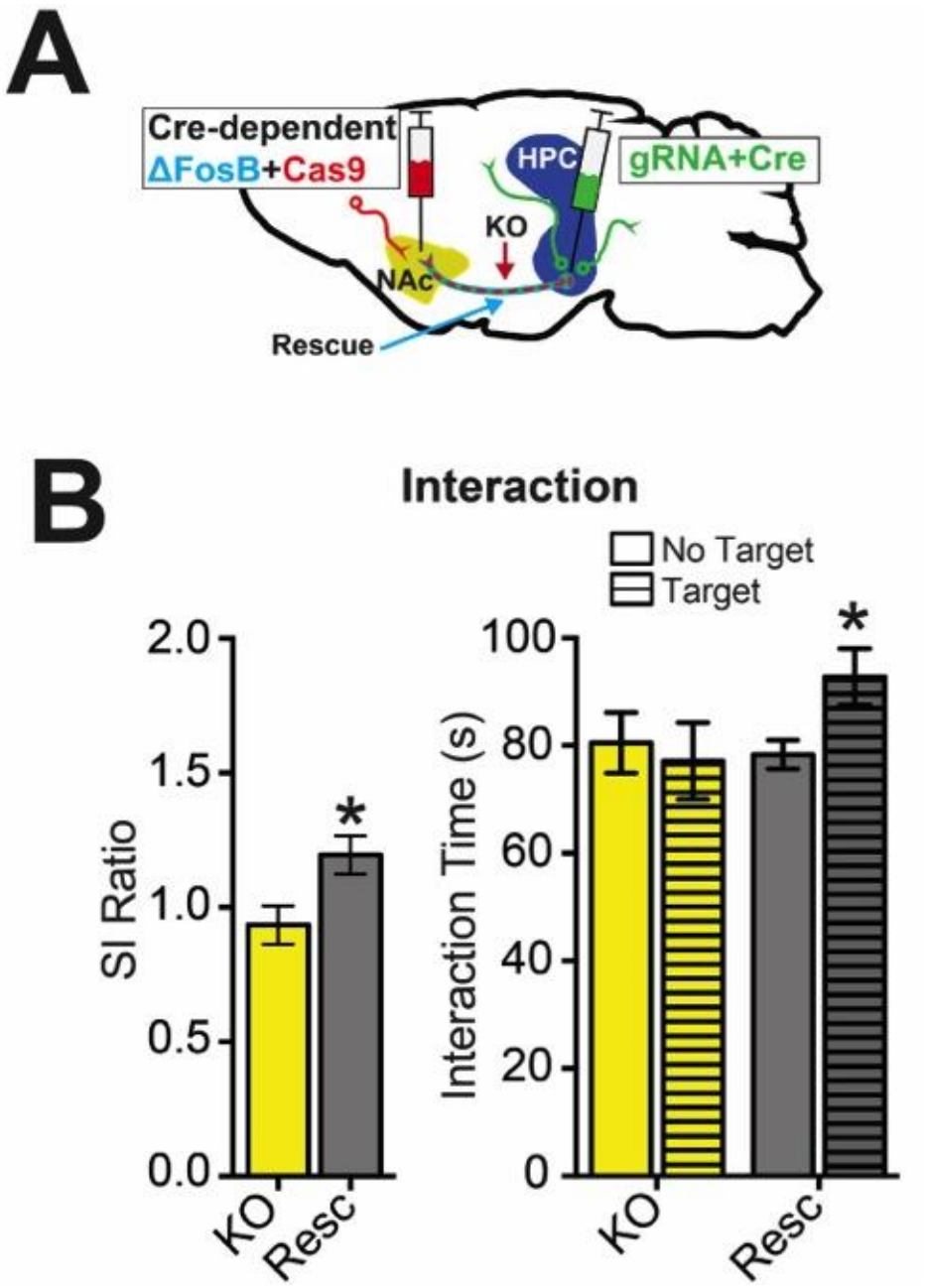

Figure 23 | Rescue of vHPC–NAc ΔFosB enhances stress resilience. (A) Schematic of ΔFosB rescue experiments in vHPC-NAc afferent neurons. **(B)** ΔFosB rescue (Resc) in vHPC-NAc neurons reverses stress-induced social avoidance, indicated by enhanced social interaction ratio (left) and increased investigation of a social target (right). **P*<0.05 (n=13 KO, n=12 Resc; SI ratio: independent samples t-test compared to KO; Investigation time: two-way mixed ANOVA with Holm-Sidak post-test KO No Target vs Target).

recombinant ΔFosB back into the same circuit in which we use CRISPR to silence *FosB* gene expression (Fig 23A). These tools cause retrograde Cre-dependent ΔFosB and Cas9 expression (Resc) or Cre-dependent Cas9 expression alone (KO). We injected these into NAc, and subsequently injected local HSV expressing Cre and the FosB gRNA into vHPC of adult mice (Fig 23A). Critically, ΔFosB rescue in *FosB* KO vHPC-NAc neurons reversed the enhancement in stress-induced social avoidance (Fig 23B). Similarly, ΔFosB rescue in *FosB* KO vHPC-BLA neurons (Fig 24A) blocked the *FosB* KO-mediated reduction in basal anxiety (Fig 24B) and impairment in avoidance learning (Fig 24C). To control for the presence of CRISPR-Cas9-mediated *FosB* KO, ΔFosB was independently overexpressed in these same circuits by injecting retrograde Cre-inducible ΔFosB in NAc or BLA (HSV- hEF1α-LSIL-ΔFosB) and persistent Cre (AAV2-CMV-Cre-GFP) into vHPC (Figs 26A, 28A), which produces ΔFosB over expression specifically in circuit-specific cells (Fig 25A,B). In the absence of *FosB* KO, ΔFosB overexpression did not affect basal anxiety (Figs 27A, 28C) or avoidance learning (Figs 27B, 28B) in either projection. This suggests that ΔFosB in vHPC-BLA is necessary, but not sufficient, for the expression of for the expression of fear and anxiety.Interestingly, we found that overexpression of ΔFosB in vHPC-NAc produced a resilient phenotype to stress-induced social avoidance (Fig 26B), coupled with a small decrease in locomotor activity (Fig 29A). Together these data elucidate a clear role for ΔFosB in vHPC projections: ΔFosB in vHPC-NAc is necessary and sufficient for resilience to stress, and ΔFosB in vHPC-BLA is necessary for the expression of fear and anxiety. Moreover, the complete behavioral rescue by ΔFosB overexpression in the same circuit in which we use the novel CRISPR system to silence the *FosB* gene indicates that our behavioral effects are indeed mediated

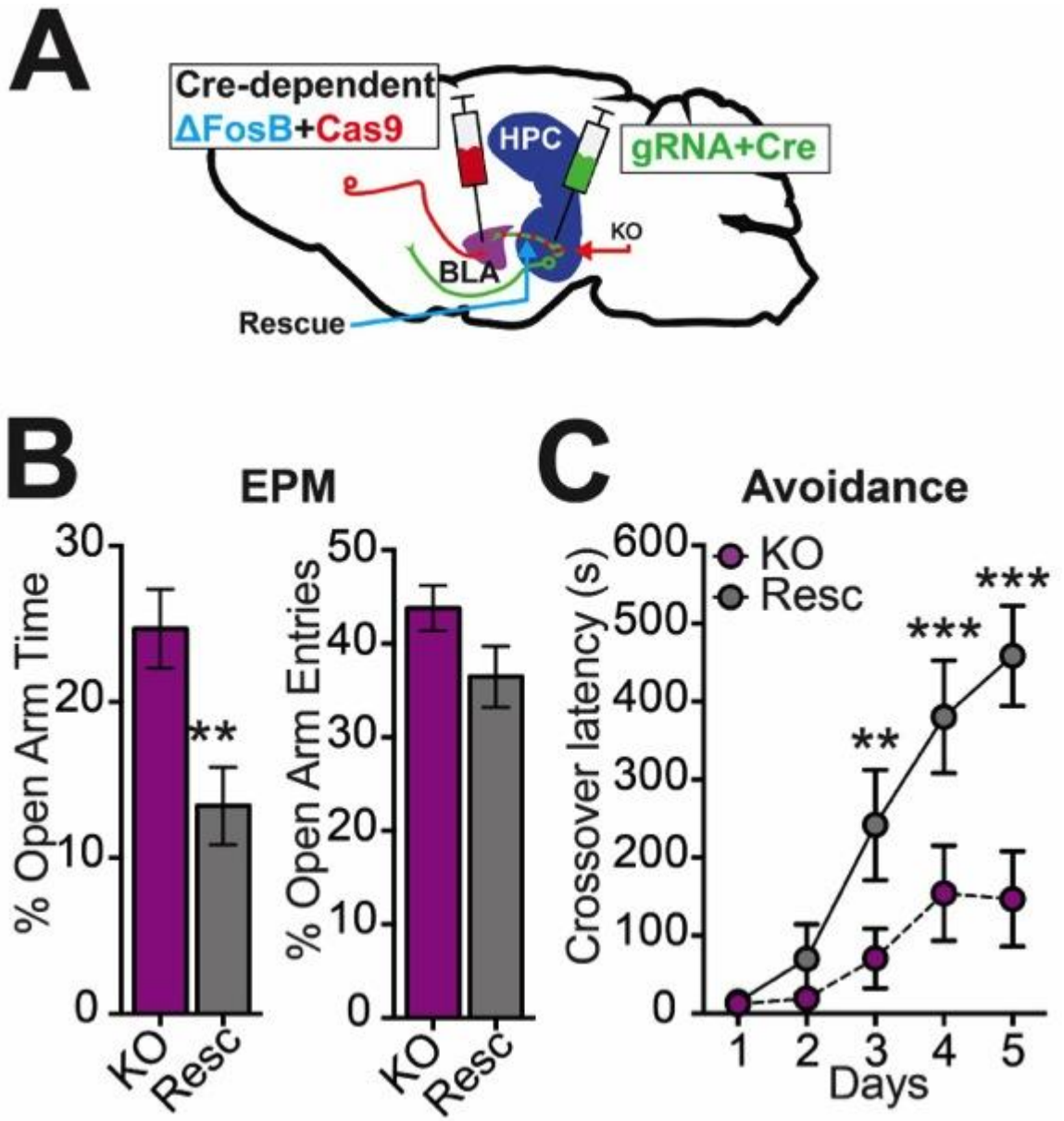

Figure 24 | Rescue of vHPC-BLA ΔFosB mediates anxiety-like behavior. (A) Schematic of ΔFosB rescue experiments in vHPC-BLA afferent neurons. **(B)** ΔFosB rescue in vHPC-BLA neurons reverses the anxiolytic effects of *FosB* silencing, decreasing open arm time in the EPM. ***P*<0.01 (n=15 KO, n=12 Resc; independent samples t-test compared to KO). **(C)** ΔFosB rescue also reverses avoidance learning impairment. ****P*<0.001 (two-way mixed ANOVA with Holm-Sidak post-tests compared to KO).

by *FosB* knockout, and not through off-target effects of the CRISPR system. Our results demonstrate that individual genes can have disparate roles within a single brain structure based not only on heterogenous cell types but on the specific projections of the neurons

in which they are expressed, which is a significant step toward illuminating the role of vHPC circuits in stress-related neuropsychiatric disease and a key finding to expand our understanding of the molecular mechanisms of complex brain functions and behaviors.

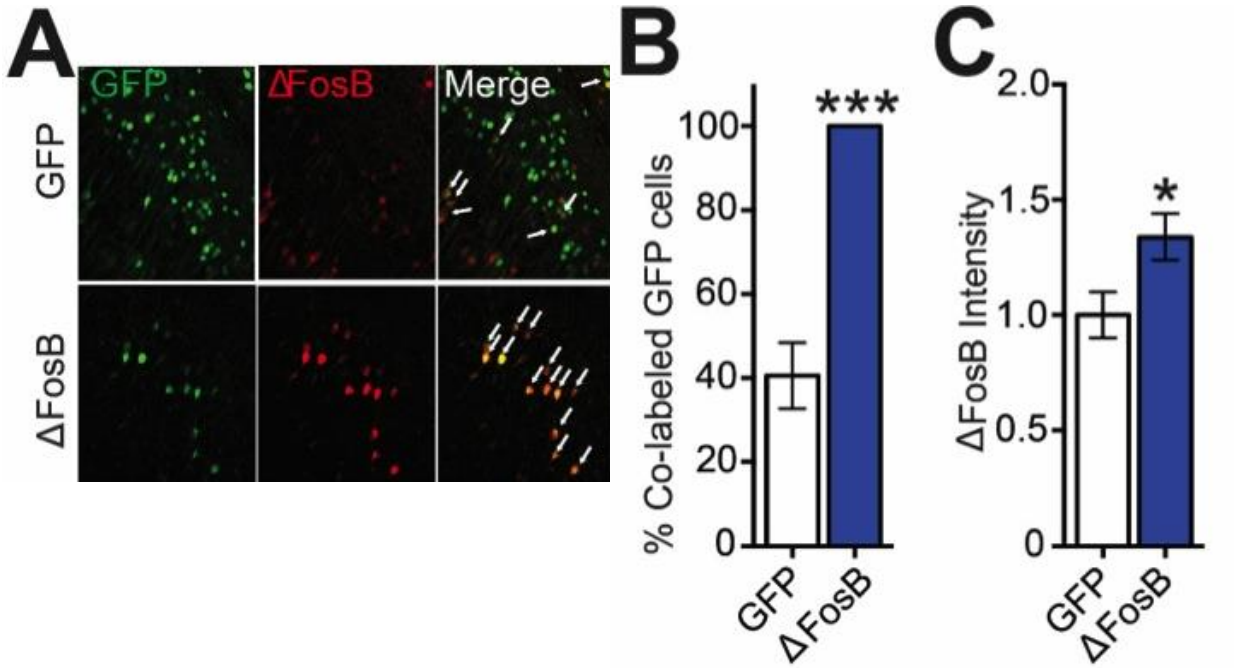

Figure 25 | ΔFosB overexpression in vHPC neurons projecting to NAc. (A) Representative coronal vHPC images (40X) of FosB (red, left), GFP (green, middle), and merged image (right) from vHPC of mice that receive control (top) or ΔFosB-overexpressing vectors (ΔFosB, bottom). White arrows indicate co-labeled GFP+ ΔFosB-expressing cells. Overexpression of ΔFosB expressed more ΔFosB co-labeled GFP projections compared to control quantified in **(B)** ΔFosB significantly increases the % of co-labeling of GFP+ ΔFosB-expressing vHPC-NAc neurons. ****P*<0.001 (n=5 control, n=6 ΔFosB; independent samples t-test compared to GFP). **(C)** Quantitative intensity analysis reveals greater ΔFosB signal intensity in GFP+ vHPC-NAc neurons after ΔFosB overexpression. **P*<0.05 (n=37 control cells, n=46 ΔFosB cells; independent samples t-test compared to GFP).

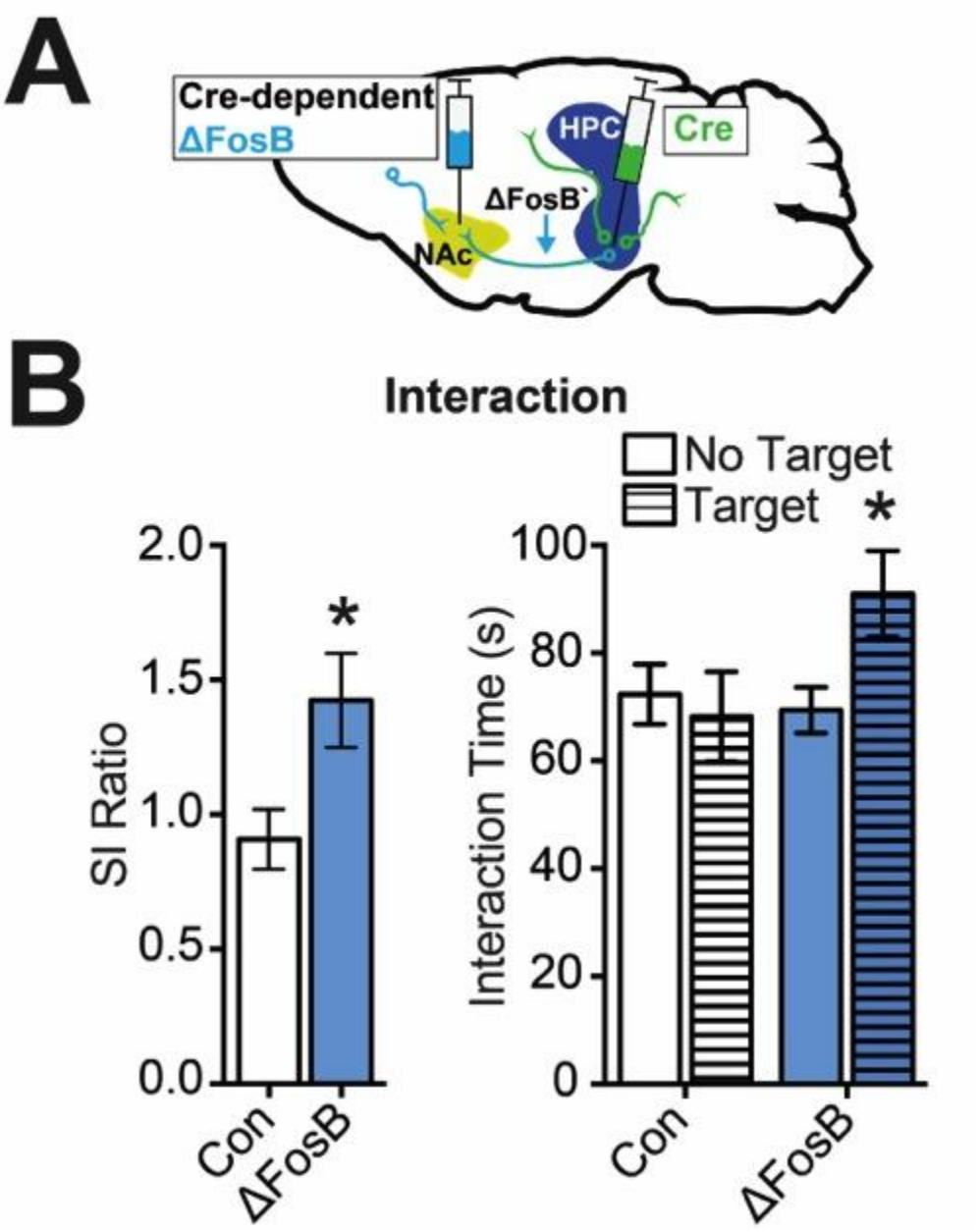

Figure 26 | vHPC-NAc ΔFosB overexpression enhances stress resilience. (A) Schematic of ΔFosB overexpression in vHPC-NAc afferent neurons. Retrograde vector expressing Cre-dependent ΔFosB is injected into NAc while local vector expressing Cre is injected into vHPC. ΔFosB overexpression is driven by Cre only in co-transduced vHPC-NAc neurons (ΔFosB). **(B)** ΔFosB overexpression in vHPC-NAc enhances social interaction following stress, producing a resilient phenotype. **P*<0.05 (n=18 control, n=12 ΔFosB; SI ratio: independent samples t-test compared to control; Interaction time: two-way ANOVA followed by Holm-Sidak post-test ΔFosB No Target vs Target).

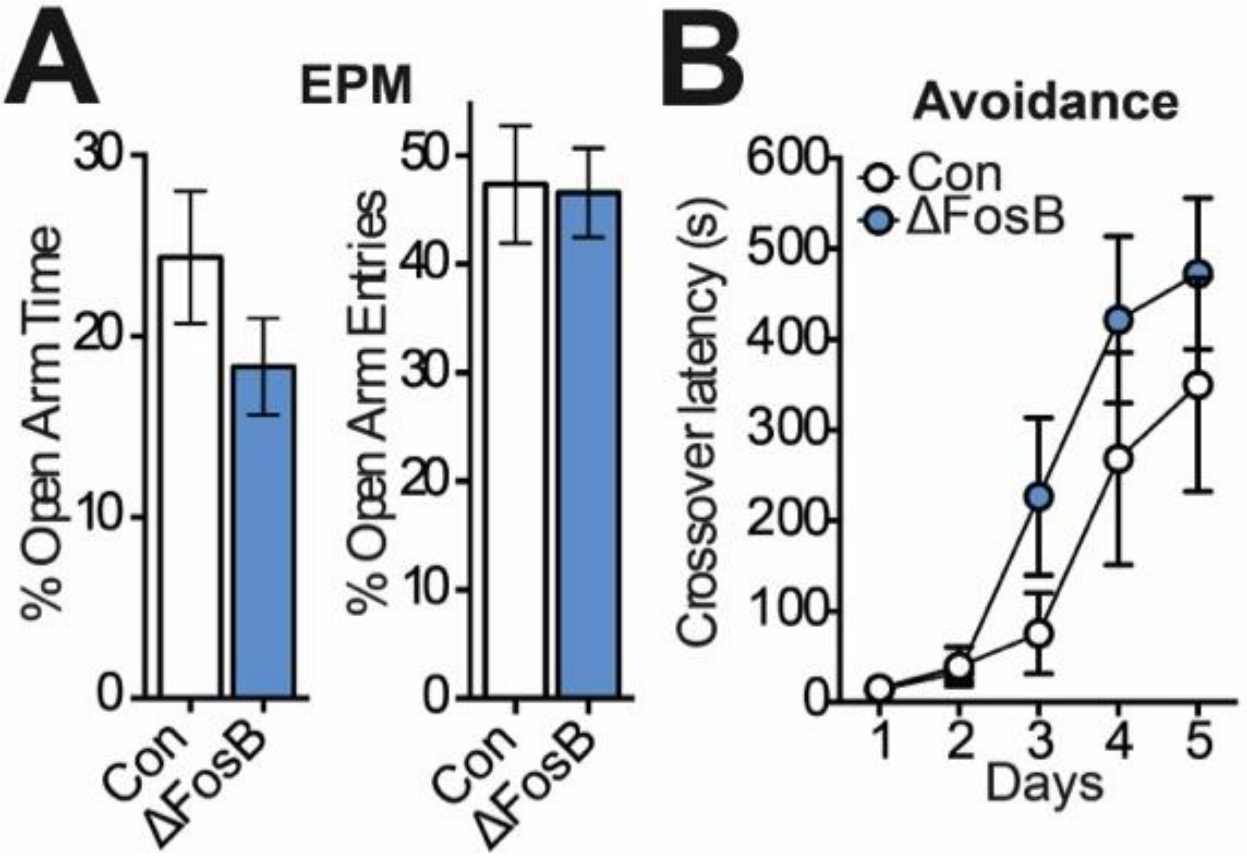

Figure 27 | vHPC-NAc ΔFosB overexpression does not alter aversive behavior. **(A)** ΔFosB overexpression in vHPC-NAc does not alter anxiety-like behavior or **(B)** avoidance learning (n=7 control, n=8 ΔFosB).

FosB knockout in vHPC-NAc increases circuit excitability

As previous findings demonstrated that increased activity in vHPC-NAc neurons underlies CSDS susceptibility[377], we next sought to ascertain the role of ΔFosB in the physiological properties of the vHPC-NAc circuit. We have previously observed ΔFosB decreases amplitude of evoked action potentials and decreased the frequency of spontaneous synaptic currents in dHPC CA1 neurons[387]. This suggests that ΔFosB expression reduces the excitability of vHPC neurons, likely via changes in intrinsic membrane properties. Importantly, in the vHPC-NAc circuit, stress-induced increases in

ΔFosB could cause the decreased excitability previously shown to drive resilience to CSDS[377], thus providing a novel molecular mechanism for this important circuit-level underpinning of stress resilience.

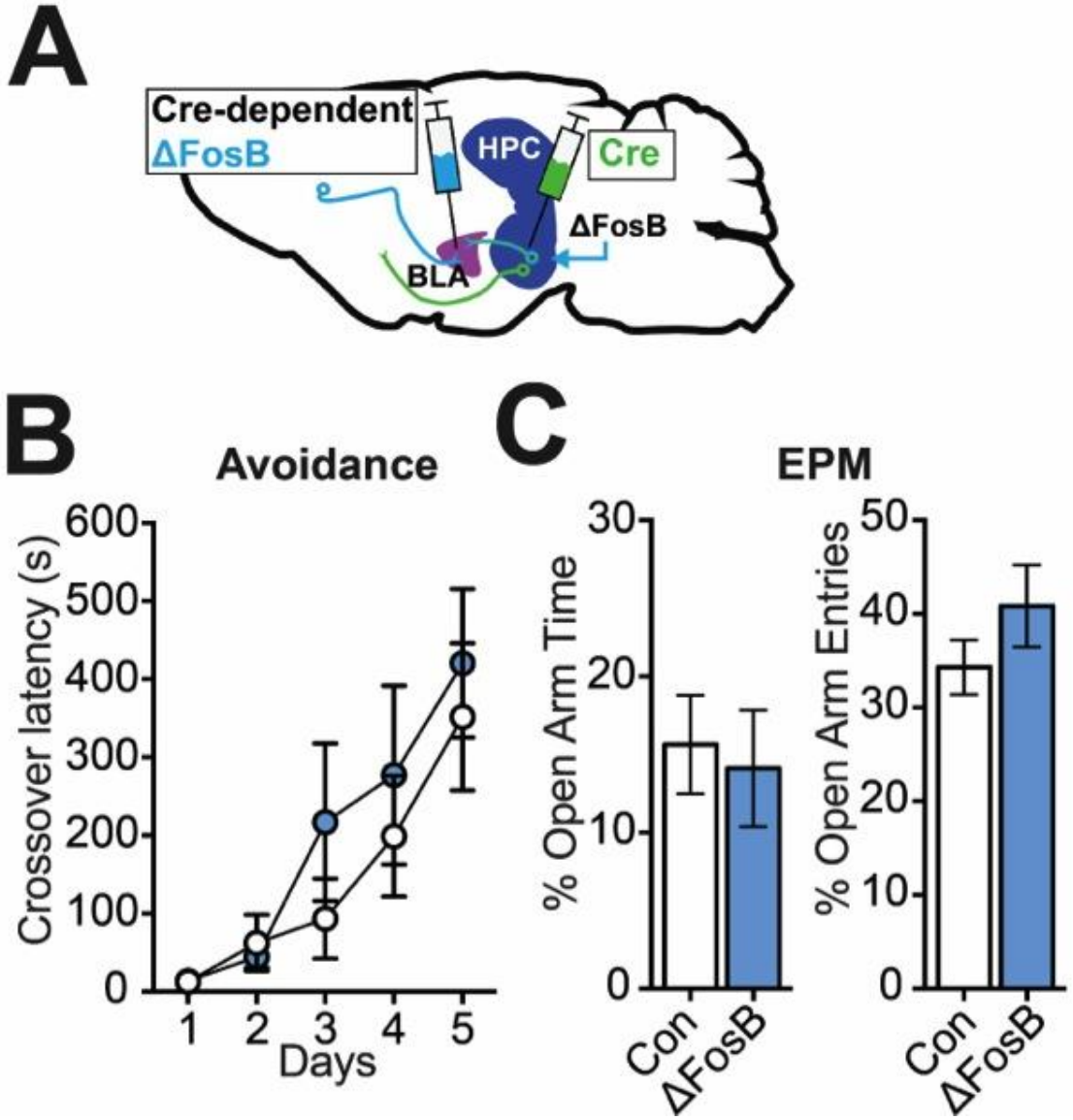

Figure 28 | vHPC-BLA ΔFosB overexpression does not alter anxiety-like behavior. (A) Schematic of ΔFosB overexpression in vHPC-BLA afferent neurons. **(B and C)** ΔFosB overexpression in vHPC-BLA does not alter anxiety-like behavior or avoidance learning (n=7/group).

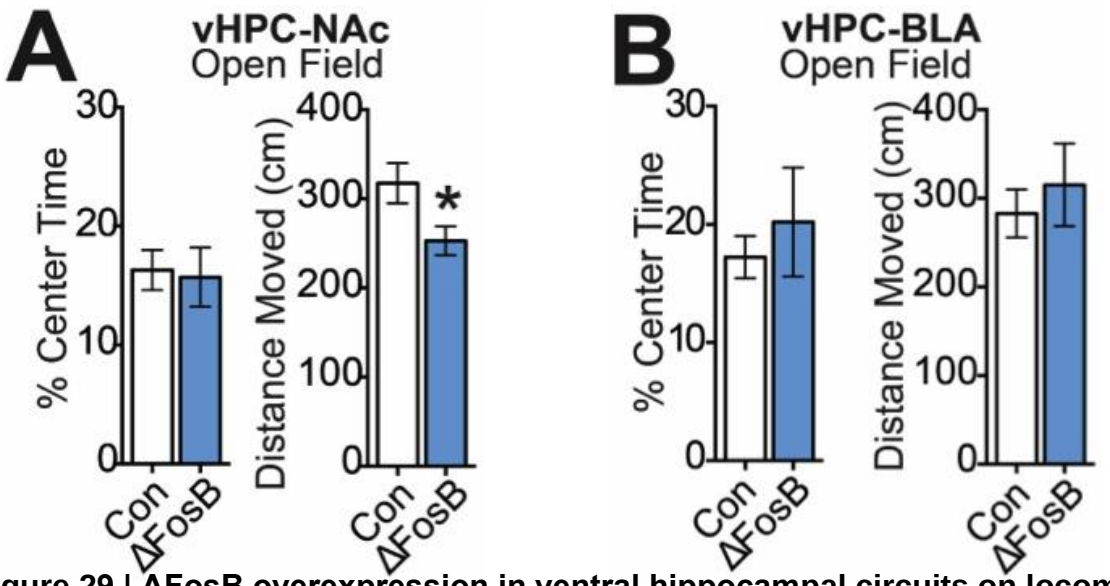

Figure 29 | ΔFosB overexpression in ventral hippocampal circuits on locomotor activity. (A) Overexpression of ΔFosB in vHPC-NAc reduces total activity in the open field, but not time spent in the center. **P*<0.05 (independent samples t-test compared to GFP). **(B)** ΔFosB overexpression in vHPC-BLA does not affect locomotor activity (n=7/group).

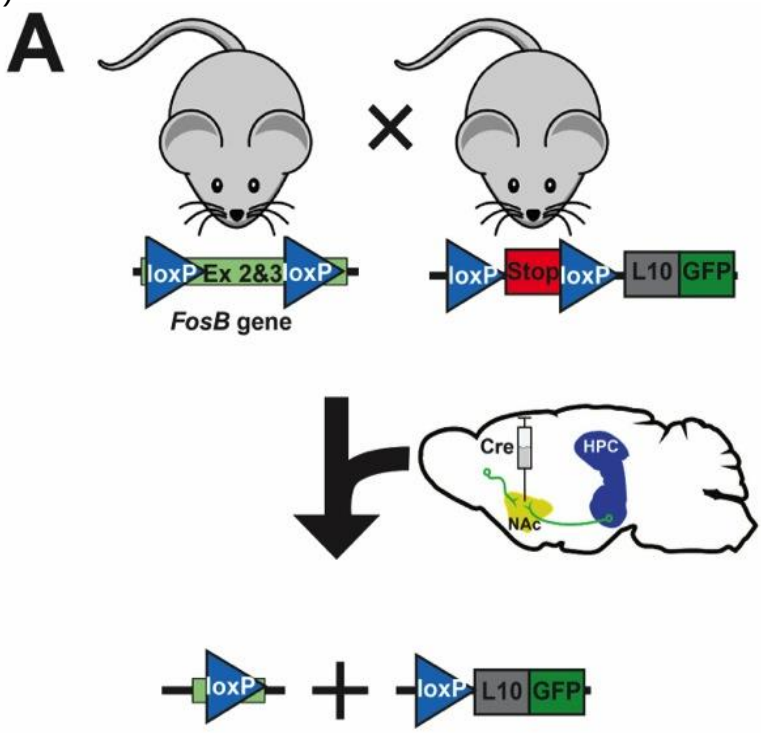

Figure 30 | Schematic of *FosB* knockout in NAc-projecting neurons. (A) *Floxed FosB* mice (*FosB*$^{fl/fl}$; removal of exon 2 & 3) were crossed with mice expressing Cre-dependent GFP-L10 ribosomal fusion protein (*Rosa26*$^{eGFP\text{-}L10a}$) to generate floxed FosB/GFP-L10 mice (KO) and non-floxed GFP-L10 littermate controls (WT). Retrograde Cre vector was injected in NAc to both drive GFP-L10 expression and knock out *FosB* in NAc-projecting neurons.

In order to determine whether ΔFosB regulates excitability of vHPC-NAc projection neurons specifically, we crossed *floxed FosB* mice (*FosB*$^{fl/fl}$)[399] with a line expressinga Cre-dependent GFP-L10a ribosomal subunit fusion protein to generate floxed FosB/GFP-L10a mice (*FosB* KO) and non-floxed GFP-L10a littermate controls (WT) (Fig 30). Injection into NAc of a retrograde HSV expressing Cre drives GFP-L10a expression in vHPC-NAc neurons of all mice, and knocks out ΔFosB expression in vHPC-NAc neurons of the KO, but not WT, mice (Figs 30, 31). Whole-cell *ex vivo* slice recordings from GFP-expressing vCA1-NAc neurons showed that *FosB* KO produces hyperexcitability in NAc-projecting vHPC neurons (Fig 32A,B) and essentially creates

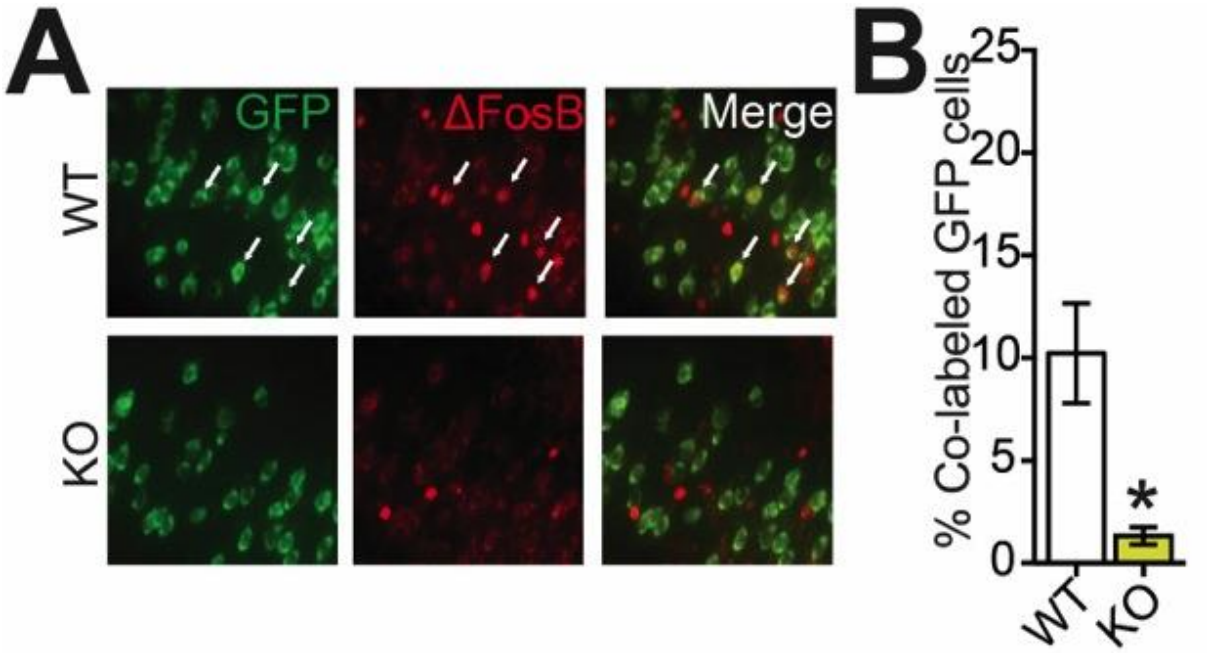

Figure 31 | Validation of adult vHPC-NAc *FosB* knockout. (A) Representative coronal vHPC images (20X) showing NAc-projecting neurons expressing GFP (green, top), ΔFosB (red, middle), and merge (bottom). White arrows indicate co-labeled GFP+ ΔFosB-expressing cells. WT (left) expressed more ΔFosB co-labeled GFP projections compared to KO quantified in **(B)** KO significantly reduces the % of co-labeling of GFP+ ΔFosB-expressing vHPC-NAc neurons. **P*<0.05 (n=6 mice/group; independent samples t-test compared to WT).

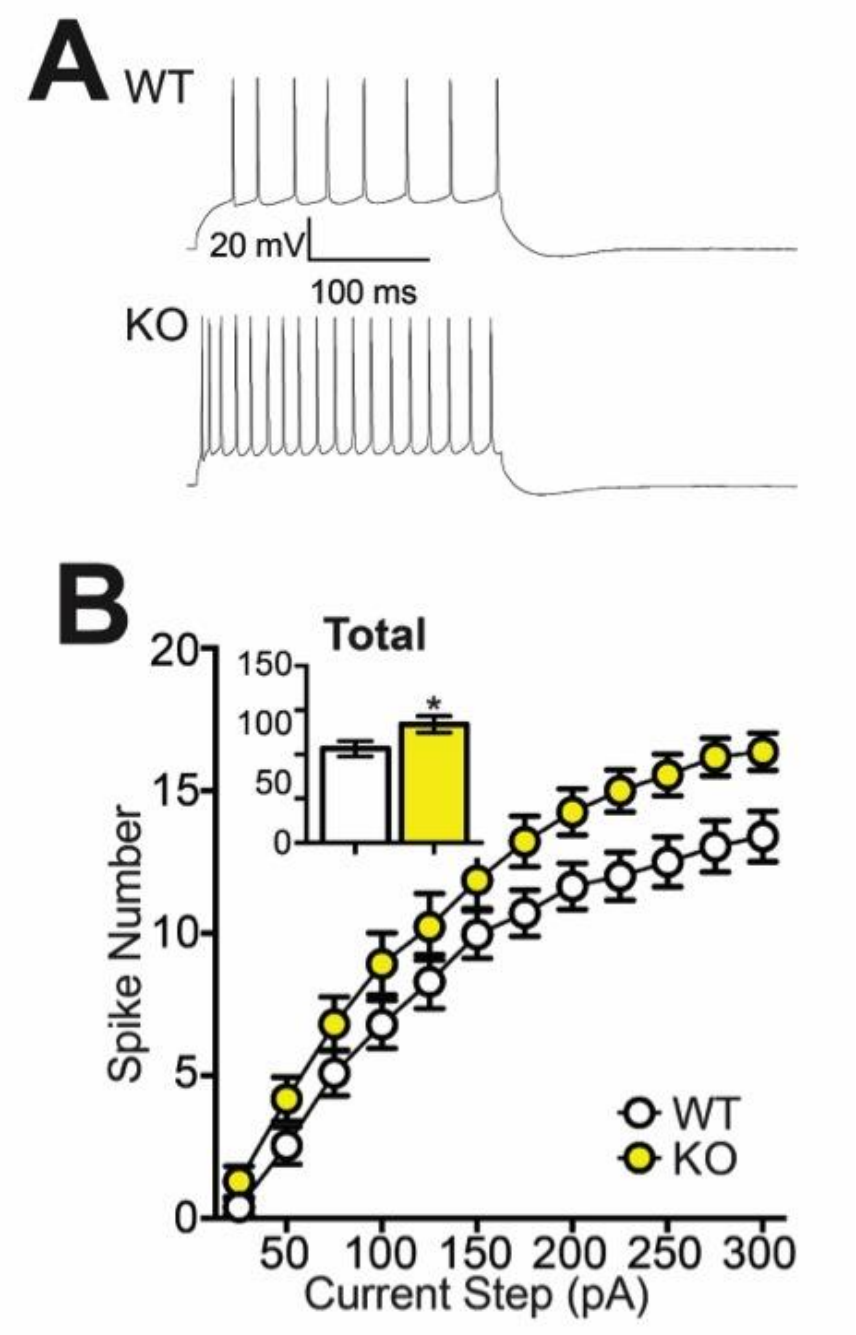

Figure 32 | ΔFosB regulates the cellular excitability of NAc-projecting vHPC neurons. (A) Representative voltage traces from 200 pA depolarizing current injection in NAc-projecting GFP-labeled vCA1 neurons from WT and KO mice. **(B)** KO of *FosB* increases the number of elicited spikes in NAc-projecting vCA1 neurons across increasing current steps (25-300 pA) or the total spikes for all steps (inset). **P*<0.05 (n=20 WT cells, n=27 KO cells; Total: independent samples t-test; Across steps: two-way mixed ANOVA with Holm-Sidak post-tests versus WT).

the opposite phenotype from ΔFosB overexpression[387]. As reduced activity in vHPC glutamatergic neurons synapsing onto NAc MSNs confers resilience to CSDS and increased activity enhances susceptibility[377], and our results above show that vHPC-NAc ΔFosB is necessary for CSDS resilience, this work supports a model in which stress-induced ΔFosB promotes hypoexcitability of NAc-projecting vHPC neurons to drive resilience to CSDS-induced social avoidance.

Identifying downstream *FosB* targets in vHPC-NAc:

In order to uncover potential mechanisms by which ΔFosB regulates vHPC-NAc excitability and related behaviors, we interrogated gene expression regulated by ΔFosB in NAc-projecting vHPC neurons. We used the same retrograde Cre floxed FosB/GFP-L10a strategy as above, but bilateral punches containing vHPC-NAc projections were taken 3 weeks following viral Cre infusions and processed for circuit-specific translating ribosome affinity purification (TRAP) to enrich for actively translating mRNA in vHPC-NAc neurons (Fig 33A). Purified mRNA was used to prepare cDNA libraries that were sequenced, and we found that there was significant enrichment of neuron-specific mRNA (like kalirin) in our TRAP samples compared to input controls, with no change in enrichment of genes common to all cells (like actin; Fig 33B), indicating that our TRAP technique successfully isolated mRNA from neurons. Furthermore, mRNA from *floxed FosB* mice showed a nearly complete absence of *FosB* gene expression compared to mRNA purified from WT controls (Fig 33C), indicating that our purified mRNA comes from vHPC neurons projecting to NAc, as retrograde viral infection in NAc is the only source of Cre in these animals. When we compared mRNAs differentially enriched in WT vs *floxed FosB* vHPC-NAc neurons, we uncovered hundreds of potential ΔFosB

gene targets (a subsection seen in Table 3). In order to begin validation of some of the most interesting potential targets, we overexpressed ΔFosB in Neuro2a cells and used qPCR to assess expression of target genes (Fig 34A). ΔFosB overexpression in cell culture regulated a number of genes identified in the vHPC-NAc TRAP-Seq, including, Adrenergic receptor 2α (Adra2a), neurofilament medium polypeptide (Nefm), and protein kinase C Beta (Prkcb, also known as PKCβ. This indicates that ΔFosB could alter neuronal responses to norepinephrine, the cytoskeleton, and a PKC isoform integral in learning-related signal transduction mechanisms [400]. Thus ΔFosB-dependent changes in gene expression in vHPC-NAc may underlie decreased excitability of this circuit driving stress resilience (Fig 35).

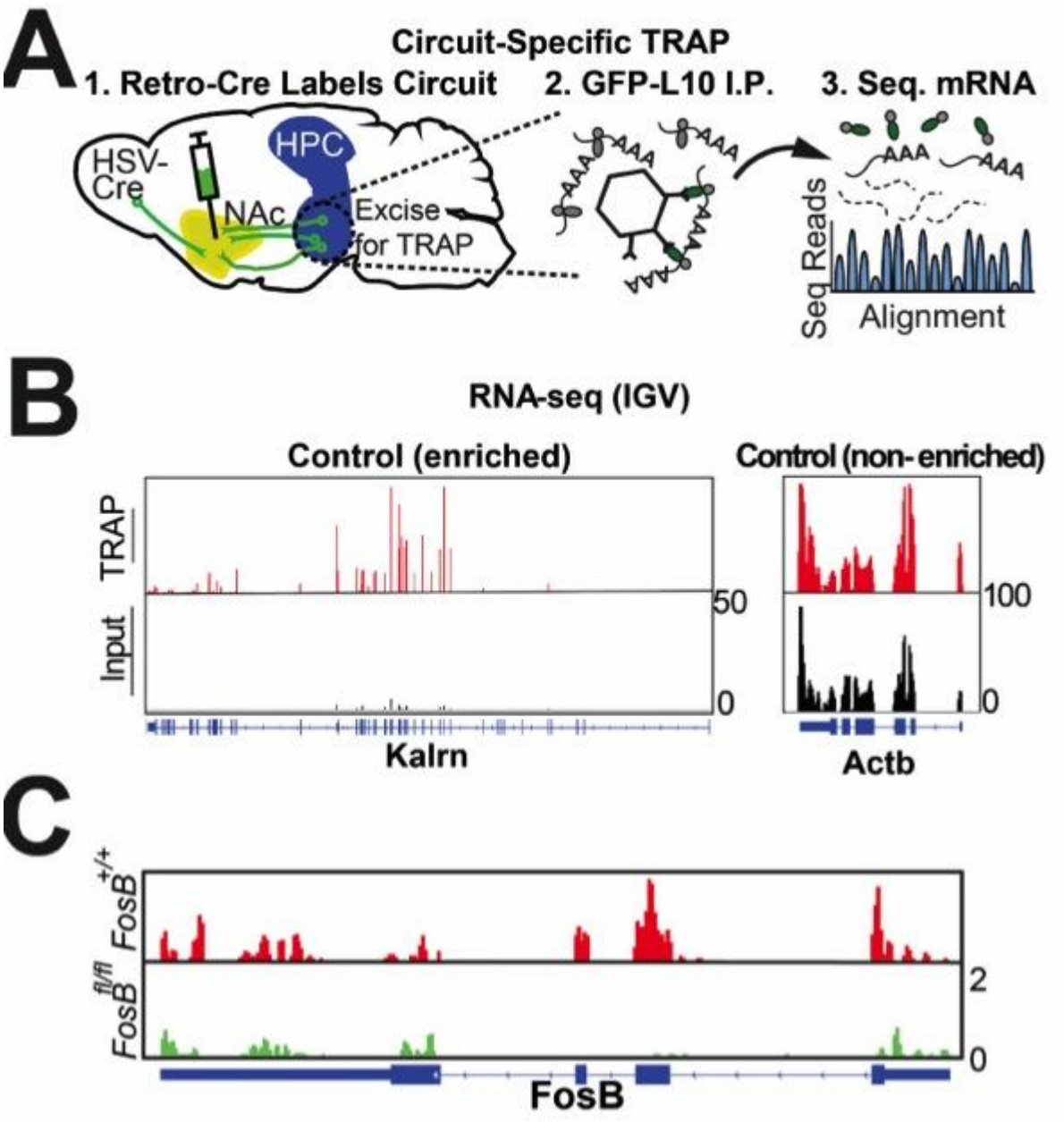

Figure 33 | FosB TRAP validation of vHPC-NAc. (A) Experimental design for circuit-specific TRAP. Retrograde Cre vector is injected into NAc and vHPC is harvested for immunoprecipitation of ribosomes from L10-GFP expressing NAc-projecting cells and sequencing of actively translating mRNA. **(B)** Visualization of mRNA reads from input and vHPC-NAc TRAP-Seq of a neuron-specific (*Kalrn*) and non neuron-specific (*Actb*) gene. **(C)** Sequencing reads (red or green peaks) for *FosB* gene (exons indicated by thick blue bars beneath graph) from WT ($FosB^{+/+}$) and *FosB* KO ($FosB^{fl/fl}$) vHPC-NAc neuron mRNA.

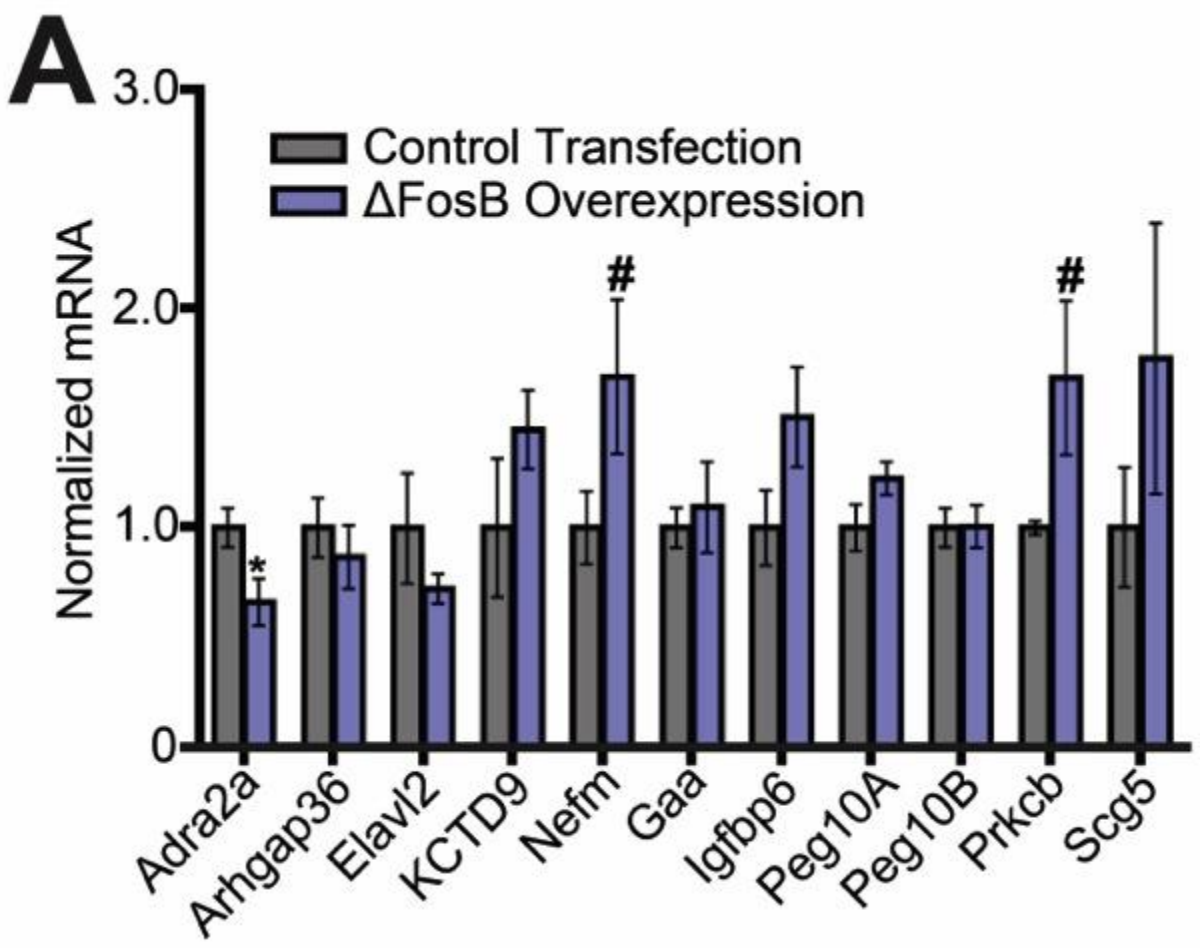

Figure 34 | Validation of vHPC-NAc identified ΔFosB downstream targets. (A) ΔFosB overexpression in Neuro2A cells regulates mRNA expression of some vHPC-NAc TRAP-identified target genes. **P*<0.05, $^{\#}$*P*<0.10 (n=6-12/group; independent samples t-test compared to Control Transfection).

Discussion

The data presented in this chapter indicate that ΔFosB is induced in response to stress in glutamatergic vHPC neurons projecting to NAc, altering gene expression to reduce circuit excitability and drive CSDS resilience (Fig 23E). In addition to showing ΔFosB's accumulation in vHPC-NAc is sufficient for resilience to stress, the experiments in this chapter which compare ΔFosB's role in vHPC-NAc and vHPC-BLA neurons are the first to show that divergent patterns of behavior can be elicited by the same manipulation of a single hippocampal population based on differences in projection target.

Additionally, as we observed that ΔFosB alters vHPC-NAc neuronal excitability, it is also possible that ΔFosB may mediate stress-associated synaptic plasticity in vHPC. In keeping with this possibility, CSDS, like ΔFosB, increases the number of thin immature dendritic spines on dorsal hippocampal CA1 neurons[337, 401], and decreases AMPA receptor subunit levels at the postsynaptic density[401]. Indeed, many postsynaptic structural/signaling proteins were uncovered in our screen of vHPC-NAc ΔFosB gene targets (Table 3), and future studies will use these data to explore the mechanisms by which stress alters both intrinsic excitability and synaptic inputs onto the vHPC-NAc and vHPC-BLA circuits.

Ventral hippocampal circuits are key regulators of multiple emotionally-driven behaviors and hold promise for future treatments of neuropsychiatric disease if we can reveal the molecular mechanisms of their regulation. In keeping with this, recent clinical studies have demonstrated that coherence of the hippocampal-amygdala circuit correlates with anxiety phenotypes in patients[402]. However, the mechanisms for differences in circuit coherence cannot yet be explored in humans, emphasizing the need for preclinical models and circuit-based tools for uncovering molecular mechanisms that could yield potential treatments. Although it is possible that drugs targeting ΔFosB could be developed, we have adopted the strategy that ΔFosB acts as an orchestrator of disease-relevant changes in gene expression, and thus uncovering the downstream targets of ΔFosB transcriptional regulation may reveal myriad druggable pathways for the systemic or circuit-specific treatment of depression.

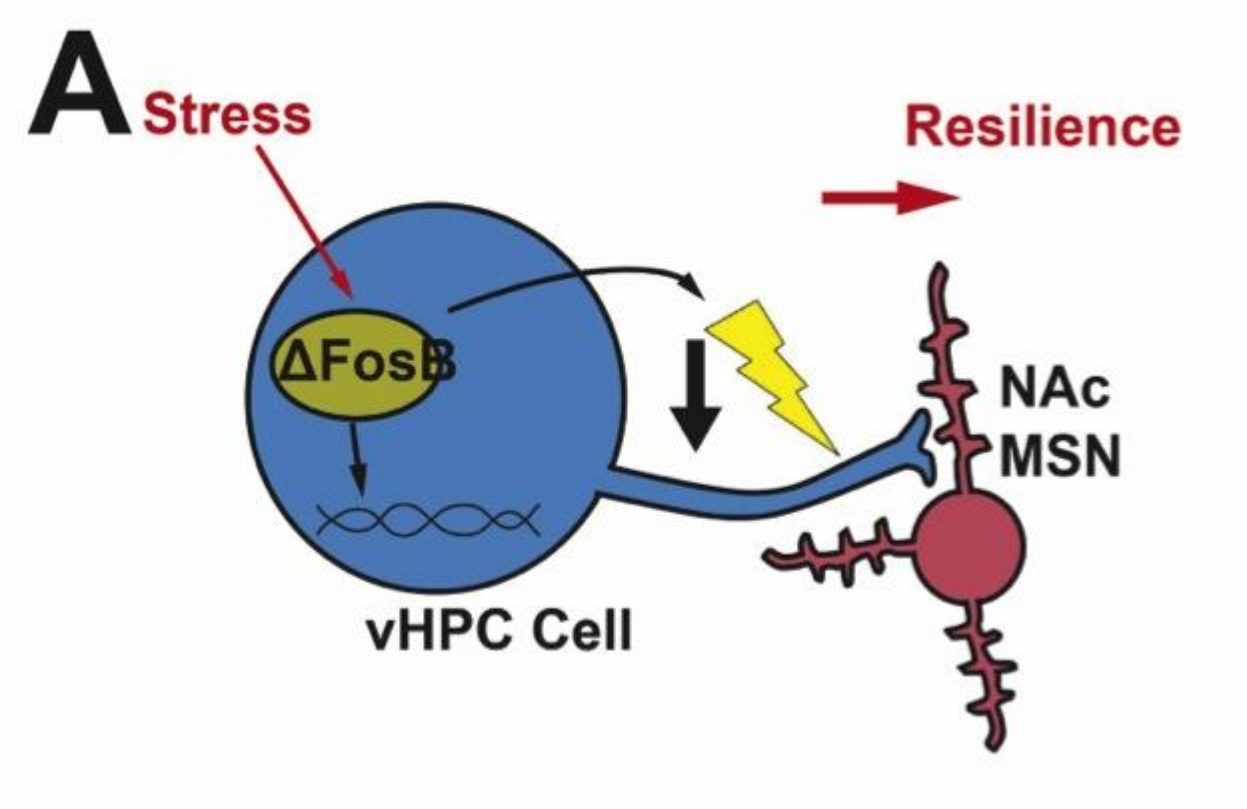

Figure 35 | Proposed model of ΔFosB orchestrating stress resilience. (A) Proposed model: in resilient mice, stress strongly induces ΔFosB in vHPC-NAc neurons, thereby changing gene expression related to stress signaling and decreasing excitability of the projection.

Although these experiments present compelling preliminary evidence for the circuit-specific control of stress resilience with implications for the treatment of depression, they were only performed in male mice. This confounds the utility of potential therapeutic strategies developed as a result of this work due to the prevalence pf depression in women. Therefore, in chapters 5 and 6 I examined sex as a variable, explicitly comparing sex differences in vHPC projections and stress phenotypes, and if ΔFosB was necessary and sufficient in the vHPC-NAc for stress resilience in both sexes.

Table 3 | Top 25 genes of interest in vHPC-NAc floxed FosB TRAP

Gene	Ensemble Gene ID	WT-TRAP % Error	KO-TRAP % Error	WT Enriched?	KO Enriched?	Reg	Fold Change	Sig. (P Value)
Peg10	ENSMUSG00000092035	3.82	2.00	FALSE	TRUE	Up	1.00	<0.001
Igfbp6	ENSMUSG00000023046	5.90	16.64	TRUE	FALSE	Down	-0.54	<0.001
Scg5	ENSMUSG00000023236	10.95	1.11	FALSE	TRUE	Down	-0.52	<0.001
Siae	ENSMUSG00000001942	41.37	8.78	FALSE	TRUE	Up	0.51	<0.001
Arhgap36	ENSMUSG00000036198	34.61	16.32	FALSE	TRUE	Up	0.49	<0.001
Dusp4	ENSMUSG00000031530	6.32	11.79	TRUE	FALSE	Down	-0.47	0.001
Zcchc12	ENSMUSG00000036699	7.17	3.26	FALSE	TRUE	Up	0.45	<0.001
Fosb	ENSMUSG00000003545	10.33	14.46	TRUE	FALSE	Down	-0.44	0.002
Kcng1	ENSMUSG00000074575	9.46	5.50	FALSE	TRUE	Up	0.44	<0.001
Nefm	ENSMUSG00000022054	7.32	2.81	TRUE	FALSE	Down	-0.44	<0.001
Ier5	ENSMUSG00000056999	11.97	15.58	TRUE	FALSE	Down	-0.43	0.003
Timm50	ENSMUSG00000003438	4.40	1.68	TRUE	TRUE	Down	-0.43	0.002
Gpr101	ENSMUSG00000036357	5.90	28.32	FALSE	TRUE	Up	0.42	0.004
Adra2a	ENSMUSG00000033717	11.01	10.10	FALSE	TRUE	Up	0.40	0.005
Sstr1	ENSMUSG00000035431	5.03	9.45	FALSE	TRUE	Up	0.40	0.006
Grp	ENSMUSG00000024517	16.83	5.80	TRUE	TRUE	Up	0.40	0.005
Peli3	ENSMUSG00000024901	5.87	2.41	FALSE	TRUE	Up	0.40	0.006
Poll	ENSMUSG00000025218	16.57	26.40	FALSE	TRUE	Up	0.40	0.005
Pdcd6	ENSMUSG00000021576	5.34	7.11	TRUE	FALSE	Down	-0.39	0.004
Rwdd2a	ENSMUSG00000032417	9.60	4.95	FALSE	TRUE	Up	0.39	0.004
Scube1	ENSMUSG00000016763	32.20	3.71	TRUE	TRUE	Down	-0.39	0.008
Grasp	ENSMUSG00000000531	10.72	6.05	TRUE	TRUE	Down	-0.39	0.001
Ap2s1	ENSMUSG00000008036	12.51	2.41	TRUE	TRUE	Down	-0.38	0.001
Scamp4	ENSMUSG00000079020	8.51	7.92	TRUE	FALSE	Down	-0.38	0.009

Table 3 (cont'd)

Rab3b	**ENSMUSG00000003411**	**5.97**	**15.06**	**FALSE**	**TRUE**	**Up**	**0.38**	**0.003**

Table 4 | Statistical comparisons in chapter 4

Figure	Test	Comparison	Stat	p-value	Summary
Fig 10C	Independent samples t-test	Control vs Defeat	t (18) = 1.770	P = 0.0936	NS
Fig 11B (Left)	Independent samples t-test	Saline vs Fluoxetine	t (10) = 3.908	P = 0.0029	**
Fig 11B (Middle)	Independent samples t-test	Saline vs Fluoxetine	t (10) = 7.951	P < 0.0001	***
Fig 11B (Right)	Independent samples t-test	Saline vs Fluoxetine	t (10) = 5.674	P = 0.0002	***
Fig 12C	Independent samples t-test	Control vs Defeat	t (254) = 2.847	P = 0.0048	**
Fig 14C (Left)	Independent samples t-test	GFP vs ΔJunD	t (35) = 2.632	P = 0.0125	*
Fig 14C (Right)	2-way Mixed ANOVA	Group: GFP vs ΔJunD	F (1, 35) = 1.790	P = 0.1896	NS
		Trial: No Target vs Target	F (1, 35) = 21.16	P < 0.0001	***
		Group X Trial	F (1, 35) = 9.955	P = 0.0033	**
Fig 14D (Left)	Independent samples t-test	GFP vs ΔJunD	t (16) = 0.4163	P = 0.6827	NS
Fig 14D (Right)	2-way Mixed ANOVA	Group: GFP vs ΔJunD	F (1, 16) = 0.7639	P = 0.3950	NS
		Trial: No Target vs Target	F (1, 16) = 2.378	P = 0.1426	NS
		Group X Trial	F (1, 16) = 0.0928	P = 0.7646	NS
Fig 15A (Left)	Independent samples t-test	GFP vs ΔJunD	t (23) = 1.517	P = 0.1430	NS
Fig 15A (Right)	Independent samples t-test	GFP vs ΔJunD	t (23) = 1.118	P = 0.2750	NS
Fig 15B (Left)	Independent samples t-test	GFP vs ΔJunD	t (23) = 1.494	P = 0.1489	NS
Fig 15B (Right)	Independent samples t-test	GFP vs ΔJunD	t (23) = 1.240	P = 0.2275	NS
Fig 16B	Independent samples t-test	NT vs GFP	t (6) = 0.0616	P = 0.9529	NS
Fig 16B	Independent samples t-test	NT vs gRNA1	t (6) = 1.529	P = 0.1771	NS
Fig 16B	Independent samples t-test	NT vs gRNA2	t (6) = 2.901	P = 0.0273	*

Table 4 (cont'd)

Fig 17B	Independent samples t-test	GFP vs FosB gRNA	t (23) = 2.813	P = 0.0099	**
Fig 18C	Independent samples t-test	Control vs FosB gRNA	t (266) = 5.876	P < 0.0001	***
Fig 19B	Independent samples t-test	Control vs FosB KO	t (13) = 3.056	P = 0.0092	**
Fig 19C (Left)	Independent samples t-test	Control vs FosB KO	t (13) = 1.203	P = 0.2504	NS
Fig 19C (Right)	Independent samples t-test	Control vs FosB KO	t (13) = 2.527	P = 0.0253	*
Fig 20A	2-way Mixed ANOVA	Group: Control vs FosB KO	F (1, 13) = 0.343	P = 0.5682	NS
		Day: (1,2,3,4,5)	F (4, 52) = 12.150	P < 0.0001	***
		Group X Day	F (4, 52) = 0.337	P = 0.8516	NS
Fig 20B (Left)	Independent samples t-test	Control vs FosB KO	t (13) = 0.144	P = 0.8877	NS
Fig 20B (Right)	Independent samples t-test	Control vs FosB KO	t (13) = 2.082	P = 0.0576	NS
Fig 21B	Independent samples t-test	Control vs FosB KO	t (19) = 0.872	P = 0.3939	NS
Fig 21C (Left)	Independent samples t-test	Control vs FosB KO	t (12) = 0.930	P = 0.3706	NS
Fig 21C (Right)	Independent samples t-test	Control vs FosB KO	t (12) = 1.341	P = 0.2049	NS
Fig 22A	2-way Mixed ANOVA	Group: Control vs FosB KO	F (1, 12) = 3.896	P = 0.0719	NS
		Day: (1,2,3,4,5)	F (4, 48) = 9.332	P < 0.0001	***
		Group X Day	F (4, 48) = 2.667	P = 0.0434	*
Fig 22B (Left)	Independent samples t-test	Control vs FosB KO	t (11) = 3.241	P = 0.0079	**
Fig 22B (Right)	Independent samples t-test	Control vs FosB KO	t (11) = 3.956	P = 0.0022	**
Fig 23B (Left)	Independent samples t-test	KO vs Rescue	t (23) = 2.597	P = 0.0161	*
Fig 23B (Right)	2-way Mixed ANOVA	Group: KO vs Rescue	F (1, 23) = 0.9440	P = 0.3414	NS
		Trial: No Target vs Target	F (1, 23) = 2.495	P = 0.1278	NS
		Group X Trial	F (1, 23) = 6.452	P = 0.0183	*

Table 4 (cont'd)

Fig 24B (Left)	Independent samples t-test	KO vs Rescue	t (25) = 3.154	P = 0.0042	**
Fig 24B (Right)	Independent samples t-test	KO vs Rescue	t (25) = 1.841	P = 0.0776	NS
Fig 24C	2-way Mixed ANOVA	Group: KO vs Rescue	F (1, 26) = 10.45	P = 0.0033	**
		Day (1,2,3,4,5)	F (4, 104) = 20.11	P < 0.0001	***
		Group X Day	F (4, 104) = 4.828	P = 0.0013	**
Fig 25B	Independent samples t-test	GFP vs ΔFosB	t (9) = 8.407	P < 0.0001	***
Fig 25C	Independent samples t-test	GFP vs ΔFosB	t (81) = 2.350	P = 0.0212	*
Fig 26B (Left)	Independent samples t-test	Control vs ΔFosB	t (31) = 2.575	P = 0.0150	*
Fig 26B (Right)	2-way Mixed ANOVA	Group: Control vs ΔFosB	F (1, 31) = 1.703	P = 0.2015	NS
		Trial: No Target vs Target	F (1, 31) = 2.073	P = 0.1600	NS
		Group X Trial	F (1, 31) = 4.533	P = 0.0413	*
Fig 27A (Left)	Independent samples t-test	Control vs ΔFosB	t (13) = 1.359	P = 0.1972	NS
Fig 27A (Right)	Independent samples t-test	Control vs ΔFosB	t (13) = 0.114	P = 0.9113	NS
Fig 27B	2-way Mixed ANOVA	Group: Control vs ΔFosB	F (1, 13) = 1.473	P = 0.2465	NS
		Day (1,2,3,4,5)	F (4, 52) = 17.96	P < 0.0001	***
		Group X Day	F (4, 52) = 0.9139	P = 0.4629	NS
Fig 28B	2-way Mixed ANOVA	Group: Control vs ΔFosB	F (1, 12) = 0.5060	P = 0.4905	NS
		Day (1,2,3,4,5)	F (4, 48) = 13.91	P < 0.0001	***
		Group X Day	F (4, 48) = 0.5236	P = 0.7189	NS
Fig 28C (Left)	Independent samples t-test	Control vs ΔFosB	t (12) = 0.310	P = 0.7619	NS
Fig 28C (Right)	Independent samples t-test	Control vs ΔFosB	t (12) = 1.244	P = 0.2371	NS
Fig 29A (Left)	Independent samples t-test	Control vs ΔFosB	t (13) = 0.194	P = 0.8493	NS

Table 4 (cont'd)

Fig 29A (Right)	Independent samples t-test	Control vs ΔFosB	t (13) = 2.380	P = 0.0333	*
Fig 29B (Left)	Independent samples t-test	Control vs ΔFosB	t (12) = 0.601	P = 0.5590	NS
Fig 29B (Right)	Independent samples t-test	Control vs ΔFosB	t (12) = 0.599	P = 0.5603	NS
Fig 31B	Independent samples t-test	WT vs KO	t (10) = 3.603	P = 0.0048	**
Fig 32B (main)	2-way Mixed ANOVA	Group: WT vs KO	F (1, 45) = 4.391	P = 0.0418	*
		Current	F (11, 495) = 294.4	P < 0.0001	****
		Group X Current	F (11, 495) = 1.694	P = 0.0715	NS
Fig 32B (inset)	Independent samples t-test	WT vs KO	t (45) = 2.095	P = 0.0418	*
Fig 34A (Adra2a)	Independent samples t-test	Control vs ΔFosB	t (22) = 2.4239	P = 0.0240	*
Fig 34A (Arhgap36)	Independent samples t-test	Control vs ΔFosB	t (10) = 0.6722	P = 0.5167	NS
Fig 34A (Elavl2)	Independent samples t-test	Control vs ΔFosB	t (10) = 1.0636	P = 0.3125	NS
Fig 34A (KCTD9)	Independent samples t-test	Control vs ΔFosB	t (9) = 1.1526	P = 0.2788	NS
Fig 34A (Nefm)	Independent samples t-test	Control vs ΔFosB	t (22) = 1.7655	P = 0.0914	NS
Fig 34A (Gaa)	Independent samples t-test	Control vs ΔFosB	t (10) = 0.4133	P = 0.6881	NS
Fig 34A (Igfbp6)	Independent samples t-test	Control vs ΔFosB	t (10) = 1.7649	P = 0.1081	NS
Fig 34A (Peg10A)	Independent samples t-test	Control vs ΔFosB	t (10) = 1.7305	P = 0.1142	NS
Fig 34A (Peg10B)	Independent samples t-test	Control vs ΔFosB	t (10) = 0.0383	P = 0.9702	NS
Fig 34A (Prkcb)	Independent samples t-test	Control vs ΔFosB	t (10) = 1.9366	P = 0.0815	NS
Fig 34A (Scg5)	Independent samples t-test	Control vs ΔFosB	t (10) = 1.1394	P = 0.2811	NS

CHAPTER 5: ANDROGEN-DEPENDENT EXCITABILITY OF MOUSE VENTRAL HIPPOCAMPAL AFFERENTS TO NUCLEUS ACCUMBENS UNDERLIES SEX-SPECIFIC SUSCEPTIBILITY TO STRESS

Author contributions:

Conceived and designed the experiments: Manning, Williams, and Robison

Performed the experiments: Manning, Williams, Eagle, Duque-Wilckens, Chinnusamy

Analyzed the data: Williams, Manning, Robison

Contributed reagents/materials/analysis tools: Swift-Gallant, Moeser, Jordan, Leinninger

**Williams and Manning contributed equally to this work, Williams on electrophysiology experiments and Manning for behavioral experiments*

Introduction

Affective disorders such as major depression disproportionately affect women[403, 404], but studies investigating depression-related behaviors in animal models that include both female and male subjects are lacking. There are sex differences in brain regions that regulate reward and motivation following some stress paradigms, including subchronic variable stress (SCVS)[335], chronic mild stress[405] and *Peromyscus californicus* social defeat stress[406]. However, neurophysiological mechanisms causing sex differences in stress responses and depression-related behaviors remain unclear. Numerous studies have demonstrated the importance of the nucleus accumbens (NAc) in regulating depression-like behaviors after stress[53, 128, 305, 407], and glutamatergic inputs to NAc from areas such as prefrontal cortex and ventral hippocampus (vHPC) alter NAc activity and ultimately behavioral responses to stress[408, 409]. Critically, the vHPC is essential

for social and affective memories[193, 410, 411], and glutamatergic vHPC afferents to the NAc directly regulate male behavioral responses to chronic social defeat stress (demonstrated in chapter 4)[127], making this circuit a potential candidate mediating sex differences in mood-related disorders.

Unfortunately, most circuit-specific animal model studies investigating depression-related behaviors have not included female subjects. This gap in study design exists despite sex differences in several depression-related brain regions, including the hippocampus. For example, hippocampal spine morphology differs between male and female rodents prior to stress, and can exhibit sex-specific responses to stressful events[412], and male and female rodents differ in hippocampal LTP and hippocampus-dependent contextual learning[413]. Sex differences in responses to stress are also well-documented, and one key model in mice is subchronic variable stress (SCVS), after which only female mice exhibit anhedonic behaviors[63, 335] analogous to human depression patients. To this end, gonadal steroid hormone receptors have been identified in the NAc as modulators of female susceptibility to SCVS[64]. However, whether vHPC-NAc activity in male and female mice is regulated by gonadal hormones has not been tested. We report testosterone-dependent differences in adult male and female vHPC-NAc excitability as well as corresponding changes in susceptibility to SCVS. Importantly, we demonstrate a causal link between vHPC-NAc activity and anhedonia following SCVS using a circuit-specific viral DREADD system to artificially manipulate vHPC-NAc excitability. Here, we show that stress-induced anhedonia is dependent upon long-term adaptation of vHPC-NAc projections, as activation of this circuit for a week prior to behavioral assessment,

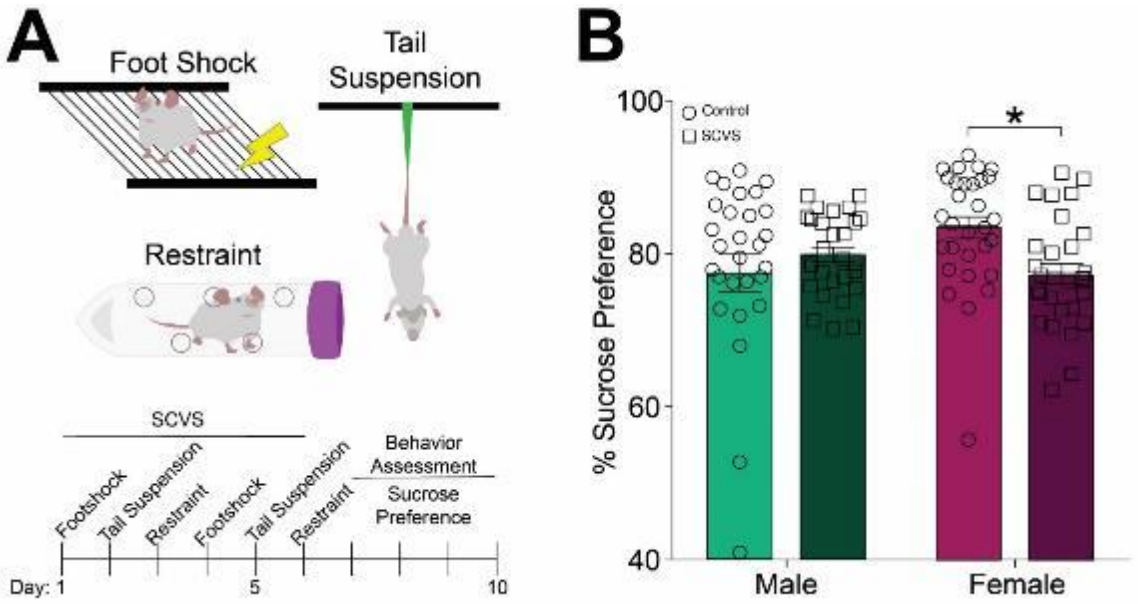

Figure 36 | Selective female susceptibility to SCVS. (A) Schematic depicting stressors used in SCVS (top) and experimental time course of stress and sucrose preference (bottom). **(B)** Only female mice displayed reduced sucrose preference after SCVS.

and not simply during behavior, is necessary for expression of anhedonia. This study introduces a novel, circuit-specific physiological difference between male and female mice driving corresponding depression-related stress outcomes that may enhance future understanding of sex differences in depression susceptibility and potential treatments in men and women.

Results

Female mice have increased vHPC-NAc circuit excitability and are selectively susceptible to SCVS:

We observe that female mice are selectively vulnerable to SCVS-induced anhedonia, in agreement with prior studies[63, 335, 414]. Following either the 6-day SCVS battery of stressors (foot shock, tail suspension, and restraint; Fig 36A) or 6 days of control handling,

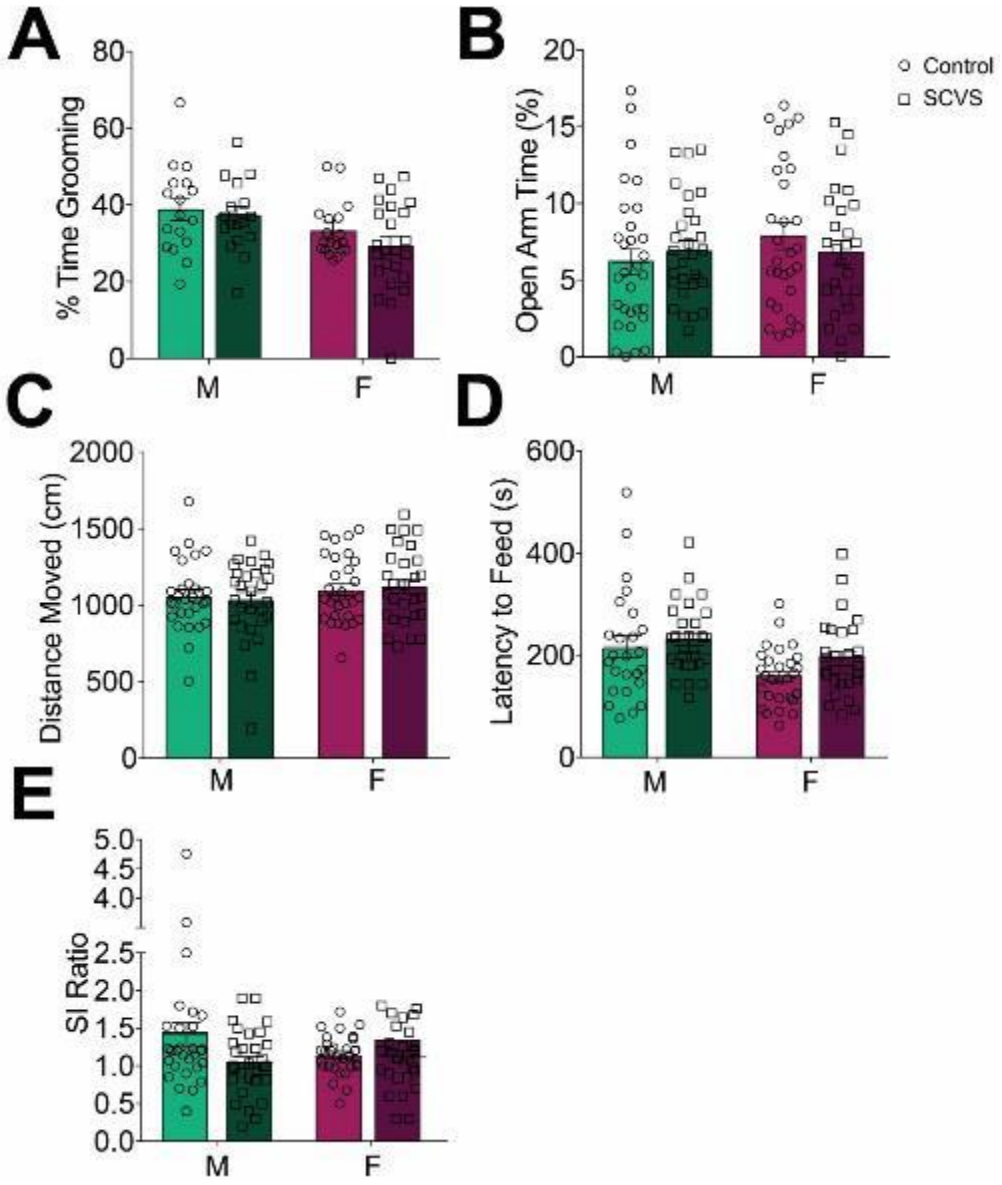

Figure 37 | Additional behavioral assays of male vs. female SCVS. All behavioral assays other than sucrose preference did not reflect sex differences in SCVS as there was no interaction of stress and sex in any of the following measures: **(A)** Percent time grooming in splash test; **(B)** Percent open arm time in EPM; **(C)** Distance moved (cm) in EPM; **(D)** Latency to feed (s) in novelty suppressed feeding test; and **(E)** SI Ratio in social interaction test

stressed female mice had a significant reduction in free-choice preference for sucrose solution over water alone compared to their control counterparts (Fig 36B), with a significant interaction between stress and sex. Although animals still display a preference for sucrose, this reduction in preference compared to normal animals is an indicator of

anhedonia[53, 61, 415], SCVS thus models an aspect of enhanced female depression vulnerability. We also used a variety of other assays to measure anxiety, autogrooming, and social withdrawal in the same mice (Fig 37A-E), but we did not

observe the robust, sex-specific vulnerability to stress in any measure other than sucrose preference. Therefore, we focused on sucrose preference and anhedonia for the remainder of the current study, though we report all other measures throughout.

This sex difference in susceptibility to SCVS suggests an underlying difference in physiology between male and female mice. Glutamatergic vHPC-NAc projections have been linked to stress susceptibility and reward in several elegant studies[127, 409]. To explore the vHPC-NAc circuit and its role in mediating anhedonic responses in mice, we employed whole cell patch clamp electrophysiology and a circuit-specific retrograde HSV-Cre labeling strategy[416] to record from vHPC-NAc cells in both male and female mice. Transgenic mice expressing the Cre-inducible L10-GFP[339] were injected in NAc with a retrograde herpes simplex virus (HSV) expressing Cre recombinase (Fig 38A, top), leading to GFP expression in all neurons projecting to or within NAc. After 21 daysto allow full retrograde expression, brain slices containing vHPC were prepared for whole-cell recordings from GFP-positive vHPC neurons projecting to NAc. In hippocampus, only pyramidal neurons of the ventral CA1/subiculum region were found to project to NAc using this method (Fig 38A, right). Female vHPC-NAc neurons were more excitable than those of male mice, as indicated by an elevated number of action potentials elicited by increasing depolarizing current injections (Fig 38B top, example traces for each group below).

To demonstrate circuit-specificity of this sex difference in excitability, we injected retrograde HSV-Cre into basolateral amygdala (BLA) of a separate cohort of male and female mice. Whole-cell recordings obtained from vHPC-BLA projections revealed no significant difference in excitability of female vHPC-NAc neurons compared to male (Fig 38C top, example traces for each group below). These findings, contrasted with the above vHPC-NAc circuit observations, demonstrate the specificity of the vHPC-NAc difference in excitability between male and female mice. Overall, these findings suggest a circuit-specific physiological difference that could underlie the sex differences in susceptibility to the anhedonia following stress.

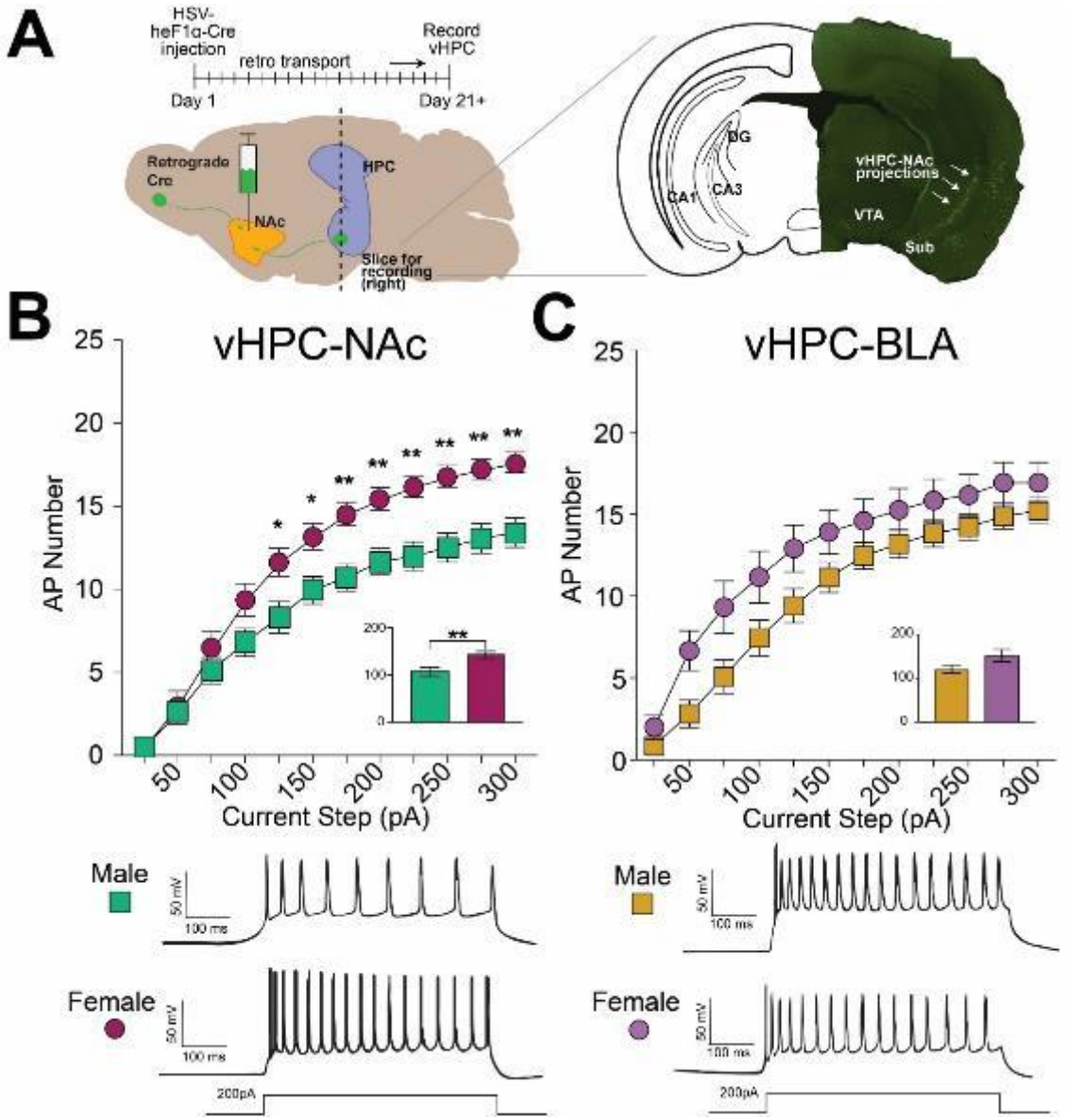

Figure 38 | Selective female vHPC-NAc hyper-excitability. (A) Schematic depicting retrograde Cre viral vector strategy and electrophysiology time course (left) and L10-GFP vHPC stained with anti-GFP demonstrating vHPC-NAc projections (right). **(B, top)** Action potential (AP) number across sequential depolarizing current steps (25-300 pA) for male (n = 20 cells from n = 6 animals) and female (n = 19 cells from n = 5 animals) vHPC-NAc projections. Females showed significantly higher AP number at all steps ≥ 125 pA (inset: sum of AP number across all current steps). **(B, bottom)** Representative traces for male and female vHPC-NAc groups, 200 pA step. **(C, top)** AP number across sequential depolarizing steps for male (n = 22 cells from n = 7 animals) and female (n = 12 cells from n = 4 animals) vHPC-BLA projections. Male and female AP number did not differ at any current step. Inset: sum of AP number across all current steps. **(C, bottom)** Representative traces for male and female vHPC-BLA groups, 200 pA step. DG: Dentate Gyrus; VTA: Ventral Tegmental Area; Sub: Subiculum.

Adult testosterone is necessary for male resilience to SCVS-induced anhedonia and reduced excitability of vHPC-NAc neurons:

To investigate the role of adult sex hormones in susceptibility to SCVS, male mice were orchidectomized (ORCH), allowed to recover for 10 or 28 days, and exposed to SCVS (Figs 39 and 40). Ten days of recovery resulted in main effects of ORCH and stress without interaction between the two (Fig 39), suggesting that SCVS this close to the stressful surgery (sham or ORCH) was sufficient to render male mice susceptible to SCVS-induced anhedonia. In contrast, twenty-eight days following ORCH, male mice displayed reduced sucrose preference following SCVS, while those undergoing sham

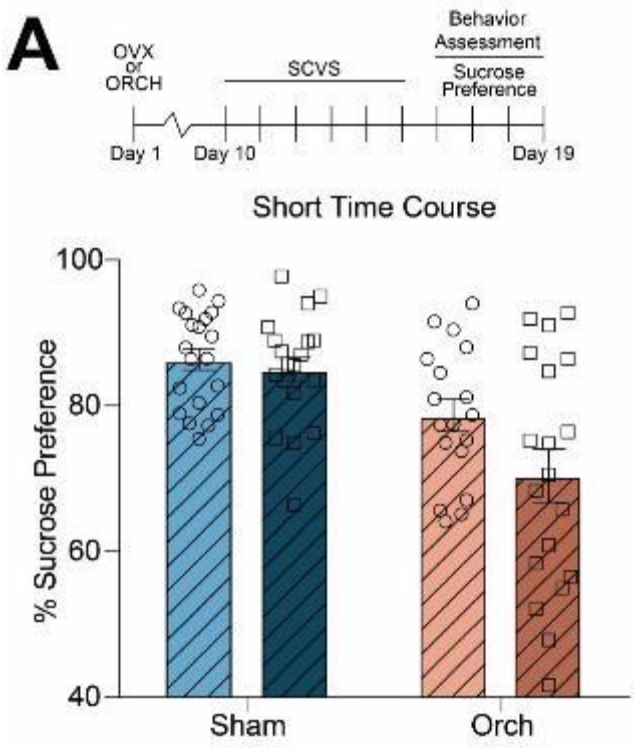

Figure 39 | Orchidectomy does not susceptibility to SCVS in a short time course. **(A, top)** Schematic depicting experimental time course of surgery, stress, and measurement of sucrose preference for short time course orchidectomy experiment. **(A, bottom)** Short time course sham vs orchidectomized male mice showed no interaction between control and stress.

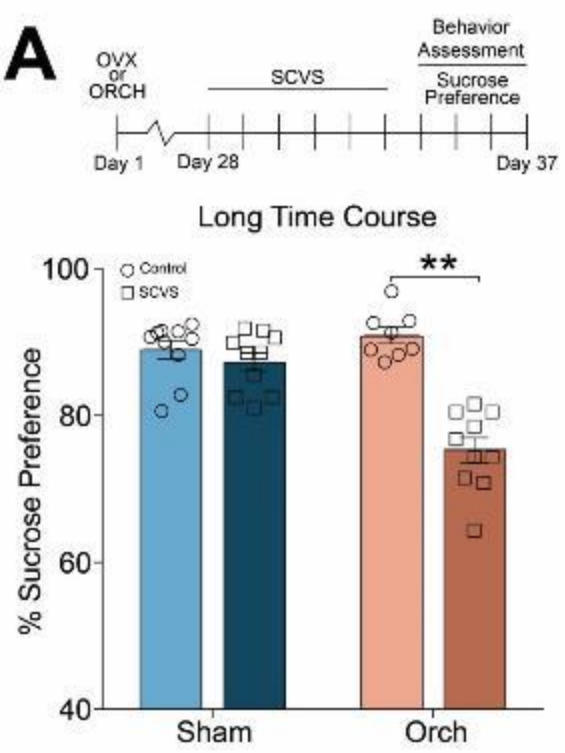

Figure 40 | Orchidectomy induces susceptibility to SCVS. (A, top) Schematic depicting experimental time course of surgery, stress, and measurement of sucrose preference for long time course orchidectomy experiment. **(A, bottom)** Orchidectomized male mice showed significant reduction in sucrose preference compared to non-stress controls, while sham male sucrose preference was unaffected by SCVS.

surgeries remained resilient to decrease in sucrose preference (Fig 40), with an interaction between the two variables. There were no differences between sham and ORCH groups in any other behavioral measure at either time point (Fig 41A-D). These data thus suggest that long-term reduction in androgen signaling is sufficient for SCVS-induced anhedonia in male mice.

To determine whether the sex difference we observed in vHPC-NAc excitability is also dependent on adult sex hormones, we compared vHPC-NAc excitability in ORCH vs. sham male and OVX vs. sham female mice at 10 days post-gonadectomy. Retrograde Cre was injected into NAc, 10 days following intracranial injection gonads were removed,

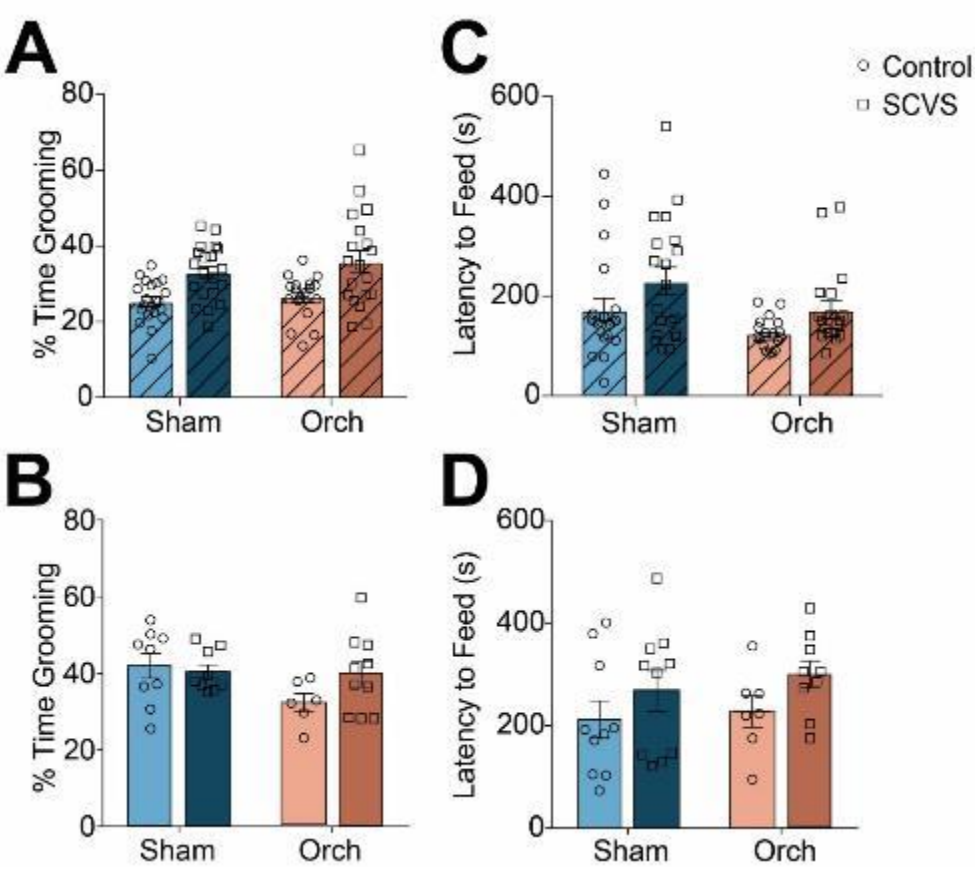

Figure 41 | Additional behavioral assays of sham vs. orchidectomy in SCVS. All behavioral assays other than sucrose preference did not reflect an interaction of hormone status and stress in any of the following measures: Percent time grooming in splash test in the 10-day **(A)** and 28-day **(B)** time courses; and latency to feed (s) in novelty suppressed feeding test in the 10-day **(C)** and 28-day **(D)** time courses.

and 10 days following gonadectomy, vHPC-NAc activity was recorded (Fig 42A). ORCH significantly increased the excitability of male vHPC-NAc neurons compared to that of sham controls (Fig 42B left, example traces for each group right). In contrast, OVX had no effect on the excitability of female vHPC-NAc neurons (Fig 43).

These data suggest that reduction of circulating androgens causes a change in vHPC-NAc excitability that may require time-dependent restructuring of vHPC-NAc neurons over weeks that causes susceptibility to SCVS-induced anhedonia similar to that seen in female mice.

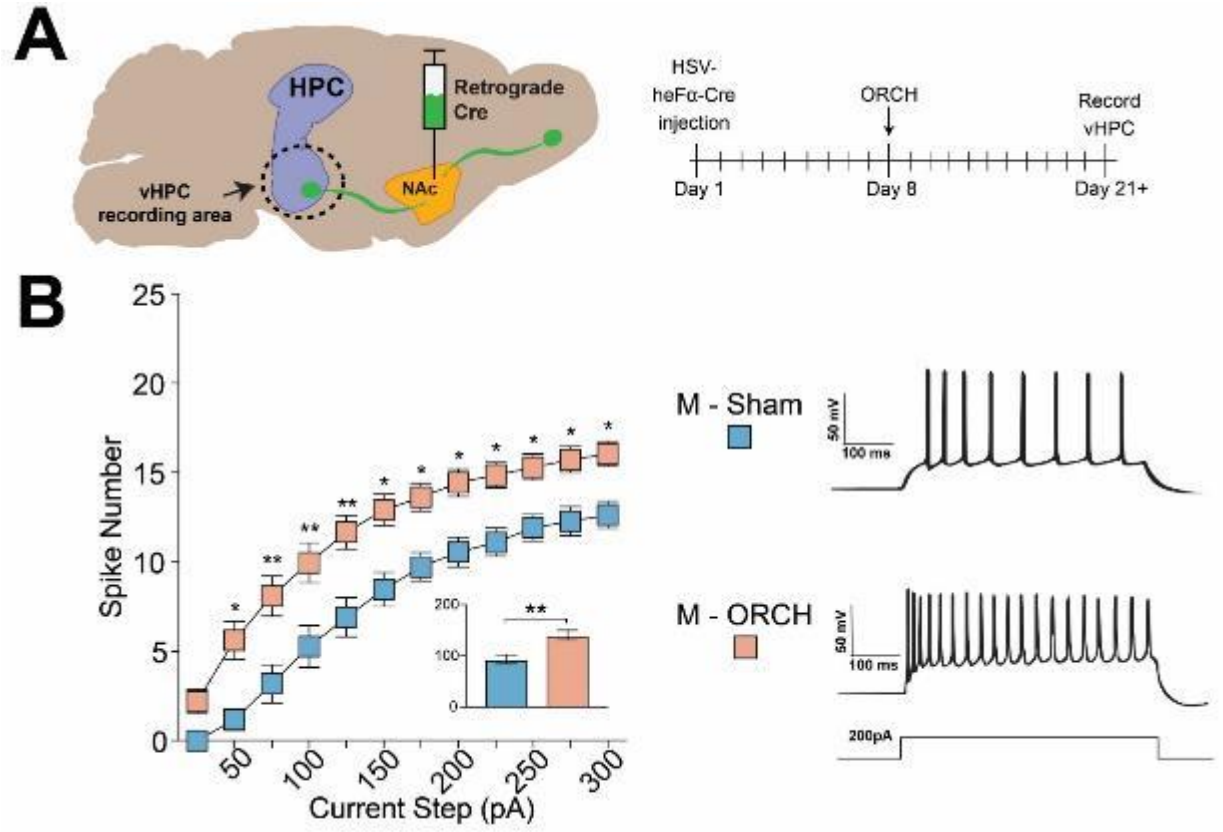

Figure 42 | Orchidectomy increases vHPC-NAc excitability. (A) Schematic depicting retrograde Cre viral strategy for labeling vHPC-NAc projections (left) and experimental time course for surgery and recording (right). **(B, left)** Action potential number across sequential depolarizing current steps (25-300 pA) for sham male (n = 11 cells from n = 3 animals) and orchiectomized male (n = 31 cells from n = 6 animals) vHPC-NAc projections. Orchiectomized male projections showed significantly higher AP number at all steps > 25 pA (inset: sum of AP number across all current steps). **(B, right)** Representative traces for sham and ORCH vHPC-NAc projections, 200 pA step.

Androgen receptor antagonism increases male vHPC-NAc excitability:

We next questioned whether androgen receptors (ARs) are directly involved in the regulation of vHPC-NAc physiology. To verify that ARs are present on vHPC-NAc projection neurons, we used double-label immunofluorescence to stain for AR and GFP in vHPC of L10-GFP reporter mice injected with retrograde HSV-Cre in NAc. As predicted, vHPC-NAc projection neurons, as well as many of the surrounding pyramidal cells in

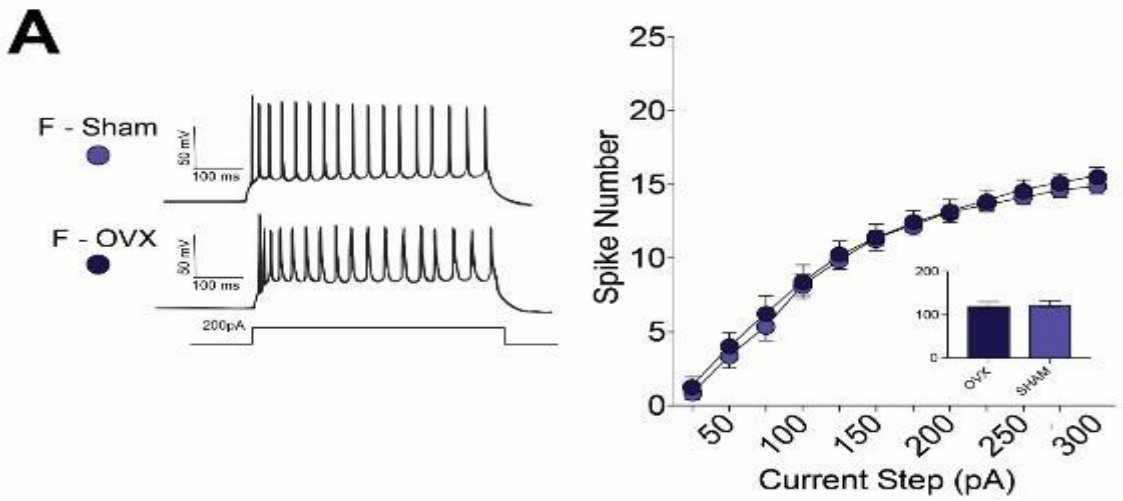

Figure 43 | Excitability in sham vs. ovariectomy female vHPC-NAc projections. **(A)** Sham and OVX female vHPC-NAc neurons did not differ in excitability as measured by number of spikes per 25 pA current injection step from 25-300 pA; inset: total number of spikes summed over all current injection steps did not differ between sham and OVX groups.

vHPC CA1, do indeed express AR (Fig 44). To test whether ARs are directly involved in the regulation of vHPC-NAc neuronal excitability, the AR antagonist flutamide was used in conjunction with slice electrophysiology to determine effects on projection physiology. Either vehicle (DMSO) or flutamide + picrotoxin-spiked aCSF solutions were used in the slice incubation chamber as well as the main bath to record from vHPC-NAc cells in L10-GFP mice injected with retrograde Cre virus at NAc (Fig 45). Those cells exposed to flutamide + picrotoxin aCSF were found to have increased excitability compared to those treated with vehicle aCSF, as indicated by a significantly elevated total number of spikes across all current injections (Fig 45, inset), although no significant differences were revealed at any current injections (Fig 45).These data support AR activation, possibly through androgen stimulation as suggested by our orchidectomy findings, as a potential direct regulator of excitability of male vHPC-NAc neurons that could mediate resilience to anhedonia following SCVS.

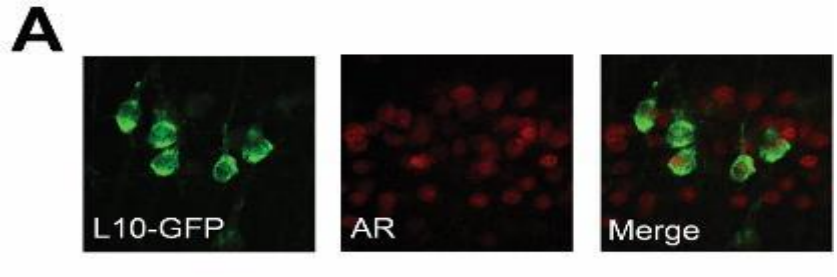

Figure 44 | vHPC-NAc Express Androgen Receptors. (A) Representative AR staining of vHPC slices from a male L10-GFP mouse; left panel shows L10-GFP staining, middle panel shows AR staining, and the left panel shows a merged image demonstrating AR expression on vHPC-NAc projection cells. All images at 100x magnification.

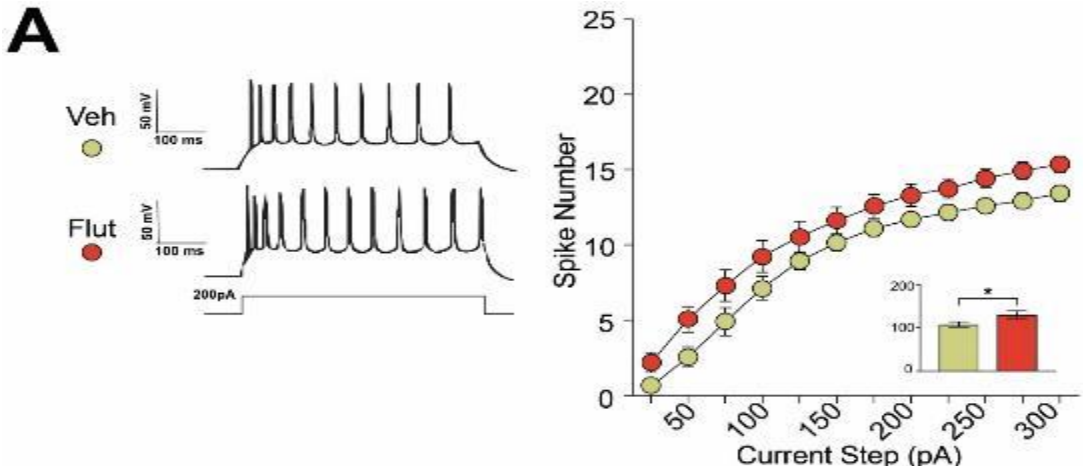

Figure 45 | Androgen receptor antagonism increases male vHPC-NAc excitability. (A, left) Representative traces for vehicle- and flutamide-treated vHPC-NAc neurons, 200 pA step. **(A, right)** Action potential number across sequential depolarizing current steps (25-300 pA) for vehicle- (n = 20 cells from n = 7 animals) and flutamide-treated (n = 16 cells from n = 6 animals) vHPC-NAc projections. Total number of spikes for flutamide-treated cells vs vehicle-treated cells (inset) was increased.

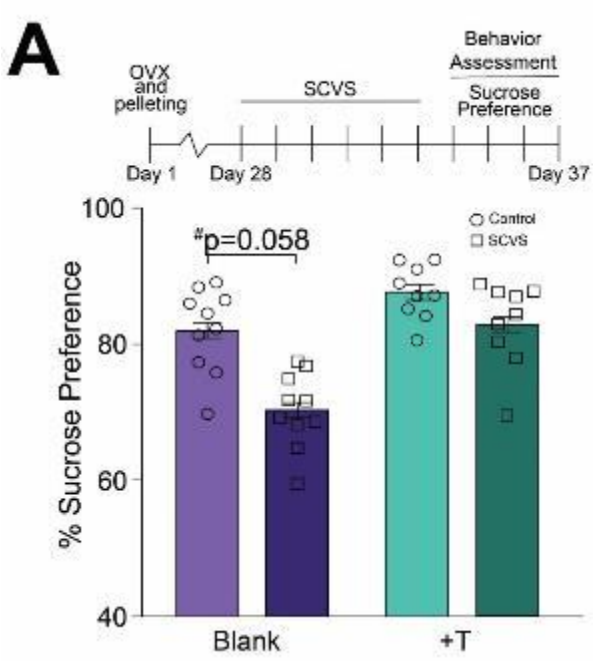

Figure 46 | Susceptibility to SCVS-induced anhedonia are dependent on adult testosterone. (A, top) Schematic depicting experimental time course of surgery, stress, and measurement of sucrose preference. **(A, bottom)** OVX females with blank pellet implants maintained a reduction in sucrose preference following SCVS, while OVX female mice exposed to testosterone showed no reduction in sucrose preference following SCVS, indicating resilience.

Exogenous testosterone in female mice ameliorates susceptibility to SCVS and decreases vHPC-NAc excitability:

To determine whether exogenous testosterone could protect female mice against the anhedonic effects of SCVS, we implanted 6mm Silastic blank or testosterone pellets in adult female mice simultaneously with ovariectomy (OVX). Following OVX and implantation, 28 days were allowed for healing and equilibration of hormones. Mice were then exposed to SCVS, and behavioral assessment began immediately following the last day of SCVS (Fig 46, top). There was a trend towards an interaction between stress and hormone status, with female mice implanted with blank pellets having reduced sucrose preference after SCVS and those implanted with testosterone pellets showed no effect of stress on sucrose preference, indicating resilience similar to that of male mice. (Fig 46,

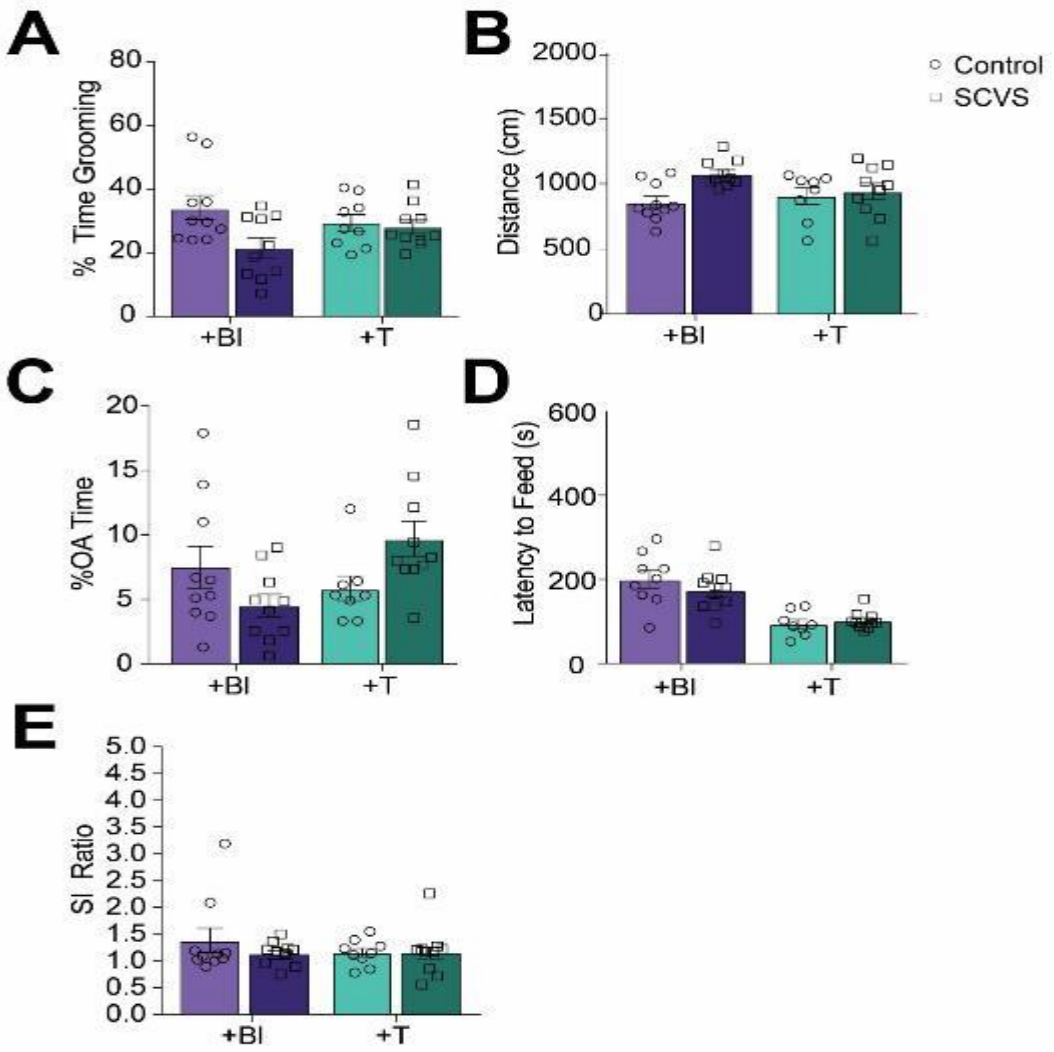

Figure 47 | Additional behavioral assays of female OVX + Blank and OVX + T SCVS. All behavioral assays other than sucrose preference were unaffected by hormone interaction with SCVS in OVX + Blank and OVX + T groups, with no interaction of stress and hormone status in any of the following measures: **(A)** Percent time grooming in splash test; **(B)** Distance moved (cm) in EPM; **(D)** Latency to feed (s) in novelty suppressed feeding test; and **(E)** SI Ratio in social interaction test. **(C)** Percent open arm (OA) time in EPM did show a significant interaction between stress and hormone status, but no differences between stress and control in either the OVX + Bl or OVX + T group.

bottom). Several other behaviors differed between blank and testosterone pellet-implanted female mice, including a main effect of testosterone on NSF and an interaction

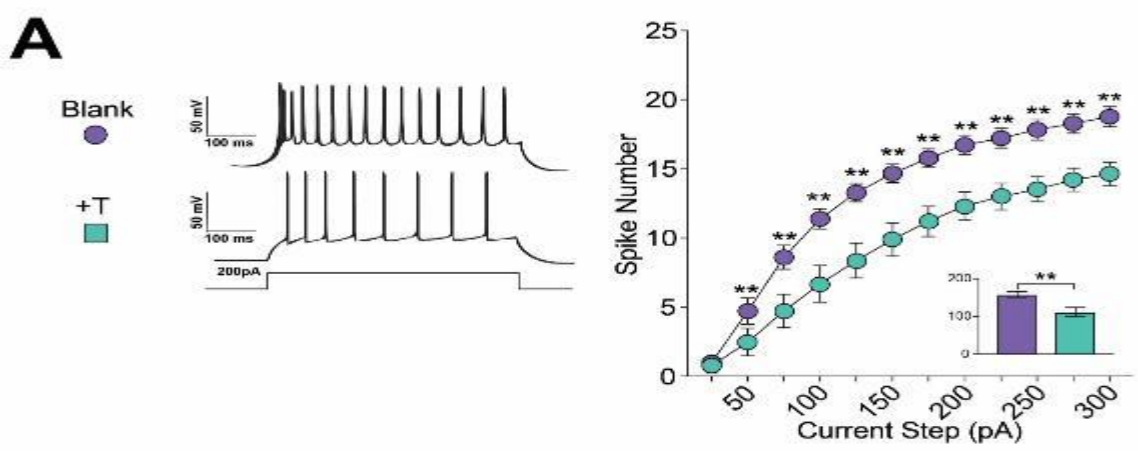

Figure 48 | vHPC-NAc excitability is dependent on adult testosterone. (A, left) Representative traces for OVX + BLANK and OVX + T vHPC-NAc projections, 200 pA step. **(A, right)** Action potential number across sequential depolarizing current steps (25-300 pA) for OVX + BLANK (n = 11 cells from n = 3 animals) and OVX + T (n = 19 cells from n = 5 animals) vHPC-NAc projections. OVX + T projections showed significantly lower AP number at all steps > 25 pA (inset: sum of AP number across all current steps).

between stress and testosterone status on EPM (Fig 47A-E). These data suggest a direct protective effect of testosterone or its derivatives against the anhedonic effects of SCVS.

To investigate whether exogenous testosterone could also reduce excitability of vHPC-NAc neurons in female mice, we injected L10-GFP female mice with retrograde HSV-Cre in NAc. One week later, OVX and pellet implantation were performed in a single procedure. Two weeks following implantation, we performed whole-cell slice physiology on vHPC-NAc projection neurons. OVX mice implanted with testosterone pellets exhibited significantly decreased excitability in vHPC-NAc neurons compared to OVX mice implanted with blank pellets (Fig 48 bottom, example traces for each group top). These results suggest that exogenous testosterone or its derivatives reduce excitability of female vHPC-NAc neurons and drives resilience to SCVS-induced anhedonia in females.

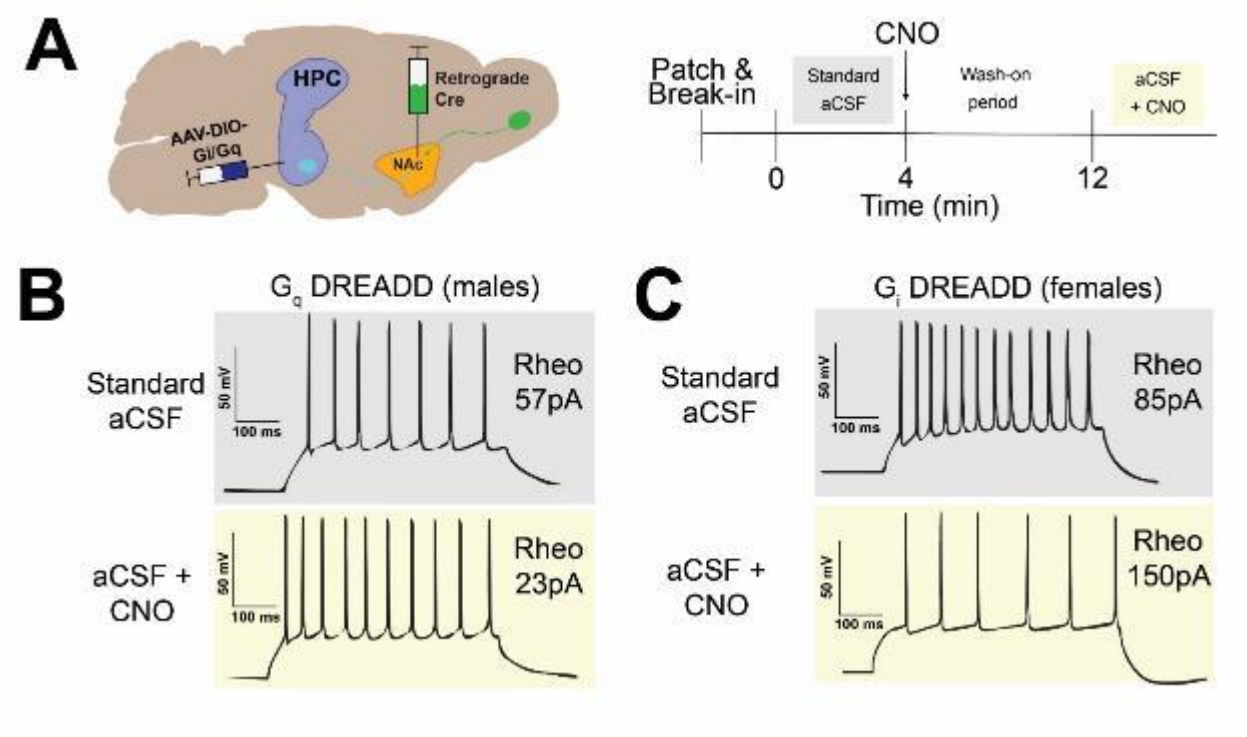

Figure 49 | Circuit-specific DREADD validation. (A, left) Schematic depicting intersecting viral DREADD strategy for circuit-specific manipulation of vHPC-NAc excitability and experimental time course. AAV encoding Cre-inducible DREADD (either G_q- or G_i-coupled) was injected in vHPC, and retrograde HSV-Cre was injected in NAc, causing circuit-specific receptor expression. **(A, right)** Schematic depicting time course for DREADD recordings. Cells were first recorded in regular aCSF, then CNO-containing aCSF was washed on and the same cell was recorded 8-10 minutes later. **(B and C)** Whole-cell slice electrophysiology demonstrating CNO activating G_q- **(B)** and G_i-coupled **(C)** receptors. Example traces before (grey) and after (yellow) CNO application along with rheobase at time of each recording.

vHPC-NAc excitability directly mediates susceptibility to anhedonia:

To determine whether the excitability of vHPC-NAc neurons is directly responsible for susceptibility to SCVS-induced anhedonia, we employed an intersecting viral DREADD strategy. In wild-type mice, retrograde HSV-Cre was injected into NAc, and a Cre-dependent AAV-mCherry-hM3D_q (Gq-coupled DREADD in male mice) or AAV-mCherry-hM4D_i (Gi-coupled DREADD in female mice) was injected into vHPC (Fig 49A, left). Using this strategy, only vHPC-NAc neurons transduced by both viruses were altered by systemic CNO administration. We verified the efficacy of the DREADDs using slice

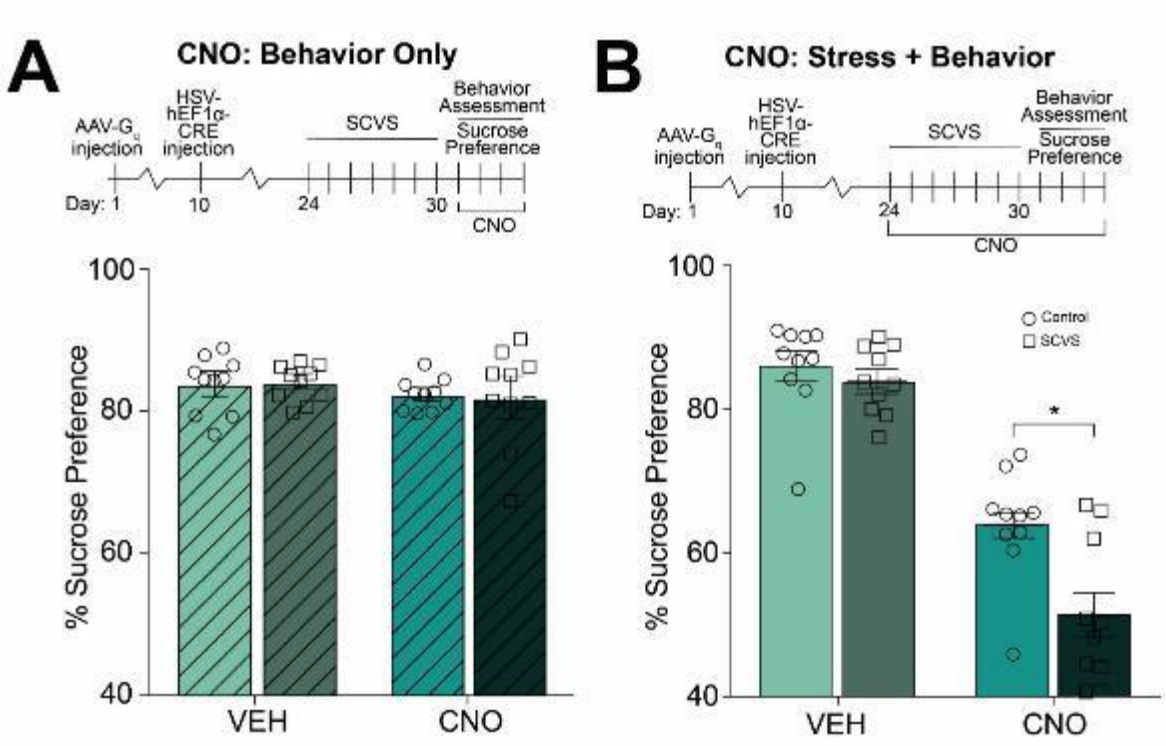

Figure 50 | Prolonged vHPC-NAc activation causes susceptibility to SCVS-induced anhedonia. (A, top) Experimental timeline of DREADD surgery, retrograde Cre surgery, SCVS, and subsequent behavioral assessment for short (behavior-only) DREADD experiment for male mice. **(A, bottom)** Male mice expressing excitatory G_q-coupled DREADD in vHPC-NAc projections and exposed to CNO only during behavior assessment did not show any change in sucrose preference following SCVS. **(B, top)** Experimental timeline for long (CNO during both SCVS and behavior assessment) DREADD experiment for male mice. **(B, bottom)** Male mice expressing excitatory G_q-coupled DREADD in vHPC-NAc projections and exposed to CNO during both SCVS and behavior assessment experienced an overall reduction in sucrose preference and a further reduction in sucrose preference following SCVS.

electrophysiology in vHPC guided by the mCherry tag and recording before and after CNO wash-on (timeline Fig 49A, right). We used exemplar neurons expressing mCherry in vHPC, thus presumably epressing the G_q-coupled DREADD in male increased in excitability following CNO wash-on, with an increase in number of spikes at 150 pA injected current, as well as a decrease in rheobase (Fig 49B). Female vHPC-NAc neurons expressing the G_i-coupled DREADD decreased in excitability following CNO wash-on,

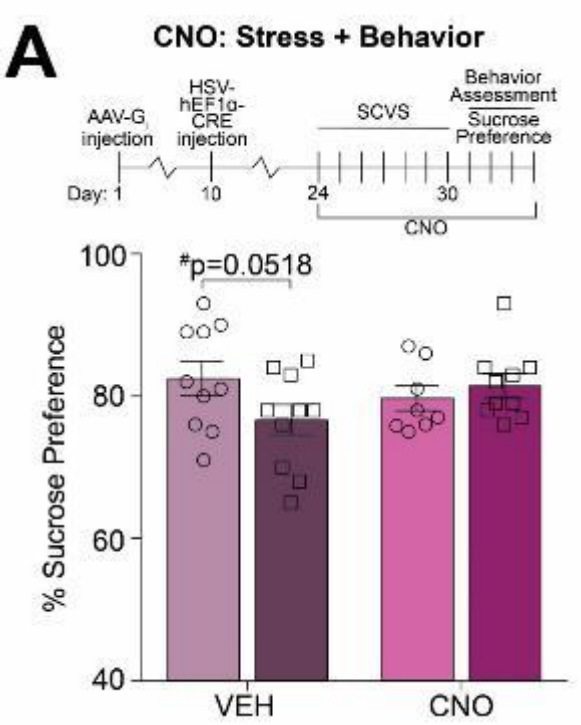

Figure 51 | vHPC-NAc inhibition prevents susceptibility to SCVS-induced anhedonia. (A, top) Experimental timeline for female mice. **(A, bottom)** Female mice expressing inhibitory G_i-coupled DREADD in vHPC-NAc projections and exposed to activating CNO showed no change in sucrose preference following SCVS.

with a decrease in the number of spikes at 150 pA injected current, as well as an increase in rheobase (Fig 49C).

Three weeks after surgery, male mice expressing the excitatory G_q-coupled DREADD in vHPC-NAc were exposed to SCVS followed by CNO or saline administration via i.p. injection each day of behavioral testing (Fig 50A, top). Intriguingly, CNO failed to directly evoke changes in sucrose preference (Fig 50A, bottom), indicating that short-term increased activity of the circuit does not cause anhedonia. A second cohort of males expressing G_q-coupled DREADD in vHPC-NAc was exposed to SCVS with CNO or saline exposure throughout both stress and behavioral testing (Fig 50B, top).

These long-term CNO-treated male mice showed a decrease in sucrose preference overall, as well as a further SCVS-induced decrease in sucrose preference (Fig 50B, bottom). There was a significant interaction between stress and CNO treatment in the measure of SI ratio (Fig 52B), but no interaction between stress and CNO treatment in EPM open arm time (Fig 53B). Because CNO can be metabolized into clozapine which can affect animal behavior, we also performed a control experiment in which male mice without DREADD overexpression were stressed and administered CNO using the same protocol, and we observed no change in sucrose preference (Fig 54). These data suggest that short-term artificial stimulation of the vHPC-NAc circuit does not directly cause anhedonia in stressed or non-stressed animals. However, prolonged increase in excitability of this circuit elicits anhedonia at baseline, and if these changes in excitability are paired with stress, the anhedonic response in male mice is enhanced.

Female mice expressing inhibitory G_i-coupled DREADD in vHPC-NAc were exposed to SCVS while CNO or saline was administered via i.p. injection each day of stress and throughout behavioral testing (Fig 51, top). Saline-treated female mice showed a decrease in sucrose preference following SCVS that reached p=0.0518, while CNO-treated female mice showed an amelioration of this susceptibility to anhedonia following stress (Fig 51, bottom). There was no significant interaction between stress and CNO treatment in the measures of SI ratio (Fig 52C) or EPM open arm time (Fig 53C). Overall, these data indicate that prolonged, but not acute, alterations in vHPC-NAc neuronal excitability can elicit or relieve anhedonic behavioral effect of SCVS.

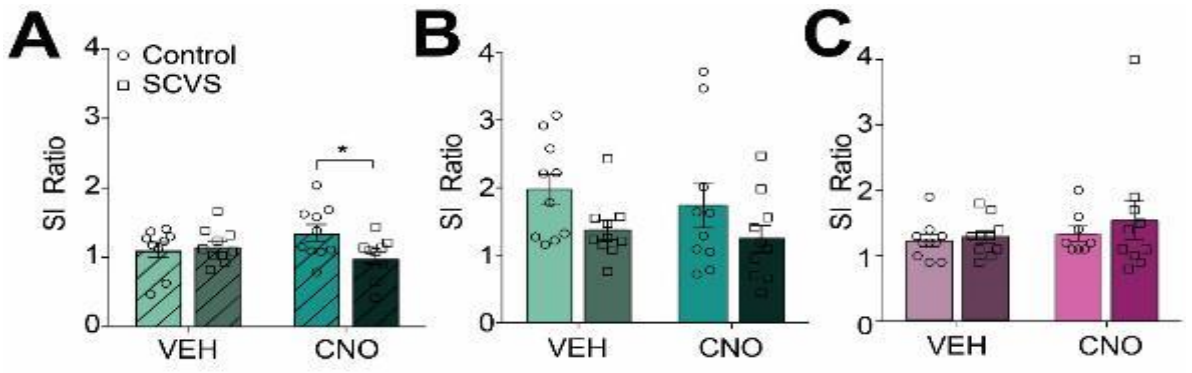

Figure 52 | Social Interaction of Gq-coupled (male) and Gi-coupled (female) DREADD-expressing vHPC-NAc mice. For the short CNO administration Gq DREADD vHPC-NAc activation, there was also an interaction between SCVS and male vHPC-NAc activation in **(A)** SI ratio in social interaction test; with CNO injections reducing social interaction after stress. No interaction was observed between SCVS and long CNO administration in SI ratio in **(B)** male Gq DREADD vHPC-NAc activation or **(C)** female Gi DREADD vHPC-NAc inhibition.

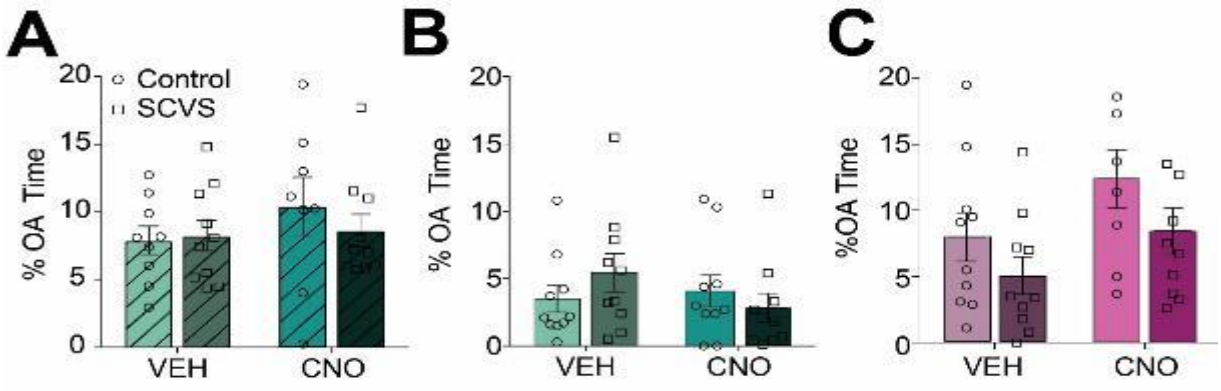

Figure 53 | Anxiety measures of Gq-coupled (male) and Gi-coupled (female) DREADD-expressing vHPC-NAc mice. (A) For the short CNO administration Gq DREADD vHPC-NAc activation, percent open arm time in EPM remained unaffected. Furthermore, no interactions were observed between SCVS and long CNO administration percent open arm (OA) time in EPM in **(B)** male Gq DREADD vHPC-NAc activation or **(C)** female Gi DREADD vHPC-NAc inhibition.

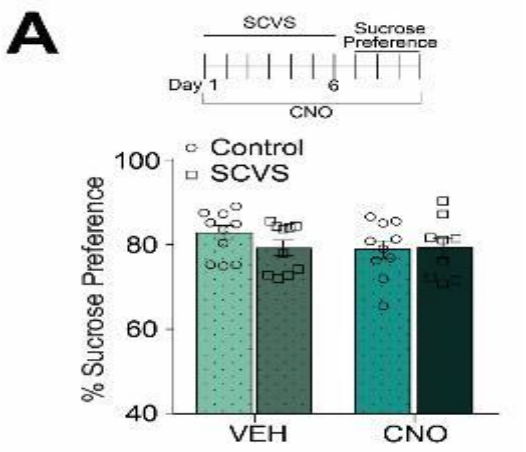

Figure 54 | Long-term CNO administration effect on anhedonia in males. (A) CNO or vehicle was administered in male mice without the presence of DREADD expression throughout the duration of SCVS stress battery and sucrose preference assessment. There was no interaction between stress and treatment, and no differences in sucrose preference were observed in either vehicle- or CNO-treated control and stressed groups.

Sex-specific transcriptomics of vHPC-NAc neurons:

To investigate potential mechanisms by which the excitability of male and female vHPC-NAc neurons differ, we utilized translating ribosome affinity purification (TRAP) to interrogate circuit-specific gene expression. Using the retrograde Cre strategy described above, vHPC-NAc neurons of male and female mice were labeled with L10-GFP and bilateral ventral hippocampus punches were collected and pooled. Thus, actively translating mRNA from this circuit was purified and used to prepare cDNA libraries for sequencing (Fig 55A). RNAseq revealed enrichment of neuron-specific mRNA (e.g. *Vamp2,* Fig 55B) in the pulldown samples compared to input, while genes specific to glia (e.g. *Slc14a1* and *Bcas1)* were depleted (Fig 56A,B). Moreover, we observed that more transcripts were higher than were lower in abundance in male mice compared to female mice (Fig 55C), suggesting the possibility of an active mechanism in this circuit driving resilience to stress-induced anhedonia. Importantly, we also observed the largest

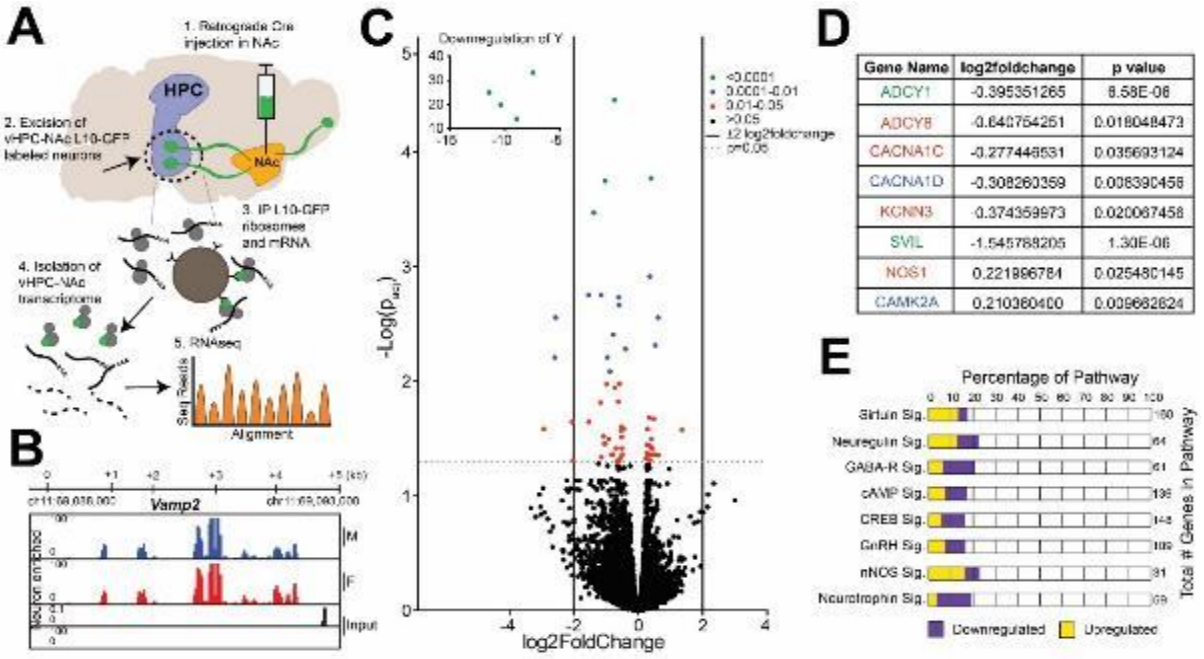

Gene Name	log2foldchange	p value
ADCY1	-0.395351265	8.58E-06
ADCY8	-0.640754251	0.018048473
CACNA1C	-0.277446531	0.035693124
CACNA1D	-0.308260359	0.008390456
KCNN3	-0.374359973	0.020087458
SVIL	-1.545788205	1.30E-06
NOS1	0.221896784	0.025480145
CAMK2A	0.210360400	0.009682624

Figure 55 | Male and female vHPC-NAc transcriptomes. (A) Schematic depicting retrograde L10-GFP labeling strategy and general TRAP and sequencing steps. **(B)** RNA sequencing reads for neuron-specific gene vesicle-associated membrane protein 2 (*VAMP2)* in male (top) and female (middle) TRAP samples compared to input (bottom). **(C)** Volcano plot showing distribution of transcript enrichment in female vs. male vHPC-NAc TRAP. Inset shows Y-linked genes: *Uty* [-log(p_{adj})=32.662]; *Eif2s3y* [-log(p_{adj})=13.517]; *Kdm5d* [-log(p_{adj})=19.380]; *Ddx3y* [-log(p_{adj})=24.487]. X-linked genes that were greatly significantly enriched in female mice were omitted for clarity of illustration. **(D)** Table listing significantly differentially regulated genes. Log2foldchange listed for female vHPC-NAc neurons compared to male vHPC-NAc neurons. **(E)** Selected pathways affected by sex as determined by Ingenuity Pathway Analysis. Down- and upregulated gene numbers (female vs male) represented as a percentage of the total number of genes within the given pathway.

difference in transcript abundance between the sexes in Y-linked genes (many orders of magnitude more abundant in males, see inset Fig 55C), indicating that our methodology for uncovering sexually dimorphic gene expression in this circuit was sound.

Sequencing of TRAP mRNA revealed many differentially regulated genes between female and male vHPC-NAc neurons, a number of which are highlighted in Figure 55D. Many of these genes are potential mediators of the basal sex difference in excitability in this circuit. Moreover, Ingenuity pathway analysis (IPA, Qiagen; Hilden, Germany) applied

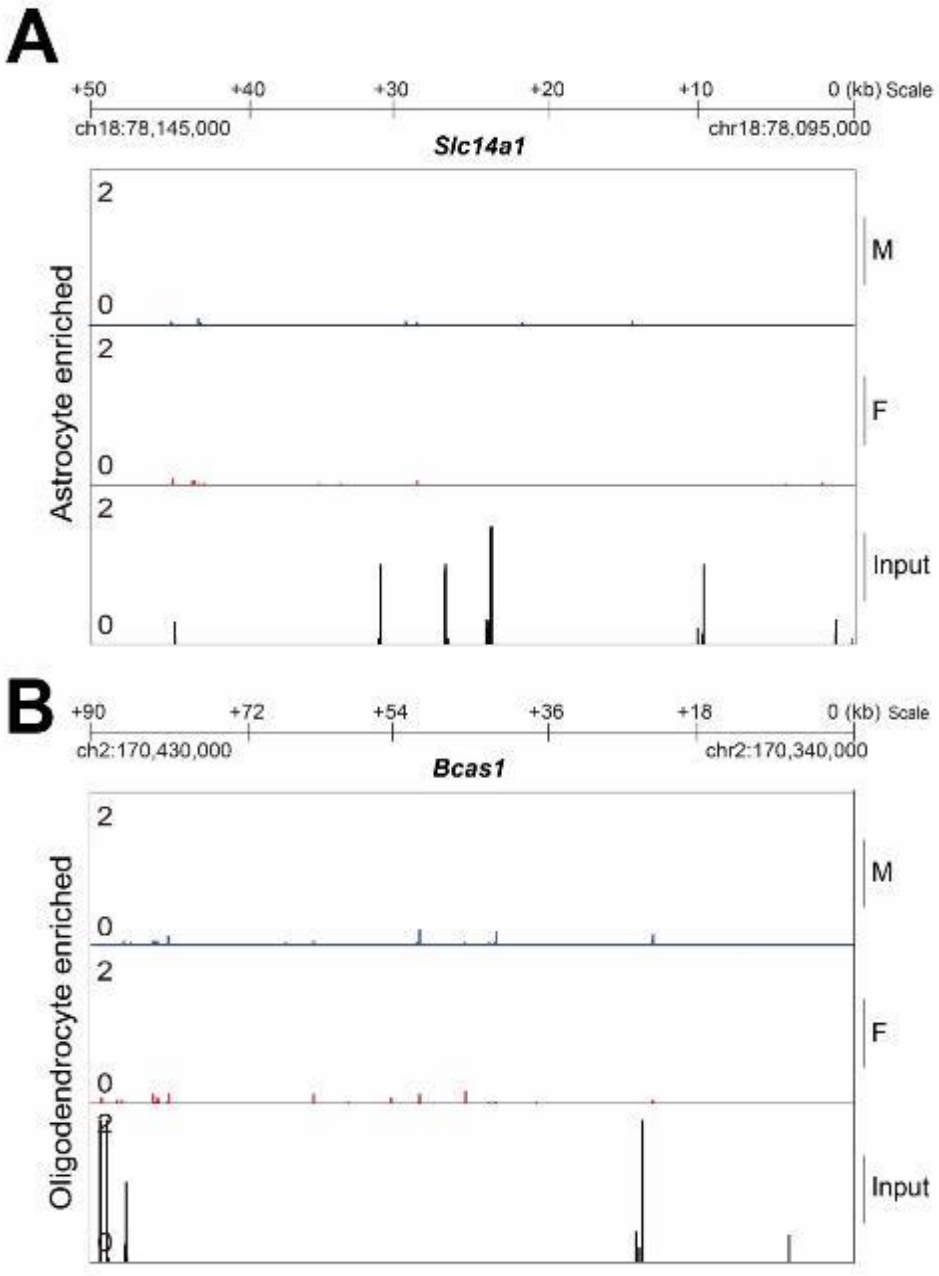

Figure 56 | Example glia-related genes depleted in male and female TRAP samples. Gene depletion was verified for genes related to glia, as these genes were expected not to be enriched in the neuron-specific TRAP pulldown. **(A)** Astrocyte-related gene *Slc14a1* was depleted in male and female TRAP samples (top and middle) compared to input (bottom). **(B)** Oligodendrocyte-related gene *Bcas1* depleted in male and female TRAP samples (top and middle) compared to input (bottom). Depletion of glia-related genes in TRAP samples verifies that the TRAP pulldowns were neuron-specific.

involved in regulating hippocampal excitability (Fig 55E). These analyses demonstrate successful enrichment of vHPC-NAc mRNA and reveal clear sex differences in the transcriptome of this circuit, including several potential mechanisms for the differential excitability between male and female mice to be explored in future studies.

Discussion

In this chapter, we use mouse behavior, slice electrophysiology, and intersecting DREADD viral manipulation of circuit function to define a novel neurophysiological mechanism for sex differences in anhedonic responses to stress. We found that susceptibility to SCVS-induced anhedonia correlates with a sex-dependent heightened vHPC-NAc excitability of female mice. Further, we demonstrated that circulating adult gonadal hormones underlie these sex differences in behavior and circuit-specific excitability. Additionally, we show that vHPC-NAc circuit physiology indirectly regulates susceptibility to stress over time: increasing the activity of male vHPC-NAc neurons is sufficient to induce anhedonia following SCVS, but only when the activity is increased over a prolonged period, suggesting a long-term adaptation to circuit activity that drives behavior. Conversely, we demonstrate that decreasing the activity of female vHPC-NAc neurons over a prolonged period is sufficient to induce resilience to anhedonia following SCVS.

Exploring sex as a biological variable in preclinical models of mood disorders is essential, as there is an enigmatic sex difference in human depression diagnostic rates. Women are more likely than men to be diagnosed with depression across the lifespan[417], and these diagnoses often surround changes to the reproductive cycle such as puberty,

menstruation, postpartum, and menopause[28, 418]. Moreover, meta-analyses of studies totaling nearly one thousand subjects demonstrate that adult (18-60yrs) but not aged (>60yrs) males with reduced testosterone are more likely to suffer depression and their symptoms, including anhedonia, can be significantly relieved by testosterone supplement[419]. However, exploring the circuit and molecular underpinnings of sex differences in depression has been difficult, in part due to many preclinical behavioral models of depression and stress-induced behaviors focusing on intersexual aggression, leaving female models understudied[38, 46, 53]. In the last decade, there has been a proliferation of models attempting to address this disparity[37, 39, 58, 420], including SCVS[63, 335]. Previous studies have highlighted the importance of the NAc in the regulation of SCVS-induced behaviors, including processes such as transcriptional and epigenetic regulation, and many of these studies have implicated steroid hormones and their receptors[44, 63, 64]. Furthermore, recent work demonstrates that stress-induced changes in females may be presynaptic, either through glutamatergic inputs onto NAc medium spiny neurons or in other reward-related circuits[65, 335]. This is concordant with previous work in males suggesting the strength of vHPC glutamatergic synapses in the NAc underlies susceptibility to chronic social defeat stress[127]. These studies, along with human studies that demonstrate a decreased hippocampal volume in patients with MDD[421], suggest that the vHPC may be a mediator of sex differences in stress outcomes and depression-related behaviors, especially through its projections to the NAc. Additionally, circulating hormones are known to dramatically affect vHPC CA1 structure and function[422-424] as well as social and hippocampal-dependent learning[425, 426].

We show that vHPC afferents to NAc, but not BLA, have increased excitability in female mice and that the presence of testosterone is sufficient to decrease the excitability of the vHPC-NAc circuit while conferring resilience to SCVS. Previously, vHPC-NAc afferents have been implicated in modulating social behaviors[300, 427]. Here, we demonstrate vHPC-NAc projection-specific regulation of the likewise positively-valenced measure of sucrose preference, a well-validated measure of anhedonia[53, 428, 429]. We show that reduced sucrose preference after SCVS is female-specific and that this correlates with higher vHPC-NAc, but not vHPC-BLA, excitability. This sex difference appears to be dependent on circulating gonadal hormones, as orchidectomy in male mice feminizes the vHPC-NAc excitability and SCVS-induced anhedonia, and testosterone in female mice decreased vHPC-NAc excitability and prevents anhedonia. However, our gonadal hormone manipulations were systemic and may therefore act in a non-cell autonomous manner, perhaps exerting their effects at the level of adjacent circuitry or even via support cells such as glia. In addition, androgens may be aromatized to estrogens in the brain further complicating the mechanism of androgens' actions. However, as we show that vHPC-NAc neurons express AR and their excitability is unchanged following ovariectomy, while bath application of AR antagonist increases vHPC-NAc excitability, we hypothesize that direct activation of androgen receptors mediates these effects, potentially within the vHPC-NAc cells themselves.

The basal sex differences we demonstrate in vHPC-NAc excitability and behavioral responses to stress are in agreement with work in males that highlights the activity of vHPC-NAc afferents as a driver of behavioral responses to chronic social defeat stress[127, 409]. To demonstrate the causal link between vHPC-NAc excitability and

susceptibility to SCVS, we utilized DREADDs in both male and female mice to artificially increase or decrease projection excitability, respectively. We found that 10 days of systemic administration of CNO in males with excitatory DREADDs in vHPC-NAc directly induced anhedonia as measured by decreased sucrose-preference and promoted susceptibility to anhedonia following SCVS with application of CNO. Intriguingly, recent report suggests a chronic multimodal stress model reduces vHPC synaptic strength onto D1 medium spiny neurons of the NAc in stress-susceptible males[127, 409]. This discordance may be due to our study's inability to distinguish between D1 and D2 expressing projections in the NAc or due to other long term changes in reward related circuits in response to chronic activity of vHPC-NAc. Indeed, prolonged changes in activity may lead to a number of neuroadaptations, including changes in gene expression and synaptic strength, to drive differential responses to stress, both within vHPC-NAc neurons or adjacent circuitry. This notion is supported by literature demonstrating that long-term changes in the strength of vHPC synapses onto NAc medium spiny neurons drive motivated behaviors in multiple contexts including chronic stress and drug of abuse[127, 409]

As our short time courses of orchidectomy or vHPC-NAc activity manipulation did not elicit the same robust behavioral effects as prolonged manipulations of the circuit, we hypothesize that vHPC-NAc neuronal excitability primes neuroadaptations which elicit stress-induced anhedonia. Thus, uncovering the mechanisms underlying both the basal sex differences in vHPC-NAc excitability, like androgens' precise mechanism action, and neuroadaptations, including changes gene expression and synaptic strength in both sexes provide exciting subjects for future studies.

The experiments presented in this chapter uncover a basal sex difference in excitability of the vHPC-NAc circuit driven by adult testosterone that is causally linked to susceptibility to anhedonia, a key behavioral phenotype of mood disorders. This discovery may in part explain the clinical observation that women are more than twice as likely as men to experience depressive disorders, paving the way for sex-specific treatment of depression. However, these experiments did not examine sex-specific changes in gene expression following stress. In chapter 4, I showed that vHPC afferent expression of the IEG ΔFosB was necessary and sufficient for behavioral responses to CSDS in males. Therefore, in the next chapter I sought to elucidate if males and females had differences in vHPC afferent ΔFosB expression and whether manipulation of ΔFosB would affect basal and stress-dependent behavior in a sex-specific manner.

Table 5 | Statistical comparisons in chapter 5

Figure	Test	Comparison	Stat	p Value	Sum-mary
Fig 36B	2-way ANOVA	Group: Male vs Female	F(1,112)=1.109	p = 0.2946	n.s.
		Trial: Control vs Stress	F(1,112)=1.212	p = 0.2734	n.s.
		Group X Trial	F(1,112)=6.518	p = 0.0120	*
Fig 37A	2-way ANOVA	Group: Male vs Female	F(1,73)=6.223	p = 0.0149	*
		Trial: Control vs Stress	F(1,73)=1.481	p = 0.2276	n.s.
		Group X Trial	F(1,73)=0.1272	p = 0.7223	n.s.
Fig 37B	2-way ANOVA	Group: Male vs Female	F(1,111)=0.9638	p = 0.3284	n.s.
		Trial: Control vs Stress	F(1,111)=0.0319	p = 0.8585	n.s.
		Group X Trial	F(1,111)=1.358	p = 0.2465	n.s.
Fig 37C	2-way ANOVA	Group: Male vs Female	F(1,112)=2.112	p = 0.1489	n.s.
		Trial: Control vs Stress	$F(1,112)=4.352x10^{-6}$	p = 0.9983	n.s.
		Group X Trial	F(1,112)=0.2906	p = 0.5909	n.s.
Fig 37D	2-way ANOVA	Group: Male vs Female	F(1,107)=10.23	p = 0.0018	**
		Trial: Control vs Stress	F(1,107)=2.92	p = 0.0904	n.s.
		Group X Trial	F(1,107)=0.5162	p = 0.4741	n.s.
Fig 37E	2-way ANOVA	Group: Male vs Female	F(1,115)=0.8692	p = 0.3531	n.s.
		Trial: Control vs Stress	F(1,115)=3.712	p = 1.087	n.s.
		Group X Trial	F(1,115)=3.093	p = 0.0813	n.s.
Fig 38B	2-way RM ANOVA	Male vs Female			
		25pA	t(444)=0.1142	p = 0.9091	n.s.
		50pA	t(444)=0.4545	p = 0.8773	n.s.

Table 5 (cont'd)

		75pA	t(444)=1.147	p = 0.5816	n.s.
		100pA	t(444)=2.322	p = 0.0801	n.s.
		125pA	t(444)=3.012	p = 0.0163	*
		150pA	t(444)=2.901	p = 0.0194	*
		175pA	t(444)=3.46	p = 0.0047	**
		200pA	t(444)=3.41	p = 0.0050	**
		225pA	t(444)=3.76	p = 0.0019	**
		250pA	t(444)=3.879	p = 0.0015	**
		275pA	t(444)=3.762	p = 0.0019	**
		300pA	t(444)=3.826	p = 0.0016	**
Fig 38B, inset	Two-tailed t-test	Male vs Female	t(37)=2.96	p = 0.0053	**
Fig 38C	2-way RM ANOVA	Male vs Female			
		25pA	t(384)=0.745	p = 0.9993	n.s.
		50pA	t(384)=2.523	p = 0.1352	n.s.
		75pA	t(384)=2.781	p = 0.0661	n.s.
		100pA	t(384)=2.434	p = 0.1699	n.s.
		125pA	t(384)=2.3	p = 0.2343	n.s.
		150pA	t(384)=1.823	p = 0.5765	n.s.
		175pA	t(384)=1.396	p = 0.8828	n.s.
		200pA	t(384)=1.356	p = 0.9019	n.s.
		225pA	t(384)=1.321	p = 0.9169	n.s.
		250pA	t(384)=1.272	p = 0.9356	n.s.

Table 5 (cont'd)

		275pA	t(384)=1.346	p = 0.9063	n.s.
		300pA	t(384)=1.108	p = 0.9766	n.s.
Fig 38c, inset	Two-tailed t-test	Male vs Female	t(32)=1.861	p = 0.0720	n.s.
Fig 39A	2-way ANOVA	Group: Sham vs ORCH	F(1,73)=21.78	p < 0.0001	***
		Trial: Control vs Stress	F(1,73)=4.115	p = 0.0462	*
		Group X Trial	F(1,73)=2.116	p = 0.15	n.s.
Fig 40A	2-way ANOVA	Group: Sham vs ORCH	F(1,34)=24.76	p <0.0001	****
		Trial: Control vs Stress	F(1,34)=12.74	p=0.0011	**
		Group X Trial	F(1,34)=38.33	p<0.0001	****
Fig 41A	2-way ANOVA	Group: Sham vs ORCH	F(1,73)=1.244	p = 0.2684	n.s.
		Trial: Control vs Stress	F(1,73)=20.28	p < 0.0001	****
		Group X Trial	F(1,73)=0.2295	p = 0.6333	n.s.
Fig 41B	2-way ANOVA	Group: Sham vs ORCH	F(1,30)=0.0934	p = 0.1460	n.s.
		Trial: Control vs Stress	F(1,30)=0.3237	p = 0.3237	n.s.
		Group X Trial	F(1,30)=0.1460	p = 0.1460	n.s.
Fig 41C	2-way ANOVA	Group: Sham vs ORCH	F(1,73)=6.339	p = 0.0140	*
		Trial: Control vs Stress	F(1,73)=6.258	p = 0.0146	*
		Group X Trial	F(1,73)=0.06081	p = 0.8059	n.s.
Fig 41D	2-way ANOVA	Group: Sham vs ORCH	F(1,32)=0.45	p = 0.5072	n.s.
		Trial: Control vs Stress	F(1,32)=3.28	p = 0.0795	n.s.
		Group X Trial	F(1,32)=0.0534	p = 0.8187	n.s.
Fig 42B	2-way RM ANOVA;	Sham vs ORCH			

Table 5 (cont'd)

	Holm-Sidak multiple comparisons	25pA	t(360)=1.614		
		50pA	t(360)=3.27	p = 0.1073	n.s.
		75pA	t(360)=3.621	p = 0.0102	*
		100pA	t(360)=3.449	p = 0.0040	**
		125pA	t(360)=3.506	p = 0.0063	**
		150pA	t(360)=3.28	p = 0.0056	**
		175pA	t(360)=2.868	p = 0.0102	*
		200pA	t(360)=2.862	p = 0.0302	*
		225pA	t(360)=2.776	p = 0.0302	*
		250pA	t(360)=2.489	p = 0.0302	*
		275pA	t(360)=2.536	p = 0.0457	*
		300pA	t(360)=2.514	p = 0.0457	*
Fig 42B, inset	Two-tailed t-test	Sham vs ORCH	t(30)=3.131	p = 0.0039	**
Fig 43A	2-way RM ANOVA;	Sham vs OVX			
	Holm-Sidak multiple comparisons	25pA	t(348)=0.5113	p = 0.9997	n.s.
		50pA	t(348)=0.6087	p = 0.9996	n.s.
		75pA	t(348)=0.8684	p = 0.9971	n.s.
		100pA	t(348)=0.2069	p = 0.9998	n.s.
		125pA	t(348)=0.3165	p = 0.9998	n.s.
		150pA	t(348)=0.0244	p = 0.9998	n.s.

Table 5 (cont'd)

		175pA	t(348)=0.1461	p = 0.9998	n.s.
		200pA	t(348)=0.0730	p = 0.9998	n.s.
		225pA	t(348)=0.3003	p = 0.9998	n.s.
		250pA	t(348)=0.5275	p = 0.9997	n.s.
		275pA	t(348)=0.4951	p = 0.9997	n.s.
		300pA	t(348)=0.7061	p = 0.9993	n.s.
Fig 45A	2-way RM ANOVA;	Veh vs Flut			
	Holm-Sidak multiple comparisons	25pA	t(408)=1.626	p = 0.4664	n.s.
		50pA	t(408)=2.573	p = 0.1182	n.s.
		75pA	t(408)=2.471	p = 0.1426	n.s.
		100pA	t(408)=2.151	p = 0.2782	n.s.
		125pA	t(408)=1.652	p = 0.4664	n.s.
		150pA	t(408)=1.511	p = 0.4664	n.s.
		175pA	t(408)=1.498	p = 0.4664	n.s.
		200pA	t(408)=1.652	p = 0.4664	n.s.
		225pA	t(408)=1.639	p = 0.4664	n.s.
		250pA	t(408)=1.882	p = 0.3542	n.s.
		275pA	t(408)=2.036	p = 0.3231	n.s.
		300pA	t(408)=1.972	p = 0.3328	n.s.
Fig 45, inset	Two-tailed t-test	Veh vs Flut	t(34)=2.119	p = 0.0415	*
Fig 46A	2-way ANOVA	Group: OVX + Bl vs OVX + T	F(1,34)=26.00	p < 0.0001	****

Table 5 (cont'd)

		Trial: Control vs Stress	F(1,34)=20.79	p < 0.0001	****
		Group X Trial	F(1,34)=3.849	p = 0.0580	#
Fig 47A	2-way ANOVA	Group: OVX + Bl vs OVX + T	F(1,35)=0.0884	p = 0.7680	n.s.
		Trial: Control vs Stress	F(1,35)=5.449	p = 0.0254	*
		Group X Trial	F(1,35)=3.598	p = 0.0661	n.s.
Fig 47B	2-way ANOVA	Group: OVX + Bl vs OVX + T	F(1,34)=0.6634	p = 0.4210	n.s.
		Trial: Control vs Stress	F(1,34)=5.778	p = 0.0218	*
		Group X Trial	F(1,34)=3.132	p = 0.0857	n.s.
Fig 47C	2-way ANOVA	Group: OVX + Bl vs OVX + T	F(1,34)=1.78	p = 0.1910	n.s.
		Trial: Control vs Stress	F(1,34)=0.0865	p = 0.7705	n.s.
		Group X Trial	F(1,34)=7.131	p = 0.0114	*
Fig 47D	2-way ANOVA	Group: OVX + Bl vs OVX + T	F(1,33)=36.41	p < 0.0001	****
		Trial: Control vs Stress	F(1,33)=0.4705	p = 0.4975	n.s.
		Group X Trial	F(1,33)=1.291	p = 0.2641	n.s.
Fig 47E	2-way ANOVA	Group: OVX + Bl vs OVX + T	F(1,35)=0.3507	p = 0.5575	n.s.
		Trial: Control vs Stress	F(1,35)=0.4839	p = 0.4913	n.s.
		Group X Trial	F(1,35)=0.681	p = 0.4148	n.s.
Fig 48A	2-way RM ANOVA;	OVX + Bl vs OVX + T			
	Holm-Sidak multiple comparisons	25pA	t(420)=0.165	p = 0.8690	n.s.
		50pA	t(420)=1.762	p = 0.1514	n.s.
		75pA	t(420)=3.036	p = 0.0076	**

Table 5 (cont'd)

		100pA	t(420)=3.687	p = 0.0026	**
		125pA	t(420)=3.847	p = 0.0017	**
		150pA	t(420)=3.739	p = 0.0023	**
		175pA	t(420)=3.579	p = 0.0035	**
		200pA	t(420)=3.453	= 0.0049	**
		225pA	t(420)=3.309	p = 0.0061	**
		250pA	t(420)=3.375	p = 0.0056	**
		275pA	t(420)=3.187	p = 0.0062	**
		300pA	t(420)=3.249	p = 0.0062	**
Fig 48, inset	Two-tailed t-test	OVX + Bl vs OVX + T	t(35)=3.254	p = 0.0025	**
Fig 50A	2-way ANOVA	Group: Vehicle vs CNO	F(1,36)=0.9478	p = 0.3368	n.s.
		Trial: Control vs Stress	F(1,36)=0.001178	p = 0.9728	n.s.
		Group X Trial	F(1,36)=0.03545	p = 0.8517	n.s.
Fig 50B	2-way ANOVA	Group: Vehicle vs CNO	F(1,36)= 133.6	p < 0.0001	****
		Trial: Control vs Stress	F(1,36)= 9.481	p = 0.0040	**
		Group X Trial	F(1,36)= 5.086	p = 0.0303	*
Fig 51A	2-way ANOVA	Group: Vehicle vs CNO	F(1,34)=0.2236	p = 0.6393	n.s.
		Trial: Control vs Stress	F(1,34)=1.041	p = 0.3147	n.s.
		Group X Trial	F(1,34)=4.064	p = 0.0518	#
Fig 52A	2-way ANOVA	Group: Vehicle vs CNO	F(1,35)= 0.1444	p = 0.7063	n.s.
		Trial: Control vs Stress	F(1,35)=0.2276	p = 0.1387	n.s.
		Group X Trial	F(1,35)=4.212	p = 0.0477	*

Table 5 (cont'd)

Fig 52B	2-way ANOVA	Group: Vehicle vs CNO	F(1,36)=0.5818	p = 0.4506	n.s.
		Trial: Control vs Stress	F(1,36)=5.372	p = 0.0263	*
		Group X Trial	F(1,36)=0.0530	p = 0.8192	n.s.
Fig 52C	2-way ANOVA	Group: Vehicle vs CNO	F(1,36)=0.7445	p = 0.3939	n.s.
		Trial: Control vs Stress	F(1,36)=0.0876	p = 0.7689	n.s.
		Group X Trial	F(1,36)=1.832	p = 0.1844	n.s.
Fig 53A	2-way ANOVA	Group: Vehicle vs CNO	F(1,33)=1.097	p = 0.3025	n.s.
		Trial: Control vs Stress	F(1,33)=0.2781	p = 0.6015	n.s.
		Group X Trial	F(1,33)=0.59	p = 0.4479	n.s.
Fig 53B	2-way ANOVA	Group: Vehicle vs CNO	F(1,34)=0.3007	p = 0.3213	n.s.
		Trial: Control vs Stress	F(1,34)=0.5462	p = 0.4650	n.s.
		Group X Trial	F(1,34)=0.161	p = 0.6908	n.s.
Fig 53C	2-way ANOVA	Group: Vehicle vs CNO	F(1,34)=4.658	p = 0.0381	*
		Trial: Control vs Stress	F(1,34)=3.642	p = 0.0648	n.s.
		Group X Trial	F(1,34)=0.0797	p = 0.7794	n.s.
Fig 54A	2-way ANOVA	Group: Vehicle vs CNO	F(1,35)=0.7583	p = 0.3898	n.s.
		Trial: Control vs Stress	F(1,35)=0.5333	p = 0.4701	n.s.
		Group X Trial	F(1,35)=0.7462	p = 0.3935	n.s.

CHAPTER 6: EFFECTS CIRCUIT-SPECIFIC HIPPOCAMPAL ΔFOSB IN BOTH SEXES

Introduction

In chapters 4 and 5, I determined that ΔFosB in vHPC afferents is critical for male CSDS behaviors, and that there is a critical sex difference in the excitability of vHPC-NAc projections which drives differences in behavioral responses to SCVS. However, ΔFosB has not been studied in these projections under basal conditions, nor in both sexes in the context of stress. Therefore, in this chapter I sought to elucidate ΔFosB's role in mediating the contributions of vHPC projection neurons to baseline behaviors and if it is a common regulator of stress-induced behaviors in females as well as males.

While the bulk of this dissertation focuses on the role of vHPC afferents in the context of stress, these same circuits also play a central role in other maladaptive reward contexts such as drug seeking [45, 430, 431]. It therefore follows that the vHPC and its afferents are populations that might affect natural rewarding behaviors under basal conditions [432, 433], and that any manipulation of these circuits could also result in changes in behaviors such as social interaction, feeding, or drinking.

Consistent with this hypothesis, the vHPC is one of many regions implicated in modulation of anorectic and orexigenic behaviors. For example, the vHPC contains the neuroendocrine receptors for Glucagon-like peptide-1(GLP-1,) leptin, and ghrelin, hormones from the periphery which communicate satiety and energy status to the CNS [434-436]. Furthermore, lesion experiments have demonstrated the role of vHPC in meal onset [437], as well as in social transmission of food preferences through social conditioning, consumption, and learning [438-444]. Indeed, vHPC afferents to the lateral

septum have been implicated in controlling feeding behavior; although, these are derived from the vDG-CA3, where leptin receptors are expressed, rather than the vCA1 layer which projects to NAc and BLA [129, 445, 446]. Nevertheless, glutamatergic activity in the NAc also transiently stops feeding while antagonizing ionotropic glutamate receptors in the NAc stimulates ingestion [447, 448]. As the vHPC is the largest contributor of glutamatergic projections to the NAc [129, 130], vHPC-NAc projections may also contribute to some aspects of feeding behaviors in addition their role in affective memories. Furthermore, lesions of the vHPC and BLA result in obesity [449, 450], implicating the vHPC and perhaps its afferents in feeding behavior. Because different vHPC afferents can orchestrate distinct behavioral phenotypes (chapter 4) and alterations in gene expression within these circuits can drive differential outcomes in stress-induced behavior ([127, 300]] and see chapter 4), I sought to characterize how changes in gene expression in these circuits may also underlie natural feeding behavior or energy expenditure.

ΔFosB, a transcription factor and splice variant of the *FosB* gene, has been well characterized in stress and maladaptive rewards ([280, 281, 305, 326, 383, 384, 451]] and see chapter 4). However, the role of ΔFosB in weight and natural reward is poorly understood. To date, the accumulation of ΔFosB in the NAc is concordant with increases in male sexual experience, sucrose consumption, and consumption of high fat diets [304, 350, 387, 452, 453]. Additionally, prolonged intermittent access to sucrose induces ΔFosB in the NAc and BLA [454, 455]. Together, these data suggest that ΔFosB has a role in natural reward, including consummatory behavior. Though there is preliminary evidence for this, it is drawn from studies using male subjects. Indeed, studies examining

the role of ΔFosB in the neural circuitry of both sexes are rare, and thus potential sex differences have not been extensively characterized. There are no differences in the dHPC between males and females in the basal state of many Fos and Jun proteins, although, ΔFosB was not specifically assayed [456]. In the NAc, there are no sex differences in the extent to which cocaine seeking [457] or sexual experience [458] induce ΔFosB. However, stress paradigms produce conflicting results. While there are no reported sex differences in ΔFosB expression in PVN or PFC following stress [459, 460], stress does precipitate sex differences in ΔFosB expression in the BNST [459]. Importantly, an early life stress paradigm causes sex-specific changes in ΔFosB in mPFC which correlate to behavioral outcomes [461]. Thus, ΔFosB induction vHPC afferents in response to stress could be sexually dimorphic and regulate sex differences in behavior. Nevertheless, the specific function of ΔFosB in the vHPC has yet to be fully characterized for both males and females.

To test the hypothesis that ΔFosB in vHPC afferents is a common mechanism to elicit stress-induced behavior, I examined ΔFosB induction in vHPC afferents to NAc and BLA in males and females under control conditions and after SCVS, a paradigm which elicits stress behaviors in females but not males. I used dual viral manipulation of vHPC afferents coupled with behavioral and metabolic assays to examine whether ΔFosB differentially contributes to basal physiological states or behavior. I then used dual viral manipulations to test the hypothesis that ΔFosB is necessary and sufficient in vHPC-NAc circuity for resilience to SCVS in male and female mice, respectively. Together, these studies elucidate ΔFosB's role in vHPC afferents in metabolism, basal ingestive

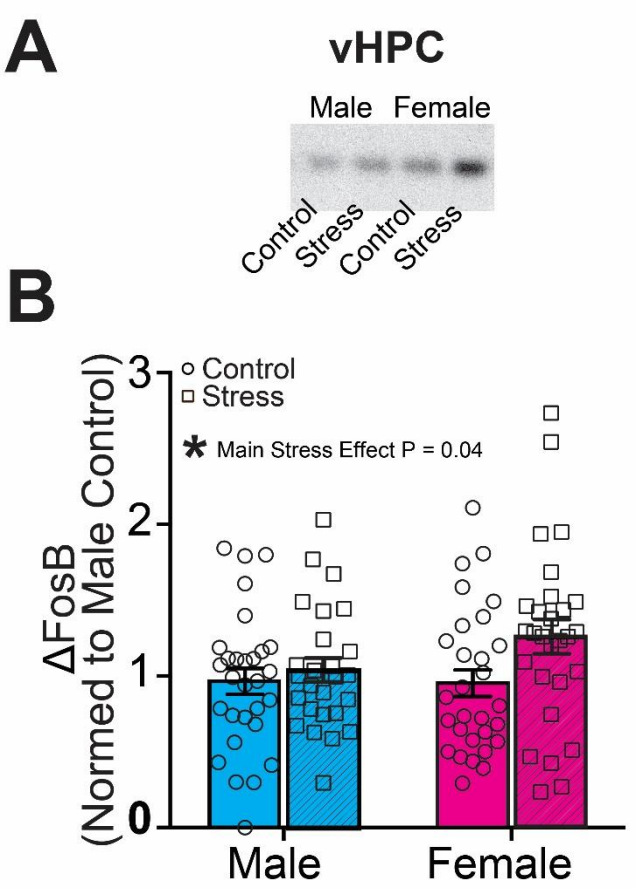

Figure 57 | SCVS induces ΔFosB in the vHPC. (A) Representative image of Western blots for ΔFosB from males and females that underwent stress or control handling. **(B)** SCVS resulted a main effect of stress on ΔFosB induction in the vHPC.

behaviors, affective behaviors of both sexes, and its role in shaping sex differences in behavioral responses to stress.

Results

Stress induces ΔFosB in the vHPC, while males have increased vHPC-NAc ΔFosB at baseline compared to females:

To test whether stress would induce vHPC ΔFosB in females as it does in males (as in chapter 4), I put both males and females through SCVS or control handling, which elicits anhedonia in females, but not males ([63] and chapter 5). Following stress, bilateral punches were taken of the dHPC and vHPC, and then Western blotted for ΔFosB (Figs

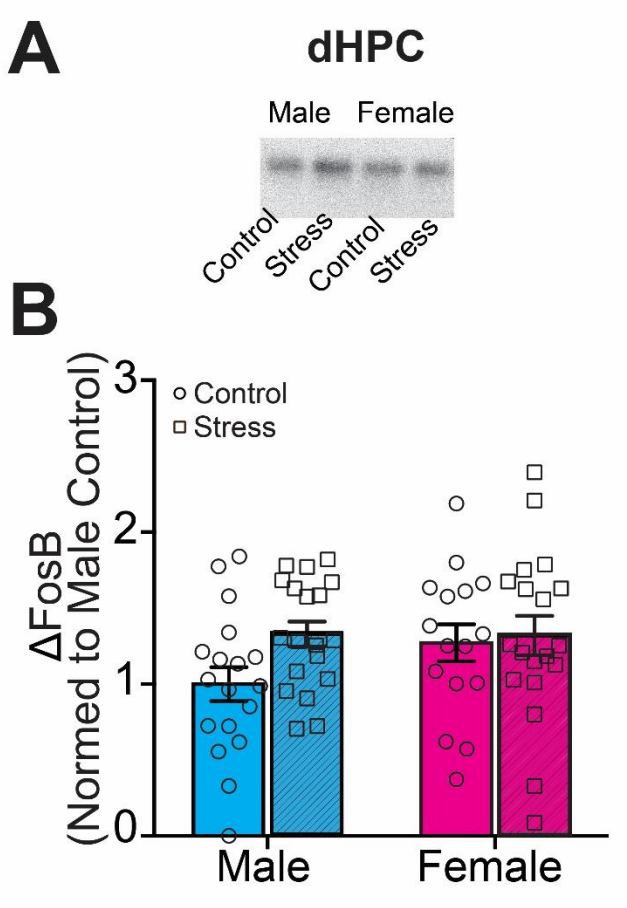

Figure 58 | ΔFosB after SCVS in the dHPC. (A) Representative image of Western blots for ΔFosB from males and females that underwent stress or control handling. **(B)** SCVS resulted in no effect of stress or sex on ΔFosB levels in dHPC, but **(D)** a main effect of stress on ΔFosB induction in the vHPC.

57 and 58). We found a main effect of stress on ΔFosB in vHPC (Fig 57) though there was no significant change in the dHPC (Fig 58). This induction of ΔFosB in vHPC implies a potential effect on vHPC projection neurons. To determine whether ΔFosB is induced specifically in either vHPC-NAc or vHPC-BLA projections, I injected HSV-hef1α-Cre into either NAc or BLA of a Cre-dependent GFP mouse line as described in previous chapters (Figs 59A, 60A). Surgeries were followed by either SCVS or control handling. I performed quantitative immunohistochemistry for ΔFosB

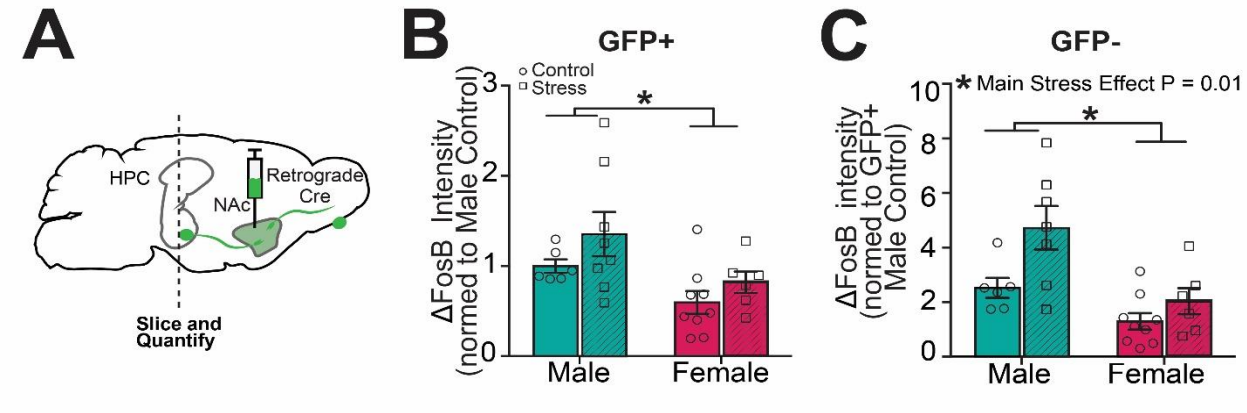

Figure 59 | Sex differences in ΔFosB in vHPC-NAc afferents. (A) Schematic depicting retrograde Cre viral vector injections to the NAc of GFP reporter mice. **(B)** Males vHPC-NAc neurons (GFP+) have significantly more ΔFosB expression than females, regardless of stress. **(C)** Males and stressed animals have significantly more ΔFosB expression in other vCA1 cells (GFP-) .

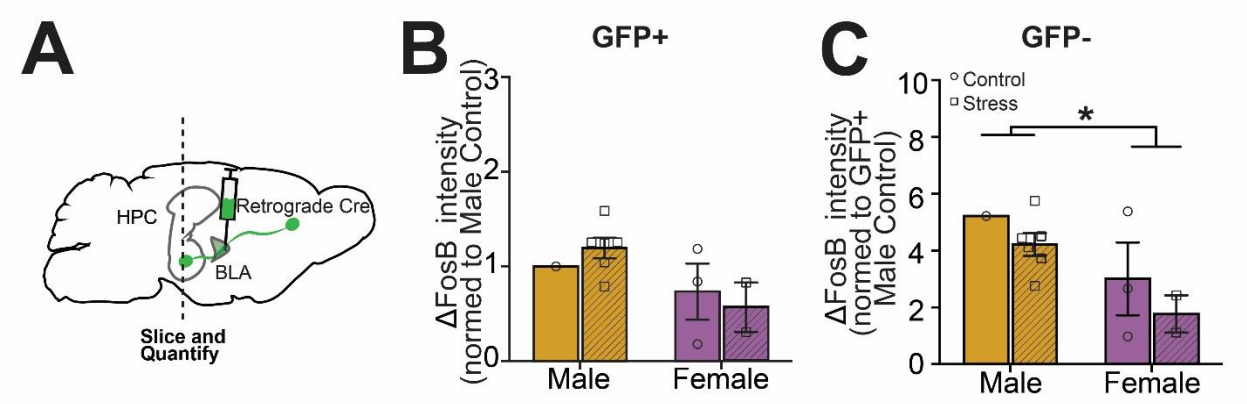

Figure 60 | Sex differences in ΔFosB in vHPC-BLA afferents. (A) Schematic depicting retrograde Cre viral vector injections to the BLA of GFP reporter mice. **(B)** In vCA1-BLA projections there were no significant differences in ΔFosB based on stress or sex. However, **(C)** males have more robust ΔFosB expression compared to females other cells of the vCA1 cell layer after BLA surgeries.

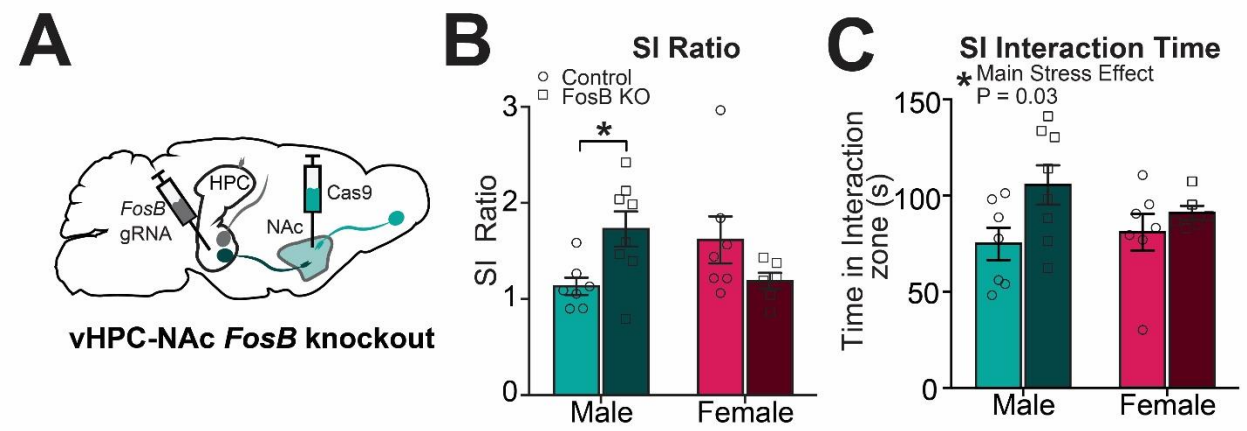

Figure 61 | FosB KO in vHPC-NAc has sex specific effects on social interaction. **(A)** Schematic depicting dual viral vector strategy for NAc circuit-specific mutation of FosB gene. **(B)** Unstressed males have increased SI ratios after FosB knockout compared to females. **(C)** This is reflected in the main effect of FosB knockout increasing the time spent interacting with a novel mouse.

and GFP in the vHPC, thereby enabling projection-specific quantification. While therewas no effect of stress in either NAc or BLA projection neurons (Fig 59B, 59B), quantification of other vCA1 cells showed ΔFosB was induced in both sexes following stress, which replicated the Western blot data (Fig 59C). It should be noted that the number of animals in projection-specific analysis was low, and this experiment will be repeated in the future. Analysis of the vCA1 did show a main effect of sex on ΔFosB expression such that males had more ΔFosB than females (Fid 59C) in nonspecific vCA1 cells and in vHPC-NAc projections, regardless of stress (Fig 59B, 59C). Overall, these data suggest that there are sex differences in the basal expression of ΔFosB in vCA1. Given that a sex difference is not observed in Western blot analysis of the whole vHPC, these findings indicate that ΔFosB may be differentially expressed between sexes within specific cell types or subregions of the vHPC.

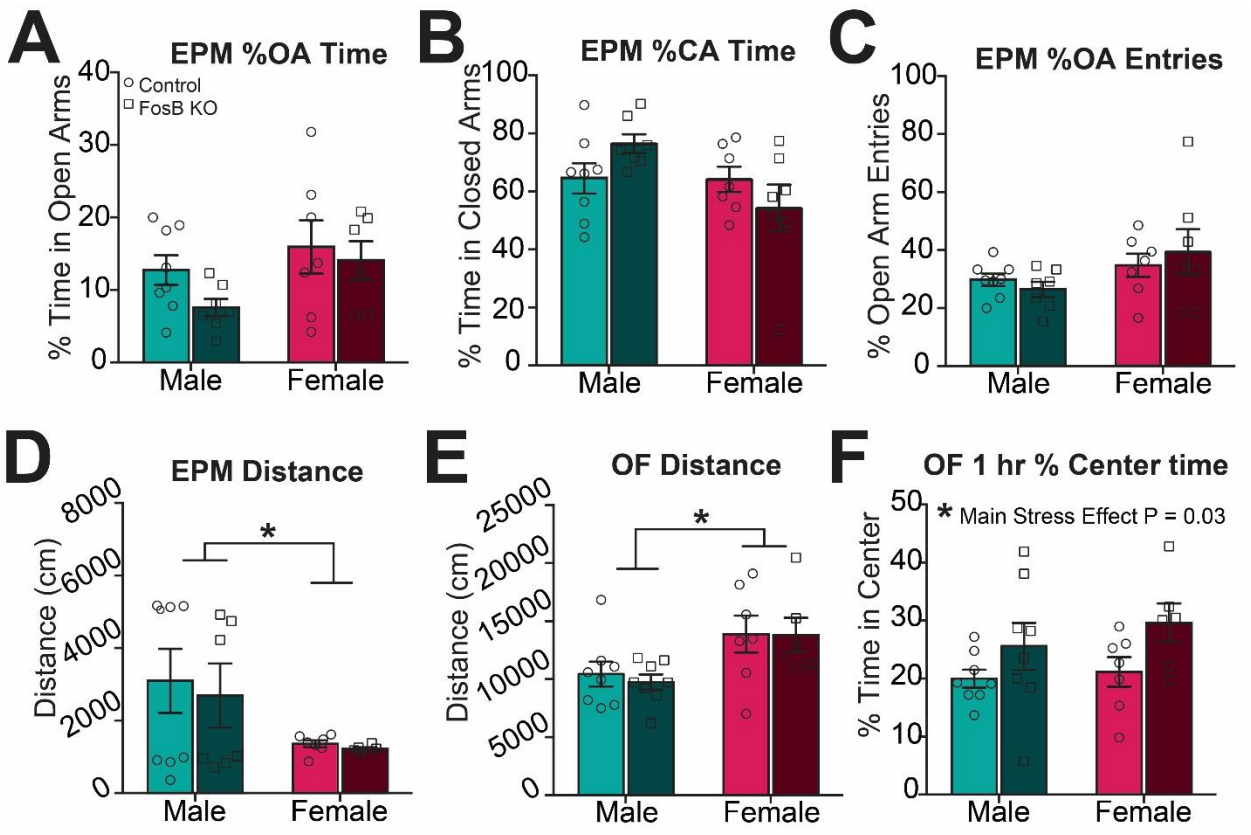

Figure 62 | Effects of FosB knockout in vHPC-NAc on anxiety and locomotor behaviors. (A-C) FosB KO and sex did not affect EPM metrics of anxiety **(D-E)** Males moved more in the EPM, but less in the Open Field. **(F)** FosB KO in vHPC-NAc increased time spent in the center of the Open field over the course of an hour.

vHPC-NAc *FosB* knockout contributes to sex differences in weight gain and social behavior:

To test if sex differences in vHPC afferent ΔFosB differentially contributes to baseline behavior, I utilized the dual viral CRISPR Cas9 system described in chapter 4 to induce a circuit-specific knockout of the *FosB* gene in vHPC afferents to the NAc of males and females (Fig 61A). I then tested mice in a suite of affective behavioral assays, including EPM, OF, and SI, that examine anxiety-like and social behaviors. Following behavioral assessment, mice underwent body composition analysis and were singly housed in metabolic cages to track energy expenditure for three days to assess the effect of ΔFosB

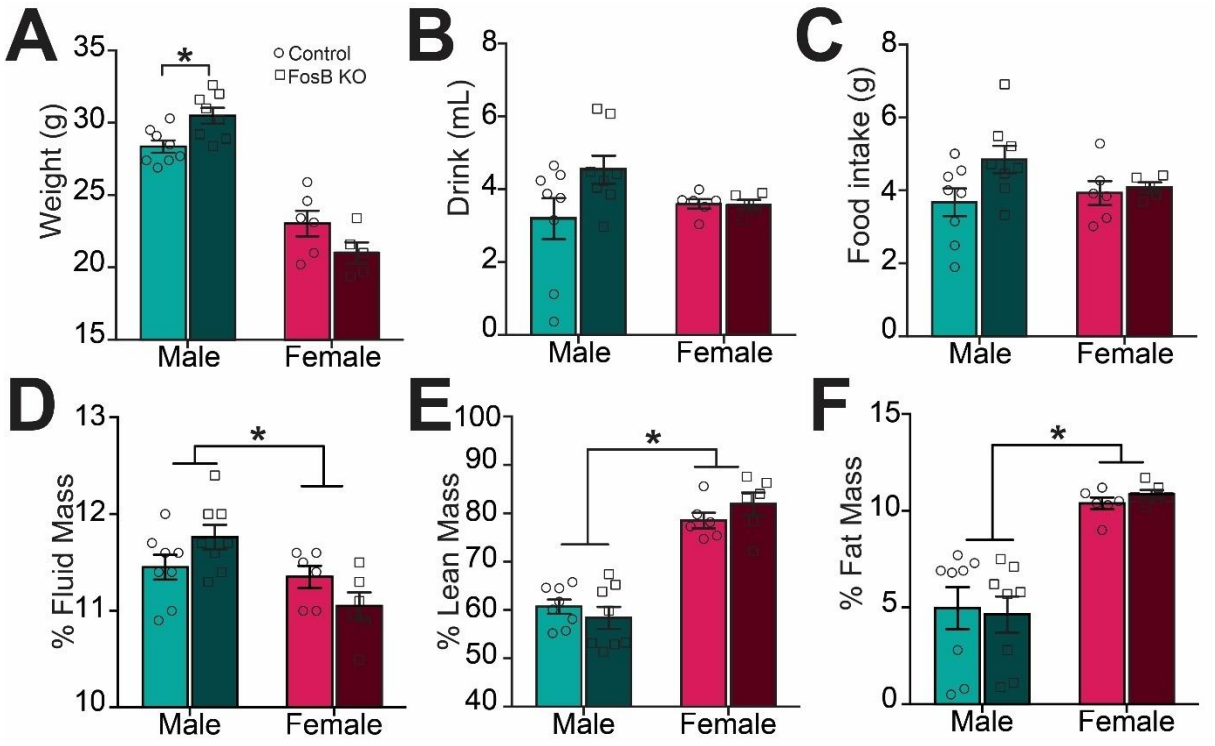

Figure 63 | FosB KO in vHPC-NAc has increases weight of males. (A) Males weigh more than females after vHPC-NAc FosB KO, and there is a main effect of sex on weight. **(B-C)** This is accompanied trends for increased intake in males, although this is not significant. **(D-F)** There are main effects of sex on body composition, with females having less fluid mass, and higher lean and fat mass than males. **(D)** There is also an interaction of sex and FosB KO on percent fluid mass, although neither group is different from their control counterparts.

on consummatory behaviors, calorimetry, and activity. Intriguingly, vHPC-NAc *FosB* knockout results in enhanced prosocial behavior in males but not females (Fig 61B, C). There was no effect of knockout on anxiety like behavior in EPM or OF (Fig 62A-C), but was a main effect of sex on locomotion in both tests, with females moving less than males in EPM, but more in the OF (Fig 62D, E), suggesting that females may freeze more in short-term anxiety provoking contexts. Additional sex-specific effects of vHPC-NAc *FosB* knockout emerged in the metabolic profiles of these animals.

Males with vHPC-NAc *FosB* knockout had increased weight compared to their control counterparts (Fig 63A). This was accompanied by trends for increased consumption in

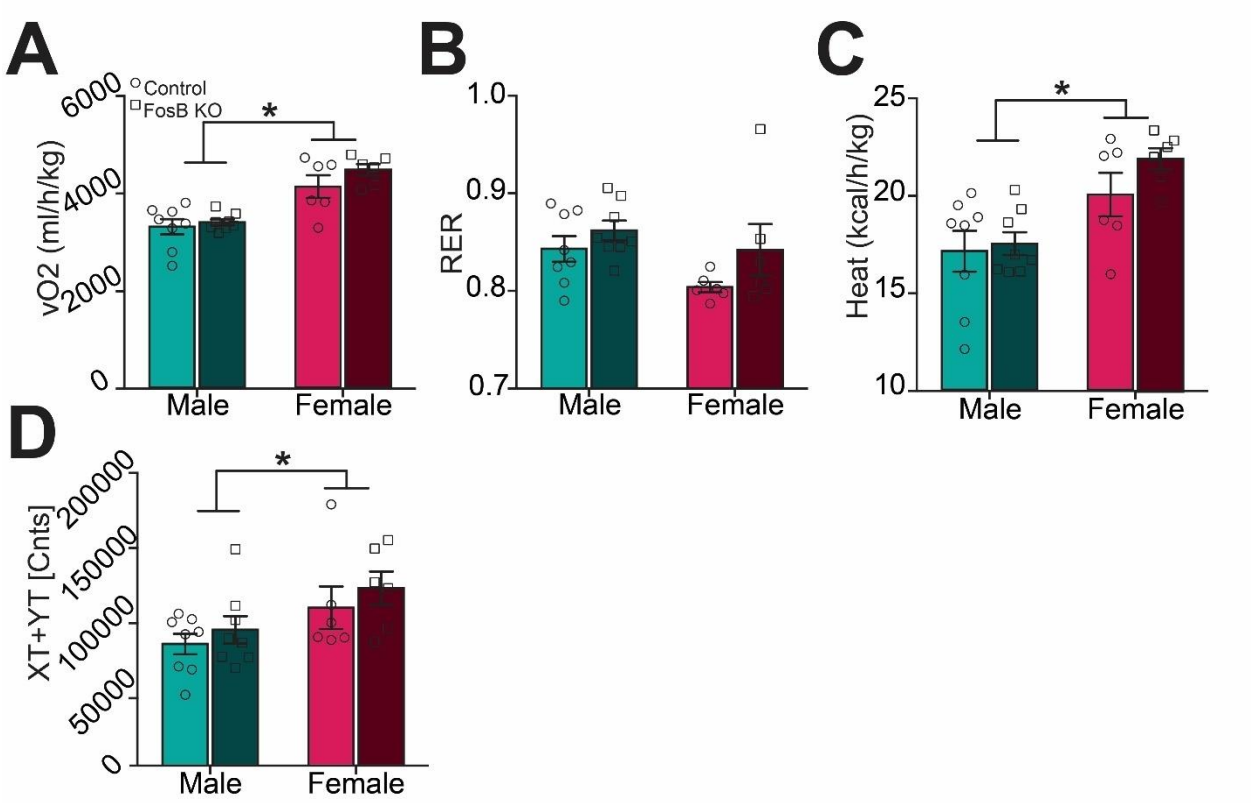

Figure 64 | Sex effects on metabolism. FosB KO had no effect on energy expenditure. Females have higher **(A)** oxygen consumption, **(C)** energy output, and **(D)** locomotor activity than males. There was no effect of sex or stress on **(B)** RER.

males (Fig 63B-C) and a significant interaction between sex and vHPC-NAc *FosB* knockout on free fluids in the body, although this did not result in significant post-hoc comparisons (Fig 63D). There were main effects of sex on body composition (Fig 63D-F), energy expenditure (Fig 64A,C), and activity (Fig 64D), which indicate that females had increased lean and fat mass compared to males, decreased fluid mass, and higher rates of activity, energy expenditure, and O2 use, but vHPC-NAc *FosB* KO did not affect any of these measures. Altogether, these data highlight a role for vHPC-NAc ΔFosB male-specific enhancement of social behavior and increased weight, providing preliminary evidence for ΔFosB regulation of the role of this circuit in natural reward.

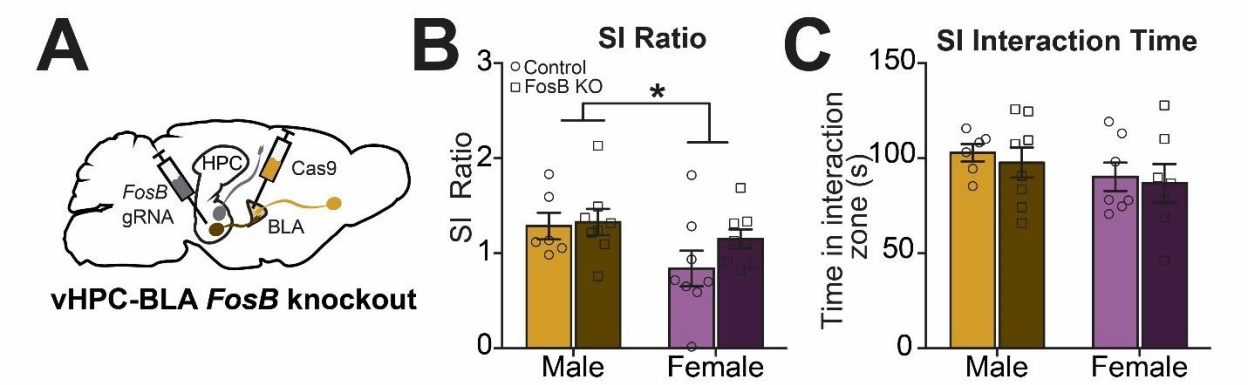

Figure 65 | Effects of FosB KO in vHPC-BLA on social interaction. (A) Schematic depicting dual viral vector strategy for BLA circuit-specific mutation of FosB gene. **(B)** FosB KO in vHPC-BLA resulted in a male effect of sex of social interaction ratio. However, this was not reflected in time interacting with a novel mouse **(C)**.

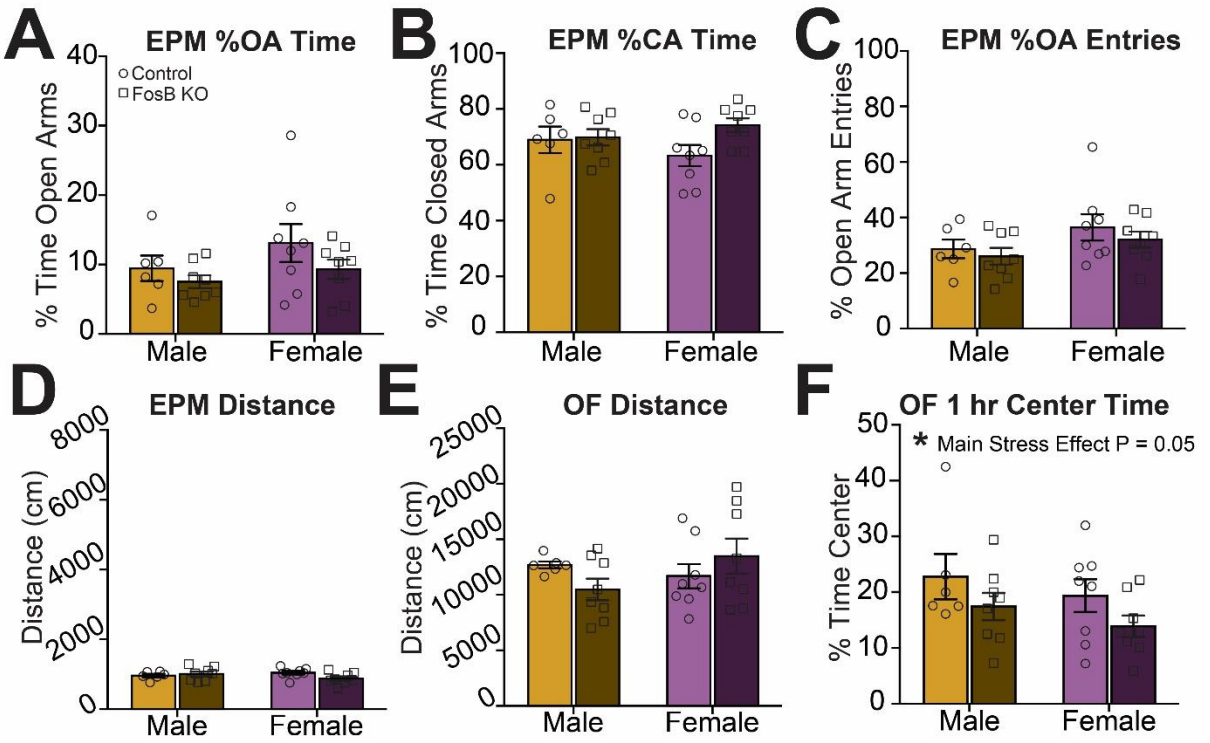

Figure 66 | FosB KO in vHPC-BLA does not affect EPM or locomotor behaviors. (A-C) FosB KO and sex did not affect EPM metrics of anxiety, **(D-E)** nor were there any effects on locomotion **(F)** FosB KO decreased time spent in the center of the Open field over the course of an hour.

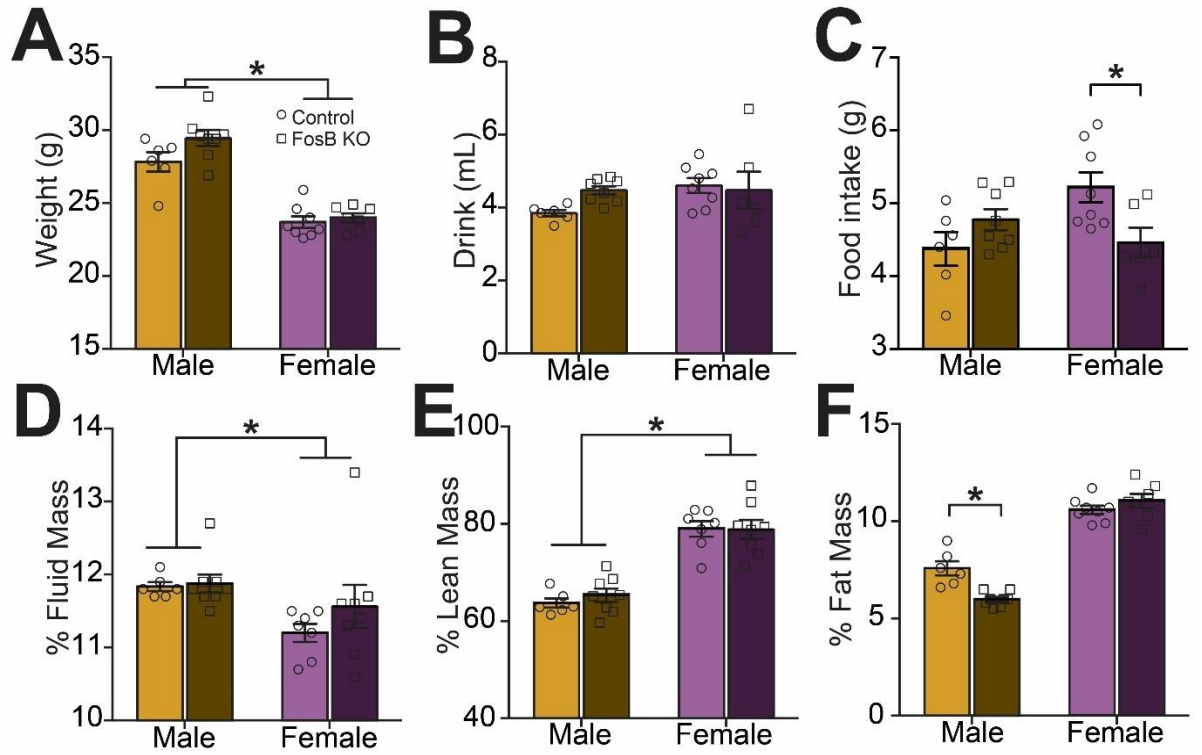

Figure 67 | FosB KO in vHPC-BLA has sex specific effects on consumption and body composition. (A) vHPC-BLA FosB KO does not affect weight, while males weigh more than females. **(B)** There are no effects of FosB KO or sex on fluid intake. **(C)** However, FosB KO in vHPC-BLA results in females eating less than their intact counterparts. **(D-E)** Females have lower fluid mass, and higher lean mass than males. **(F)** Females also have a higher fat mass of males, and FosB KO in males is concurrent with decreased fat mass compared to control males.

vHPC-BLA *FosB* knockout differentially contributes to food intake, but not affective behaviors:

In order to investigate the role of ΔFosB in vHPC neurons projecting to BLA, I used the same circuit-specific CRISPR method (Fig 65A). Indeed, vHPC-BLA *FosB* knockout under baseline conditions did not alter any behavioral phenotype (Figs 65 and 66). vHPC-BLA *FosB* knockout specifically altered female's food intake while not affecting their weight, consistent with trends for reduced metabolic expenditure (Fig 67A, C and Fig 68A-D). vHPC-BLA *FosB* knockout also significantly altered male body composition

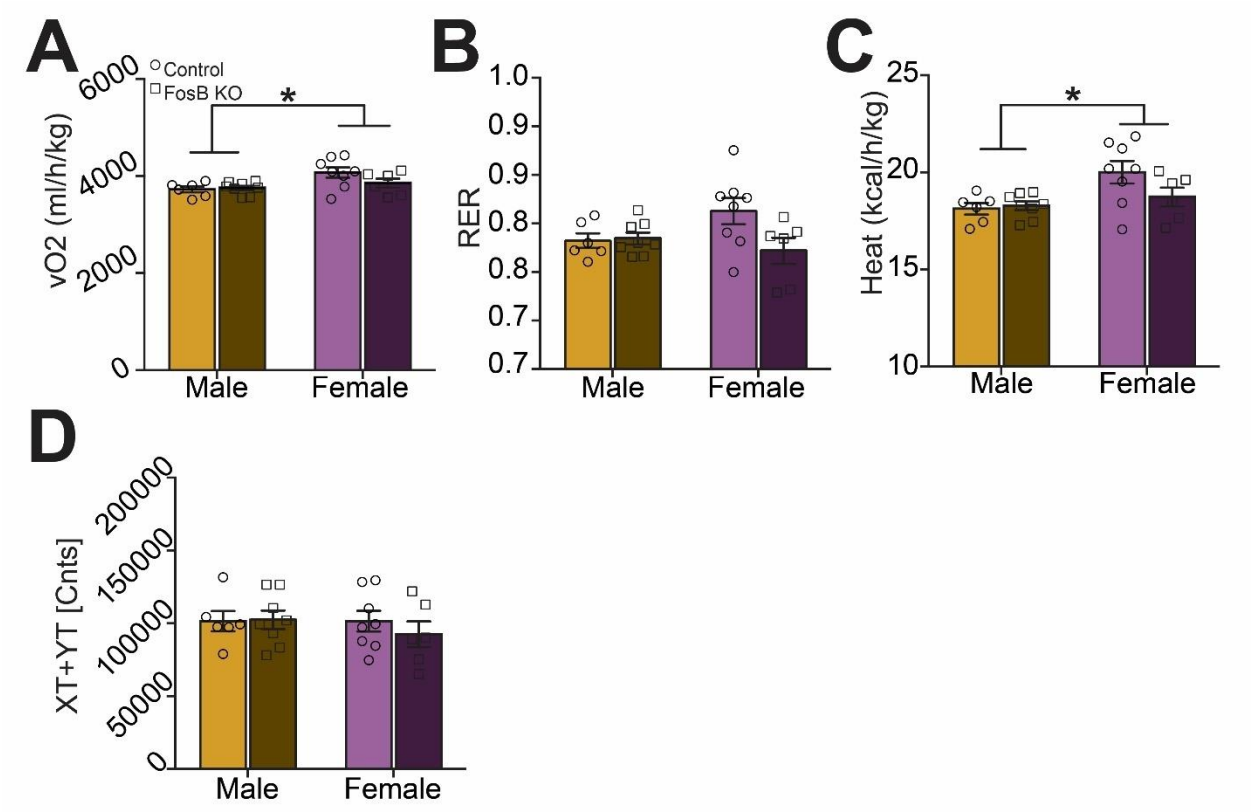

Figure 68 | Sex effects on metabolism. FosB KO had no significant effect on energy expenditure. Females have higher **(A)** oxygen consumption and **(C)** energy output. There was no effect of sex on **(B)** RER or **(D)** locomotion.

by decreasing percentage of fat mass (Fig 67F). This is also consistent with trends for increased weight, food consumption, and percentage of lean body mass (Fig 67A, C, and E), without altering energy expenditure or locomotor activity (Fig 68A-D). Taken together, these data suggest that vHPC-BLA *FosB* gene products may differentially regulate appetitive behaviors between the sexes by influencing food intake and perhaps metabolism.

vHPC-NAc *FosB* knockout is not sufficient to drive stress-susceptibility to SCVS in males:

In chapter 4, I showed that vHPC-NAc *FosB* knockout caused stress susceptibility of males in CSDS paradigm, indicating *FosB* gene products are necessary for resilience to stress (chapter 4). Although males are resilient to SCVS under normal conditions [44, 63], manipulation of the brain or extension of SCVS can elicit depression-related behavior in males ([44]] and chapter 5). Therefore, I tested whether *FosB* knockout in the vHPC-NAc circuit in males would precipitate vulnerability to a subthreshold stress (SCVS), similar to effects after CSDS. To do this, I used the dual virus CRISPR system to silence the *FosB* gene in males (Fig 61A) followed by SCVS or control handling. Counter to my hypothesis, *FosB* knockout in the vHPC-NAc circuit did not elicit any interactions or main effects of viral manipulation or stress on sucrose preference, a robust output of SCVS (Fig 69A). There was a main effect of stress reducing social interaction with a novel mouse (Fig 69B, C), but no effects on EPM, NSF, or the splash test (Fig 70). This suggests *FosB* knockout in this circuit is not sufficient to elicit susceptibility to a subthreshold stress, and therefore ΔFosB in this circuit likely does not play a role in male resilience to SCVS effects on behavior.

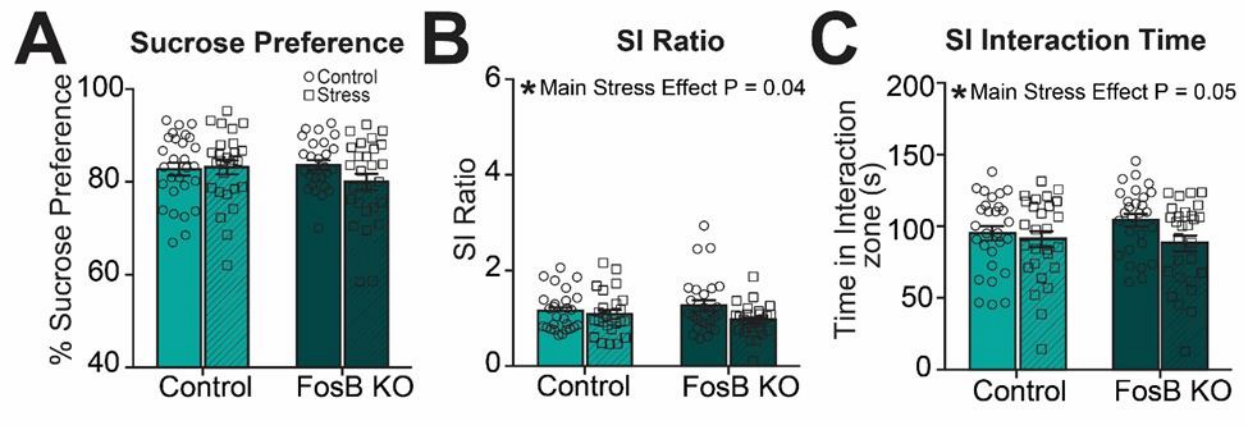

Figure 69 | Male vHPC-NAc FosB KO does not cause changes to anhedonia following SCVS, (A) Neither stress nor vHPC-NAc FosB KO effect sucrose preference in males following SCVS **(B, C)** Stress has a main effect on SI ratio, decreasing social interaction following SCVS which is also reflected in a main effect of stress on the time spent interacting with a novel mouse.

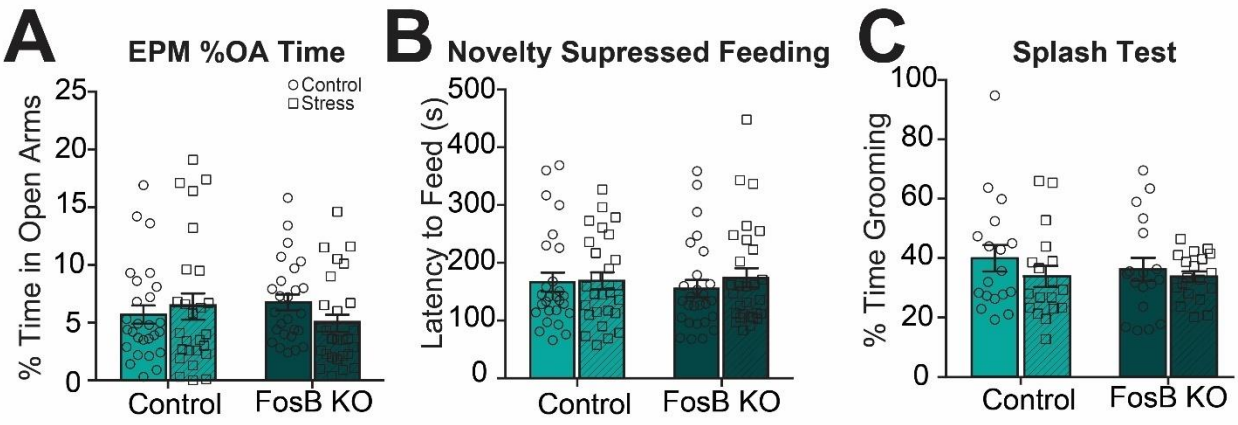

Figure 70 | Male vHPC-NAc FosB KO does not cause anxiety after SCVS. There is no effect of stress or FosB KO in **(A)** EPM, **(B)** NSF, or **(C)** Splash Test following SCVS.

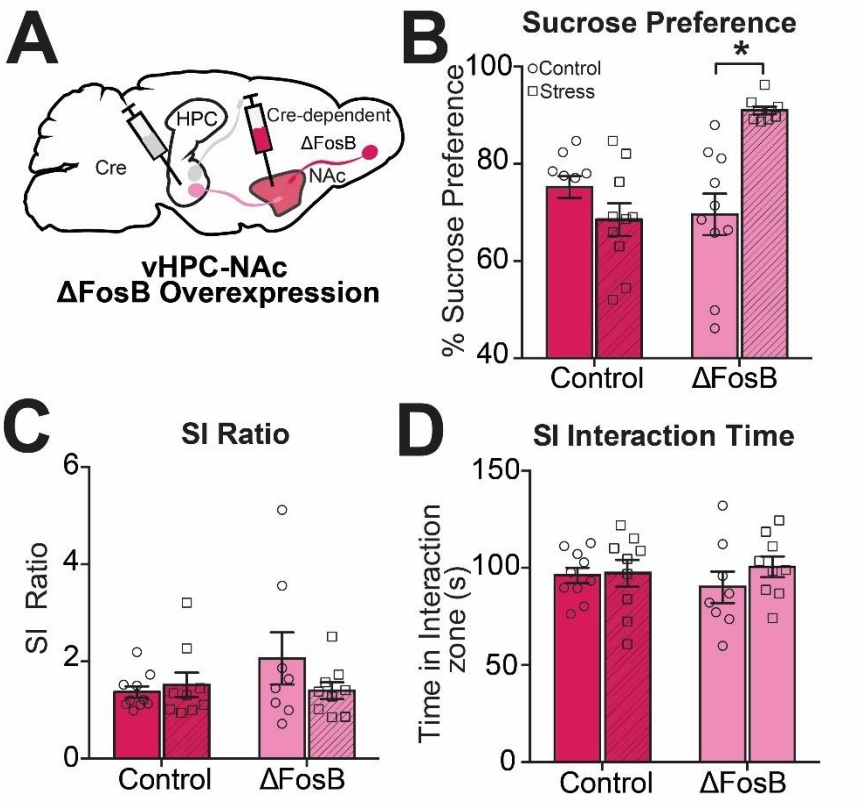

Figure 71 | Female vHPC-NAc ΔFosB overexpression causes context specific behavioral changes. **(A)** Schematic depicting dual viral vector strategy for NAc circuit-specific overexpression of ΔFosB. **(B)** vHPC-NAc ΔFosB overexpression enhances sucrose preference only after exposure to SCVS. **(C-D)** vHPC-NAc ΔFosB overexpression had no effect on social interaction ratio or time spent with a novel animal

Female ΔFosB overexpression in the vHPC-NAc circuit has experience dependent effects on behavior:

Although *FosB* gene products in vHPC-NAc may not be necessary for behavioral resilience to stress, ΔFosB in this circuit may be sufficient for stress resilience. As ΔFosB is known to decrease neuronal excitability, which has previously been tied to stress resilience ([127, 337, 387]] and chapter 4) and females have low levels of ΔFosB at baseline and an increased susceptibility to stress (Figs 3,4 and chapter 5), the accumulation of ΔFosB may be protective in behavioral responses to stress. I tested this hypothesis using a dual viral ΔFosB circuit-specific specific overexpression method

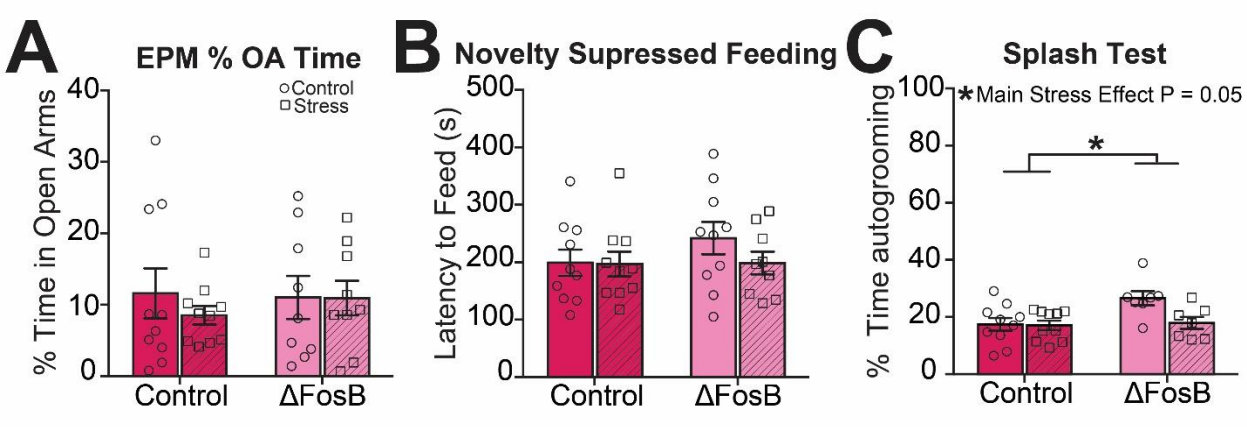

Figure 72 | Effects of female vHPC-NAc ΔFosB overexpression on anxiety. Neither stress nor FosB overexpression affect (A) open arm time in the EPM or (B) latency to feed in NSF. (C) Both stress and ΔFosB overexpression affect autogrooming in the Splash Test, with ΔFosB increases autogrooming and stress decreasing autogrooming.

previously described in chapter 4 (Fig 71A), and then exposing female mice to SCVS or control handling. When ΔFosB was overexpressed in this circuit in the context of stress, it greatly increased sucrose preference, a measure typically reduced in females after SCVS (Fig 71B). However, SCVS did not change social interaction (Fig 71C, D). The was concurrent with trends for reduced latency to feed, increased time spent with a novel mouse, and reduced grooming following SCVS, with no change in EPM (Fig 71C, D and Fig 72A-C). As with the male *FosB* knockout behavior, this indicates that the presence of ΔFosB itself is not sufficient for increases in affective behavior (Fig 71A). However, ΔFosB and its signaling cascades may influence the integration of the valence of an experience with subsequent decision making or the coordination future behavioral responses to stimuli, and thus result in behavioral resilience following stress.

Discussion

In this chapter, I used wild-type mice coupled with viral vectors to visualize and manipulate *FosB* gene expression in the vHPC afferents to NAc and BLA. For the first time, I show that stress induces ΔFosB in the vHPC of both male and female mice, and that while stress induces ΔFosB in the vCA1 of both sexes, males have increased basal ΔFosB expression compared to females in the vCA1-NAc circuit. Previously, ΔFosB has been shown to decrease the excitability of HPC pyramidal neurons, including vHPC afferents, and its accumulation in vHPC-NAc causes resilience to CSDS in male mice ([387] and chapter 4). This is consistent with males' reduced excitability in this circuit and resilience to SCVS, shown in chapter 5, and supports the hypothesis that accumulation of ΔFosB in the vHPC-NAc may be pro-resilient in both sexes. This suggests that males' resilience to SCVS may be derived, in part, from their innate abundance of ΔFosB in this circuit. Previously, no sex differences in expression of the Fos family has been reported in HPC [456]. Since ΔFosB is induced by chronic neuronal activation [282, 311, 383, 384], this suggests that sex differences in basal ΔFosB expression may arise from differential profiles of gene expression, either at the level of epigenetic regulation [287, 462], or through differential activation of these projections in response to normal experiences [413, 463-466]. This begs the question: what effects do ΔFosB in vHPC afferents have on normal behaviors?

The vHPC is thought to integrate affective memories: the integration of the internal and external contextual environments and the valence of an experience [467, 468]. This may include the integration of interoceptive contexts like energy status with experiences to influence feeding behavior. Indeed, learned feeding has been attributed, in part, to vHPC

CA1 neurons [439, 469]. Therefore, ΔFosB expression in vHPC CA1 afferents may communicate to other limbic regions some aspects of these learned behaviors, including interoceptive energy status, external animal location, or valence of an experience. Due in part to sex differences in basal ΔFosB, the manipulation of ΔFosB in circuits then results in sex-specific changes in normal affective behaviors including feeding and social interaction.

Initial analysis of sex differences in vHPC afferent *FosB* knockout supports the idea that vHPC afferents play a role in feeding behavior. vHPC-NAc knockout increased weight in males, consistent with increased fluid mass (Fig 5). This suggest vHPC-NAc *FosB* gene products are necessary for appropriate weight in males, but not females. The mechanism by which this occurs is unclear, as there were no significant changes in food/water intake, locomotor activity, or metabolism (Fig 6). Perhaps this change in weight is a result of the timing of meals which can alter body weight independent of intake through neuropeptides like ghrelin [470, 471], or changes water retention, indicating the potential influence of altered glutamatergic signaling in the NAc on downstream inflammation or micturition [40, 236, 420, 472-474]. When I induced *FosB* knockout in the vHPC-BLA projection, there was a male-specific reduction in fat mass, which coincided with nonsignificant trends for increased lean mass, food consumption, and weight gain. In contrast, there was a female-specific reduction in food consumption which coincided with trends for reduced energy expenditure (Figs 9 and 10). Sex differences in energy balance are based in part on glutamatergic and neuroendocrine responses attributed to amygdaloid subregions and cell-types, such as leptin receptors and estrogen receptors on Sim-1 neurons of the amygdala [475-479]. Sex differences in food intake have also been reported after vHPC

lesions, providing evidence to support the idea that the vHPC of males and females have subtle differences in their function, connectivity, or ability to integrate stimuli related to feeding [480]. Taken together, these changes suggest that perturbing vHPC afferents changes facets of ingestive behavior in a sex-specific manner.

Manipulation of the *FosB* gene in vHPC afferents also elicited sex differences in mood- and reward-related behaviors in the absence of stress. vHPC-NAc *FosB* knockout resulted in male-specific increased basal social interaction (Fig 3). This was particularly surprising as male vHPC-NAc *FosB* gene knockout resulted in increased susceptibility to stress-induced social withdrawal in chapter 4. Taken together, this suggests the importance of the animals' experiences during which *FosB* gene expression is manipulated.

ΔFosB accumulation reduces the excitability of vHPC-NAc neurons (chapter 4), and inhibition of ΔFosB activity increases dHPC CA1 excitability [387]. It follows that *FosB* knockout also increases the activity of the vHPC-NAc circuit. This implies that increasing the activity of the male circuit facilitates social interactions under basal conditions but induces social withdrawal following CSDS. By comparison, females are unaffected by *FosB* knockout in this circuit (Figs 2, 3). This may be due to different neurobiological sequelae associated with interaction with a novel male. Alternatively, *FosB* knockout may not have an effect in females due to low levels of ΔFosB at baseline in the vHPC-NAc circuit, and therefore reducing its expression reached a floor effect on its contributions to behavior.

Conversely, vHPC-BLA *FosB* knockout did not create consistent changes in behavior, including a failure to replicate anxiolytic behaviors in males previously reported in chapter

4. Indeed, the *FosB* knockout trended to increase anxiety behaviors in both sexes. This suggests that the rules governing vHPC-BLA projections contributions to behaviors are not clear cut. BLA can regulate many aspects of behavior, including consummatory behaviors and energy status [475, 481-484]. The BLA is hypothesized to be organized in a “salt and pepper” model where BLA neurons are not segregated based on behavioral contributions or valence [144, 485]. In addition, vHPC-BLA projections are sometimes reported to be glutamatergic, but other reports suggest that vHPC projections to the BLA may be GABAergic [486, 487]. Therefore, although we targeted the same cell population across these studies, the specific nature of the cell populations which were manipulated in these studies may have biased for one cell type over another to influence these incongruous results between chapters.

The NAc, while also containing anatomical and cell type complexity, has been more robustly studied in the context of these behaviors. vHPC-NAc neurons are mostly glutamatergic and synapse on D1 and D2 medium spiny neurons of the NAc shell [45, 130, 199, 488]. Presynaptic changes in NAc glutamatergic signaling is implicated in sex differences in stress susceptibility [335]. Although changes in synaptic plasticity in response to stress is shown primarily at NAc D1 MSNs [45, 114, 126], I previously showed ΔFosB in the all vHPC-NAc afferents is necessary and sufficient for male resilience to CSDS social interaction and works in part through decreasing the activity of this circuit ([194, 387]] and chapter 4). Furthermore, in chapter 5, I showed there are sex differences in susceptibility to stress that rely, in part, on males having lower excitability of the vHPC-NAc circuit compared to females. SCVS induces ΔFosB in the vCA1 of males and females, which may act to reduce the activity of vHPC-NAc corresponding to behavioral

resilience. As males have more ΔFosB in this circuit at baseline, males may then achieve an activity threshold which results in behavioral resilience more rapidly than females. Thus, ΔFosB may be a mediator of stress behaviors in both sexes.

Contrary to this hypothesis, removal of *FosB* in the vHPC-NAc selectively enhances social interaction in males indicating a "protoresilient" phenotype. Furthermore, this manipulation failed to produce anhedonia and social withdrawal after SCVS. Although SCVS is a "subthreshold" stress for males, if my hypotheses were correct, *FosB* knockout would have increased susceptibility. These data provide evidence which counter the idea that *FosB* gene products are necessary for stress resilience, but rather suggest their role in behavior is dependent upon the animal's experiences during *FosB* gene product expression. This is consistent with the suggestion that HPC ΔFosB is associated with engrams encoding specific experiences [337].

Additionally, ΔFosB overexpression in females did not affect non-stressed animals, but in the context of stress actually *enhanced* sucrose preference. This indicates that ΔFosB itself is not sufficient for "protoresilient" phenotypes in females, but rather specifically interacted with the stress context for behavioral resilience. Taken together, these data suggest that the presence of ΔFosB alone cannot specifically encode sensitivity to stress or protoresilient affective behaviors. Rather, this implicates the accumulation of ΔFosB in this circuit as interacting with the encoding and sequalae of experiences to affect responses to future stimuli, rather than changing the valence involved in the features of experience itself. This is consistent with previous reports indicating that increased vHPC activation in response to appetitive cues is dependent on internal context [471] and the vHPC is critical in effort-based responding, but not for the formation of preferences [469].

Together, these experiments shed light on disease states at the intersection of valence and experience, such as depression. These studies highlight that transcriptional changes in vHPC neurons themselves do not necessarily remodel behavior: rather the transcriptome interacts with patterns of activation (i.e. experiences) to elicit behavior. Therefore, future studies of the entire memory trace--- such as how the vHPC-NAc circuit interacts with projections to other brain regions to encode stress memories and govern stress-induced behaviors--- provide an attractive focus for future studies.

Table 6 | Statistical comparisons in chapter 6

Figure	Test	Comparison	Stat	p-value	Sum-mary
Fig 57B	2-way ANOVA	Group: Male vs Female	F (1, 108) = 1.183	P = 0.279	ns
		Trial: Control vs Stress	F (1, 108) = 4.151	P = 0.044	*
		Group x Trial	F (1, 108) = 1.507	P = 0.222	ns
Fig 58B	2-way ANOVA	Group: Male vs Female	F (1, 68) = 1.364	P = 0.247	ns
		Trial: Control vs Stress	F (1, 68) = 2.770	P = 0.101	ns
		Group x Trial	F (1, 68) = 1.540	P = 0.219	ns
Fig 59B	2-way ANOVA	Group: Male vs Female	F (1, 25) = 7.614	P = 0.011	*
		Trial: Control vs Stress	F (1, 25) = 2.913	P = 0.100	ns
		Group x Trial	F (1, 25) = 0.1453	P = 0.706	ns
Fig 59C	2-way ANOVA	Group: Male vs Female	F (1, 24) = 13.93	P = 0.001	**
		Trial: Control vs Stress	F (1, 24) = 7.840	P = 0.010	**
		Group x Trial	F (1, 24) = 1.961	P = 0.174	ns
Fig 60B	2-way ANOVA	Group: Male vs Female	F (1, 8) = 3.142	P = 0.114	ns
		Trial: Control vs Stress	F (1, 8) = 0.002938	P = 0.958	ns
		Group x Trial	F (1, 8) = 0.5140	P = 0.494	ns
Fig 60C	2-way ANOVA	Group: Male vs Female	F (1, 8) = 5.589	P = 0.046	*
		Trial: Control vs Stress	F (1, 8) = 1.293	P = 0.289	ns
		Group x Trial	F (1, 8) = 0.01416	P = 0.908	ns
Fig 61B	2-way ANOVA	Group: Male vs Female	F (1, 24) = 0.02855	P = 0.867	ns
		Trial: Control vs FosB KNOCKOUT	F (1, 24) = 0.2300	P = 0.636	ns
		Group x Trial	F (1, 24) = 8.766	P = 0.007	**

Table 6 (cont'd)

	Sidak's multiple comparisons	scr-gRNA – FosB-gRNA			
		Male	t (24) = 2.526	P = 0.015	*
		Female	t(24) = 1.694	P = 0.152	ns
Fig 61C	2-way ANOVA	Group: Male vs Female	F (1, 24) = 0.2282	P = 0.637	ns
		Trial: Control vs FosB KNOCKOUT	F (1, 24) = 5.330	P = 0.030	*
		Group x Trial	F (1, 24) = 1.369	P = 0.254	ns
Fig 62A	2-way ANOVA	Group: Male vs Female	F (1, 24) = 3.602	P = 0.070	ns
		Trial: Control vs FosB KNOCKOUT	F (1, 24) = 1.906	P = 0.180	ns
		Group x Trial	F (1, 24) = 0.4283	P = 0.519	ns
Fig 62B	2-way ANOVA	Group: Male vs Female	F (1, 25) = 4.209	P = 0.051	ns
		Trial: Control vs FosB KNOCKOUT	F (1, 25) = 0.03834	P = 0.846	ns
		Group x Trial	F (1, 25) = 3.950	P = 0.058	ns
Fig 62C	2-way ANOVA	Group: Male vs Female	F (1, 25) = 3.869	P = 0.060	ns
		Trial: Control vs FosB KNOCKOUT	F (1, 25) = 0.02258	P = 0.882	ns
		Group x Trial	F (1, 25) = 0.7606	P = 0.391	ns
Fig 62D	2-way ANOVA	Group: Male vs Female	F (1, 24) = 5.546	P = 0.027	*
		Trial: Control vs FosB KNOCKOUT	F (1, 24) = 0.1555	P = 0.697	ns
		Group x Trial	F (1, 24) = 0.03894	P = 0.845	ns
Fig 62E	2-way ANOVA	Group: Male vs Female	F (1, 25) = 9.656	P = 0.005	**
		Trial: Control vs FosB KNOCKOUT	F (1, 25) = 0.09996	P = 0.755	ns
		Group x Trial	F (1, 25) = 0.06540	P = 0.800	ns

Table 6 (cont'd)

Fig 62F	2-way ANOVA	Group: Male vs Female	F (1, 25) = 0.7175	P = 0.405	ns
		Trial: Control vs FosB KNOCKOUT	F (1, 25) = 5.322	P = 0.030	*
		Group x Trial	F (1, 25) = 0.2216	P = 0.642	ns
Fig 63A	2-way ANOVA	Group: Male vs Female	F (1, 23) = 135.3	P < 0.001	***
		Trial: Control vs FosB KNOCKOUT	F (1, 23) = 0.009544	P = 0.923	ns
		Group x Trial	F (1, 23) = 10.67	P = 0.003	**
	Sidak's multiple comparisons	scr-gRNA – FosB-gRNA			
		Male	t(23) = 2.641	P = 0.008	*
		Female	t (23) = 2.054	P = 0.118	ns
Fig 63B	2-way ANOVA	Group: Male vs Female	F (1, 23) = 0.4221	P = 0.522	ns
		Trial: Control vs FosB KNOCKOUT	F (1, 23) = 2.374	P = 0.137	ns
		Group x Trial	F (1, 23) = 2.591	P = 0.121	ns
Fig 63C	2-way ANOVA	Group: Male vs Female	F (1, 23) = 0.5043	P = 0.485	ns
		Trial: Control vs FosB KNOCKOUT	F (1, 23) = 3.329	P = 0.081	ns
		Group x Trial	F (1, 23) = 1.976	P = 0.173	ns
Fig 63D	2-way ANOVA	Group: Male vs Female	F (1, 24) = 9.670	P = 0.005	**
		Trial: Control vs FosB KNOCKOUT	F (1, 24) = 0.002289	P = 0.962	ns
		Group x Trial	F (1, 24) = 5.495	P = 0.028	*
	Sidak's multiple comparisons	scr-gRNA – FosB-gRNA			
		Male	t (24) = 1.827	P = 0.105	ns

Table 6 (cont'd)

		Female	t (24) = 1.519	P = 0.130	ns
Fig 63E	2-way ANOVA	Group: Male vs Female	F (1, 24) = 108.3	P < 0.001	****
		Trial: Control vs FosB KNOCKOUT	F (1, 24) = 0.08014	P = 0.780	ns
		Group x Trial	F (1, 24) = 2.112	P = 0.159	ns
Fig 63F	2-way ANOVA	Group: Male vs Female	F (1, 24) = 46.77	P < 0.001	****
		Trial: Control vs FosB KNOCKOUT	F (1, 24) = 0.006936	P = 0.934	ns
		Group x Trial	F (1, 24) = 0.2166	P = 0.646	ns
Fig 64A	2-way ANOVA	Group: Male vs Female	F (1, 24) = 40.51	P < 0.001	****
		Trial: Control vs FosB KNOCKOUT	F (1, 24) = 2.098	P = 0.160	ns
		Group x Trial	F (1, 24) = 0.7121	P = 0.407	ns
Fig 64B	2-way ANOVA	Group: Male vs Female	F (1, 24) = 3.887	P = 0.060	ns
		Trial: Control vs FosB KNOCKOUT	F (1, 24) = 3.665	P = 0.066	ns
		Group x Trial	F (1, 24) = 0.4316	P = 0.516	ns
Fig 64C	2-way ANOVA	Group: Male vs Female	F (1, 24) = 17.08	P < 0.001	***
		Trial: Control vs FosB KNOCKOUT	F (1, 24) = 1.596	P = 0.219	ns
		Group x Trial	F (1, 24) = 0.6751	P = 0.419	ns
Fig 64D	2-way ANOVA	Group: Male vs Female	F (1, 24) = 6.478	P = 0.018	*
		Trial: Control vs FosB KNOCKOUT	F (1, 24) = 1.215	P = 0.281	ns
		Group x Trial	F (1, 24) = 0.02832	P = 0.868	ns
Fig 65B	2-way ANOVA	Group: Male vs Female	F (1, 25) = 5.647	P = 0.026	*
		Trial: Control vs FosB KNOCKOUT	F (1, 25) = 0.8595	P = 0.363	ns

Table 6 (cont'd)

		Group x Trial	F (1, 25) = 0.4166	P = 0.525	ns
Fig 65C	2-way ANOVA	Group: Male vs Female	F (1, 24) = 2.124	P = 0.158	ns
		Trial: Control vs FosB KNOCKOUT	F (1, 24) = 0.2779	P = 0.603	ns
		Group x Trial	F (1, 24) = 0.01134	P = 0.916	ns
Fig 66A	2-way ANOVA	Group: Male vs Female	F (1, 25) = 1.747	P = 0.198	ns
		Trial: Control vs FosB KNOCKOUT	F (1, 25) = 2.477	P = 0.128	ns
		Group x Trial	F (1, 25) = 0.3237	P = 0.576	ns
Fig 66B	2-way ANOVA	Group: Male vs Female	F (1, 25) = 0.01970	P = 0.890	ns
		Trial: Control vs FosB KNOCKOUT	F (1, 25) = 2.819	P = 0.106	ns
		Group x Trial	F (1, 25) = 2.065	P = 0.163	ns
Fig 66C	2-way ANOVA	Group: Male vs Female	F (1, 25) = 2.718	P = 0.112	ns
		Trial: Control vs FosB KNOCKOUT	F (1, 25) = 1.340	P = 0.258	ns
		Group x Trial	F (1, 25) = 0.1992	P = 0.659	ns
Fig 66D	2-way ANOVA	Group: Male vs Female	F (1, 25) = 0.1233	P = 0.728	ns
		Trial: Control vs FosB KNOCKOUT	F (1, 25) = 0.8150	P = 0.375	ns
		Group x Trial	F (1, 25) = 2.721	P = 0.112	ns
Fig 66E	2-way ANOVA	Group: Male vs Female	F (1, 25) = 0.3112	P = 0.582	ns
		Trial: Control vs FosB KNOCKOUT	F (1, 25) = 0.2435	P = 0.626	ns
		Group x Trial	F (1, 25) = 2.086	P = 0.161	ns
Fig 66F	2-way ANOVA	Group: Male vs Female	F (1, 25) = 1.924	P = 0.177	ns
		Trial: Control vs FosB KNOCKOUT	F (1, 25) = 4.261	P = 0.050	*

Table 6 (cont'd)

		Group x Trial	F (1, 25) = 0.03836	P = 0.846	ns
Fig 67A	2-way ANOVA	Group: Male vs Female	F (1, 25) = 97.18	P < 0.001	****
		Trial: Control vs FosB KNOCKOUT	F (1, 25) = 3.910	P = 0.059	ns
		Group x Trial	F (1, 25) = 1.948	P = 0.175	ns
Fig 67B	2-way ANOVA	Group: Male vs Female	F (1, 24) = 2.153	P = 0.155	ns
		Trial: Control vs FosB KNOCKOUT	F (1, 24) = 0.9046	P = 0.351	ns
		Group x Trial	F (1, 24) = 2.134	P = 0.157	ns
Fig 67C	2-way ANOVA	Group: Male vs Female	F (1, 24) = 1.823	P = 0.190	ns
		Trial: Control vs FosB KNOCKOUT	F (1, 24) = 0.8243	P = 0.373	ns
		Group x Trial	F (1, 24) = 8.748	P = 0.007	**
	Sidak's multiple comparisons	scr-gRNA – FosB-gRNA			
		Male	t (24) = 1.449	P = 0.145	ns
		Female	t (24) = 2.733	P = 0.025	*
Fig 67D	2-way ANOVA	Group: Male vs Female	F (1, 25) = 6.143	P = 0.020	*
		Trial: Control vs FosB KNOCKOUT	F (1, 25) = 1.122	P = 0.300	ns
		Group x Trial	F (1, 25) = 0.7068	P = 0.409	ns
Fig 67E	2-way ANOVA	Group: Male vs Female	F (1, 25) = 82.95	P < 0.001	****
		Trial: Control vs FosB KNOCKOUT	F (1, 25) = 0.2285	P = 0.637	ns
		Group x Trial	F (1, 25) = 0.2906	P = 0.595	ns
Fig 67F	2-way ANOVA	Group: Male vs Female	F (1, 25) = 228.2	P < 0.001	****
		Trial: Control vs FosB KNOCKOUT	F (1, 25) = 4.440	P = 0.045	***

Table 6 (cont'd)

		Group x Trial	F (1, 25) = 14.94	P = 0.001	*
	Sidak's multiple comparisons	scr-gRNA – FosB-gRNA			
		Male	t (25) = 4.136	P < 0.001	***
		Female	t (25) = 1.270	P = 0.261	ns
Fig 68A	2-way ANOVA	Group: Male vs Female	F (1, 24) = 7.124	P = 0.013	*
		Trial: Control vs FosB KNOCKOUT	F (1, 24) = 1.352	P = 0.256	ns
		Group x Trial	F (1, 24) = 2.221	P = 0.149	ns
Fig 68B	2-way ANOVA	Group: Male vs Female	F (1, 24) = 0.6646	P = 0.423	ns
		Trial: Control vs FosB KNOCKOUT	F (1, 24) = 3.217	P = 0.086	ns
		Group x Trial	F (1, 24) = 3.962	P = 0.058	ns
Fig 68C	2-way ANOVA	Group: Male vs Female	F (1, 24) = 7.221	P = 0.013	*
		Trial: Control vs FosB KNOCKOUT	F (1, 24) = 1.666	P = 0.209	ns
		Group x Trial	F (1, 24) = 2.648	P = 0.117	ns
Fig 68D	2-way ANOVA	Group: Male vs Female	F (1, 24) = 0.4650	P = 0.502	ns
		Trial: Control vs FosB KNOCKOUT	F (1, 24) = 0.3073	P = 0.585	ns
		Group x Trial	F (1, 24) = 0.4668	P = 0.501	ns
Fig 69A	2-way ANOVA	Group: Control vs FosB KNOCKOUT	F (1, 105) = 0.5822	P = 0.447	ns
		Trial: Control vs Stress	F (1, 105) = 1.266	P = 0.263	ns
		Group x Trial	F (1, 105) = 1.922	P = 0.169	ns
Fig 69B	2-way ANOVA	Group: Control vs FosB KNOCKOUT	F (1, 104) = 0.004628	P = 0.946	ns
		Trial: Control vs Stress	F (1, 104) = 4.549	P = 0.035	*

Table 6 (cont'd)

		Group x Trial	F (1, 104) = 2.031	P = 0.157	ns
Fig 69C	2-way ANOVA	Group: Control vs FosB KNOCKOUT	F (1, 107) = 0.3583	P = 0.551	ns
		Trial: Control vs Stress	F (1, 107) = 3.960	P = 0.049	*
		Group x Trial	F (1, 107) = 1.360	P = 0.246	ns
Fig 70A	2-way ANOVA	Group: Control vs FosB KNOCKOUT	F (1, 102) = 0.05629	P = 0.813	ns
		Trial: Control vs Stress	F (1, 102) = 0.4183	P = 0.519	ns
		Group x Trial	F (1, 102) = 2.161	P = 0.145	ns
Fig 70B	2-way ANOVA	Group: Control vs FosB KNOCKOUT	F (1, 106) = 0.03543	P = 0.851	ns
		Trial: Control vs Stress	F (1, 106) = 0.4539	P = 0.502	ns
		Group x Trial	F (1, 106) = 0.2906	P = 0.591	ns
Fig 70C	2-way ANOVA	Group: Control vs FosB KNOCKOUT	F (1, 69) = 0.6963	P = 0.407	ns
		Trial: Control vs Stress	F (1, 69) = 0.4692	P = 0.496	ns
		Group x Trial	F (1, 69) = 0.08350	P = 0.774	ns
Fig 71B	2-way ANOVA	Group: Control vs ΔFosB	F (1, 35) = 7.687	P = 0.009	**
		Trial: Control vs Stress	F (1, 35) = 5.904	P = 0.020	*
		Group x Trial	F (1, 35) = 21.38	P < 0.001	****
	Sidak's multiple comparisons	Control vs Stress			
		Control	t (35) = 1.573	P = 0.115	ns
		ΔFosB	t (35) = 4.922	P < 0.001	****
Fig 71C	2-way ANOVA	Group: Control vs ΔFosB	F (1, 32) = 0.9960	P = 0.326	ns
		Trial: Control vs Stress	F (1, 32) = 0.7924	P = 0.380	ns

Table 6 (cont'd)

		Group x Trial	F (1, 32) = 1.967	P = 0.170	ns
Fig 71D	2-way ANOVA	Group: Control vs ΔFosB	F (1, 32) = 0.05179	P = 0.821	ns
		Trial: Control vs Stress	F (1, 32) = 0.9243	P = 0.344	ns
		Group x Trial	F (1, 32) = 0.6024	P = 0.443	ns
Fig 72A	2-way ANOVA	Group: Control vs ΔFosB	F (1, 34) = 0.1145	P = 0.737	ns
		Trial: Control vs Stress	F (1, 34) = 0.3387	P = 0.564	ns
		Group x Trial	F (1, 34) = 0.3059	P = 0.584	ns
Fig 72B	2-way ANOVA	Group: Control vs ΔFosB	F (1, 35) = 0.9063	P = 0.348	ns
		Trial: Control vs Stress	F (1, 35) = 0.9326	P = 0.341	ns
		Group x Trial	F (1, 35) = 0.7681	P = 0.387	ns
Fig 72C	2-way ANOVA	Group: Control vs ΔFosB	F (1, 30) = 5.293	P = 0.029	*
		Trial: Control vs Stress	F (1, 30) = 4.385	P = 0.045	*
		Group x Trial	F (1, 30) = 3.786	P = 0.061	ns

CHAPTER 7: CONCLUSIONS AND FUTURE DIRECTIONS

Summary

The work presented in this dissertation contributes to the fields of mood disorder research and behavioral neuroscience in several ways. First, these data describe several mechanisms of *FosB* gene products in HPC affecting behavioral responses to experience (i.e. learning and memory). Regulation of transcription in dHPC is necessary for spatial learning [337], though its mechanism(s) and location of action in hippocampal function are not fully understood. As the process of learning and memory consolidation can take place over timescales of up to days or weeks, mechanisms controlling gene expression over these timescales, like ΔFosB, have become a key area of study in the formation and expression of memories. Previous work from our lab and others has shown that ΔFosB is induced in rodent dHPC following multiple forms of experience including stress, drugs, exercise, and spatial learning [326, 328, 337, 348, 384, 451]. As the HPC has distinct patterns of information flow [162, 489], and functional segregation of cognitive and affective memories across the dorsoventral axis [189], specific hippocampal subpopulations may be involved in different aspects of learning and memory. The experiments in chapters 3, 4, and 6 therefore sought to uncover subpopulation-specific contributions of ΔFosB to behavior following neutral and affective experiences through the use of transgenic mouse lines and viral vectors.

The experiments in chapter 3 examined the effects of *FosB* gene products in the SGZ of the DG on learning and memory. To this end I collaborated with Dr. Gina Leinninger who developed the *NtsR2-Cre* mouse, in which hippocampal Cre expression is confined to the SGZ [330]. Crossing this line with our floxed *FosB* line produced knock out of *FosB* gene

products in in the SGZ. SGZ *FosB* knockout reduced multiple markers of neurogenesis: BrdU and DCX preferentially in the dHPC, indicating dHPC SGZ *FosB* is necessary in normal cell proliferation. In addition, *FosB* knockout reduced the time spent with a novel object in the NOR task, without impacting anxiety phenotypes. These results suggest *FosB* gene products regulate dHPC neurogenesis in a manner necessary for normal cognition.

As the vHPC is implicated in affective learning and memory through its connectivity to limbic regions, in chapters 4 and 6 I examined the role of vHPC ΔFosB in stress-induced affective behaviors. To test ΔFosB's role in multiple cell populations of the vHPC, I collaborated with Dr. Rachel Neve at Massachusetts General Hospital, who produced the novel viruses allowing circuit-specific guidance of Cas9 to the *FosB* gene and subsequent *FosB* knockout. The specific guide RNA for this system was validated in our lab and caused marked reduction in *FosB* protein products in cell culture, local brain injections, and in circuit specific manipulations. I used these technologies in combination with CSDS and SCVS to unveil a previously unknown role for ΔFosB in vHPC neurons projecting to NAc in orchestrating resilience to stress-induced behaviors.

The data presented in this thesis also demonstrate a novel dissociation of vHPC afferents' contributions to stress phenotypes. In addition to showing ΔFosB's accumulation in vHPC-NAc is sufficient for resilience to stress, the experiments in chapter 4 comparing ΔFosB's role in vHPC-NAc and vHPC-BLA neurons are the first to show that divergent patterns of behavior can be elicited by the same manipulation of a single hippocampal population based solely on differences in projection. These data elucidate a clear role for ΔFosB in male vHPC projections: ΔFosB in vHPC-NAc is necessary and sufficient for

resilience to stress, and ΔFosB in vHPC-BLA is necessary for the expression of fear and anxiety. Our results demonstrate that individual genes can have disparate roles within a single brain region based not only on heterogenous cell types but on the specific projections of the neurons in which they are expressed.

Third, the experiments in chapter 5 describe the first finding of a circuit-specific sex difference which drives stress-induced behavior. Glutamatergic projection neurons from vHPC-NAc were previous implicated in stress and reward behavior in males [45, 127], and we show they display a basal sex difference in excitability which is driven by adult testosterone. Analysis of the NAc following stress suggests that sex differences in stress responses are due in part to changes in glutamatergic signaling [335]. These data show vHPC-NAc activity is causally linked to the sex difference in susceptibility to stress-induced anhedonia. This relationship is dependent upon long-term adaptation of vHPC-NAc projections and may reflect on the biological underpinning of female vulnerability to mood disorders related to stress.

Final Summary

The molecular mediators which underlie the symptoms of human depression are still largely unknown. To help bridge this knowledge gap, this dissertation used preclinical mouse models to evaluate the hypothesis that cell-specific hippocampal ΔFosB drives behavioral responses to chronic stress. Multiple chapters investigated the transcriptional underpinnings of vHPC-NAc its contributions to stress behavior, summarized in Figure 73. In chapter 4, the modulation of ΔFosB expression in male vHPC-NAc led to changes in stress induced behavior. Specifically, knockout of vHPC-NAc ΔFosB increased the circuit's excitability concurrent with decreased social interaction following stress. This

indicates ΔFosB is a molecular mediator which reduces vHPC-NAc excitability and leads to stress resilience. The relationship between vHPC-NAc excitability and stress resilience was further characterized in chapter 5. Chronically driving vHPC-NAc excitability through projection-specific chemogenetics caused anhedonia, while inhibiting the circuit prevented the phenomenon. This indicated that the higher excitability of the female vHPC-NAc circuit compared to males caused the female-specific susceptibility to stress-induced anhedonia. Furthermore, circulating adult androgens exerted a protective effect against vHPC-NAc excitability and stress susceptibility. This implicates androgens as another potentially independent transcriptional modulator of vHPC-NAc which influences sex differences in stress responses. The intersection of androgens and ΔFosB is unclear. In chapter 6, males expressed more ΔFosB in vHPC-NAc compared to females regardless of stress, supporting synergistic interactions of androgens and ΔFosB. However, ΔFosB overexpression in both male and female vHPC-NAc circuit prevented stress-induced behavioral deficits in naturally cycling animals (e.g. increased social interaction following CSDS in males from chapter 4 and increased sucrose preference following SCVS in females in chapter 6) indicating that ΔFosB accumulation in vHPC-NAc is sufficient for stress resilience in both sexes regardless of androgens. Taken together, these studies suggest that persistent presence of androgens and accumulation ΔFosB can act upon the vHPC-NAc circuit in similar fashions, perhaps in tandem, to elicit decreases in circuit excitability and subsequent behavioral resilience.

While the findings in the above chapters provide further evidence for the involvement of the *FosB* gene and sex in the hippocampus in learned and affective behaviors, the mechanisms behind their involvement are complex. In order to gain a more complete understanding of hippocampal ΔFosB function and its role in orchestrating behavior, many more experiments will be necessary. Five particular themes suggest themselves for future exploration of the molecular mechanisms of hippocampal effects on behavior: 1) Projection-specific considerations; 2) Cell-specific importance of gene expression; 3) Validation of ΔFosB gene targets; 4) Intersections of Sex, Stress, and *FosB;* and 5) Potential Therapeutic interventions.

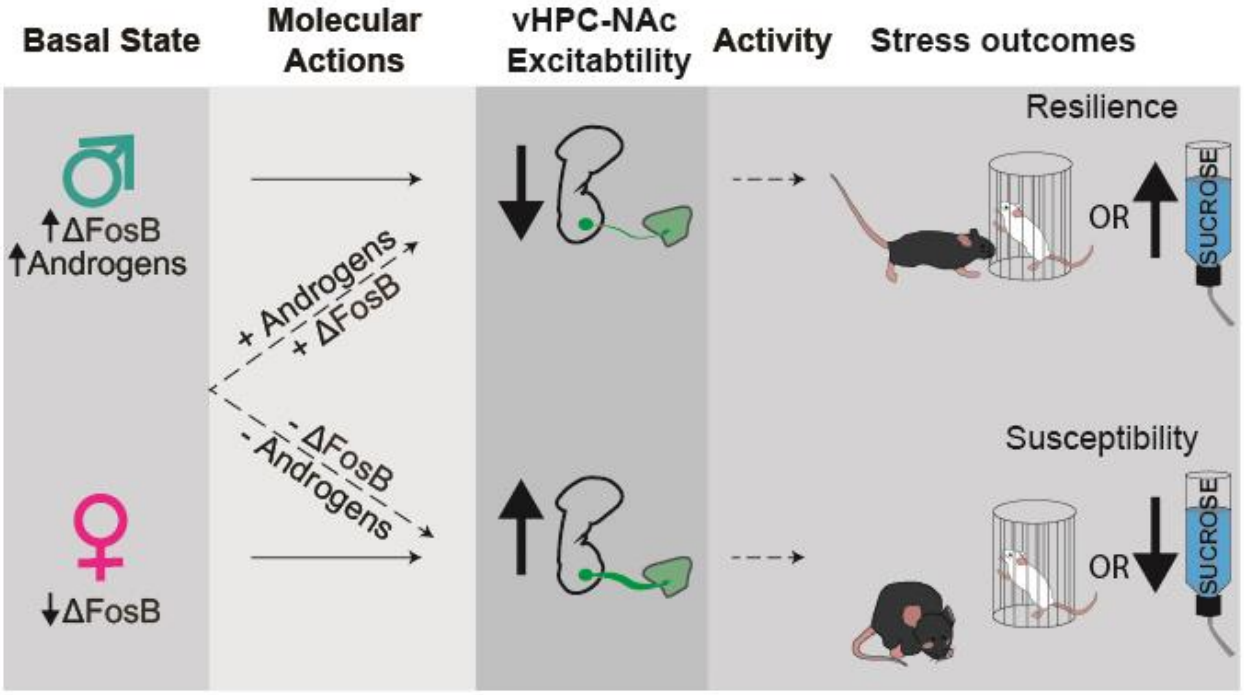

Figure 73 | Model of ΔFosB and androgens' contributions to chronic stress phenotypes. Persistent actions of both vHPC-NAc ΔFosB and circulating androgens lead to reduced vHPC-NAc excitability and subsequent stress resilience, while preventing either mechanism leads to stress susceptibility. Solid arrows indicate phenomena, while dashed lines represent manipulations performed in the thesis.

Projection-specific Considerations

The HPC, unlike many other limbic regions, displays an exquisite degree of spatial organization. The delineation of the HPC into distinct anatomical subregions corresponds to their functional connectivity in the trisynaptic circuit [162, 490]. In an extension of this principle, recent work shows that vHPC afferent cell bodies also have discrete and non-overlapping spatial patterns within the CA1 and subiculum (e.g. deep vs superficial, medial vs lateral, dorsal vs ventral) which correspond both with afferent projection targets and distinct patterns of gene expression [199, 488, 491, 492]. These findings have several implications in the context of this thesis. Despite all being glutamatergic projection neurons, the transcription profiles are distinct, suggesting there are fundamental differences in the mechanisms maintaining gene expression across the vHPC CA1 and subiculum, perhaps through epigenetics. If this is the case, the transcription factor ΔFosB may bind to different AP-1 consensus sequences in vHPC-NAc vs vHPC-BLA based on differential states of the chromatin in those populations, leading to differences in ΔFosB gene targets and functional effects [493]. One experiment that would provide evidence for this hypothesis would be projection-specific TRAP from both vHPC-BLA and vHPC-NAc neurons in floxed *FosB* and control mice and subsequent comparisons of gene expression. However, if these experiments do not support differential effects of ΔFosB on gene expression, then the projection-specific changes in behavior reported in chapter 4 and 6 may be due to the identity of the postsynaptic cells.

The work presented in this dissertation exclusively uses viruses to identify and manipulate a subpopulation of vHPC neurons projecting to NAc or BLA. Future studies may instead be able to use spatial registration in vCA1 to identify projection targets rather than viral

labeling [494], expediting scientific questions by removing the need for retrograde labeling, or developing mouse lines to manipulate whole projection populations, like Trophoblast glycoprotein (Tpbg)-expressing neurons which exclusively project to the mPFC [488].

vHPC neurons project to a number of limbic regions, including NAc, BLA, and PFC [129], and its activity is critical in several aspects of affective learning and memory [146, 495, 496]. Other labs have shown vHPC-NAc neurons modulate reward and stress phenotypes [45, 127], but our lab was the first to examine divergent vHPC projections' roles in behavior. The experiments of chapters 4 and 6 show that vHPC's role in affective behavior is not monolithic, but rather vHPC neurons contribute differentially to enhance anxiety- or reward-related behavior, depending on their projection targets. These results suggest that the contributions of vHPC to other limbic regions, such as PFC, are a critical next step to understanding vHPC contributions to afferent behavior.

Colocalization:

There is an insidious assumption in the experiments described in this thesis. Identification of vHPC projection neurons were based upon regrade tracing, which prevented rigorous identification of collateral axons of vHPC afferents [129, 130, 149]. Thus, vHPC afferents were purported to be mutually exclusive. However, several reports suggest that individual vHPC afferents may send multiple collateral projections to a number of limbic regions [45, 497, 498]. If this is true for the entirely of these cell populations, our "circuit-specific" approach to label, record, and manipulate vHPC afferents is flawed, and results in direct manipulation of multiple limbic circuits. In contrast to these reports of individual collateralizing vHPC afferents, analysis across vHPC populations suggests the afferent

subpopulations are on the whole mutually exclusive [488, 499, 500]. To do a preliminary assessment of collaterals between vHPC-NAc and vHPC-BLA projection neurons, I injected the two regions simultaneously with retrograde viruses expressing mCherry and Cre in our L10-GFP reporter line (Fig 74). These images show a single colabelled neuron projecting from vHPC to both NAc and BLA, supporting the existence of collateralizing vHPC afferents. However, these images provide preliminary evidence that these neurons represent a minute fraction of vHPC afferents to BLA or NAc. Thus, there is support that an overwhelming majority of NAc and BLA projecting neurons in vHPC are mutually exclusive populations, and the circuit-specific manipulations of these populations do indeed target distinct neurons.

This retrograde dual labeling strategy to identify collateralization between brain regions prevents analysis of multiple brain regions, and thus is subject to the same pitfalls as single retrograde labeling. Whole dye fills coupled with anatomical reconstruction prevent characterization of projection populations as a whole. An intermediate strategy to characterize population collaterals could use a dual viral strategy. A retrogradely expressing viral vector encoding Cre recombinase and a reporter injected into one vHPC afferent region, like NAc, while a Cre-dependent AAV encoding GFP is injected into the vHPC, would allow circuit specific GFP expression. Unlike our Cre-dependent reporter line which expresses GFP on ribosomes, viral GFP is freely diffusible and fills neurons which allows clear visualization of neurites including collateral projection sites. Similar strategies have been used to this effect in the hypothalamus [501]. Thus, reporter signal will confirm injection sites, and GFP in the projecting axons throughout potential target sites will characterize relative densities of innervation. However, as vHPC-PFC neurons

have a distinct pattern of gene expression [491], and my preliminary images show little colabeling between vHPC-BLA and vHPC-NAc, I predict vHPC afferents are almost all exclusive projections. Nonetheless, this information is critical for the interpretation of all of our projection-specific manipulations.

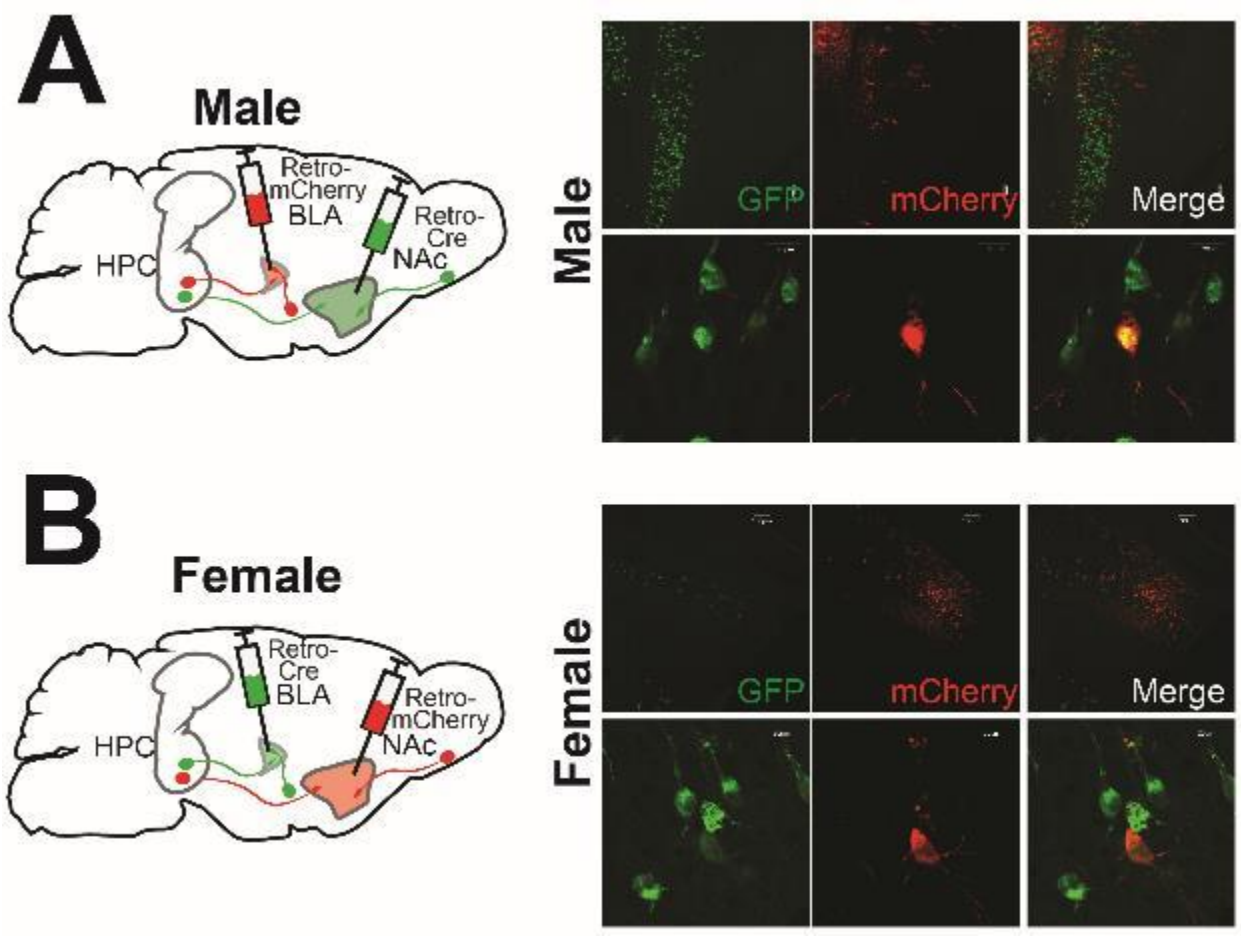

Figure 74 | Example of double labeling of vHPC afferents. (A, left) Schematic of male GFP reporter mouse with double lablled with Retrograde mCherry into the BLA, and Retrograde Cre into the NAc. **(A, right)** Images of vHPC at 10x and 100x show a single colabelled cell in the vCA1 cell layer. **(B, left)** Schematic of female GFP reporter mouse receiving Retro-Cre in BLA and Retro mCherry in the NAc. **(B,right)** Images of vHPC at 10x and 100x show no colabelling in the vCA1.

Cell-type specific importance of gene expression

The role of HPC ΔFosB in behavior is determined by the cells in which it is expressed. ΔFosB accumulates in dHPC in response to experiences like drugs, stress, learning, and

exercise [326, 337, 348, 451], suggesting that it is potentially important in the formation of memories about these experiences. However, it also accumulates in Alzheimer's disease mouse models and patients [324, 371, 372]. This accumulation may be an attempted compensation against the disease state. However, ΔFosB viral overexpression throughout the dHPC results in impaired cognition, while viral inhibition of ΔFosB impairs cognition in wild type mice but prevents cognitive decline in an Alzheimer's model [337, 502]. Coupled with data from chapter 3 that show SGZ *FosB* is necessary for normal cognition, this suggests that cell-specific hippocampal ΔFosB is necessary for normal cognition, but aberrant or non-specific ΔFosB may result in cognitive deficits, perhaps through obscuring relevant neuronal activity in the trisynaptic path[337].

This concept of cell-specific importance is also borne out in the examinations of vHPC afferents. Indeed, the vHPC CA1 projections are characterized as a homogeneous cell-type and the same gross anatomical location, but the same manipulation of gene expression results in gross differences in behavior dependent on projection regions. These differences may arise at the level of individual cell gene expression (i.e. the heterogeneity of the projection transcriptome, described above), or through the downstream patterns of connectivity engaged though such projection-specific expression. Adding additional layers of complexity to cell-specific engagement is a discussion surrounding the heterogeneity of cells targeted by vHPC afferents. For example, vHPC projections to the NAc synapse onto both D1 and D2 MSNs, preferentially in the NAc shell. Therefore, previous work using optogenetics and the manipulations in chapters 4-6 which show vHPC-NAc activity drives stress behavior, actually affected several subpopulations of neurons in the NAc which may engage both the direct and indirect

paths to mediate affective behaviors. Furthermore, studies of vHPC-NAc synapses show regulation at D1, but not D2 synapses, following stress [45]. This is also reflected in general studies of the NAc, wherein chronic stress causes LTD and alters D1 morphology but has no effect on D2 neurons [124, 126, 447]. This cell-type specific sensitivity to stress results in opposing roles of MSN activity in stress phenotypes, where D1 and D2 activation promotes resilience and susceptibility to stress, respectively [114]. These effects are reflected in and caused by gene expression, as ΔFosB induction in D1 neurons causes a proresilient phenotype, while FosB induction in D2 neurons causes stress susceptibility [285, 287]. This suggests that activity and the transcriptome intersect for cell-type specific changes in responses to chronic stress. Because the projection-specific manipulations used in this thesis are not exclusive to axons synapsing onto either D1 or D2 MSNs, it is difficult to interpret our results in the context of the known roles of vHPC synapses onto each of these cell types.

Increased D1 MSN activity can drive both reward and aversion outcomes, and recent work suggests that DA signaling in the NAc supports valueless learning [503, 504]. In addition, both D1 and D2 MSNs are necessary for reward behavior [114]. Whether this arises from parallel processing of information or local microcircuits influencing information flow between D1 and D2 neurons is unknown. In the NAc core, it's hypothesized that the coincidence of firing between D1 and D2 MSNs facilitates goal directed behavior, while dichotomy in firing rates leads to divergent behavioral responses. In support of this idea, strong D1 neuronal firing patterns can cause long-lasting potentiation (LLP) of excitatory transmission at D2 MSNs within the core [505]. If this mechanism of D1 influence on D2 neurons also holds true in the NAc shell, this would provide a mechanism which supports

the findings of both vHPC-NAc behavior experiments and vHPC-NAc plasticity experiments. Although stress and reward can bidirectionally alter D1 synapses, D2 neurons remain relatively inflexible to changes in response to stimulation, and thus are positioned to robustly control the proportion of D1 and D2 activity and downstream behaviors. With this hypothesis of shell D1-D2 influence, stimulation the whole vHPC-NAc may result in stress susceptibility through direct activation of D1 neurons and both direct activation and LLP of D2 neurons, leading to D2 activity bias and behavioral aversion. Under these same assumptions, vHPC-NAc activity in response to stress could cause LTD at specifically at D1 neurons, also biasing for D2 population activation, and thus aversion. In support of this idea of LLP at D2 neurons driving behavior, multiple manipulations from chapter 5 caused anhedonia under long time courses, but the short time courses yielded no differences. This suggests that acute activity of vHPC-NAc is not sufficient to cause stress phenotypes, but chronic activity causally changes behavior, perhaps through plasticity of synapses.

Taken altogether, the data presented in this thesis demonstrate that changes in gene expression result in grossly different behavioral outcomes, not solely based on cell type, but also the functional connectivity of the brain. Although populations of neurons may have similarities like anatomical location, cell types, or pattern of gene expression, it is patterns of activity which intersect with gene expression to orchestrate behavior in response to stimuli.

Validation of Downstream ΔFosB targets

Hippocampal ΔFosB is a critical modulator of behavior, and its activity as a transcription factor alters expression of many genes. However, as ΔFosB targets include several other transcription factors and epigenetic modifiers, ΔFosB is a master regulator. In such a position, ΔFosB may not be an attractive druggable target as specific downstream effects may be accompanied with other off-target effects. Prior to this work, ΔFosB's downstream targets were frequently identified in microarray and candidate-based approaches in limbic brain regions [506], with one study of HPC *FosB* ChiP [315]. These targets include molecules in glutamatergic signaling cascades and receptor subunits[291, 292, 318-320] and epigenetic modifications[312, 313, 315-317, 502], and glial markers[321-323]. Use of Cre-dependent GFP reporter line in combination with a retrograde cre viral vector allowed isolation of circuit-specific transcriptomes. In Chapter 4, crossing the cre-dependent line to a floxed FosB line allowed the comparison of the vHPC-NAc transcriptome of males with and without the *FosB* gene specifically in this circuit. This allowed elucidation of ΔFosB gene targets in an unbiased manner and highlighted a number of genes, including g-proteins, metabolism associated genes, and

ion channels. To validate the interaction of ΔFosB with these transcripts, Neuro2A cells were transfected with ΔFosB, followed by qPCR for transcripts of interest. ΔFosB changed transcripts of Adrenergic receptor 2α (Adra2a), neurofilament medium polypeptide (Nefm), and protein kinase C Beta (Prkcb, also known as PKCβ). The indicates that ΔFosB could alter neuronal responses to norepinephrine, the cytoskeleton, and a PKC isoform integral in learning-related signal transduction mechanisms [400].

However, the experiments from Chapter 4 only utilized males, leaving open questions about *FosB* downstream targets in females.

Conversely the TRAP experiments from Chapter 5 examine sex differences in the same vHPC-NAc neuronal population but was performed in wild type animals. This experiment suggested changes in almost 150 genes which passed false discovery rate analysis, many of which are associated with cell excitability and plasticity. These results have not yet been validated in cell culture, but qPCR of punches of whole vHPC tissue are underway. Quantifying transcripts of supervillain (SVIL, an AR chaperone) and adenyl cyclase 1 (ADCY1) indicate that sex differences in gene expression identified in circuit-specific TRAP may robust enough to influence the reads of the whole region, or these sex differences exist across the vHPC (Fig 75). To further validate these results, TRAP could be performed, followed by qPCR for our transcripts of interest. This approach, while cumbersome, would allow us to confirm projection specific gene regulation. Indeed, a preliminary use of this technique has been performed in the lab in male mice exposed to stress (Fig 76). These data confirm stress upregulation of ΔFosB in vHPC-NAc neurons and show minor changes in microtuble-associated protein 2 (map2). Interestingly, map2 is also one of the sexually dimorphic genes identified by TRAP in this circuit, suggesting that changes in the cytoskeleton of vHPC to NAc may be part of the mechanism of stress susceptibility. However, TRAP followed by qPCR is extremely low yield. Alternative approaches like *in situ* hybridization or IHC in male and female labelled projections may allow a higher throughput analysis to confirm sex differences of circuit-specific transcripts. This indicates that comparing TRAP studies may identify common regulators of cell

excitability between *FosB* targets and sex. This may identify proteins suited for therapeutic potential in males and females.

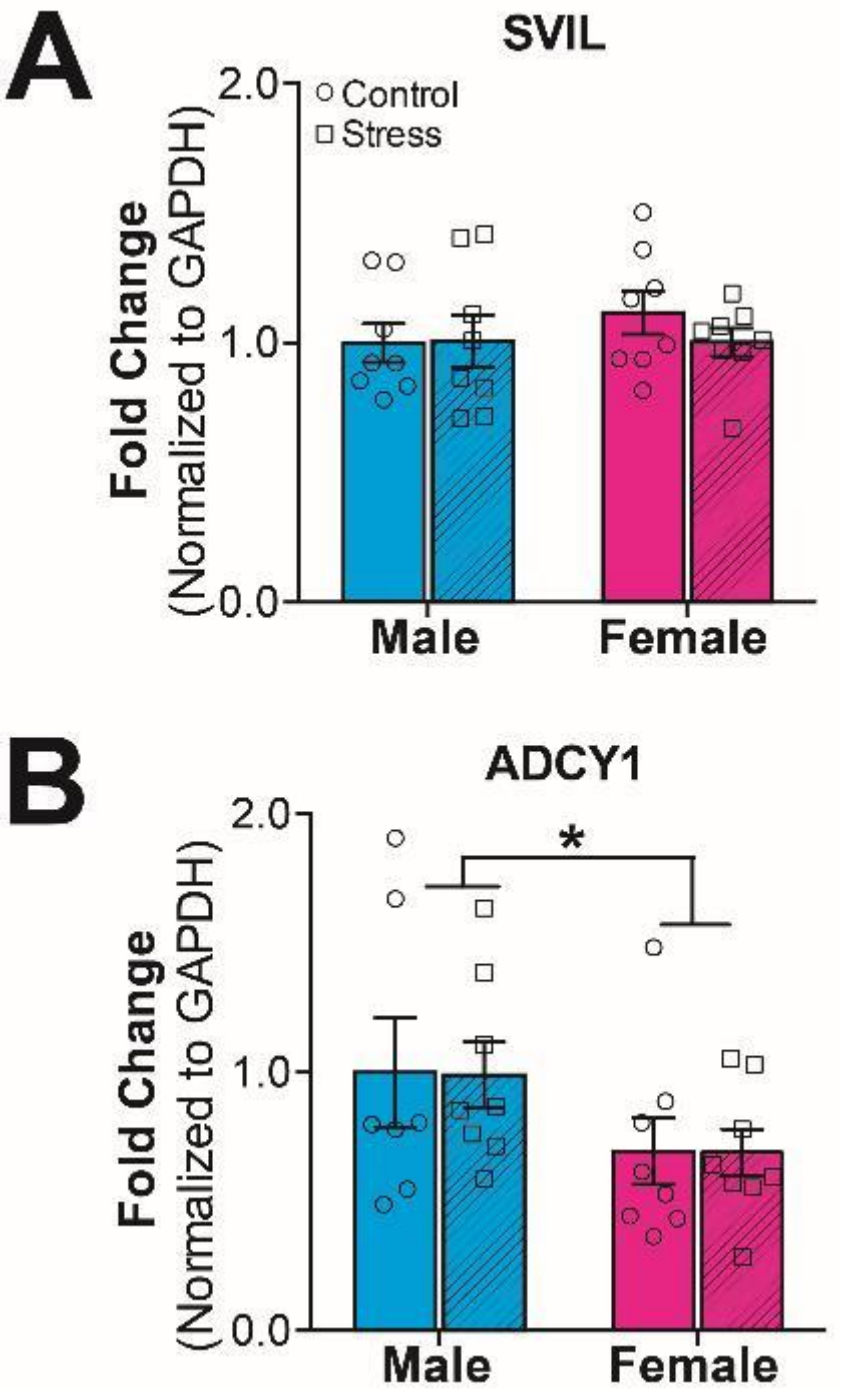

Figure 75 | qPCR of general vHPC transcriptome after stress. Transcripts levels of **(A)** SVIL (supervillain) or **(B)** ADCY1 (adenyl cyclase 1) from punches of vHPC tissue from males and females taken 24 hours after SCVS or control handling. *Main effect of sex, $P < 0.05$, main effect of stress $P = 0.955$, interaction $P = 0.989$.

This method of identifying sex differences in *FosB* gene targets produces candidate molecules but will not directly determine whether *FosB* gene products produce differences in gene expression based on the sex of the animal. One approach to this question is the use TRAP in both males and females from our GFP reporter line. It is customary to give animals chronic stimuli to induce ΔFosB, but this thesis shows there are sex differences response to stress and general basal excitability. Furthermore, there are sex differences in response to antidepressants and drugs of abuse, potentially confounding the comparison [24, 507]. Therefore, to induce ΔFosB at equivalent levels, I propose intracranial injections of a retrograde cre and ΔFosB overexpressing virus, followed TRAP and RNA-Seq with an analysis by sex. Although this experiment does not allow for the comparison of *FosB* knockout between sexes, it will show potential ΔFosB

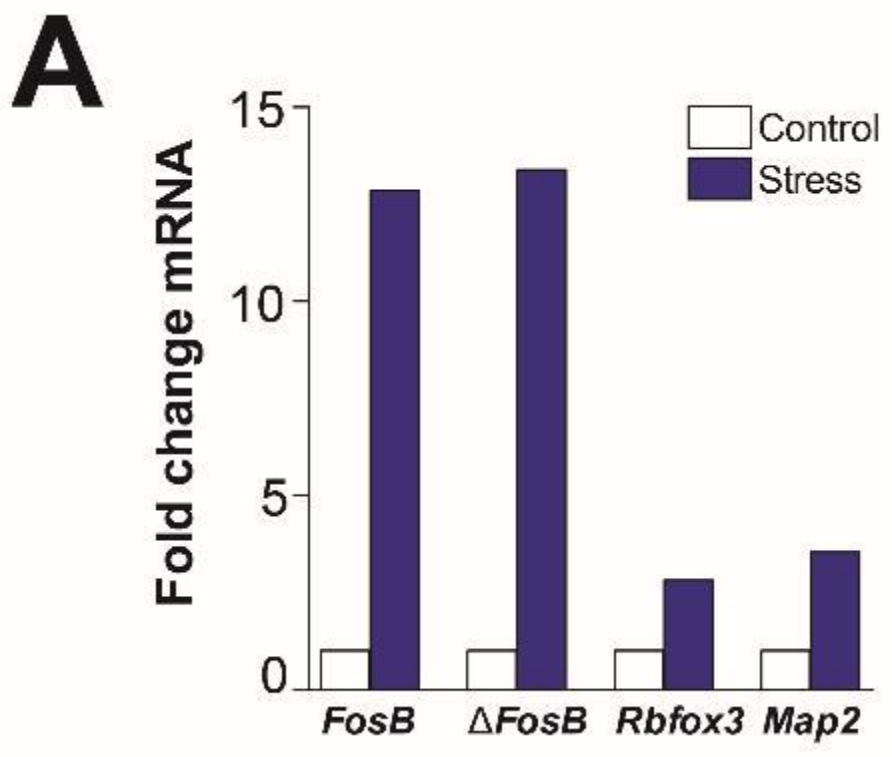

Figure 76 | Proof of concept quantification of TRAP-qPCR. (A) A single biological replicate of male GFP reporter animals that underwent CSDS show enhanced FosB, ΔFosB, Rbfox3, and Map2 mRNA in vHPC-NAc neurons.

interactions with sex in gene expression. If there are few differentially regulated genes, this will reflect a common mechanism of ΔFosB action between the sexes. If ΔFosB does indeed influence gene expression on the basis of sex, it may provide foundational information in the development of sex-specific drugs for the treatment of depression.

Intersection of Sex, Stress, and ΔFosB

The studies described Chapters 5 and 6 examine the interplay of stress experiences, sex, and *FosB* gene products. The intersection between stress and gonadal hormones' contributions to the vHPC-NAc circuit and stress behaviors provides a rich environment for future study. For example, exposure to SCVS results in female-specific corticosteroid increases, but not changes to estrus cycle [63, 508]. SCVS also results in female-specific anhedonia while males were resilient to stress [63], and this effect on anhedonia was dependent on increased vHPC-NAc excitability. Critically, circulating androgens reduced the excitability of this circuit and ameliorated stress-induced anhedonia, while estrogens are not necessary for SCVS anhedonia [508] and did not change vHPC-NAc excitability. This indicates that androgens specifically temper the effects of stress, but the peripheral manipulation and levels of analysis (cell physiology and behavior) obscures the mechanisms of action. This leads to three lines of future study: steroid hormone specificity, cell autonomous vs non-cell autonomous effects of hormones, and steroid receptor actions.

Steroid hormone specificity:

One line of inquiry is at the level of gonadal hormone binding. Although circulating androgens are necessary and sufficient for resilience to SCVS, our manipulations used

testosterone, which can be aromatized to 17β-estradiol (E2) in the hippocampus [509-511]. E2 is a potent estrogen which binds to all ERs, and therefore androgen's effects on stress resilience might be through the actions of estradiol. Future studies in the lab may use 5α-dihydrotestosterone (DHT), which has a high affinity for androgen receptors and cannot be converted to estradiol [512]. If ovariectomy and DHT replacement followed by SCVS also prevents stress-induced anhedonia (as with testosterone in Chapter 5), then androgens are not working through the majority of ERs. One DHT metabolite, however, is a potent ERβ receptor agonist and may confound the interpretation of these results [512]. To test ERβ contributions to vHPC-NAc, the lab can use an ERβ specific agonist [513] in conjunction with vHPC-NAc labeling and *ex vivo* slice electrophysiology to elucidate which gonadal ligands drive physiological and behavioral responses to stress. However, as OVX failed to change vHPC-NAc phsyiology and still resulted in stress-induced anhedonia, I predict that androgens exert their protective effects on stress resilience and decreased neuronal excitability by binding to ARs, not through estrogen signaling.

Cell autonomous vs non-cell autonomous effects of hormones:

ARs are not exclusively expressed in the hippocampus [514], and decreasing androgen levels thus affect neurons and glia across the brain, resulting in numerous changes including increases in circulating stress hormones [460, 515, 516]. However, both sexes do express ARs in HPC [514, 517] and form new synapses in HPC in response to testosterone [518]. Furthermore, vHPC-NAc projections also show AR staining and can increase excitability in responses to an AR antagonist in *ex vivo* slices (Chapter 5). It follows that Androgens can have cell autonomous effects on this circuit, and activation of

AR on vHPC-NAc would reduce excitability, leading to stress resilience. To directly test cell autonomous effects of AR on vHPC- NAc physiology, our lab has collaborated with Dr. Aritro Sen to cross *floxed AR* mice with our GFP reporter line to develop $AR^{flox/flox}$;GFP mice and $AR^{+/+}$;GFP littermates. We can inject retrograde Cre into the NAc, similar to the experiments described in this thesis, and then perform *ex vivo* slice electrophysiology on vHPC-NAc neurons to determine AR's cell autonomous role in cellular excitability.

Steroid receptor actions:

After determining if androgens exert their effects cell autonomously, and which hormone metabolites are exerting effects on vHPC-NAc excitability and subsequent behavior, there is still a crucial question concerning steroid hormones' mechanisms of action and ways in which stress experiences and sex hormones may interact with vHPC-NAc excitability. In addition to second messenger signaling in the cytosol, steroid hormone receptors including ERs, ARs, and GRs are all transcription factors. When stimulated, steroid receptors undergo conformational changes and translocate to the nucleus where they exert transcriptional effects by binding to Androgen, Estrogen, and Glucocorticoid Response Elements, respectively (AREs, EREs, and GREs) [519]. Thus, steroid hormones are each capable of independently regulating gene expression, perhaps providing mechanisms for the sex-differences in stress induced behaviors shown in Chapter 5.

However, biochemical and cell culture, work show deeply complex interactions among the steroid hormone receptors and other transcription factors[520]. For example, GRs and ARs have identical binding motifs, and thus can bind to the overlapping recognition sequences *in vitro* and *in vivo* [521-525]. Despite the significant overlap of GREs and

AREs, these steroid hormones frequently produce differential gene expression *in vivo*, in part dependent on epigenetic factors [522, 526]. Furthermore, transcription factors can bind to enhancer and promotor regions to promote AR and GR selectivity [527-529], and GR can alter chromatin state to facilitate other transcription factor binding [530]. A complex of interest is AP-1, of which ΔFosB is a component. Indeed, ARs and AP-1 can inhibit the transcriptional activity of each other [531, 532], while ERs, in addition to their canonical function, can bind to AP-1 through a tethering mechanism and exert transcriptional actions at AP-1 consensus sites [533, 534]. Furthermore, AP-1 primes chromatin accessibility and facilitates GR recruitment to its binding sites [535]. In turn, GR increases chromatin accessibility to modulate estrogen receptor actions specifically though AP-1 [536, 537]. This crosstalk between stress hormones, AP-1, and gonadal hormones provide a complex web of interactions to influence the brain's transcriptome. Taken together, this suggests that experiences of stress, presumably through the HPA axis and activation of neuronal circuits, can directly intersect with circulating gonadal hormones to orchestrate sex differences in gene expression [538, 539].

Since persistent changes in behavior come about through long term changes in neuronal activity and gene expression, it follows then that stressful experiences may cause sex-specific changes in behavior though regulating interaction with long-term sex-specific patterns of gene regulation, and through direct downstream targets of gonadal hormones in the brain. This is consistent with the data from chapter 5 showing androgens tempering stress responses at the physiological and behavioral level, and the sex-specific effects of ΔFosB on stress behavior reported in Chapter 6. This is also consistent with human reports of exacerbated depression symptoms during times of hormonal change and sex

differences in transcriptomes of depressed humans [25, 27, 262, 418, 540]. Thus, our growing understanding of the interactions of hormones, gene expression, and brain circuits could potentially be leveraged to enable sex-specific therapies for mood disorders.

Potential Therapeutic Interventions

Depression affects up to twenty percent of the population and results in more than 350 billion dollars in losses per year, while standard SSRIs are ineffective in up to half of all patients [1-3, 403, 541]. This disease state shows remarkable sex differences in diagnostic rates, and changes in disease state frequently accompany hormonal status and life stresses [25]. The majority of preclinical studies on depression have been done in exclusively male rodents. Despite failing to include females, the literature suggests there are both activity and transcriptional signatures associated with stress phenotypes and antidepressant responses [127, 128, 197, 300, 542, 543], in agreement with the data in this thesis. Although there are still many future studies needed to elucidate the molecular underpinnings of sex differences in stress-induced behaviors, the work presented in this thesis is also in accordance with reported sex differences in gene expression of stressed mice [63, 299, 463] and depressed human subjects [262]. Furthermore, this thesis contributes new knowledge which highlights critical roles for both cell type- and projection-specific HPC neurons in shaping behavioral responses to experience. All of the above have implications on the treatment of hippocampal atrophy associated with diseases like depression or Alzheimer's disease.

Developing Novel Drug Targets:

The studies in Chapter 3 elucidate cell type-specific molecular mechanisms which contribute to neurogenesis and learning and memory in mice. Neurogenesis, while confirmed in rodents and nonhuman primates, is a subject of controversy in humans. SGZ cellular proliferation does occur in humans, but the contention is whether this process continues into adulthood and results in integrated neurons [207-210, 544]. However, our studies of rodent SGZ *FosB* gene expression implicate *FosB* gene products in this region in induced cell proliferation and learning and memory processes, although aberrant ΔFosB expression is linked to cognitive decline [314, 315, 337]. Taken together, this suggests that *FosB* expression in specific cells is critical for normal learning and memory. ΔFosB accumulation in the dHPC results in a number of downstream changes in gene expression, including epigenetic alterations at target genes. Of note is histone deacetylation at the *Calb1* gene, a calcium binding protein and marker of mature neurons [314, 315, 371, 372], whose regulation by ΔFosB may be critical for the altered neurogenesis seen in *FosB* SGZ knockout. *Calb1* expression governs neuronal maturation and cell survival [209, 502]. Although manipulation of the *FosB* gene leads to a host of downstream targets and may thus be unsuitable for drug development, this suggests manipulation of specific ΔFosB downstream targets like *Calb1* could assist in increasing the maturation and survival of newly proliferating cells in diseases with hippocampal atrophy like Alzheimer's disease or depression.

Genomic Medicine:

Although there are sex differences in vulnerability to stress, increased vHPC-NAc activity governs stress phenotypes in both males and females ([127] and Chapters 4 and 5).

These phenotypes, social withdrawal and anhedonia, respectively, were captured using different paradigms. However, these phenotypes are both in the domain of reducing known pleasurable behaviors and decreasing activity of this circuit in proscribed ways corresponds to behavioral resilience to stress in both sexes.

This suggests that there may be ways to stimulate the human brain to result in behavioral resilience, without invasive probes like DBS [210]. Indeed, non-invasive stimulation has gained traction in clinical populations using mechanisms like Transcranial Magnetic Stimulation and transcranial Direct Current Stimulation (tDCS) [545]. Although brain stimulating paradigms exist and are gaining specificity to promising effect, the involvement of neurons within the same region and cell-type contributing to different aspects of behavior shown in this thesis further complicate the implementation of regional stimulation studies. To this end, the work presented in this thesis also show that changes in gene expression are sufficient to change the excitability of specific subpopulations of interest and orchestrate affective behavior. Indeed, the development of the circuit-specific CRISPR/Cas9 system allows precision manipulation the genome in the absence of other manipulations. CRISPR/Cas9 technology has been so promising that several human embryos have been treated for disease states, although many ethical questions remain in these studies [546]. Nevertheless, genomic medicine is making strides, with the first children recently being born with genetic material from three individuals [547]. CRISPR/Cas9 tools still require thorough investigation and substantial development to ensure safe use in humans. In addition, circuit-specific manipulation of the genome currently relies upon direct injection of the brain, an inherently invasive procedure that may deter use in patients. However, human studies that access the brain for direct

therapeutic intervention produce promising results [548], and recent developments in viral vector compatibility and precise delivery [549, 550] suggest that circuit-specific genomic medicine could become a reality. Altogether, the CRISPR/Cas9 manipulations developed in this thesis represent a novel mechanism for circuit-specific genome manipulation and may be able to shape human behavior in precise ways not currently available in the clinic.

LITERATURE CITED

LITERATURE CITED

1. Kessler, R.C., et al., *Lifetime prevalence and age-of-onset distributions of DSM-IV disorders in the National Comorbidity Survey Replication.* Archives of general psychiatry, 2005. **62**: p. 593-602.

2. Kessler, R.C., et al., *Anxious and non-anxious major depressive disorder in the World Health Organization World Mental Health Surveys.* Epidemiol Psychiatr Sci, 2015. **24**(3): p. 210-26.

3. Auerbach, R.P., et al., *WHO World Mental Health Surveys International College Student Project: Prevalence and distribution of mental disorders.* J Abnorm Psychol, 2018. **127**(7): p. 623-638.

4. Ewens, E.F.W., *Six Cases of Melancholic Stupor.* Ind Med Gaz, 1902. **37**(10): p. 381-385.

5. Maclachlan, J.T., *Clinical Essays on Insanity: I. Melancholic, Maniacal, and Demented States.* Glasgow Med J, 1897. **47**(1): p. 11-18.

6. Jiang, X., et al., *BDNF variation and mood disorders: a novel functional promoter polymorphism and Val66Met are associated with anxiety but have opposing effects.* Neuropsychopharmacology, 2005. **30**(7): p. 1353-61.

7. Kohli, M.A., et al., *The neuronal transporter gene SLC6A15 confers risk to major depression.* Neuron, 2011. **70**(2): p. 252-65.

8. Tolentino, J.C. and S.L. Schmidt, *DSM-5 Criteria and Depression Severity: Implications for Clinical Practice.* Front Psychiatry, 2018. **9**: p. 450.

9. Barlow, D.H., et al., *Co-morbidity and depression among the anxiety disorders. Issues in diagnosis and classification.* J Nerv Ment Dis, 1986. **174**(2): p. 63-72.

10. Pelicier, Y., *[SEROTONIN AND PSYCHIATRY].* Pathol Biol, 1964. **12**: p. 1107-9.

11. Tissot, R., *The common pathophysiology of monaminergic psychoses: a new hypothesis.* Neuropsychobiology, 1975. **1**(4): p. 243-60.

12. Vetulani, J. and F. Sulser, *Action of various antidepressant treatments reduces reactivity of noradrenergic cyclic AMP-generating system in limbic forebrain.* Nature, 1975. **257**(5526): p. 495-6.

13. Sulser, F., J. Vetulani, and P.L. Mobley, *Mode of action of antidepressant drugs.* Biochem Pharmacol, 1978. **27**(3): p. 257-61.

14. Charney, D.S., D.B. Menkes, and G.R. Heninger, *Receptor sensitivity and the mechanism of action of antidepressant treatment. Implications for the etiology and therapy of depression.* Arch Gen Psychiatry, 1981. **38**(10): p. 1160-80.

15. Duman, R.S., *Neurobiology of stress, depression, and rapid acting antidepressants: remodeling synaptic connections.* Depress Anxiety, 2014. **31**(4): p. 291-6.

16. Holtzheimer, P.E. and H.S. Mayberg, *Stuck in a rut: rethinking depression and its treatment.* Trends Neurosci, 2011. **34**(1): p. 1-9.

17. Kendler, K.S., L.M. Karkowski, and C.A. Prescott, *Causal relationship between stressful life events and the onset of major depression.* Am J Psychiatry, 1999. **156**(6): p. 837-41.

18. Kilpatrick, D.G., et al., *National estimates of exposure to traumatic events and PTSD prevalence using DSM-IV and DSM-5 criteria.* Journal of traumatic stress, 2013. **26**(5): p. 537-547.

19. Charney, D.S., *Psychobiological mechanisms of resilience and vulnerability: implications for successful adaptation to extreme stress.* Am J Psychiatry, 2004. **161**(2): p. 195-216.

20. Andermann, L., *Culture and the social construction of gender: mapping the intersection with mental health.* Int Rev Psychiatry, 2010. **22**(5): p. 501-12.

21. Roberts, T., et al., *Factors associated with health service utilisation for common mental disorders: a systematic review.* BMC Psychiatry, 2018. **18**(1): p. 262.

22. Laman-Maharg, A. and B.C. Trainor, *Stress, sex, and motivated behaviors.* J Neurosci Res, 2017. **95**(1-2): p. 83-92.

23. Ma, L., et al., *What do we know about sex differences in depression: A review of animal models and potential mechanisms.* Prog Neuropsychopharmacol Biol Psychiatry, 2019. **89**: p. 48-56.

24. LeGates, T.A., M.D. Kvarta, and S.M. Thompson, *Sex differences in antidepressant efficacy.* Neuropsychopharmacology, 2019. **44**(1): p. 140-154.

25. Deecher, D., et al., *From menarche to menopause: exploring the underlying biology of depression in women experiencing hormonal changes.* Psychoneuroendocrinology, 2008. **33**(1): p. 3-17.

26. Gobinath, A.R., R. Mahmoud, and L.A. Galea, *Influence of sex and stress exposure across the lifespan on endophenotypes of depression: focus on behavior, glucocorticoids, and hippocampus.* Front Neurosci, 2014. **8**: p. 420.

27. Bromberger, J.T. and C.N. Epperson, *Depression During and After the Perimenopause: Impact of Hormones, Genetics, and Environmental Determinants of Disease.* Obstet Gynecol Clin North Am, 2018. **45**(4): p. 663-678.

28. Stickel, S., et al., *Neural correlates of depression in women across the reproductive lifespan - An fMRI review.* J Affect Disord, 2018. **246**: p. 556-570.

29. Wang, H., et al., *Age at Onset of Puberty and Adolescent Depression: "Children of 1997" Birth Cohort.* Pediatrics, 2016. **137**(6).

30. Walther, A., J. Breidenstein, and R. Miller, *Association of Testosterone Treatment With Alleviation of Depressive Symptoms in Men: A Systematic Review and Meta-analysis.* JAMA Psychiatry, 2019. **76**(1): p. 31-40.

31. McKinney, W.T., *Animal models of depression: an overview.* Psychiatr Dev, 1984. **2**(2): p. 77-96.

32. O'Leary, O.F. and J.F. Cryan, *Towards translational rodent models of depression.* Cell Tissue Res, 2013. **354**(1): p. 141-53.

33. Foy, M.R., et al., *Behavioral stress impairs long-term potentiation in rodent hippocampus.* Behav Neural Biol, 1987. **48**(1): p. 138-49.

34. Uno, H., et al., *Hippocampal damage associated with prolonged and fatal stress in primates.* J Neurosci, 1989. **9**(5): p. 1705-11.

35. Kudryavtseva, N.N., I.V. Bakshtanovskaya, and L.a. Koryakina, *Social model of depression in mice of C57BL/6J strain.* Pharmacology, biochemistry, and behavior, 1991. **38**(2): p. 315-320.

36. Watanabe, Y., E. Gould, and B.S. McEwen, *Stress induces atrophy of apical dendrites of hippocampal CA3 pyramidal neurons.* Brain Research, 1992. **588**(2): p. 341-345.

37. Takahashi, A., et al., *Establishment of a repeated social defeat stress model in female mice.* Sci Rep, 2017. **7**(1): p. 12838.

38. Sial, O.K., et al., *Vicarious social defeat stress: Bridging the gap between physical and emotional stress.* J Neurosci Methods, 2016. **258**: p. 94-103.

39. Riggs LM, A.J., Hernandez M, Flores-Ramirez FJ, Iñiguez SD. , *Witness defeat: A novel animal model of vicarious stress-induced depression in female c57bl/6 mice.* Poster. International Behavioral Neuroscience Society (IBNS), Victoria, Canada., 2015.

40. Pelton, G.H., Y. Lee, and M. Davis, *Repeated stress, like vasopressin, sensitizes the excitatory effects of corticotropin releasing factor on the acoustic startle reflex.* Brain Res, 1997. **778**(2): p. 381-7.

41. Kuroda, Y. and B.S. McEwen, *Effect of chronic restraint stress and tianeptine on growth factors, growth-associated protein-43 and microtubule-associated protein 2 mRNA expression in the rat hippocampus.* Brain Res Mol Brain Res, 1998. **59**(1): p. 35-9.

42. Bourke, C.H. and G.N. Neigh, *Exposure to repeated maternal aggression induces depressive-like behavior and increases startle in adult female rats.* Behav Brain Res, 2012. **227**(1): p. 270-5.

43. Perrine, S.A., et al., *Severe, multimodal stress exposure induces PTSD-like characteristics in a mouse model of single prolonged stress.* Behav Brain Res, 2016. **303**: p. 228-37.

44. LaPlant, Q., et al., *Role of Nuclear Factor κB in Ovarian Hormone-Mediated Stress Hypersensitivity in Female Mice.* Biological psychiatry, 2009. **65**(10): p. 874-880.

45. LeGates, T.A., et al., *Reward behaviour is regulated by the strength of hippocampus-nucleus accumbens synapses.* Nature, 2018. **564**(7735): p. 258-262.

46. Berton, O., et al., *Essential role of BDNF in the mesolimbic dopamine pathway in social defeat stress.* Science, 2006. **311**(5762): p. 864-8.

47. Alfonso, J., et al., *Regulation of hippocampal gene expression is conserved in two species subjected to different stressors and antidepressant treatments.* Biol Psychiatry, 2006. **59**(3): p. 244-51.

48. Miczek, K.a., et al., *Escalated or suppressed cocaine reward, tegmental BDNF, and accumbal dopamine caused by episodic versus continuous social stress in rats.* The Journal of neuroscience : the official journal of the Society for Neuroscience, 2011. **31**(27): p. 9848-57.

49. Trainor, B.C., et al., *Sex Differences in Social Interaction Behavior Following Social Defeat Stress in the Monogamous California Mouse (Peromyscus californicus).* 2011. **6**(2).

50. Markham, C.M., S.L. Taylor, and K.L. Huhman, *Role of amygdala and hippocampus in the neural circuit subserving conditioned defeat in Syrian hamsters.* Learn Mem, 2010. **17**(2): p. 109-16.

51. Björkqvist, K., *Social defeat as a stressor in humans.* Physiology and Behavior, 2001. **73**(3): p. 435-442.

52. Powers, S.I., et al., *Depression and anxiety predict sex-specific cortisol responses to interpersonal stress.* Psychoneuroendocrinology, 2016. **69**: p. 172-9.

53. Krishnan, V., et al., *Molecular Adaptations Underlying Susceptibility and Resistance to Social Defeat in Brain Reward Regions.* Cell, 2007. **131**(2): p. 391-404.

54. Greenberg, G.D., et al., *Effects of social defeat on dopamine neurons in the ventral tegmental area in male and female California mice.* Eur J Neurosci, 2015. **42**(12): p. 3081-94.

55. Warren, B.L., et al., *Neurobiological sequelae of witnessing stressful events in adult mice.* Biol Psychiatry, 2013. **73**(1): p. 7-14.

56. Palanza, P., *Animal models of anxiety and depression: how are females different?* Neurosci Biobehav Rev, 2001. **25**(3): p. 219-33.

57. Beery, A.K. and I. Zucker, *Sex bias in neuroscience and biomedical research.* Neurosci Biobehav Rev, 2011. **35**(3): p. 565-72.

58. Harris, A.Z., et al., *A Novel Method for Chronic Social Defeat Stress in Female Mice.* Neuropsychopharmacology, 2018. **43**(6): p. 1276-1283.

59. Lin, D., et al., *Functional identification of an aggression locus in the mouse hypothalamus.* Nature, 2011. **470**(7333): p. 221-226.

60. Newman, E.L., et al., *Fighting Females: Neural and Behavioral Consequences of Social Defeat Stress in Female Mice.* Biol Psychiatry, 2019.

61. Willner, P., et al., *Reduction of sucrose preference by chronic unpredictable mild stress, and its restoration by a tricyclic antidepressant.* Psychopharmacology (Berl), 1987. **93**(3): p. 358-64.

62. Maras, P.M., et al., *Preferential loss of dorsal-hippocampus synapses underlies memory impairments provoked by short, multimodal stress.* Molecular Psychiatry, 2014. **19**: p. 811.

63. Hodes, G.E., et al., *Sex Differences in Nucleus Accumbens Transcriptome Profiles Associated with Susceptibility versus Resilience to Subchronic Variable Stress.* J Neurosci, 2015. **35**(50): p. 16362-76.

64. Lorsch, Z.S., et al., *Estrogen receptor alpha drives pro-resilient transcription in mouse models of depression.* Nat Commun, 2018. **9**(1): p. 1116.

65. Zhang, S., et al., *Sex Differences in the Neuroadaptations of Reward-related Circuits in Response to Subchronic Variable Stress.* Neuroscience, 2018. **376**: p. 108-116.

66. Selye, H., *The evolution of the stress concept.* Am Sci, 1973. **61**(6): p. 692-9.

67. Wehrwein, E.A., H.S. Orer, and S.M. Barman, *Overview of the Anatomy, Physiology, and Pharmacology of the Autonomic Nervous System.* Comprehensive Physiology, 2016.

68. Chrousos, G.P., *Stress and disorders of the stress system.* Nature Reviews Endocrinology, 2009. **5**: p. 374.

69. Droste, S.K., et al., *Corticosterone Levels in the Brain Show a Distinct Ultradian Rhythm but a Delayed Response to Forced Swim Stress.* Endocrinology, 2008. **149**(7): p. 3244-3253.

70. Ulrich-Lai, Y.M. and J.P. Herman, *Neural Regulation of Endocrine and Autonomic Stress Responses.* Nature Reviews Neuroscience, 2009. **10**: p. 397.

71. McEwen, B.S., *Physiology and Neurobiology of Stress and Adaptation: Central Role of the Brain.* Physiological Reviews, 2007. **87**(3): p. 873-904.

72. McEwen, B.S., et al., *Mechanisms of stress in the brain.* Nat Neurosci, 2015. **18**(10): p. 1353-63.

73. McEwen, B.S. and J.H. Morrison, *The brain on stress: vulnerability and plasticity of the prefrontal cortex over the life course.* Neuron, 2013. **79**(1): p. 16-29.

74. Myers, B., et al., *Ascending mechanisms of stress integration: Implications for brainstem regulation of neuroendocrine and behavioral stress responses.* Neurosci Biobehav Rev, 2017. **74**(Pt B): p. 366-375.

75. Haines, D.E., ed. *Fundamental Neuroscience for Basic and Clinical Applications*. 4 ed. 2013, Elsevier/Saunders. 504.

76. Charmandari, E., C. Tsigos, and G. Chrousos, *Endocrinology of the Stress Response.* Annual Review of Physiology, 2005. **67**(1): p. 259-284.

77. Sapolsky, R.M., L.M. Romero, and A.U. Munck, *How Do Glucocorticoids Influence Stress Responses? Integrating Permissive, Suppressive, Stimulatory, and Preparative Actions*.* Endocrine Reviews, 2000. **21**(1): p. 55-89.

78. Grad, I. and D. Picard, *The glucocorticoid responses are shaped by molecular chaperones.* Mol Cell Endocrinol, 2007. **275**(1-2): p. 2-12.

79. Zalachoras, I., R. Houtman, and O.C. Meijer, *Understanding stress-effects in the brain via transcriptional signal transduction pathways.* Neuroscience, 2013. **242**: p. 97-109.

80. Calfa, G., et al., *Characterization and functional significance of glucocorticoid receptors in patients with major depression: modulation by antidepressant treatment.* Psychoneuroendocrinology, 2003. **28**(5): p. 687-701.

81. O'Keane, V., T. Frodl, and T.G. Dinan, *A review of Atypical depression in relation to the course of depression and changes in HPA axis organization.* Psychoneuroendocrinology, 2012. **37**(10): p. 1589-99.

82. Owens, M.J. and C.B. Nemeroff, *The role of corticotropin-releasing factor in the pathophysiology of affective and anxiety disorders: laboratory and clinical studies.* Ciba Found Symp, 1993. **172**: p. 296-308; discussion 308-16.

83. Mason, J.W., et al., *Urinary free-cortisol levels in posttraumatic stress disorder patients.* J Nerv Ment Dis, 1986. **174**(3): p. 145-9.

84. Yehuda, R., et al., *The ACTH response to dexamethasone in PTSD.* Am J Psychiatry, 2004. **161**(8): p. 1397-403.

85. Yehuda, R., et al., *Enhanced sensitivity to glucocorticoids in peripheral mononuclear leukocytes in posttraumatic stress disorder.* Biol Psychiatry, 2004. **55**(11): p. 1110-6.

86. Elnazer, H.Y. and D.S. Baldwin, *Investigation of cortisol levels in patients with anxiety disorders: a structured review.* Curr Top Behav Neurosci, 2014. **18**: p. 191-216.

87. Fischer, S. and U. Ehlert, *Hypothalamic-pituitary-thyroid (HPT) axis functioning in anxiety disorders. A systematic review.* Depress Anxiety, 2018. **35**(1): p. 98-110.

88. Patel, P.D., et al., *Glucocorticoid and mineralocorticoid receptor mRNA expression in squirrel monkey brain.* Journal of Psychiatric Research, 2000. **34**(6): p. 383-392.

89. Sousa, R.J., N.H. Tannery, and E.M. Lafer, *In situ hybridization mapping of glucocorticoid receptor messenger ribonucleic acid in rat brain.* Molecular Endocrinology, 1989. **3**(3): p. 481-494.

90. Rodrigues, S.M., J.E. LeDoux, and R.M. Sapolsky, *The Influence of Stress Hormones on Fear Circuitry.* Annual Review of Neuroscience, 2009. **32**(1): p. 289-313.

91. Sapolsky, R.M., *Stress and Plasticity in the Limbic System.* Neurochemical Research, 2003. **28**(11): p. 1735-1742.

92. Nestler, E.J. and W.a. Carlezon, *The Mesolimbic Dopamine Reward Circuit in Depression.* Biological Psychiatry, 2006. **59**(12): p. 1151-1159.

93. Nestler, E.J., *Role of the Brain's Reward Circuitry in Depression: Transcriptional Mechanisms.* Int Rev Neurobiol, 2015. **124**: p. 151-70.

94. Mac, L.P., *Psychosomatic disease and the visceral brain; recent developments bearing on the Papez theory of emotion.* Psychosom Med, 1949. **11**(6): p. 338-53.

95. Papez, J.W., *A proposed mechanism of emotion. 1937.* J Neuropsychiatry Clin Neurosci, 1995. **7**(1): p. 103-12.

96. Gerfen, C.R., et al., *D1 and D2 dopamine receptor-regulated gene expression of striatonigral and striatopallidal neurons.* Science, 1990. **250**(4986): p. 1429-32.

97. Robison, A.J. and E.J. Nestler, *Translational and Epigenetic Mechanisms of Addiction.* 2012. **12**(11): p. 623-637.

98. Clark, D. and F.J. White, *D1 dopamine receptor—the search for a function: a critical evaluation of the D1/D2 dopamine receptor classification and its functional implications.* Synapse, 1987. **1**(4): p. 347-388.

99. Mangiavacchi, S. and M.E. Wolf, *D1 dopamine receptor stimulation increases the rate of AMPA receptor insertion onto the surface of cultured nucleus accumbens neurons through a pathway dependent on protein kinase A.* J Neurochem, 2004. **88**(5): p. 1261-71.

100. Self, D.W. and E.J. Nestler, *Molecular mechanisms of drug reinforcement and addiction.* Annu Rev Neurosci, 1995. **18**: p. 463-95.

101. Nicola, S.M. and R.C. Malenka, *Dopamine depresses excitatory and inhibitory synaptic transmission by distinct mechanisms in the nucleus accumbens.* J Neurosci, 1997. **17**(15): p. 5697-710.

102. Higley, M.J. and B.L. Sabatini, *Competitive regulation of synaptic Ca2+ influx by D2 dopamine and A2A adenosine receptors.* Nat Neurosci, 2010. **13**(8): p. 958-66.

103. Cooper, S., A.J. Robison, and M.S. Mazei-Robison, *Reward Circuitry in Addiction.* Neurotherapeutics, 2017. **14**(3): p. 687-697.

104. Kupchik, Y.M., et al., *Coding the direct/indirect pathways by D1 and D2 receptors is not valid for accumbens projections.* Nat Neurosci, 2015. **18**(9): p. 1230-2.

105. Yang, H., et al., *Nucleus Accumbens Subnuclei Regulate Motivated Behavior via Direct Inhibition and Disinhibition of VTA Dopamine Subpopulations.* Neuron, 2018. **97**(2): p. 434-449.e4.

106. Lammel, S., et al., *Input-specific control of reward and aversion in the ventral tegmental area.* Nature, 2012. **491**(7423): p. 212-7.

107. Lammel, S., B.K. Lim, and R.C. Malenka, *Reward and aversion in a heterogeneous midbrain dopamine system.* Neuropharmacology, 2014. **76 Pt B**: p. 351-9.

108. Pascoli, V., et al., *Sufficiency of Mesolimbic Dopamine Neuron Stimulation for the Progression to Addiction.* Neuron, 2015. **88**(5): p. 1054-1066.

109. Klawonn, A.M. and R.C. Malenka, *Nucleus Accumbens Modulation in Reward and Aversion.* Cold Spring Harb Symp Quant Biol, 2019.

110. Root, D.H., et al., *The ventral pallidum: Subregion-specific functional anatomy and roles in motivated behaviors.* Prog Neurobiol, 2015. **130**: p. 29-70.

111. Wulff, A.B., et al., *Ventral pallidal modulation of aversion processing.* Brain Research, 2019. **1713**: p. 62-69.

112. Bock, R., et al., *Strengthening the accumbal indirect pathway promotes resilience to compulsive cocaine use.* Nat Neurosci, 2013. **16**(5): p. 632-8.

113. Creed, M., et al., *Convergence of Reinforcing and Anhedonic Cocaine Effects in the Ventral Pallidum.* Neuron, 2016. **92**(1): p. 214-226.

114. Francis, T.C., et al., *Nucleus accumbens medium spiny neuron subtypes mediate depression-related outcomes to social defeat stress.* Biol Psychiatry, 2015. **77**(3): p. 212-222.

115. Gallo, E.F., et al., *Accumbens dopamine D2 receptors increase motivation by decreasing inhibitory transmission to the ventral pallidum.* Nat Commun, 2018. **9**(1): p. 1086.

116. Faure, A., et al., *Mesolimbic dopamine in desire and dread: enabling motivation to be generated by localized glutamate disruptions in nucleus accumbens.* J Neurosci, 2008. **28**(28): p. 7184-92.

117. Cao, J.L., et al., *Mesolimbic dopamine neurons in the brain reward circuit mediate susceptibility to social defeat and antidepressant action.* J Neurosci, 2010. **30**(49): p. 16453-8.

118. Friedman, A.K., et al., *KCNQ channel openers reverse depressive symptoms via an active resilience mechanism.* Nat Commun, 2016. **7**: p. 11671.

119. Parkinson, J.A., et al., *Disconnection of the anterior cingulate cortex and nucleus accumbens core impairs Pavlovian approach behavior: further evidence for limbic cortical-ventral striatopallidal systems.* Behav Neurosci, 2000. **114**(1): p. 42-63.

120. Di Ciano, P., et al., *Differential involvement of NMDA, AMPA/kainate, and dopamine receptors in the nucleus accumbens core in the acquisition and performance of pavlovian approach behavior.* J Neurosci, 2001. **21**(23): p. 9471-7.

121. Salamone, J.D. and M. Correa, *The mysterious motivational functions of mesolimbic dopamine.* Neuron, 2012. **76**(3): p. 470-85.

122. Gal, G., D. Schiller, and I. Weiner, *Latent inhibition is disrupted by nucleus accumbens shell lesion but is abnormally persistent following entire nucleus accumbens lesion: The neural site controlling the expression and disruption of the stimulus preexposure effect.* Behav Brain Res, 2005. **162**(2): p. 246-55.

123. Floresco, S.B., et al., *Dissociable roles for the nucleus accumbens core and shell in regulating set shifting.* J Neurosci, 2006. **26**(9): p. 2449-57.

124. Francis, T.C., et al., *Molecular basis of dendritic atrophy and activity in stress susceptibility.* Mol Psychiatry, 2017. **22**(11): p. 1512-1519.

125. Campioni, M.R., M. Xu, and D.S. McGehee, *Stress-induced changes in nucleus accumbens glutamate synaptic plasticity.* J Neurophysiol, 2009. **101**(6): p. 3192-8.

126. Lim, B.K., et al., *Anhedonia requires MC4R-mediated synaptic adaptations in nucleus accumbens.* Nature, 2012. **487**(7406): p. 183-9.

127. Bagot, R.C., et al., *Ventral hippocampal afferents to the nucleus accumbens regulate susceptibility to depression.* Nat Commun, 2015. **6**: p. 7062.

128. Muir, J., et al., *In Vivo Fiber Photometry Reveals Signature of Future Stress Susceptibility in Nucleus Accumbens.* Neuropsychopharmacology, 2018. **43**(2): p. 255-263.

129. Britt, J.P., et al., *Synaptic and behavioral profile of multiple glutamatergic inputs to the nucleus accumbens.* Neuron, 2012. **76**(4): p. 790-803.

130. Li, Z., et al., *Cell-Type-Specific Afferent Innervation of the Nucleus Accumbens Core and Shell.* Front Neuroanat, 2018. **12**: p. 84.

131. Holland, P.C. and M. Gallagher, *Amygdala circuitry in attentional and representational processes.* Trends Cogn Sci, 1999. **3**(2): p. 65-73.

132. Balleine, B.W. and S. Killcross, *Parallel incentive processing: an integrated view of amygdala function.* Trends Neurosci, 2006. **29**(5): p. 272-9.

133. Weiskrantz, L., *Behavioral changes associated with ablation of the amygdaloid complex in monkeys.* J Comp Physiol Psychol, 1956. **49**(4): p. 381-91.

134. Orsini, C.A. and S. Maren, *Neural and cellular mechanisms of fear and extinction memory formation.* Neurosci Biobehav Rev, 2012. **36**(7): p. 1773-802.

135. Stuber, G.D., J.P. Britt, and A. Bonci, *Optogenetic modulation of neural circuits that underlie reward seeking.* Biol Psychiatry, 2012. **71**(12): p. 1061-7.

136. Janak, P.H. and K.M. Tye, *From circuits to behaviour in the amygdala.* Nature, 2015. **517**(7534): p. 284-92.

137. Gill, K.M. and A.A. Grace, *Heterogeneous processing of amygdala and hippocampal inputs in the rostral and caudal subregions of the nucleus accumbens.* Int J Neuropsychopharmacol, 2011. **14**(10): p. 1301-14.

138. Maren, S. and M.S. Fanselow, *Synaptic plasticity in the basolateral amygdala induced by hippocampal formation stimulation in vivo.* J Neurosci, 1995. **15**(11): p. 7548-64.

139. Biedenkapp, J.C. and J.W. Rudy, *Hippocampal and extrahippocampal systems compete for control of contextual fear: role of ventral subiculum and amygdala.* Learn Mem, 2009. **16**(1): p. 38-45.

140. Pitkanen, A., et al., *Reciprocal connections between the amygdala and the hippocampal formation, perirhinal cortex, and postrhinal cortex in rat. A review.* Ann N Y Acad Sci, 2000. **911**: p. 369-91.

141. Richardson, M.P., B.A. Strange, and R.J. Dolan, *Encoding of emotional memories depends on amygdala and hippocampus and their interactions.* Nat Neurosci, 2004. **7**(3): p. 278-85.

142. Felix-Ortiz, A.C. and K.M. Tye, *Amygdala inputs to the ventral hippocampus bidirectionally modulate social behavior.* J Neurosci, 2014. **34**(2): p. 586-95.

143. Felix-Ortiz, A.C., et al., *BLA to vHPC inputs modulate anxiety-related behaviors.* Neuron, 2013. **79**(4): p. 658-64.

144. Beyeler, A., et al., *Organization of Valence-Encoding and Projection-Defined Neurons in the Basolateral Amygdala.* Cell Rep, 2018. **22**(4): p. 905-918.

145. Zhang, J.Y., et al., *Chronic Stress Remodels Synapses in an Amygdala Circuit-Specific Manner.* Biol Psychiatry, 2019. **85**(3): p. 189-201.

146. Ortiz, S., et al., *Anterior cingulate cortex and ventral hippocampal inputs to the basolateral amygdala selectively control generalized fear.* J Neurosci, 2019.

147. Bian, X.L., et al., *Anterior Cingulate Cortex to Ventral Hippocampus Circuit Mediates Contextual Fear Generalization.* J Neurosci, 2019. **39**(29): p. 5728-5739.

148. Carlen, M., *What constitutes the prefrontal cortex?* Science, 2017. **358**(6362): p. 478-482.

149. Sesack, S.R. and A.A. Grace, *Cortico-Basal Ganglia reward network: microcircuitry.* Neuropsychopharmacology, 2010. **35**(1): p. 27-47.

150. Kalivas, P.W., N. Volkow, and J. Seamans, *Unmanageable motivation in addiction: a pathology in prefrontal-accumbens glutamate transmission.* Neuron, 2005. **45**(5): p. 647-50.

151. Liu, X. and A.G. Carter, *Ventral Hippocampal Inputs Preferentially Drive Corticocortical Neurons in the Infralimbic Prefrontal Cortex.* J Neurosci, 2018. **38**(33): p. 7351-7363.

152. Sotres-Bayon, F., et al., *Gating of fear in prelimbic cortex by hippocampal and amygdala inputs.* Neuron, 2012. **76**(4): p. 804-12.

153. Milner, B. and W. Penfield, *The effect of hippocampal lesions on recent memory.* Trans Am Neurol Assoc, 1955(80th Meeting): p. 42-8.

154. Penfield, W. and B. Milner, *Memory deficit produced by bilateral lesions in the hippocampal zone.* AMA Arch Neurol Psychiatry, 1958. **79**(5): p. 475-97.

155. Squire, L.R. and S. Zola-Morgan, *The neuropsychology of memory: new links between humans and experimental animals.* Ann N Y Acad Sci, 1985. **444**: p. 137-49.

156. Squire, L.R., *Mechanisms of memory.* Science, 1986. **232**(4758): p. 1612-9.

157. Deadwyler, S.A., T.C. Foster, and R.E. Hampson, *Processing of sensory information in the hippocampus.* CRC Crit Rev Clin Neurobiol, 1987. **2**(4): p. 335-55.

158. Burgess, N., E.A. Maguire, and J. O'Keefe, *The human hippocampus and spatial and episodic memory.* Neuron, 2002. **35**(4): p. 625-41.

159. Ranganath, C., *A unified framework for the functional organization of the medial temporal lobes and the phenomenology of episodic memory.* Hippocampus, 2010. **20**(11): p. 1263-90.

160. Eichenbaum, H., A.P. Yonelinas, and C. Ranganath, *The medial temporal lobe and recognition memory.* Annu Rev Neurosci, 2007. **30**: p. 123-52.

161. Diana, R.A., A.P. Yonelinas, and C. Ranganath, *Imaging recollection and familiarity in the medial temporal lobe: a three-component model.* Trends Cogn Sci, 2007. **11**(9): p. 379-86.

162. Amaral, D.G. and M.P. Witter, *The three-dimensional organization of the hippocampal formation: a review of anatomical data.* Neuroscience, 1989. **31**(3): p. 571-91.

163. Andersen, P., T.V. Bliss, and K.K. Skrede, *Lamellar organization of hippocampal pathways.* Exp Brain Res, 1971. **13**(2): p. 222-38.

164. Nguyen, P.V., T. Abel, and E.R. Kandel, *Requirement of a critical period of transcription for induction of a late phase of LTP.* Science, 1994. **265**(5175): p. 1104-7.

165. Nguyen, P.V. and E.R. Kandel, *A macromolecular synthesis-dependent late phase of long-term potentiation requiring cAMP in the medial perforant pathway of rat hippocampal slices.* J Neurosci, 1996. **16**(10): p. 3189-98.

166. Rubin, A., et al., *Hippocampal ensemble dynamics timestamp events in long-term memory.* Elife, 2015. **4**.

167. Levy, W.B. and O. Steward, *Temporal contiguity requirements for long-term associative potentiation/depression in the hippocampus.* Neuroscience, 1983. **8**(4): p. 791-7.

168. Goelet, P., et al., *The long and the short of long-term memory--a molecular framework.* Nature, 1986. **322**(6078): p. 419-22.

169. Eccles, J.C., *Mechanisms of long-term memory.* J Physiol (Paris), 1986. **81**(4): p. 312-7.

170. Squire, L.R. and S.H. Barondes, *Actinomycin-D: effects on memory at different times after training.* Nature, 1970. **225**(5233): p. 649-50.

171. Squire, L.R., S.S. John, and H.P. Davis, *Inhibitors of protein synthesis and memory: dissociation of amnesic effects and effects on adrenal steroidogenesis.* Brain Res, 1976. **112**(1): p. 200-6.

172. Bear, M.F., *Mechanism for a sliding synaptic modification threshold.* Neuron, 1995. **15**(1): p. 1-4.

173. Lynch, G., et al., *Intracellular injections of EGTA block induction of hippocampal long-term potentiation.* Nature, 1983. **305**(5936): p. 719-21.

174. Lynch, D.R. and R.P. Guttmann, *NMDA receptor pharmacology: perspectives from molecular biology.* Curr Drug Targets, 2001. **2**(3): p. 215-31.

175. Banke, T.G., et al., *Control of GluR1 AMPA receptor function by cAMP-dependent protein kinase.* J Neurosci, 2000. **20**(1): p. 89-102.

176. Matamales, M. and J.A. Girault, *Signaling from the cytoplasm to the nucleus in striatal medium-sized spiny neurons.* Front Neuroanat, 2011. **5**: p. 37.

177. Bading, H., D.D. Ginty, and M.E. Greenberg, *Regulation of gene expression in hippocampal neurons by distinct calcium signaling pathways.* Science, 1993. **260**(5105): p. 181-6.

178. Bekinschtein, P., et al., *Persistence of long-term memory storage requires a late protein synthesis- and BDNF- dependent phase in the hippocampus.* Neuron, 2007. **53**(2): p. 261-77.

179. Bito, H., K. Deisseroth, and R.W. Tsien, *CREB phosphorylation and dephosphorylation: a Ca(2+)- and stimulus duration-dependent switch for hippocampal gene expression.* Cell, 1996. **87**(7): p. 1203-14.

180. Bourtchuladze, R., et al., *Deficient long-term memory in mice with a targeted mutation of the cAMP-responsive element-binding protein.* Cell, 1994. **79**(1): p. 59-68.

181. Cammarota, M., et al., *Learning-associated activation of nuclear MAPK, CREB and Elk-1, along with Fos production, in the rat hippocampus after a one-trial avoidance learning: abolition by NMDA receptor blockade.* Brain Res Mol Brain Res, 2000. **76**(1): p. 36-46.

182. Davis, S., et al., *The MAPK/ERK cascade targets both Elk-1 and cAMP response element-binding protein to control long-term potentiation-dependent gene expression in the dentate gyrus in vivo.* J Neurosci, 2000. **20**(12): p. 4563-72.

183. Frey, U., Y.Y. Huang, and E.R. Kandel, *Effects of cAMP simulate a late stage of LTP in hippocampal CA1 neurons.* Science, 1993. **260**(5114): p. 1661-4.

184. Huber, K.M., M.S. Kayser, and M.F. Bear, *Role for rapid dendritic protein synthesis in hippocampal mGluR-dependent long-term depression.* Science, 2000. **288**(5469): p. 1254-7.

185. Manahan-Vaughan, D., A. Kulla, and J.U. Frey, *Requirement of translation but not transcription for the maintenance of long-term depression in the CA1 region of freely moving rats.* J Neurosci, 2000. **20**(22): p. 8572-6.

186. Xu, L., et al., *Glucocorticoid receptor and protein/RNA synthesis-dependent mechanisms underlie the control of synaptic plasticity by stress.* Proc Natl Acad Sci U S A, 1998. **95**(6): p. 3204-8.

187. Alberini, C.M., et al., *A molecular switch for the consolidation of long-term memory: cAMP-inducible gene expression.* Ann N Y Acad Sci, 1995. **758**: p. 261-86.

188. Moser, M.B. and E.I. Moser, *Functional differentiation in the hippocampus.* Hippocampus, 1998. **8**(6): p. 608-19.

189. Fanselow, M.S. and H.-W. Dong, *Are The Dorsal and Ventral Hippocampus functionally distinct structures?* Neuron, 2010. **65**(1): p. 7-7.

190. Moser, M.B., et al., *Spatial learning with a minislab in the dorsal hippocampus.* Proc Natl Acad Sci U S A, 1995. **92**(21): p. 9697-701.

191. Jung, M.W., S.I. Wiener, and B.L. McNaughton, *Comparison of spatial firing characteristics of units in dorsal and ventral hippocampus of the rat.* J Neurosci, 1994. **14**(12): p. 7347-56.

192. Pothuizen, H.H., et al., *Dissociation of function between the dorsal and the ventral hippocampus in spatial learning abilities of the rat: a within-subject, within-task comparison of reference and working spatial memory.* Eur J Neurosci, 2004. **19**(3): p. 705-12.

193. Ramirez, S., et al., *Activating positive memory engrams suppresses depression-like behaviour.* Nature, 2015. **522**(7556): p. 335-9.

194. Bagot, R.C., et al., *Ventral hippocampal afferents to the nucleus accumbens regulate susceptibility to depression.* Nature Communications, 2015. **6**(May): p. 7062-7062.

195. Henke, P.G., *Hippocampal pathway to the amygdala and stress ulcer development.* Brain Res Bull, 1990. **25**(5): p. 691-5.

196. Anacker, C., et al., *Antidepressants increase human hippocampal neurogenesis by activating the glucocorticoid receptor.* Mol Psychiatry, 2011. **16**(7): p. 738-50.

197. Anacker, C., et al., *Neuroanatomic Differences Associated With Stress Susceptibility and Resilience.* Biol Psychiatry, 2016. **79**(10): p. 840-849.

198. Swanson, L.W. and W.M. Cowan, *An autoradiographic study of the organization of the efferent connections of the hippocampal formation in the rat.* J Comp Neurol, 1977. **172**(1): p. 49-84.

199. Cembrowski, M.S., et al., *Dissociable Structural and Functional Hippocampal Outputs via Distinct Subiculum Cell Classes.* Cell, 2018. **173**(5): p. 1280-1292.e18.

200. Tye, K.M., et al., *Amygdala circuitry mediating reversible and bidirectional control of anxiety.* Nature, 2011. **471**(7338): p. 358-62.

201. Phillipson, O.T. and A.C. Griffiths, *The topographic order of inputs to nucleus accumbens in the rat.* Neuroscience, 1985. **16**(2): p. 275-96.

202. Floresco, S.B., C.L. Todd, and a.a. Grace, *Glutamatergic afferents from the hippocampus to the nucleus accumbens regulate activity of ventral tegmental area dopamine neurons.* The Journal of neuroscience : the official journal of the Society for Neuroscience, 2001. **21**(13): p. 4915-4922.

203. Zhao, C., W. Deng, and F.H. Gage, *Mechanisms and Functional Implications of Adult Neurogenesis.* Cell, 2008. **132**(4): p. 645-660.

204. Altman, J. and G.D. Das, *Autoradiographic and histological evidence of postnatal hippocampal neurogenesis in rats.* J Comp Neurol, 1965. **124**(3): p. 319-35.

205. Lledo, P.M. and M. Valley, *Adult Olfactory Bulb Neurogenesis.* Cold Spring Harb Perspect Biol, 2016. **8**(8).

206. Ahmed, E.I., et al., *Pubertal hormones modulate the addition of new cells to sexually dimorphic brain regions.* Nat Neurosci, 2008. **11**(9): p. 995-7.

207. Paredes, M.F., et al., *Does Adult Neurogenesis Persist in the Human Hippocampus?* Cell Stem Cell, 2018. **23**(6): p. 780-781.

208. Bergmann, O., K.L. Spalding, and J. Frisen, *Adult Neurogenesis in Humans.* Cold Spring Harb Perspect Biol, 2015. **7**(7): p. a018994.

209. Eriksson, P.S., et al., *Neurogenesis in the adult human hippocampus.* Nat Med, 1998. **4**(11): p. 1313-7.

210. Sorrells, S.F., et al., *Human hippocampal neurogenesis drops sharply in children to undetectable levels in adults.* Nature, 2018. **555**(7696): p. 377-381.

211. Ge, S., et al., *Synaptic integration and plasticity of new neurons in the adult hippocampus.* J Physiol, 2008. **586**(16): p. 3759-65.

212. Ming, G.L. and H. Song, *Adult neurogenesis in the mammalian central nervous system.* Annu Rev Neurosci, 2005. **28**: p. 223-50.

213. Schoenfeld, T.J., et al., *Stress and Loss of Adult Neurogenesis Differentially Reduce Hippocampal Volume.* Biol Psychiatry, 2017. **82**(12): p. 914-923.

214. Deng, W., J.B. Aimone, and F.H. Gage, *New neurons and new memories: how does adult hippocampal neurogenesis affect learning and memory?* Nat Rev Neurosci, 2010. **11**(5): p. 339-50.

215. Danielson, N.B., et al., *Distinct Contribution of Adult-Born Hippocampal Granule Cells to Context Encoding.* Neuron, 2016. **90**(1): p. 101-12.

216. Surget, A., et al., *Antidepressants recruit new neurons to improve stress response regulation.* Mol Psychiatry, 2011. **16**(12): p. 1177-88.

217. Kitabatake, Y., et al., *Adult neurogenesis and hippocampal memory function: new cells, more plasticity, new memories?* Neurosurg Clin N Am, 2007. **18**(1): p. 105-13, x.

218. Akers, K.G., et al., *Hippocampal neurogenesis regulates forgetting during adulthood and infancy.* Science, 2014. **344**(6184): p. 598-602.

219. Epp, J.R., et al., *Neurogenesis-mediated forgetting minimizes proactive interference.* Nat Commun, 2016. **7**: p. 10838.

220. Clelland, C.D., et al., *A functional role for adult hippocampal neurogenesis in spatial pattern separation.* Science, 2009. **325**(5937): p. 210-3.

221. Sahay, A., et al., *Increasing adult hippocampal neurogenesis is sufficient to improve pattern separation.* Nature, 2011. **472**(7344): p. 466-70.

222. van Praag, H., G. Kempermann, and F.H. Gage, *Running increases cell proliferation and neurogenesis in the adult mouse dentate gyrus.* Nat Neurosci, 1999. **2**(3): p. 266-270.

223. Pemberton, R. and M.D. Fuller Tyszkiewicz, *Factors contributing to depressive mood states in everyday life: A systematic review.* J Affect Disord, 2016. **200**: p. 103-10.

224. Mul, J.D., et al., *Voluntary wheel running promotes resilience to chronic social defeat stress in mice: a role for nucleus accumbens ΔFosB .* Neuropsychopharmacology, 2018. **43**(9): p. 1934-1942.

225. Leem, Y.H., et al., *Exercise exerts an anxiolytic effect against repeated restraint stress through 5-HT2A-mediated suppression of the adenosine A2A receptor in the basolateral amygdala.* Psychoneuroendocrinology, 2019.

226. Zhang, J., et al., *Voluntary Wheel Running Reverses Deficits in Social Behavior Induced by Chronic Social Defeat Stress in Mice: Involvement of the Dopamine System.* Front Neurosci, 2019. **13**: p. 256.

227. Malberg, J.E., et al., *Chronic antidepressant treatment increases neurogenesis in adult rat hippocampus.* The Journal of neuroscience : the official journal of the Society for Neuroscience, 2000. **20**(24): p. 9104-9110.

228. Warner-Schmidt, J.L. and R.S. Duman, *Hippocampal neurogenesis: opposing effects of stress and antidepressant treatment.* Hippocampus, 2006. **16**(3): p. 239-49.

229. Santarelli, L., et al., *Requirement of hippocampal neurogenesis for the behavioral effects of antidepressants.* Science, 2003. **301**(5634): p. 805-9.

230. Snyder, J.S., et al., *Adult hippocampal neurogenesis buffers stress responses and depressive behaviour.* Nature, 2011. **476**(7361): p. 458-61.

231. Hill, A.S., A. Sahay, and R. Hen, *Increasing Adult Hippocampal Neurogenesis is Sufficient to Reduce Anxiety and Depression-Like Behaviors.* Neuropsychopharmacology, 2015: p. 1-11.

232. Boldrini, M., et al., *Antidepressants increase neural progenitor cells in the human hippocampus.* Neuropsychopharmacology, 2009. **34**(11): p. 2376-89.

233. Erickson, K.I., et al., *Exercise training increases size of hippocampus and improves memory.* Proc Natl Acad Sci U S A, 2011. **108**(7): p. 3017-22.

234. Lucassen, P.J., et al., *Regulation of adult neurogenesis by stress, sleep disruption, exercise and inflammation: Implications for depression and antidepressant action.* Eur Neuropsychopharmacol, 2010. **20**(1): p. 1-17.

235. Anacker, C., et al., *Hippocampal neurogenesis confers stress resilience by inhibiting the ventral dentate gyrus.* Nature, 2018. **559**(7712): p. 98-102.

236. Jacobson, L. and R. Sapolsky, *The role of the hippocampus in feedback regulation of the hypothalamic-pituitary-adrenocortical axis.* Endocr Rev, 1991. **12**(2): p. 118-34.

237. Klüver, H. and P.C. Bucy, *"Psychic blindness" and other symptoms following bilateral temporal lobectomy in Rhesus monkeys.* American Journal of Physiology, 1937. **119**: p. 352-353.

238. Finsterwald, C. and C.M. Alberini, *Stress and glucocorticoid receptor-dependent mechanisms in long-term memory: from adaptive responses to psychopathologies.* Neurobiol Learn Mem, 2014. **112**: p. 17-29.

239. Joëls, M. and H. Karst, *Corticosteroid effects on calcium signaling in limbic neurons.* Cell Calcium, 2012. **51**(3): p. 277-283.

240. Joëls, M., et al., *Corticosteroid effects on cellular physiology of limbic cells.* Brain Research, 2009. **1293**: p. 91-100.

241. Abercrombie, H.C., et al., *Cortisol variation in humans affects memory for emotionally laden and neutral information.* Behav Neurosci, 2003. **117**(3): p. 505-16.

242. Akirav, I., et al., *A facilitative role for corticosterone in the acquisition of a spatial task under moderate stress.* Learn Mem, 2004. **11**(2): p. 188-95.

243. Buchanan, T.W. and W.R. Lovallo, *Enhanced memory for emotional material following stress-level cortisol treatment in humans.* Psychoneuroendocrinology, 2001. **26**(3): p. 307-17.

244. Pavlides, C., L.G. Nivón, and B.S. McEwen, *Effects of chronic stress on hippocampal long-term potentiation.* Hippocampus, 2002. **12**(2): p. 245-257.

245. Nasca, C., et al., *Mind the gap: glucocorticoids modulate hippocampal glutamate tone underlying individual differences in stress susceptibility.* Mol Psychiatry, 2015. **20**(6): p. 755-63.

246. Alfarez, D.N., M. Joels, and H.J. Krugers, *Chronic unpredictable stress impairs long-term potentiation in rat hippocampal CA1 area and dentate gyrus in vitro.* Eur J Neurosci, 2003. **17**(9): p. 1928-34.

247. Karst, H. and M. Joels, *Effect of chronic stress on synaptic currents in rat hippocampal dentate gyrus neurons.* J Neurophysiol, 2003. **89**(1): p. 625-33.

248. Maggio, N. and M. Segal, *Persistent changes in ability to express long-term potentiation/depression in the rat hippocampus after juvenile/adult stress.* Biol Psychiatry, 2011. **69**(8): p. 748-53.

249. Maggio, N. and M. Segal, *Striking variations in corticosteroid modulation of long-term potentiation along the septotemporal axis of the hippocampus.* J Neurosci, 2007. **27**(21): p. 5757-65.

250. Howland, J.G. and B.N. Cazakoff, *Effects of acute stress and GluN2B-containing NMDA receptor antagonism on object and object-place recognition memory.* Neurobiol Learn Mem, 2010. **93**(2): p. 261-7.

251. Han, Q.Q., et al., *Differential GR Expression and Translocation in the Hippocampus Mediates Susceptibility vs. Resilience to Chronic Social Defeat Stress.* Front Neurosci, 2017. **11**: p. 287.

252. Bremner, J.D., et al., *MRI-based measurement of hippocampal volume in patients with combat-related posttraumatic stress disorder.* Am J Psychiatry, 1995. **152**(7): p. 973-81.

253. Hastings, R.S., et al., *Volumetric Analysis of the Prefrontal Cortex, Amygdala, and Hippocampus in Major Depression.* Neuropsychopharmacology, 2004. **29**(5): p. 952-959.

254. Frey, B.N., et al., *The role of hippocampus in the pathophysiology of bipolar disorder.* Behav Pharmacol, 2007. **18**(5-6): p. 419-30.

255. Bonne, O., et al., *Reduced posterior hippocampal volume in posttraumatic stress disorder.* J Clin Psychiatry, 2008. **69**(7): p. 1087-91.

256. Duman, R.S., J. Malberg, and J. Thome, *Neural plasticity to stress and antidepressant treatment.* Biol Psychiatry, 1999. **46**(9): p. 1181-91.

257. Duman, R.S., *Synaptic plasticity and mood disorders.* Mol Psychiatry, 2002. **7 Suppl 1**: p. S29-34.

258. Nestler, E.J., et al., *Neurobiology of depression*. 2002. p. 13--25.

259. Kyrke-Smith, M. and J.M. Williams, *Bridging Synaptic and Epigenetic Maintenance Mechanisms of the Engram.* Front Mol Neurosci, 2018. **11**: p. 369.

260. Yehuda, R., et al., *The role of genes in defining a molecular biology of PTSD.* Dis Markers, 2011. **30**(2-3): p. 67-76.

261. Dalton, V.S., E. Kolshus, and D.M. McLoughlin, *Epigenetics and depression: return of the repressed.* J Affect Disord, 2014. **155**: p. 1-12.

262. Labonte, B., et al., *Sex-specific transcriptional signatures in human depression.* Nat Med, 2017. **23**(9): p. 1102-1111.

263. Seney, M.L., et al., *Opposite Molecular Signatures of Depression in Men and Women.* Biol Psychiatry, 2018. **84**(1): p. 18-27.

264. Montpied, P., et al., *Repeated swim-stress reduces GABAA receptor alpha subunit mRNAs in the mouse hippocampus.* Brain Res Mol Brain Res, 1993. **18**(3): p. 267-72.

265. Smith, M.A., et al., *Stress and glucocorticoids affect the expression of brain-derived neurotrophic factor and neurotrophin-3 mRNAs in the hippocampus.* J Neurosci, 1995. **15**(3 Pt 1): p. 1768-77.

266. Alfonso, J., A.C. Frasch, and G. Flugge, *Chronic stress, depression and antidepressants: effects on gene transcription in the hippocampus.* Rev Neurosci, 2005. **16**(1): p. 43-56.

267. Dwivedi, Y., et al., *Reduced activation and expression of ERK1/2 MAP kinase in the post-mortem brain of depressed suicide subjects.* J Neurochem, 2001. **77**(3): p. 916-28.

268. Drigues, N., et al., *cDNA gene expression profile of rat hippocampus after chronic treatment with antidepressant drugs.* J Neural Transm (Vienna), 2003. **110**(12): p. 1413-36.

269. Dowlatshahi, D., et al., *Increased temporal cortex CREB concentrations and antidepressant treatment in major depression.* Lancet, 1998. **352**(9142): p. 1754-5.

270. Nibuya, M., E.J. Nestler, and R.S. Duman, *Chronic antidepressant administration increases the expression of cAMP response element binding protein (CREB) in rat hippocampus.* J Neurosci, 1996. **16**(7): p. 2365-72.

271. Thome, J., et al., *cAMP response element-mediated gene transcription is upregulated by chronic antidepressant treatment.* J Neurosci, 2000. **20**(11): p. 4030-6.

272. Chen, A.C., et al., *Expression of the cAMP response element binding protein (CREB) in hippocampus produces an antidepressant effect.* Biol Psychiatry, 2001. **49**(9): p. 753-62.

273. Sachs, B.D., J.R. Ni, and M.G. Caron, *Sex differences in response to chronic mild stress and congenital serotonin deficiency.* Psychoneuroendocrinology, 2014. **40**: p. 123-9.

274. Dalla, C., et al., *Sex differences in the effects of two stress paradigms on dopaminergic neurotransmission.* Physiol Behav, 2008. **93**(3): p. 595-605.

275. Kitraki, E., et al., *Spatial performance and corticosteroid receptor status in the 21-day restraint stress paradigm.* Ann N Y Acad Sci, 2004. **1018**: p. 323-7.

276. Covington, H.E., 3rd, et al., *Antidepressant actions of histone deacetylase inhibitors.* J Neurosci, 2009. **29**(37): p. 11451-60.

277. Wilkinson, M.B., et al., *Imipramine treatment and resiliency exhibit similar chromatin regulation in the mouse nucleus accumbens in depression models.* J Neurosci, 2009. **29**(24): p. 7820-32.

278. Manning, C.E., E.S. Williams, and A.J. Robison, *Reward Network Immediate Early Gene Expression in Mood Disorders.* Frontiers in Behavioral Neuroscience, 2017. **11**(77).

279. Madabhushi, R., et al., *Activity-Induced DNA Breaks Govern the Expression of Neuronal Early-Response Genes.* Cell, 2015. **161**(7): p. 1592-605.

280. Nakabeppu, Y. and D. Nathans, *A naturally occurring truncated form of FosB that inhibits Fos/Jun transcriptional activity.* Cell, 1991. **64**(4): p. 751-9.

281. Dobrazanski, P., et al., *Both products of the fosB gene, FosB and its short form, FosB/SF, are transcriptional activators in fibroblasts.* Mol Cell Biol, 1991. **11**(11): p. 5470-8.

282. Chen, J., et al., *Chronic Fos-related antigens: stable variants of ΔFosB induced in brain by chronic treatments.* The Journal of Neuroscience, 1997. **17**(13): p. 4933-4941.

283. Herdegen, T. and J.D. Leah, *Inducible and constitutive transcription factors in the mammalian nervous system: control of gene expression by Jun, Fos and Krox, and CREB/ATF proteins.* Brain Res Brain Res Rev, 1998. **28**(3): p. 370-490.

284. Perrotti, L.I., et al., *Induction of ΔFosB in reward-related brain structures after chronic stress.* J Neurosci, 2004. **24**(47): p. 10594-602.

285. Vialou, V., et al., *ΔFosB in brain reward circuits mediates resilience to stress and antidepressant responses.* Nature neuroscience, 2010. **13**(6): p. 745-752.

286. Nikulina, E.M., et al., *Intermittent social defeat stress enhances mesocorticolimbic ΔFosB/BDNF co-expression and persistently activates corticotegmental neurons: implication for vulnerability to psychostimulants.* Neuroscience, 2012. **212**: p. 38-48.

287. Hamilton, P.J., et al., *Cell-Type-Specific Epigenetic Editing at the Fosb Gene Controls Susceptibility to Social Defeat Stress.* Neuropsychopharmacology, 2018. **43**(2): p. 272-284.

288. Schreiber, S.S., et al., *Activation of immediate early genes after acute stress.* Neuroreport, 1991. **2**(1): p. 17-20.

289. Melia, K.R., et al., *Induction and habituation of immediate early gene expression in rat brain by acute and repeated restraint stress.* J Neurosci, 1994. **14**(10): p. 5929-38.

290. Nye, H.E., et al., *Pharmacological studies of the regulation of chronic FOS-related antigen induction by cocaine in the striatum and nucleus accumbens.* The Journal of pharmacology and experimental therapeutics, 1995. **275**(3): p. 1671-1680.

291. Robison, a.J., et al., *Behavioral and structural responses to chronic cocaine require a feedforward loop involving ΔFosB and calcium/calmodulin-dependent protein kinase II in the nucleus accumbens shell.* J Neurosci, 2013. **33**(10): p. 4295-4307.

292. Robison, A.J., et al., *Fluoxetine epigenetically alters the CaMKIIalpha promoter in nucleus accumbens to regulate ΔFosB binding and antidepressant effects.* Neuropsychopharmacology, 2014. **39**(5): p. 1178-86.

293. Vialou, V., et al., *Serum response factor and cAMP response element binding protein are both required for cocaine induction of ΔFosB .* J Neurosci, 2012. **32**(22): p. 7577-84.

294. Newton, S.S., et al., *Inhibition of cAMP response element-binding protein or dynorphin in the nucleus accumbens produces an antidepressant-like effect.* J Neurosci, 2002. **22**(24): p. 10883-90.

295. Barrot, M., et al., *CREB activity in the nucleus accumbens shell controls gating of behavioral responses to emotional stimuli.* Proc Natl Acad Sci U S A, 2002. **99**(17): p. 11435-40.

296. Heller, E.A., et al., *Targeted Epigenetic Remodeling of the Cdk5 Gene in Nucleus Accumbens Regulates Cocaine- and Stress-Evoked Behavior.* J Neurosci, 2016. **36**(17): p. 4690-7.

297. Kim, H.D., et al., *SIRT1 Mediates Depression-Like Behaviors in the Nucleus Accumbens.* J Neurosci, 2016. **36**(32): p. 8441-52.

298. Feng, J., et al., *Tet1 in Nucleus Accumbens Opposes Depression- and Anxiety-Like Behaviors.* Neuropsychopharmacology, 2017. **42**(8): p. 1657-1669.

299. Pfau, M.L., et al., *Integrative Analysis of Sex-Specific microRNA Networks Following Stress in Mouse Nucleus Accumbens.* Front Mol Neurosci, 2016. **9**: p. 144.

300. Bagot, R.C., et al., *Circuit-wide Transcriptional Profiling Reveals Brain Region-Specific Gene Networks Regulating Depression Susceptibility.* Neuron, 2016. **90**(5): p. 969-83.

301. Chandra, R., et al., *Reduced Slc6a15 in Nucleus Accumbens D2-Neurons Underlies Stress Susceptibility.* J Neurosci, 2017. **37**(27): p. 6527-6538.

302. Fox, M.E., et al., *Dendritic remodeling of D1 neurons by RhoA/Rho-kinase mediates depression-like behavior.* Mol Psychiatry, 2018.

303. Heshmati, M., et al., *Cell-type-specific role for nucleus accumbens neuroligin-2 in depression and stress susceptibility.* Proc Natl Acad Sci U S A, 2018. **115**(5): p. 1111-1116.

304. Lobo, M.K., et al., *ΔFosB induction in striatal medium spiny neuron subtypes in response to chronic pharmacological, emotional, and optogenetic stimuli.* J Neurosci, 2013. **33**(47): p. 18381-95.

305. Vialou, V., et al., *ΔFosB in brain reward circuits mediates resilience to stress and antidepressant responses.* Nat Neurosci, 2010. **13**(6): p. 745-52.

306. Eagle, A.L., et al., *Experience-Dependent Induction of Hippocampal ΔFosB Controls Learning.* J Neurosci, 2015. **35**(40): p. 13773-83.

307. Carle, T.L., et al., *Proteasome-dependent and -independent mechanisms for FosB destabilization: identification of FosB degron domains and implications for ΔFosB stability.* Eur J Neurosci, 2007. **25**(10): p. 3009-19.

308. Ulery-Reynolds, P.G., et al., *Phosphorylation of ΔFosB mediates its stability in vivo.* Neuroscience, 2009. **158**(2): p. 369-72.

309. Nestler, E.J., *FosB: a transcriptional regulator of stress and antidepressant responses.* Eur J Pharmacol, 2015. **753**: p. 66-72.

310. Jorissen, H.J., et al., *Dimerization and DNA-binding properties of the transcription factor ΔFosB .* Biochemistry, 2007. **46**(28): p. 8360-72.

311. McClung, C.A., et al., *ΔFosB : a molecular switch for long-term adaptation in the brain.* Brain Res Mol Brain Res, 2004. **132**(2): p. 146-54.

312. Russo, S.J., et al., *Nuclear factor kappa B signaling regulates neuronal morphology and cocaine reward.* J Neurosci, 2009. **29**(11): p. 3529-37.

313. Maze, I., et al., *Essential role of the histone methyltransferase G9a in cocaine-induced plasticity.* Science, 2010. **327**(5962): p. 213-6.

314. You, J.C., et al., *Epigenetic suppression of hippocampal calbindin-D28k by ΔFosB drives seizure-related cognitive deficits.* Nat Med, 2017. **23**(11): p. 1377-1383.

315. You, J.C., et al., *Genome-wide profiling reveals functional diversification of FosB gene targets in the hippocampus of an Alzheimer's disease mouse model.* PLoS One, 2018. **13**(2): p. e0192508.

316. Renthal, W., et al., *Delta FosB mediates epigenetic desensitization of the c-fos gene after chronic amphetamine exposure.* J Neurosci, 2008. **28**(29): p. 7344-9.

317. Kumar, A., et al., *Chromatin remodeling is a key mechanism underlying cocaine-induced plasticity in striatum.* Neuron, 2005. **48**(2): p. 303-14.

318. Hiroi, N., et al., *Essential role of the fosB gene in molecular, cellular, and behavioral actions of chronic electroconvulsive seizures.* J Neurosci, 1998. **18**(17): p. 6952-62.

319. Kelz, M.B., et al., *Expression of the transcription factor ΔFosB in the brain controls sensitivity to cocaine.* Nature, 1999. **401**(6750): p. 272-6.

320. Peakman, M.C., et al., *Inducible, brain region-specific expression of a dominant negative mutant of c-Jun in transgenic mice decreases sensitivity to cocaine.* Brain Res, 2003. **970**(1-2): p. 73-86.

321. Nomaru, H., et al., *Fosb gene products contribute to excitotoxic microglial activation by regulating the expression of complement C5a receptors in microglia.* Glia, 2014. **62**(8): p. 1284-1298.

322. Hong, S., et al., *Complement and microglia mediate early synapse loss in Alzheimer mouse models.* Science, 2016. **352**(6286): p. 712-716.

323. Brennan, F.H., et al., *Therapeutic targeting of complement to modify disease course and improve outcomes in neurological conditions.* Semin Immunol, 2016. **28**(3): p. 292-308.

324. Yutsudo, N., et al., *fosB-null mice display impaired adult hippocampal neurogenesis and spontaneous epilepsy with depressive behavior.* Neuropsychopharmacology, 2013. **38**(5): p. 895-906.

325. Ohnishi, Y.N., et al., *FosB is essential for the enhancement of stress tolerance, and antagonizes locomotor sensitization by ΔFosB.* Biological Psychiatry, 2011. **70**(5): p. 487-495.

326. Vialou, V., et al., *Differential induction of FosB isoforms throughout the brain by fluoxetine and chronic stress.* Neuropharmacology, 2015. **99**: p. 28-37.

327. Vialou, V., et al., *Prefrontal cortical circuit for depression- and anxiety-related behaviors mediated by cholecystokinin: role of ΔFosB .* J Neurosci, 2014. **34**(11): p. 3878-87.

328. Cooper, S.E., et al., *Comparison of chronic physical and emotional social defeat stress effects on mesocorticolimbic circuit activation and voluntary consumption of morphine.* Scientific reports, 2017. **7**(1): p. 8445-8445.

329. Eagle, A.L., et al., *ΔFosB Decreases Excitability of Dorsal Hippocampal CA1 Neurons.* eNeuro, 2018. **5**(4).

330. Woodworth, H.L., et al., *Identification of Neurotensin Receptor Expressing Cells in the Ventral Tegmental Area across the Lifespan.* eNeuro, 2018. **5**(1).

331. Ohnishi, Y.N., et al., *Generation and validation of a floxed FosB mouse line.* bioRxiv, 2017: p. 179309.

332. Overk, C.R., et al., *Effects of aromatase inhibition versus gonadectomy on hippocampal complex amyloid pathology in triple transgenic mice.* Neurobiol Dis, 2012. **45**(1): p. 479-87.

333. Morris, J.A., et al., *Sexual dimorphism and steroid responsiveness of the posterodorsal medial amygdala in adult mice.* Brain research, 2008. **1190**: p. 115-121.

334. Tsankova, N.M., et al., *Sustained hippocampal chromatin regulation in a mouse model of depression and antidepressant action.* Nat Neurosci, 2006. **9**(4): p. 519-25.

335. Brancato, A., et al., *Sub-chronic variable stress induces sex-specific effects on glutamatergic synapses in the nucleus accumbens.* Neuroscience, 2017. **350**: p. 180-189.

336. Golden, S.A., et al., *Epigenetic regulation of RAC1 induces synaptic remodeling in stress disorders and depression.* Nat Med, 2013. **19**(3): p. 337-44.

337. Eagle, A.L., et al., *Experience-dependent induction of hippocampal ΔFosB controls learning.* The Journal of Neuroscience, 2015. **35**(40): p. 13773-13783.

338. Eagle, A.L., H. Wang, and A.J. Robison, *Sensitive assessment of hippocampal learning using temporally dissociated passive avoidance task.* Bio Protoc, 2016. **6**(11).

339. Heiman, M., et al., *Cell type-specific mRNA purification by translating ribosome affinity purification (TRAP).* Nat Protoc, 2014. **9**(6): p. 1282-91.

340. Heiman, M., et al., *A translational profiling approach for the molecular characterization of CNS cell types.* Cell, 2008. **135**(4): p. 738-48.

341. Tschöp, M.H., et al., *A guide to analysis of mouse energy metabolism.* Nature methods, 2011. **9**(1): p. 57-63.

342. Minatohara, K., M. Akiyoshi, and H. Okuno, *Role of Immediate-Early Genes in Synaptic Plasticity and Neuronal Ensembles Underlying the Memory Trace.* Frontiers in Molecular Neuroscience, 2015. **8**: p. 78.

343. Liu, X., et al., *Identification and Manipulation of Memory Engram Cells.* Cold Spring Harb Symp Quant Biol, 2014. **79**: p. 59-65.

344. Tonegawa, S., et al., *Memory Engram Cells Have Come of Age.* Neuron, 2015. **87**(5): p. 918-31.

345. Ramirez, S., *Crystallizing a memory.* Science, 2018. **360**(6394): p. 1182-1183.

346. Leighton, L.J., et al., *A Functional Role for the Epigenetic Regulator ING1 in Activity-induced Gene Expression in Primary Cortical Neurons.* Neuroscience, 2018. **369**: p. 248-260.

347. Duke, C.G., et al., *Experience-dependent epigenomic reorganization in the hippocampus.* Learn Mem, 2017. **24**(7): p. 278-288.

348. Nishijima, T., M. Kawakami, and I. Kita, *Long-term exercise is a potent trigger for ΔFosB induction in the hippocampus along the dorso-ventral axis.* PLoS One, 2013. **8**(11): p. e81245.

349. Nestler, E.J., *Transcriptional Mechanisms of Drug Addiction.* Clinical Psychopharmacology and Neuroscience, 2012. **10**(3): p. 136-143.

350. Pitchers, K.K., et al., *ΔFosB in the nucleus accumbens is critical for reinforcing effects of sexual reward.* Genes Brain Behav, 2010. **9**(7): p. 831-40.

351. Robison, A.J., et al., *Behavioral and structural responses to chronic cocaine require a feedforward loop involving ΔFosB and calcium/calmodulin-dependent protein kinase II in the nucleus accumbens shell.* J Neurosci, 2013. **33**(10): p. 4295-307.

352. Lagace, D.C., et al., *Adult hippocampal neurogenesis is functionally important for stress-induced social avoidance.* Proc Natl Acad Sci U S A, 2010. **107**(9): p. 4436-41.

353. Seo, D.-o., et al., *Adult Hippocampal Neurogenesis Modulates Fear Learning through Associative and Nonassociative Mechanisms.* The Journal of Neuroscience, 2015. **35**(32): p. 11330-11345.

354. Mazella, J., et al., *Structure, functional expression, and cerebral localization of the levocabastine-sensitive neurotensin/neuromedin N receptor from mouse brain.* J Neurosci, 1996. **16**(18): p. 5613-20.

355. Nouel, D., et al., *Pharmacological, molecular and functional characterization of glial neurotensin receptors.* Neuroscience, 1999. **94**(4): p. 1189-97.

356. Sarret, P., et al., *Regional and cellular distribution of low affinity neurotensin receptor mRNA in adult and developing mouse brain.* J Comp Neurol, 1998. **394**(3): p. 344-56.

357. Lepee-Lorgeoux, I., et al., *Differential ontogenetic patterns of levocabastine-sensitive neurotensin NT2 receptors and of NT1 receptors in the rat brain revealed by in situ hybridization.* Brain Res Dev Brain Res, 1999. **113**(1-2): p. 115-31.

358. van Praag, H., G. Kempermann, and F.H. Gage, *Running increases cell proliferation and neurogenesis in the adult mouse dentate gyrus.* Nat Neurosci, 1999. **2**(3): p. 266-70.

359. Revest, J.M., et al., *Adult hippocampal neurogenesis is involved in anxiety-related behaviors.* Mol Psychiatry, 2009. **14**(10): p. 959-67.

360. Epp, J.R., et al., *Neurogenesis-mediated forgetting minimizes proactive interference.* Nat Commun, 2016. **7**.

361. Niibori, Y., et al., *Suppression of adult neurogenesis impairs population coding of similar contexts in hippocampal CA3 region.* Nat Commun, 2012. **3**: p. 1253.

362. Kogan, J.H., P.W. Frankland, and A.J. Silva, *Long-term memory underlying hippocampus-dependent social recognition in mice.* Hippocampus, 2000. **10**(1): p. 47-56.

363. Kohler, C., A.C. Radesater, and V. Chan-Palay, *Distribution of neurotensin receptors in the primate hippocampal region: a quantitative autoradiographic study in the monkey and the postmortem human brain.* Neurosci Lett, 1987. **76**(2): p. 145-50.

364. Kurushima, H., et al., *Selective induction of ΔFosB in the brain after transient forebrain ischemia accompanied by an increased expression of galectin-1, and the implication of ΔFosB and galectin-1 in neuroprotection and neurogenesis.* Cell Death Differ, 2005. **12**(8): p. 1078-96.

365. Niu, H., et al., *Effect of Long-Term Sodium Salicylate Administration on Learning, Memory, and Neurogenesis in the Rat Hippocampus.* Biomed Res Int, 2018. **2018**: p. 7807426.

366. Flood, J.F. and A. Cherkin, *Fluoxetine enhances memory processing in mice.* Psychopharmacology (Berl), 1987. **93**(1): p. 36-43.

367. Yi, J.H., et al., *Fluoxetine Inhibits Natural Decay of Long-Term Memory via Akt/GSK-3beta Signaling.* Mol Neurobiol, 2018. **55**(9): p. 7453-7462.

368. Marwari, S. and G.S. Dawe, *(R)-fluoxetine enhances cognitive flexibility and hippocampal cell proliferation in mice.* J Psychopharmacol, 2018. **32**(4): p. 441-457.

369. Ibi, D., et al., *Social isolation rearing-induced impairment of the hippocampal neurogenesis is associated with deficits in spatial memory and emotion-related behaviors in juvenile mice.* J Neurochem, 2008. **105**(3): p. 921-32.

370. Mastrodonato, A., et al., *Ventral CA3 Activation Mediates Prophylactic Ketamine Efficacy Against Stress-Induced Depressive-like Behavior.* Biol Psychiatry, 2018.

371. Corbett, B.F., et al., *ΔFosB Regulates Gene Expression and Cognitive Dysfunction in a Mouse Model of Alzheimer's Disease.* Cell Rep, 2017. **20**(2): p. 344-355.

372. Cho, K.O., et al., *Aberrant hippocampal neurogenesis contributes to epilepsy and associated cognitive decline.* Nat Commun, 2015. **6**: p. 6606.

373. LaGamma, C.T., et al., *Antidepressant but Not Prophylactic Ketamine Administration Alters Calretinin and Calbindin Expression in the Ventral Hippocampus.* Frontiers in molecular neuroscience, 2018. **11**: p. 404-404.

374. Rivera, P.D., et al., *Removal of microglial-specific MyD88 signaling alters dentate gyrus doublecortin and enhances opioid addiction-like behaviors.* Brain Behav Immun, 2018.

375. Bannerman, D.M., et al., *Regional dissociations within the hippocampus—memory and anxiety.* Neuroscience & Biobehavioral Reviews, 2004. **28**(3): p. 273-283.

376. LeGates, T.A., et al., *Reward behaviour is regulated by the strength of hippocampus–nucleus accumbens synapses.* Nature, 2018.

377. Bagot, R.C., et al., *Ventral hippocampal afferents to the nucleus accumbens regulate susceptibility to depression.* Nature Communications, 2015. **6**: p. 7062.

378. Floriou-Servou, A., et al., *Distinct proteomic, transcriptomic, and epigenetic stress responses in dorsal and ventral hippocampus.* Biol Psychiatry, 2018. **84**(7): p. 531-541.

379. Pacheco, A., et al., *Chronic stress triggers expression of immediate early genes and differentially affects the expression of AMPA and NMDA subunits in dorsal and ventral hippocampus of rats.* Front Mol Neurosci, 2017. **10**: p. 244.

380. Kenworthy, C.A., et al., *Social defeat induces changes in histone acetylation and expression of histone modifying enzymes in the ventral hippocampus, prefrontal cortex, and dorsal raphe nucleus.* Neuroscience, 2014. **264**: p. 88-98.

381. Carle, T.L., et al., *Proteasome-dependent and -independent mechanisms for FosB destabilization: identification of FosB degron domains and implications for ΔFosB stability.* European Journal of Neuroscience, 2007. **25**(10): p. 3009-3019.

382. Ulery, P.G., G. Rudenko, and E.J. Nestler, *Regulation of ΔFosB stability by phosphorylation.* The Journal of Neuroscience, 2006. **26**(19): p. 5131-5142.

383. Nestler, E.J., M.B. Kelz, and J. Chen, *ΔFosB: a molecular mediator of long-term neural and behavioral plasticity.* Brain Research, 1999. **835**(1): p. 10-17.

384. Perrotti, L.I., et al., *Induction of ΔFosB in reward-related brain structures after chronic stress.* The Journal of Neuroscience, 2004. **24**(47): p. 10594-10602.

385. Robison, A.J. and E.J. Nestler, *Transcriptional and epigenetic mechanisms of addiction.* Nat Rev Neurosci, 2011. **12**(11): p. 623-37.

386. Grueter, B.A., et al., *FosB differentially modulates nucleus accumbens direct and indirect pathway function.* Proc Natl Acad Sci U S A, 2013. **110**(5): p. 1923-8.

387. Eagle, A.L., et al., *ΔFosB decreases excitability of dorsal hippocampal CA1 neurons.* eNeuro, 2018. **5**(4): p. ENEURO.0104-18.2018.

388. Mastrodonato, A., et al., *Ventral CA3 activation mediates prophylactic ketamine efficacy against stress-induced depressive-like behavior.* Biological Psychiatry, 2018. **84**(11): p. 846-856.

389. Krishnan, V., et al., *Molecular Adaptations Underlying Susceptibility and Resistance to Social Defeat in Brain Reward Regions.* Cell, 2007. **131**(2): p. 391-404.

390. Golden, S.A., et al., *A standardized protocol for repeated social defeat stress in mice.* Nature protocols, 2011. **6**(8): p. 1183-1191.

391. Blaha, C.D., et al., *Stimulation of the ventral subiculum of the hippocampus evokes glutamate receptor-mediated changes in dopamine efflux in the rat nucleus accumbens.* European Journal of Neuroscience, 1997. **9**(5): p. 902-911.

392. Floresco, S.B., C.L. Todd, and A.A. Grace, *Glutamatergic afferents from the hippocampus to the nucleus accumbens regulate activity of ventral tegmental area dopamine neurons.* The Journal of Neuroscience, 2001. **21**(13): p. 4915-4922.

393. Fanselow, M.S. and J.E. LeDoux, *Why we think plasticity underlying pavlovian fear conditioning occurs in the basolateral amygdala.* Neuron, 1999. **23**(2): p. 229-232.

394. Etkin, A., et al., *Individual differences in trait anxiety predict the response of the basolateral amygdala to unconsciously processed fearful faces.* Neuron, 2004. **44**(6): p. 1043-1055.

395. Sierra-Mercado, D., N. Padilla-Coreano, and G.J. Quirk, *Dissociable Roles of Prelimbic and Infralimbic Cortices, Ventral Hippocampus, and Basolateral Amygdala in the Expression and Extinction of Conditioned Fear.* Neuropsychopharmacology, 2011. **36**(2): p. 529-538.

396. Kjelstrup, K.G., et al., *Reduced fear expression after lesions of the ventral hippocampus.* Proceedings of the National Academy of Sciences, 2002. **99**(16): p. 10825-10830.

397. Nakabeppu, Y. and D. Nathans, *A naturally occurring truncated form of FosB that inhibits Fos/Jun transcriptional activity.* Cell, 1991. **64**(4): p. 751-759.

398. Bading, H., et al., *N-methyl-d-aspartate receptors are critical for mediating the effects of glutamate on intracellular calcium concentration and immediate early gene expression in cultured hippocampal neurons.* Neuroscience, 1995. **64**(3): p. 653-664.

399. Ohnishi, Y.N., et al., *Generation and validation of a floxed FosB mouse line.* bioRxiv, 2017.

400. Weeber, E.J., et al., *A role for the beta isoform of protein kinase C in fear conditioning.* J Neurosci, 2000. **20**(16): p. 5906-14.

401. Iñiguez, S.D., et al., *Social defeat stress induces depression-like behavior and alters spine morphology in the hippocampus of adolescent male C57BL/6 mice.* Neurobiology of Stress, 2016. **5**: p. 54-64.

402. Kirkby, L.A., et al., *An amygdala-hippocampus subnetwork that encodes variation in human mood.* Cell, 2018. **175**(6): p. 1688-1700.e14.

403. Kessler, R.C., *Epidemiology of women and depression.* J Affect Disord, 2003. **74**(1): p. 5-13.

404. Marcus, S.M., et al., *Gender differences in depression: findings from the STAR*D study.* J Affect Disord, 2005. **87**(2-3): p. 141-50.

405. Dalla, C., et al., *Chronic mild stress impact: are females more vulnerable?* Neuroscience, 2005. **135**(3): p. 703-14.

406. Trainor, B.C., et al., *Sex differences in social interaction behavior following social defeat stress in the monogamous California mouse (Peromyscus californicus).* PLoS One, 2011. **6**(2): p. e17405.

407. LaPlant, Q., et al., *Dnmt3a regulates emotional behavior and spine plasticity in the nucleus accumbens.* Nat Neurosci, 2010. **13**(9): p. 1137-43.

408. Vialou, V., et al., *Prefrontal Cortical Circuit for Depression- and Anxiety-Related Behaviors Mediated by Cholecystokinin: Role of ΔFosB.* J Neurosci, 2011. **34**(11): p. 3878-3887.

409. LeGates, T.A., et al., *Reward behaviour is regulated by the strength of hippocampus–nucleus accumbens synapses.* Nature, 2018. **564**: p. 258-262.

410. Faneselow, M.S. and H. Dong, *Are the Dorsal and Ventral Hippocampus Functionally Distinct Structures?* Neuron, 2010. **65**: p. 7-19.

411. Okuyama, T., et al., *Ventral CA1 neurons store social memory.* Science, 2016. **353**(6307): p. 1536-1541.

412. Shors, T.J., C. Chua, and J. Falduto, *Sex differences and opposite effects of stress on dendritic spine density in the male versus female hippocampus.* J Neurosci, 2001. **21**(16): p. 6292-7.

413. Maren, S., B. De Oca, and M.S. Fanselow, *Sex differences in hippocampal long-term potentiation (LTP) and Pavlovian fear conditioning in rats: positive correlation between LTP and contextual learning.* Brain Research, 1994. **661**(1-2): p. 25-34.

414. Zhang, S., et al., *Sex Differences in the Neuroadaptations of Reward-related Circuits in Response to Subchronic Variable Stress.* Neuroscience, 2018. **376**: p. 106-116.

415. Eagle, A., M. Mazei-Robison, and A.J. Robison, *Sucrose Preference Test to Measure Stress-Induced Anhedonia.* Bio-Protocol, 2016. **6**(11).

416. Sarno, E. and A.J. Robison, *Emerging role of viral vectors for circuit-specific gene interrogation and manipulation in rodent brain.* Pharmacol Biochem Behav, 2018. **174**: p. 2-8.

417. Kessler, R.C., et al., *Lifetime prevalence and age-of-onset distributions of DSM-IV disorders in the National Comorbidity Survey Replication.* Arch Gen Psychiatry, 2005. **62**(6): p. 593-602.

418. Maki, P.M., et al., *Guidelines for the evaluation and treatment of perimenopausal depression: summary and recommendations.* Menopause, 2018. **25**(10): p. 1069-1085.

419. Amanatkar, H.R. and J.T. Chibnall, *Impact of exogenous testosterone on mood: A systematic review and meta-analysis of randomized placebo-controlled trials.* Ann Clin Psychiatry, 2014. **26**(1): p. 19-32.

420. Steinman, M.Q., et al., *Hypothalamic vasopressin systems are more sensitive to the long term effects of social defeat in males versus females.* Psychoneuroendocrinology, 2014. **51C**: p. 122-134.

421. Hastings, R., et al., *Volumetric Analysis of the Prefrontal Cortex, Amygdala, and Hippocampus in Major Depression.* Neuropsychopharmacology, 2004. **29**: p. 952-959.

422. Leranth, C., O. Petnehazy, and N.J. MacLusky, *Gonadal Hormones Affect Spine Synaptic Density in the CA1 Hippocampal Subfield of Male Rats.* J Neurosci, 2003. **23**(5): p. 1588-1592.

423. Woolley, C.S., et al., *Estradiol increases the sensitivity of hippocampal CA1 pyramidal cells to NMDA receptor-mediated synaptic input: correlation with dendritic spine density.* J Neurosci, 1997. **17**(5): p. 1848-59.

424. Woolley, C.S. and B.S. McEwen, *Estradiol mediates fluctuation in hippocampal synapse density during the estrous cycle in the adult rat.* J Neurosci, 1992. **12**(7): p. 2549-54.

425. Frick, K.M., *Estrogens and age-related memory decline in rodents: what have we learned and where do we go from here?* Horm Behav, 2009. **55**(1): p. 2-23.

426. Choleris, E., et al., *Estrogenic involvement in social learning, social recognition and pathogen avoidance.* Front Neuroendocrinol, 2012. **33**(2): p. 140-59.

427. Okuyama, T., et al., *Ventral CA1 neurons store social memory.* Science, 2016. **353**(6307): p. 1536.

428. Papp, M., P. Willner, and R. Muscat, *An animal model of anhedonia: attenuation of sucrose consumption and place preference conditioning by chronic unpredictable mild stress.* Psychopharmacology (Berl), 1991. **104**(2): p. 255-9.

429. Pizzagalli, D.A., *Depression, Stress, and Anhedonia: Toward a Synthesis and Integrated Model.* Annu Rev Clin Psychol, 2014. **10**: p. 393-423.

430. Russo, S.J. and E.J. Nestler, *The brain reward circuitry in mood disorders.* Nat Rev Neurosci, 2013. **14**(9): p. 609-25.

431. Grueter, B.A., P.E. Rothwell, and R.C. Malenka, *Integrating synaptic plasticity and striatal circuit function in addiction.* Curr Opin Neurobiol, 2012. **22**(3): p. 545-51.

432. Kelley, A.E. and K.C. Berridge, *The neuroscience of natural rewards: relevance to addictive drugs.* J Neurosci, 2002. **22**(9): p. 3306-11.

433. DiLeone, R.J., J.R. Taylor, and M.R. Picciotto, *The drive to eat: comparisons and distinctions between mechanisms of food reward and drug addiction.* Nat Neurosci, 2012. **15**(10): p. 1330-5.

434. Merchenthaler, I., M. Lane, and P. Shughrue, *Distribution of pre-pro-glucagon and glucagon-like peptide-1 receptor messenger RNAs in the rat central nervous system.* J Comp Neurol, 1999. **403**(2): p. 261-80.

435. Kanoski, S.E., et al., *Ghrelin signaling in the ventral hippocampus stimulates learned and motivational aspects of feeding via PI3K-Akt signaling.* Biol Psychiatry, 2013. **73**(9): p. 915-23.

436. Kanoski, S.E. and H.J. Grill, *Hippocampus Contributions to Food Intake Control: Mnemonic, Neuroanatomical, and Endocrine Mechanisms.* Biol Psychiatry, 2017. **81**(9): p. 748-756.

437. Hannapel, R.C., et al., *Ventral hippocampal neurons inhibit postprandial energy intake.* Hippocampus, 2017. **27**(3): p. 274-284.

438. Davidson, T.L., et al., *Contributions of the hippocampus and medial prefrontal cortex to energy and body weight regulation.* Hippocampus, 2009. **19**(3): p. 235-52.

439. Davidson, T.L., et al., *A potential role for the hippocampus in energy intake and body weight regulation.* Curr Opin Pharmacol, 2007. **7**(6): p. 613-6.

440. Davidson, T.L., et al., *The interoceptive cue properties of ghrelin generalize to cues produced by food deprivation.* Peptides, 2005. **26**(9): p. 1602-10.

441. Parent, M.B., J.N. Darling, and Y.O. Henderson, *Remembering to eat: hippocampal regulation of meal onset.* Am J Physiol Regul Integr Comp Physiol, 2014. **306**(10): p. R701-13.

442. Henderson, K.W., et al., *Long-term seizure suppression and optogenetic analyses of synaptic connectivity in epileptic mice with hippocampal grafts of GABAergic interneurons.* J Neurosci, 2014. **34**(40): p. 13492-504.

443. Carballo-Marquez, A., et al., *Muscarinic receptor blockade in ventral hippocampus and prelimbic cortex impairs memory for socially transmitted food preference.* Hippocampus, 2009. **19**(5): p. 446-55.

444. Kanoski, S.E., et al., *Hippocampal leptin signaling reduces food intake and modulates food-related memory processing.* Neuropsychopharmacology, 2011. **36**(9): p. 1859-70.

445. Sweeney, P. and Y. Yang, *An excitatory ventral hippocampus to lateral septum circuit that suppresses feeding.* Nat Commun, 2015. **6**: p. 10188.

446. Wang, X., D. Zhang, and X.Y. Lu, *Dentate gyrus-CA3 glutamate release/NMDA transmission mediates behavioral despair and antidepressant-like responses to leptin.* Mol Psychiatry, 2015. **20**(4): p. 509-19.

447. Prado, L., et al., *Activation of Glutamatergic Fibers in the Anterior NAc Shell Modulates Reward Activity in the aNAcSh, the Lateral Hypothalamus, and Medial Prefrontal Cortex and Transiently Stops Feeding.* J Neurosci, 2016. **36**(50): p. 12511-12529.

448. Maldonado-Irizarry, C.S., C.J. Swanson, and A.E. Kelley, *Glutamate receptors in the nucleus accumbens shell control feeding behavior via the lateral hypothalamus.* J Neurosci, 1995. **15**(10): p. 6779-88.

449. King, B.M., et al., *Temporal lobe lesion-induced obesity in rats: an anatomical investigation of the posterior amygdala and hippocampal formation.* Physiol Behav, 1996. **59**(4-5): p. 843-8.

450. King, B.M., et al., *Effect on food intake and body weight of lesions in and adjacent to the posterodorsal amygdala in rats.* Physiol Behav, 1994. **55**(5): p. 963-6.

451. Perrotti, L.I., et al., *Distinct patterns of ΔFosB induction in brain by drugs of abuse.* Synapse, 2008. **62**(5): p. 358-69.

452. Sharma, S., M.F. Fernandes, and S. Fulton, *Adaptations in brain reward circuitry underlie palatable food cravings and anxiety induced by high-fat diet withdrawal.* Int J Obes (Lond), 2013. **37**(9): p. 1183-91.

453. Wallace, D.L., et al., *The influence of ΔFosB in the nucleus accumbens on natural reward-related behavior.* J Neurosci, 2008. **28**(41): p. 10272-7.

454. Christiansen, A.M., et al., *"Snacking" causes long term attenuation of HPA axis stress responses and enhancement of brain FosB/ΔFosB expression in rats.* Physiol Behav, 2011. **103**(1): p. 111-6.

455. Egan, A.E., et al., *Palatable Food Affects HPA Axis Responsivity and Forebrain Neurocircuitry in an Estrous Cycle-specific Manner in Female Rats.* Neuroscience, 2018. **384**: p. 224-240.

456. Herdegen, T., et al., *Basal expression of the inducible transcription factors c-Jun, JunB, JunD, c-Fos, FosB, and Krox-24 in the adult rat brain.* J Comp Neurol, 1995. **354**(1): p. 39-56.

457. Sato, S.M., et al., *Quantitative mapping of cocaine-induced ΔFosB expression in the striatum of male and female rats.* PLoS One, 2011. **6**(7): p. e21783.

458. Acaba, L., et al., *Sex experience increases delta FosB in male and female hamsters, but facilitates sex behavior only in females.* Behav Neurosci, 2019. **133**(4): p. 378-384.

459. Sterrenburg, L., et al., *Chronic stress induces sex-specific alterations in methylation and expression of corticotropin-releasing factor gene in the rat.* PLoS One, 2011. **6**(11): p. e28128.

460. Bollinger, J.L., et al., *Gonadal hormones differentially regulate sex-specific stress effects on glia in medial prefrontal cortex.* J Neuroendocrinol, 2019: p. e12762.

461. Rincel, M., et al., *Multi-hit early life adversity affects gut microbiota, brain and behavior in a sex-dependent manner.* Brain Behav Immun, 2019.

462. Hill, R.a. and M.a. Klug, *Sex-specific disruptions in spatial memory and anhedonia in a two hit rat model correspond with alterations in hippocampal brain-derived neurotrophic factor expression and signaling.* Hippocampus, 2014. **24**(10): p. 1197--211.

463. Rowson, S.A., et al., *Chronic adolescent stress sex-specifically alters the hippocampal transcriptome in adulthood.* Neuropsychopharmacology, 2019. **44**(7): p. 1207-1215.

464. Keiser, A.A., et al., *Sex Differences in Context Fear Generalization and Recruitment of Hippocampus and Amygdala during Retrieval.* Neuropsychopharmacology, 2016. **42**: p. 397.

465. Hwang, L.L., et al., *Sex differences in high-fat diet-induced obesity, metabolic alterations and learning, and synaptic plasticity deficits in mice.* Obesity (Silver Spring), 2010. **18**(3): p. 463-9.

466. Silva-Gómez, A.B., et al., *Comparative behavioral changes between male and female postpubertal rats following neonatal excitotoxic lesions of the ventral hippocampus.* Brain Research, 2003. **973**(2): p. 285-292.

467. Maren, S. and W. Holt, *The hippocampus and contextual memory retrieval in Pavlovian conditioning.* Behav Brain Res, 2000. **110**(1-2): p. 97-108.

468. Kennedy, P.J. and M.L. Shapiro, *Retrieving memories via internal context requires the hippocampus.* J Neurosci, 2004. **24**(31): p. 6979-85.

469. Hsu, T.M., et al., *Hippocampal GLP-1 receptors influence food intake, meal size, and effort-based responding for food through volume transmission.* Neuropsychopharmacology, 2015. **40**(2): p. 327-37.

470. Lin, L., et al., *Ghrelin receptor regulates appetite and satiety during aging in mice by regulating meal frequency and portion size but not total food intake.* J Nutr, 2014. **144**(9): p. 1349-55.

471. Goldstone, A.P., et al., *Ghrelin mimics fasting to enhance human hedonic, orbitofrontal cortex, and hippocampal responses to food.* Am J Clin Nutr, 2014. **99**(6): p. 1319-30.

472. Pierce, A.N., et al., *Urinary bladder hypersensitivity and dysfunction in female mice following early life and adult stress.* Brain Res, 2016. **1639**: p. 58-73.

473. Nelson, B.S., M.K. Sequeira, and J.R. Schank, *Bidirectional relationship between alcohol intake and sensitivity to social defeat: association with Tacr1 and Avp expression.* Addict Biol, 2018. **23**(1): p. 142-153.

474. Lee, W., et al., *Social status in mouse social hierarchies is associated with variation in oxytocin and vasopressin 1a receptor densities.* Horm Behav, 2019.

475. Cakir, I., et al., *Leptin Receptor Signaling in Sim1-Expressing Neurons Regulates Body Temperature and Adaptive Thermogenesis.* Endocrinology, 2019. **160**(4): p. 863-879.

476. Balthasar, N., et al., *Divergence of melanocortin pathways in the control of food intake and energy expenditure.* Cell, 2005. **123**(3): p. 493-505.

477. Xu, P., et al., *Estrogen receptor-alpha in medial amygdala neurons regulates body weight.* J Clin Invest, 2015. **125**(7): p. 2861-76.

478. Alhadeff, A.L., et al., *Glutamate Receptors in the Central Nucleus of the Amygdala Mediate Cisplatin-Induced Malaise and Energy Balance Dysregulation through Direct Hindbrain Projections.* J Neurosci, 2015. **35**(31): p. 11094-104.

479. Bovetto, S. and D. Richard, *Lesion of central nucleus of amygdala promotes fat gain without preventing effect of exercise on energy balance.* Am J Physiol, 1995. **269**(4 Pt 2): p. R781-6.

480. Forloni, G., et al., *Role of the hippocampus in the sex-dependent regulation of eating behavior: Studies with kainic acid.* Physiology & Behavior, 1986. **38**(3): p. 321-326.

481. Koorneef, L.L., et al., *How Metabolic State May Regulate Fear: Presence of Metabolic Receptors in the Fear Circuitry.* Front Neurosci, 2018. **12**: p. 594.

482. Blume, S.R., et al., *Sex- and Estrus-Dependent Differences in Rat Basolateral Amygdala.* J Neurosci, 2017. **37**(44): p. 10567-10586.

483. Bocchio, M., S. Nabavi, and M. Capogna, *Synaptic Plasticity, Engrams, and Network Oscillations in Amygdala Circuits for Storage and Retrieval of Emotional Memories.* Neuron, 2017. **94**(4): p. 731-743.

484. Zanchi, D., et al., *The impact of gut hormones on the neural circuit of appetite and satiety: A systematic review.* Neurosci Biobehav Rev, 2017. **80**: p. 457-475.

485. Beyeler, A., et al., *Divergent Routing of Positive and Negative Information from the Amygdala during Memory Retrieval.* Neuron, 2016. **90**(2): p. 348-361.

486. Hadad-Ophir, O., et al., *Amygdala activation and GABAergic gene expression in hippocampal sub-regions at the interplay of stress and spatial learning.* Front Behav Neurosci, 2014. **8**: p. 3.

487. Lubkemann, R., et al., *Identification and Characterization of GABAergic Projection Neurons from Ventral Hippocampus to Amygdala.* Brain Sci, 2015. **5**(3): p. 299-317.

488. Cembrowski, M.S., et al., *Spatial Gene-Expression Gradients Underlie Prominent Heterogeneity of CA1 Pyramidal Neurons.* Neuron, 2016. **89**(2): p. 351-68.

489. Anderson, P. and T. Lomo, *Mode of activation of hippocampal pyramidal cells by excitatory synapses on dendrites.* Exp Brain Res, 1966. **2**(3): p. 247-60.

490. Zola-Morgan, S. and L.R. Squire, *Neuroanatomy of memory.* Annu Rev Neurosci, 1993. **16**: p. 547-63.

491. Cembrowski, M.S., et al., *The subiculum is a patchwork of discrete subregions.* Elife, 2018. **7**.

492. Bienkowski, M.S., et al., *Integration of gene expression and brain-wide connectivity reveals the multiscale organization of mouse hippocampal networks.* Nat Neurosci, 2018. **21**(11): p. 1628-1643.

493. Vierbuchen, T., et al., *AP-1 Transcription Factors and the BAF Complex Mediate Signal-Dependent Enhancer Selection.* Mol Cell, 2017. **68**(6): p. 1067-1082.e12.

494. Cembrowski, M.S. and N. Spruston, *Heterogeneity within classical cell types is the rule: lessons from hippocampal pyramidal neurons.* Nat Rev Neurosci, 2019. **20**(4): p. 193-204.

495. Yoshida, K., et al., *Serotonin-mediated inhibition of ventral hippocampus is required for sustained goal-directed behavior.* Nature Neuroscience, 2019. **22**(5): p. 770-777.

496. Bigio, B., et al., *Epigenetics and energetics in ventral hippocampus mediate rapid antidepressant action: Implications for treatment resistance.* Proc Natl Acad Sci U S A, 2016. **113**(28): p. 7906-11.

497. Arszovszki, A., Z. Borhegyi, and T. Klausberger, *Three axonal projection routes of individual pyramidal cells in the ventral CA1 hippocampus.* Front Neuroanat, 2014. **8**: p. 53.

498. Ciocchi, S., et al., *Selective information routing by ventral hippocampal CA1 projection neurons.* 2015. **348**(6234).

499. Witter, M.P. and H.J. Groenewegen, *Laminar origin and septotemporal distribution of entorhinal and perirhinal projections to the hippocampus in the cat.* J Comp Neurol, 1984. **224**(3): p. 371-85.

500. Spruston, N., *Assembling cell ensembles.* Cell, 2014. **157**(7): p. 1502-4.

501. Lo, L., et al., *Connectional architecture of a mouse hypothalamic circuit node controlling social behavior.* Proceedings of the National Academy of Sciences, 2019. **116**(15): p. 7503.

502. You, J.C., et al., *Epigenetic suppression of hippocampal calbindin-D28k by ΔFosB drives seizure-related cognitive deficits.* Nature Medicine, 2017. **23**: p. 1377.

503. Carlezon, W.A., Jr. and M.J. Thomas, *Biological substrates of reward and aversion: a nucleus accumbens activity hypothesis.* Neuropharmacology, 2009. **56 Suppl 1**: p. 122-32.

504. Sharpe, M.J., et al., *Dopamine transients delivered in learning contexts do not act as model-free prediction errors.* bioRxiv, 2019: p. 574541.

505. Francis, T.C., et al., *High-Frequency Activation of Nucleus Accumbens D1-MSNs Drives Excitatory Potentiation on D2-MSNs.* Neuron, 2019.

506. McClung, C.a. and E.J. Nestler, *Regulation of gene expression and cocaine reward by CREB and ΔFosB .* Nature neuroscience, 2003. **6**(11): p. 1208-1215.

507. Becker, J.B. and E. Chartoff, *Sex differences in neural mechanisms mediating reward and addiction.* Neuropsychopharmacology, 2019. **44**(1): p. 166-183.

508. Eid, R.S., et al., *Ovarian hormone status dictates the neuroinflammatory and behavioural consequences of sub-chronic stress exposure in middle-aged female mice.* bioRxiv, 2019: p. 706887.

509. Naftolin, F. and K.J. Ryan, *The metabolism of androgens in central neuroendocrine tissues.* J Steroid Biochem, 1975. **6**(6): p. 993-7.

510. Tabatadze, N., S.M. Sato, and C.S. Woolley, *Quantitative analysis of long-form aromatase mRNA in the male and female rat brain.* PLoS One, 2014. **9**(7): p. e100628.

511. Yague, J.G., et al., *Aromatase expression in the normal and epileptic human hippocampus.* Brain Res, 2010. **1315**: p. 41-52.

512. Marks, L.S., *5alpha-reductase: history and clinical importance.* Rev Urol, 2004. **6 Suppl 9**: p. S11-21.

513. Lacreuse, A., M.E. Wilson, and J.G. Herndon, *No effect of different estrogen receptor ligands on cognition in adult female monkeys.* Physiol Behav, 2009. **96**(3): p. 448-56.

514. Lu, S.F., et al., *Androgen receptor in mouse brain: sex differences and similarities in autoregulation.* Endocrinology, 1998. **139**(4): p. 1594-601.

515. Miyamoto, J., et al., *The pituitary function of androgen receptor constitutes a glucocorticoid production circuit.* Mol Cell Biol, 2007. **27**(13): p. 4807-14.

516. Handa, R.J., et al., *Gonadal steroid hormone receptors and sex differences in the hypothalamo-pituitary-adrenal axis.* Horm Behav, 1994. **28**(4): p. 464-76.

517. Tsai, H.-W., et al., *Age- and Sex-Dependent Changes in Androgen Receptor Expression in the Developing Mouse Cortex and Hippocampus.* Neuroscience Journal, 2015. **2015**: p. 11.

518. Hajszan, T., N.J. MacLusky, and C. Leranth, *Role of androgens and the androgen receptor in remodeling of spine synapses in limbic brain areas.* Hormones and behavior, 2008. **53**(5): p. 638-646.

519. Hartshorn, M., *Steroid reaction mechanisms*.

520. Schule, R., et al., *Many transcription factors interact synergistically with steroid receptors.* Science, 1988. **242**(4884): p. 1418-20.

521. Arora, V.K., et al., *Glucocorticoid receptor confers resistance to antiandrogens by bypassing androgen receptor blockade.* Cell, 2013. **155**(6): p. 1309-22.

522. Claessens, F., S. Joniau, and C. Helsen, *Comparing the rules of engagement of androgen and glucocorticoid receptors.* Cellular and molecular life sciences : CMLS, 2017. **74**(12): p. 2217-2228.

523. Claessens, F., et al., *Selective DNA binding by the androgen receptor as a mechanism for hormone-specific gene regulation.* J Steroid Biochem Mol Biol, 2001. **76**(1-5): p. 23-30.

524. Denayer, S., et al., *The rules of DNA recognition by the androgen receptor.* Mol Endocrinol, 2010. **24**(5): p. 898-913.

525. Devos, A., et al., *Structure of rat genes encoding androgen-regulated cystatin-related proteins (CRPs): a new member of the cystatin superfamily.* Gene, 1993. **125**(2): p. 159-67.

526. John, S., et al., *Chromatin accessibility pre-determines glucocorticoid receptor binding patterns.* Nat Genet, 2011. **43**(3): p. 264-8.

527. Bolton, E.C., et al., *Cell- and gene-specific regulation of primary target genes by the androgen receptor.* Genes Dev, 2007. **21**(16): p. 2005-17.

528. Wang, Q., et al., *A hierarchical network of transcription factors governs androgen receptor-dependent prostate cancer growth.* Mol Cell, 2007. **27**(3): p. 380-92.

529. Sahu, B., et al., *Androgen receptor uses relaxed response element stringency for selective chromatin binding and transcriptional regulation in vivo.* Nucleic Acids Res, 2014. **42**(7): p. 4230-40.

530. Voss, T.C., et al., *Dynamic exchange at regulatory elements during chromatin remodeling underlies assisted loading mechanism.* Cell, 2011. **146**(4): p. 544-54.

531. Fronsdal, K., et al., *CREB binding protein is a coactivator for the androgen receptor and mediates cross-talk with AP-1.* J Biol Chem, 1998. **273**(48): p. 31853-9.

532. Lobaccaro, J.M., et al., *Transcriptional interferences between normal or mutant androgen receptors and the activator protein 1--dissection of the androgen receptor functional domains.* Endocrinology, 1999. **140**(1): p. 350-7.

533. Kushner, P.J., et al., *Estrogen receptor pathways to AP-1.* J Steroid Biochem Mol Biol, 2000. **74**(5): p. 311-7.

534. Heldring, N., et al., *Multiple sequence-specific DNA-binding proteins mediate estrogen receptor signaling through a tethering pathway.* Mol Endocrinol, 2011. **25**(4): p. 564-74.

535. Biddie, S.C., et al., *Transcription factor AP1 potentiates chromatin accessibility and glucocorticoid receptor binding.* Mol Cell, 2011. **43**(1): p. 145-55.

536. Swinstead, E.E., et al., *Steroid Receptors Reprogram FoxA1 Occupancy through Dynamic Chromatin Transitions.* Cell, 2016. **165**(3): p. 593-605.

537. Miranda, T.B., et al., *Reprogramming the chromatin landscape: interplay of the estrogen and glucocorticoid receptors at the genomic level.* Cancer Res, 2013. **73**(16): p. 5130-9.

538. Manoli, D.S. and J. Tollkuhn, *Gene regulatory mechanisms underlying sex differences in brain development and psychiatric disease.* Ann N Y Acad Sci, 2018. **1420**(1): p. 26-45.

539. Cotella, E., et al., *Selective modulation of the glucocorticoid receptor with CORT108297 during chronic adolescent stress evokes sex-specific effects in adulthood.* bioRxiv, 2019: p. 646745.

540. Soares, C.N., *Depression and Menopause: Current Knowledge and Clinical Recommendations for a Critical Window.* Psychiatr Clin North Am, 2017. **40**(2): p. 239-254.

541. Greenberg, P.E., et al., *The economic burden of adults with major depressive disorder in the United States (2005 and 2010).* J Clin Psychiatry, 2015. **76**(2): p. 155-62.

542. Bagot, R.C., et al., *Ketamine and Imipramine Reverse Transcriptional Signatures of Susceptibility and Induce Resilience-Specific Gene Expression Profiles.* Biol Psychiatry, 2017. **81**(4): p. 285-295.

543. Hultman, R., et al., *Brain-wide Electrical Spatiotemporal Dynamics Encode Depression Vulnerability.* Cell, 2018. **173**(1): p. 166-180.e14.

544. Anacker, C. and R. Hen, *Adult hippocampal neurogenesis and cognitive flexibility - linking memory and mood.* Nat Rev Neurosci, 2017. **18**(6): p. 335-346.

545. Gandiga, P.C., F.C. Hummel, and L.G. Cohen, *Transcranial DC stimulation (tDCS): A tool for double-blind sham-controlled clinical studies in brain stimulation.* Clinical Neurophysiology, 2006. **117**(4): p. 845-850.

546. Cyranoski, D. and H. Ledford, *Genome-edited baby claim provokes international outcry.* Nature, 2018. **563**(7733): p. 607-608.

547. Kang, E., et al., *Adult Neurogenesis and Psychiatric Disorders.* Cold Spring Harb Perspect Biol, 2016. **8**(9).

548. Steinberg, G.K., et al., *Clinical Outcomes of Transplanted Modified Bone Marrow-Derived Mesenchymal Stem Cells in Stroke: A Phase 1/2a Study.* Stroke, 2016. **47**(7): p. 1817-24.

549. Dagdeviren, C., et al., *Miniaturized neural system for chronic, local intracerebral drug delivery.* Sci Transl Med, 2018. **10**(425).

550. Bowles, D.E., et al., *Phase 1 gene therapy for Duchenne muscular dystrophy using a translational optimized AAV vector.* Mol Ther, 2012. **20**(2): p. 443-55.